1988

THE MICROSTRUCTURES OF ESTUARINE PARTICLES

TITLEY, JOHN GRAHAM

http://hdl.handle.net/10026.1/1793

THE MICROSTRUCTURES OF ESTUARINE PARTICLES

BY

JOHN GRAHAM TITLEY B.Sc. (Hons.)

A thesis submitted to the Council for National

Academic Awards in partial fulfilment of the

requirements for admittance to the degree of:

DOCTOR OF PHILOSOPHY

UNDERTAKEN AT:

       PLYMOUTH POLYTECHNIC INSTITUTE. OF MARINE STUDIES
       DEPARTMENT OF MARINE SCIENCE AND TECHNOLOGY
       DRAKES CIRCUS
       PLYMOUTH
       DEVON
       U.K.

IN COLLABORATION WITH:

       PLYMOUTH MARINE LABORATORIES
       PROSPECT PLACE
       THE HOE
       PLYMOUTH
       DEVON
       U.K.

Submitted May 1988

i

COPYRIGHT

Sedimentary Reflections

DECLARATIONS

At no time during the registration for the degree of Doctor of Philosophy has the author been registered for any other C.N.A.A. or University award. This study was financed with the aid of research assistantship GR3/5712 from the Natural Environmental Research Council, and the author also held a part-time lecturing post in the Department of Marine Science and Technology. The study was undertaken in collaboration with Plymouth Marine Laboratories.

A programme of advanced study was undertaken within the Polytechnic which included a lecture course in colloid chemistry given by Dr. D.R. Glasson, a course of instruction on the use of the Scanning Electron Microscope and several courses on the use of micro and mainframe computers.

During the period of registration a number of relevant scientific meetings were attended. A number of conference papers were also presented and three papers were published as listed below.

PAPERS PUBLISHED OR IN PRESS:

Glegg, G.A., Titley, J.G., Glasson, D.R., Millward, G.E. and Morris, A.W.;
The microstructures of estuarine particles.
In: "Particle Size Analysis 1985". (Ed. P.J. Lloyd).
John Wiley, Chichester. p.591. (1987).

Titley, J.G., Glegg, G.A., Glasson, D.R., Millward, G.E.;
Surface areas and porosities of particulate matter in turbid estuaries.
Continental Shelf Research, 7, p.1363. (1987).

Glegg, G.A., Titley, J.G., Millward G.E., Glasson, D.R. and Morris, A.W.;
Sorption behaviour of waste generated trace metals in estuarine waters.
Water Science and Technology, (In press).

CONFERENCES ATTENDED:

NERC Geocolloids Meeting: "Characterisation of Natural Particles". Held at the University of Lancaster, 15-17th April, 1985.

IAWPRC/NERC Meeting: "Estuarine and Coastal Pollution". Held at Plymouth Polytechnic, 16-19th July, 1985.

Marine Chemistry Discussion Group Meeting: "Marine Chemistry in Coastal Waters". Held at the Unversity of Surrey, 11/12th September, 1985. Paper presented by J.G. Titley entitled "Particle Microstructures in Natural Waters".

Fifth Royal Society of Chemistry Conference: "Particle Size Analysis". Held at the University of Bradford, 16-19th September 1985. Paper presented by J.G. Titley entitled "The Microstructures of Estuarine Particles".

NERC Geocolloids Group Meeting: "Sorption Processes in Geocolloid Systems". Held at the University of Lancaster, 1-3rd April, 1986. Paper presented entitled: "Surface Areas and Porosities of Estuarine Sediments".

Estuarine and Brackishwater Sciences Association Meeting: "Dynamics of Turbid Coastal Environments". Held at Plymouth Polytechnic, 1-5th September 1986. Paper presented entitled: "Surface Areas and Porosities of Particulate Matter in Turbid Estuaries".

NERC Geocolloids Group Meeting: "Particle Aggregation Processes in the Natural Environment". Held at the University of Lancaster, 21-23rd April, 1987.

IAWPRC/JSWPR Meeting: "Coastal and Estuarine Pollution". Held by Kyushu University, Fukuoka, Japan, 19-21st October 1987. Paper presented by J.G. Titley entitled: "Sorption Behaviour of Waste Generated Trace Metals in Estuarine Waters".

EXTERNAL VISITS:

British Geological Survey, Wallingford for a discussion with Dr. D.G. Kinniburgh on computerised analysis of gas adsorption data, April, 1986.

Department of Oceanography, Southampton for discussions with Dr. P. Statham on clean handling of samples for trace metal analyses. April, 1986.

ACKNOWLEDGEMENTS

THE MICROSTRUCTURES OF ESTUARINE PARTICLES

John Titley

ABSTRACT

A systematic study of the surface properties of suspended and bed
sediments from the Tamar Estuary and Restronguet Creek was carried
out using a nitrogen adsorption technique. The surface areas and
porosities of the particles were determined using BET theory and
capillary models applied to the gas adsorption isotherms. The
surface areas of the suspended particles collected on axial
transects of the Tamar Estuary ranged between 8 and 22 m^2/g. The
highest values were found for particles in the turbidity maximum
region. These appeared to be related in a complex way to both
particle size and the chemical composition of the particles. Pores
in the suspended solids (total volume $1-3*10^{-2}$ ml/g) were
predominantly parallel plates in the size range 1-50 nm, suggesting
that clay structures were important. Pore size distributions were
skewed in favour of pores <10 nm diameter, and in some cases 50% of
the pore volume was located in micropores (<2 nm diameter). Bed
sediments in the Tamar Estuary had surface areas of 6-14 m^2/g. The
highest values were associated with the <45 μm and >125 μm fractions
of the sediments, and a predominant relationship was observed
between the Fe oxide content and surface area. Surface areas of
particles from Restronguet Creek were higher (15-40 m^2/g) than from
the Tamar. The distribution of surface area correlated with the
smaller grain sizes and Fe content in the bed sediments. Comparison
of these data with results from the Mersey Estuary (surface areas 6-
14 m^2/g) showed inter and intra-estuarine variability between the
C/Fe ratio in the sediment and surface area.

The microstructural information was used to refine the understanding
of adsorption mechanisms involved in dissolved phosphate adsorption,
including diffusion of ions into the particle matrix. This was then
used to describe the mechanisms controlling the intra-estuarine
variability in the transport and bioavailability of phosphate in
estuaries.

CONTENTS

CHAPTER ONE

INTRODUCTION AND LITERATURE REVIEW

1.1. RATIONALE.

Physical, chemical and biological processes in estuaries have come under intense scrutiny in recent years, particularly because of the need to refine models which predict the dispersal of anthropogenic wastes (Gerlach, 1981; Olausson and Cato, 1980).

Environmental disasters such as the mercury poisoning problem in Minimata Bay can lead to human fatalities (Gerlach, 1981; So, 1978) or may have a detrimental impact on human economic well being, as followed the construction of the Aswan Dam which led to the destruction of a productive estuarine fishery (Lockwood, 1986). The prediction and modelling of the behaviour of natural aquatic environments is therefore essential in order to reduce the impact of man's activities and avoid the need for costly environmental clean-up.

Strategic management of the estuarine environment requires a predictive modelling approach to improve the general understanding of the complex processes that can take place. Estuaries function as receptacles for a wide range of pollutants, mainly treated and un-treated sewage outputs and industrial wastes. However, due to their high biological productivity, they also support large fish populations, especially during spawning. In addition they have aesthetic value, and provide areas for recreation.

Against this background, the physical, chemical and biological

1

processes occurring within estuaries have been widely studied. Of
these, observations into the internal biogeochemical cycling of
metals and nutrients have been undertaken to refine the modelling of
these processes; for example: Ackroyd et al., 1986; Morris et al.,
1986; Loring et al., 1983; Morris et al., 1982b; 1981; Duinker et
al., 1980; Morris and Bale, 1979; Elderfield et al., 1979; Duinker
and Nolting, 1978; Morris, 1978; Duinker et al., 1974.

A complicating factor in interpreting these data is that
hydrodynamic estuarine interactions induce wide variations in
physical, chemical and biological parameters over a range of
temporal and spatial dimensions. Thus, studies in estuaries must
involve multiparameter observations: temperature, salinity, pH,
dissolved oxygen and turbidity so that chemical variability within
the estuarine environment can be properly understood (Morris et al.,
1982; Morris et al., 1978).

Development of biogeochemical models of estuaries can be hampered by
the uniqueness of each estuarine system (Olausson and Cato, 1980),
and this is best exemplified by the differential behaviour of
dissolved chemical constituents between estuarine systems. For
example the dissolved trace metals Zn, As and Mn have been observed
to behave conservatively in some U.K. and U.S. estuaries,
(Elderfield et al., 1979; Waslenchuk and Windom, 1978; Holliday and
Liss, 1976), while in others these elements showed distinct non-
conservative behaviour (Howard et al., 1984; Langston, 1983; Morris
et al., 1982b Duinker and Nolting, 1978). This differential
behaviour between estuaries is thought to be linked to the sorptive
interactions of dissolved constituents with indigenous particles.

2

Thus, processes occurring at the solid-liquid interface in estuaries are of great importance in determining the unique behaviour of dissolved constituents in the water column, especially the low salinity region of estuaries (Morris, 1986). At present there is little direct information on the nature of the particle surfaces or the precise mechanisms by which the sorption processes take place. However it is important to know where adsorbed species are located on the particle and whether they are bioavailable. The published data in this area will be reviewed in the following three sections.

1.2 PARTICLES IN THE ESTUARINE ENVIRONMENT.

1.2.1 THE ROLE OF PARTICLES IN PHYSICO-CHEMICAL REACTIONS.

It is now widely accepted that particles in the estuarine
environment have an important role to play in controlling the
geochemical behaviour of dissolved trace metals and nutrients
(Bourg, 1987; Olsen et al., 1982). Sediment surfaces are capable
of adsorbing dissolved chemical species, thus affecting their
availability to the biota and their overall transport and cycling
within the estuarine environment. Suspended particles within the
highly turbid low salinity region are especially important for
adsorption as this region is chemically reactive (Morris, 1986). In
addition riverine particles fluxing across the Freshwater-
Brackishwater Interface, may also release sorbed trace constituents
back into the water column. This latter process can occur after
resuspension of anoxic bed sediments when a change to oxidizing
conditions may lead to desorption, as well as injecting pore fluids
into the water column. Adsorption of dissolved species in the
turbidity maximum region is important because once associated with
the particulate phase, the chemical species may become incorporated
into the sediment, which can act as the ultimate sink for many trace
metals. This process is sometimes reversible, for example release
of Mn from the sediments as they become anoxic following
sedimentation has been reported (Morris et al., 1982b; Morris and
Bale, 1979). Both suspended solids and bed sediments can have
bacterial colonies attached to them (Plummer et al., 1987) and
bacterial activity can cause transformation of chemical species,
particularily heavy metals such as Sn, Pb, and Hg (Craig, 1986;

4

Craig and Rapsomanikis, 1985). However, many adsorbed species can migrate from the external surface of the particles to the matrix, thus reducing the likelihood of release from the surface by chemical transport processes or by biological mobilization.

Thus partitioning of dissolved species between the dissolved and solid phases is largely responsible for the internal biogeochemical cycling of both dissolved pollutants and naturally occurring chemical species. The importance of these processes was recognized in the Natural Environmental Research Council Multidisciplinary Workshop on "Estuarine Processes" (1982). The major recommendation made in the report concerned "*the behaviour and fate of particulate material within estuaries, with special reference to its transformation by chemical and biological activity and fluxes across the benthic boundary layer.*"

Most estuarine research into chemical processes over the last 15 years recognizes the importance of particle-water interactions in the turbidity maximum region of estuaries. In studies where chemical reactivity was observed it was concluded that sorption onto suspended and sedimentary particles and co-precipitation with Fe/Mn oxides were the most likely causes of removal, while desorption from particles or the release of trace constituents from sediment interstitial waters are the main causes of the addition of dissolved trace metals into the water column (Hart, 1982).
The sorption of trace metals and nutrients onto natural and synthetic mineral surfaces in laboratory studies have been demonstrated by a number of workers (Glegg, 1987; Anderson *et al.*, 1985; Crosby *et al.*, 1984; Li *et al.*, 1984a; Crosby, 1982; Millward

5

and Moore, 1982; Crosby *et al.*, 1981; Benjamin and Leckie, 1981; Salomons, 1980).

Once associated with the particle, the distribution and cycling of the chemical species is modified to that of the behaviour of the particles, and thus to the physical behaviour of the estuarine hydrodynamics. These physical processes cause the temporal and spatial variability in both concentration and composition of the suspended particle population (Loring *et al.*, 1983; Morris *et al.*, 1982). Dissolved Mn, Fe, Zn, Cu and Al have been shown to cycle in relationship with the physical cycling of the particles (Morris *et al.*, 1986; Morris *et al.*, 1982b). Thus understanding of both the chemical activity at the particle-water interface and the characteristics of the particulate phases in an estuary are crucial to understanding the distribution, transport and long term fate of nutrients and trace metals.

1.2.2 THE PHYSICAL BEHAVIOUR OF PARTICLES IN ESTUARIES

The importance of particles for sorption and retention of trace metals and nutrients within aquatic environments is widely appreciated amongst environmental chemists. In order to understand the transport, cycling and distribution of chemicals within aquatic environments it is important to understand the physical behaviour of particles and the physical processes that affect their distributions.

It is known that modern estuaries are relatively short lived features in comparison with geological time scales, and have appeared since the raising of sea levels in relatively recent times.

6

Estuaries function as sediment traps and most are gradually filling up as a result of continued inputs of material from both rivers and coastal seas (Olausson and Cato, 1980). Conditions for internal sediment deposition and remobilization in estuaries are much more favourable than transport to the open coastal shelf (Bale *et al.*, 1985).

Sediment deposits are continually being mobilized and transported within the estuarine regime. Two main mechanisms function to transport sediments up-estuary, both of which are related to tidal behaviour. The first of these concerns the asymmetric behaviour of the tidal cycle within macrotidal estuaries with extensive mudflats. The asymmetry results in a shorter flood tide (with greater velocity) than the ebb flow. Flood tides can be up to 2 hours shorter than the ebb, and the period of slack water at high tide can also be extended (Bale, 1987; Postma, 1980). A time lag between the tidal current rhythm and the changes in suspended matter concentrations in the water column also influences the transport of sediment over a tidal cycle. The greater current velocity on the flood tide produces a rapid resuspension of bed sediments which are carried upstream on the tide. During high water slack and during the ebb flow which has a reduced velocity, settling out of larger particles can take place. The overall result of this is net landward transport of sediments.

In addition to this mechanism, estuarine circulation patterns can also contribute to the up-estuarine transport of suspended particles especially in partially or well mixed estuaries such as the Loire, Gironde and Tamar Estuaries (Uncles *et al.*, 1985; 1983; Allen *et*

7

al., 1980; 1974; Gallenne, 1974). The landward bottom flow is sufficiently strong (especially on spring tides and low runoff conditions) to move suspended sediment up estuary to the limit of the salt intrusion and create a turbidity maximum (Bale *et al.*, 1985; Allen *et al.*, 1980).

The turbidity maximum is usually maintained at a precise location by the time averaged balance of forces between tidal power and outflowing fresh water (Bale *et al.*, 1985; Allen *et al.*, 1980). Certain specific grain sizes become entrained and trapped within the turbidity maximum. These suspended particles are usually smaller than the overall particle size distributions of the sediment; suspended particles in the turbidity maxima of 4 μm diameter were found in the Gulf of San Miguel, 8 μm diameter in the Sacramento River Estuary, 6 μm in the Loire, 5 μm in the St. Lawrence Estuary, and 10-15 μm in the Tamar (Glegg, 1987; Postma, 1980; Gallenne, 1974; d'Anglejan and Smith, 1973; Swift and Pirie, 1970). In the Tamar Estuary, the turbidity maximum represents 0.2-5% of the total bed sediment shoal. Overall the location of the turbidity maximum appears to be governed by the volume of fresh water flow (Bale *et al.*, 1985; Allen *et al.*, 1980; Postma, 1980). Under low flow conditions the turbidity maximum stabilizes in the higher reaches of the estuary. The decrease in cross sectional area of the river channel reduces the volume of water, but not the total quantity of suspended material, thus the particle concentrations show a marked increase. If low flow conditions persist, much of the readily resuspended sediment in the estuary can become incorporated in the turbidity maximum or its associated shoal of sediment. This latter

8

feature is created as a result of settling of sediment from the turbidity maximum, and the large quantity of fluid mud produced can readily exchange with the turbidity maximum (Bale, 1987; Postma, 1980; Allen et al., 1974).

As river flow increases, the turbidity maximum migrates down estuary, together with the shoal of mobilized bed sediment. The larger river channel down-estuary has a greater cross-sectional area and a larger volume of water which dilutes the particle concentration. The total amount of sediment in suspension may not change but the turbidity maximum will tend to lose definition (Bale, 1987).

The long-term transport and cycling of sediments within macrotidal estuaries therefore depends on three main parameters:
1) Tidal transport, which predominantly affects fine grained sands and silts; 2) Estuarine circulation which acts on silts and muds;
3) River run-off which controls the location of the turbidity maximum.

The seasonal pattern of sediment movement within the Tamar Estuary has been modelled by Bale (1987) and Bale et al., (1985) (Figure 1.1) who found that the average residence time of particles in the turbidity maximum in the Tamar Estuary is 2 years. The overall distribution of bed sediments within the estuary is strongly related to the volume of fresh water flow, and this is in turn seasonal, with highest discharges occurring in winter months and lowest in the summer. Under stable low flow conditions (summer) two major reservoirs of sediment are produced: the turbidity maximum and the underlying bed shoal. If the stable conditions are disturbed by
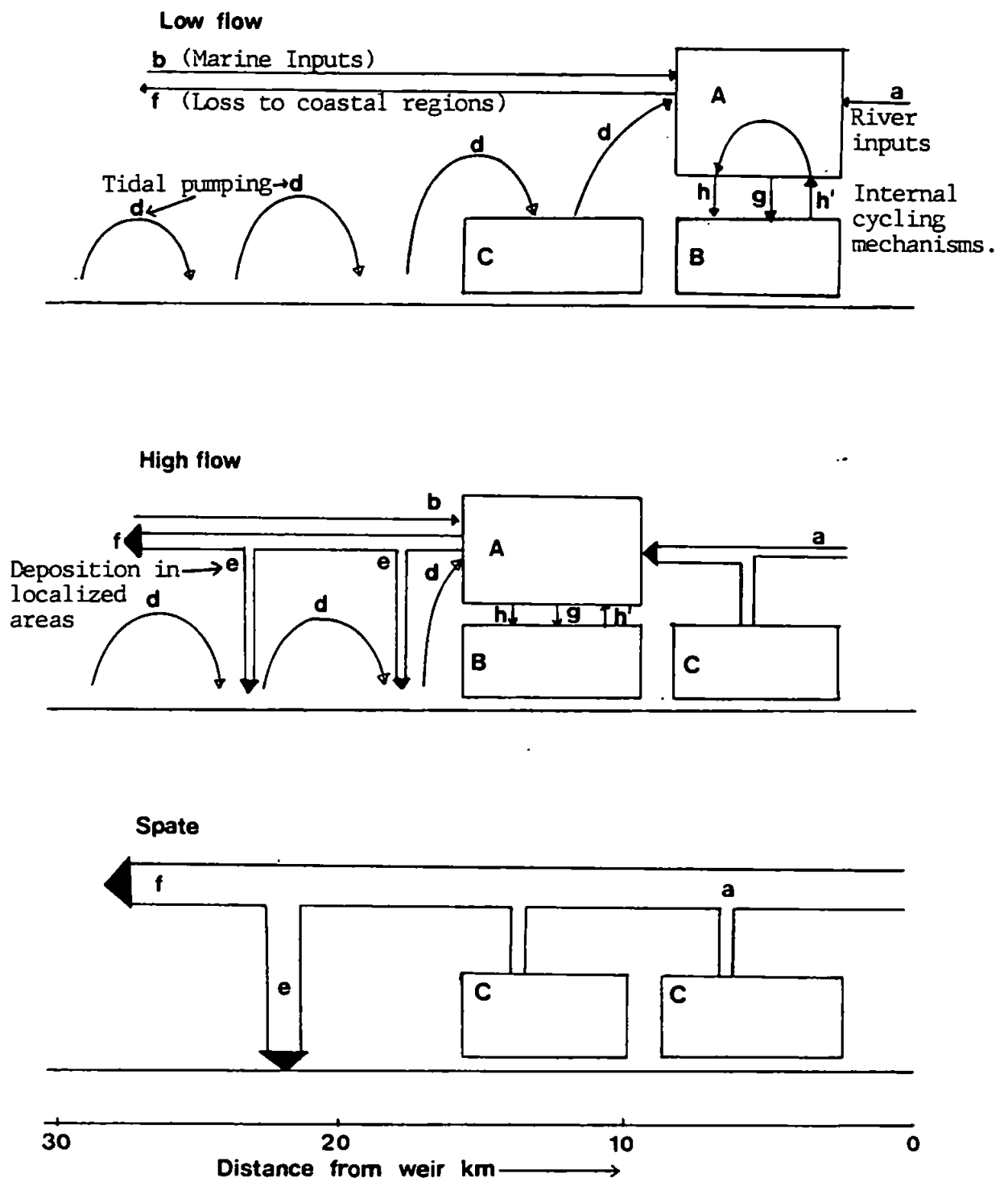
Figure 1.1. Schematic representation of suspended particle cycling in the Tamar Estuary. Three basic conditions are shown. Top: low river flow. Centre: High river flow. Bottom: Spate conditions. (Redrawn from Bale, 1987). Key: Box A, turbidity maximum. Boxes B & C are the present and previous sediment shoals associated with the turbidity maximum.

increases in run-off, the turbidity maximum can change location quickly, and a second shoal of fluid mud is created, which then gradually incorporates the original (see Figure 1.1). Under very high spate conditions (river flow > 100 m^3/s) the turbidity maximum may be lost completely and much suspended material may pass straight out to sea. The overall model suggests that as river flow increases so the amount of suspended sediment passing out of the estuary to sea increases (Bale, 1987).

Variations in the bed sediment depths were observed which fit this model (Morris *et al.*, 1986). Studies made over a complete year showed that bed sediments accumulated in the upper section of the estuary when river flow was low but were moved down estuary to localized deposition zones during the high run-off winter months. These findings were then incorporated with data on the distribution of trace metals within the sediments to provide a model which predicted the transport of Cu, Zn, Mn and Fe within the estuary (Ackroyd *et al.*, 1986; Morris *et al.*, 1986).

1.3 THE PHYSICO-CHEMICAL CHARACTERISTICS OF PARTICLES IN ESTUARIES.

1.3.1 CHEMICAL COMPOSITION.

Particles in estuaries are composed of a range materials mostly supplied from river inputs which reflect the geology and geomorphology of the catchment. Thus particles will tend to show inter-estuarine variability in composition as the geology, landuse and soil profiles in the catchment of each estuary will be different. The underlying crystalline phase identified by Titley *et al.,* (1987) and Martin *et al.,* (1986) originates in the main from leached soil particles, and comprises clay minerals, quartz grains, humic materials and iron oxide mineral phases (Berger *et al.,* 1984; Cameron and Liss, 1984; Sigleo and Helz, 1981). During high spate conditions inputs from the river bed and banks become important (Murgatroyd, 1980), and during the autumn months detrital organic material, especially leaf matter becomes important. Once incorporated in the estuarine sediment budget the organic detritus becomes part of the pool of detrital material that makes estuaries extremely productive ecosystems (McClusky, 1981).

In addition to riverborne material, *in situ* processes especially bacterial activity and photosynthetic primary production are important, as are inputs of particulate material from the marine end of the estuary. Due to the highly mobile nature of the sediments in the low salinity region of the estuary, large organisms are absent from the sediments and much of the biological reworking of the particles is carried out by either free living bacteria or colonies attached to the suspended sediments which then become part of the particulate matter (Plummer *et al.,* 1987). In the mid and

12

lower regions of the estuary larger invertebrates are able to colonise the sediments which are more compacted. These organisms are predominantly bivalve filter feeders (McClusky, 1981) and can modify the particles by removing organic coatings and bacteria and contribute fecal material.

The low salinity region of the estuary is a region of high chemical activity. Many materials are transported into this region in "dissolved" or colloidal form (one length between 1 nm and 400 nm in at least one dimension) in river water, or are stabilized by organic ligands which "complex" the materials (Cameron and Liss, 1984).

The main riverborne components transported in the "dissolved" phase are clay colloids, humic acids, organic macromolecules and Fe/Mn oxyhydroxides (Cameron and Liss, 1984; Boyle et al., 1982; Tipping, 1981; Sigleo and Helz, 1981; Eckert and Sholkovitz, 1976). On mixing with the incoming saline waters, flocculation of the dissolved species can take place as the changing ionic conditions cause compression of the electrical double layer around particles. This reduces charge induced repulsion and allows Van der Waals forces to dominate and cause particle coagulation. The flocculation processes that occur in the low salinity region as a result of these reactions are the most important mechanism for the removal of Fe from solution. The flocculation of colloidal and "dissolved" Fe oxides has been widely reported and is the principal contributing factor to the observed non-conservative behaviour of Fe in estuaries (Matsunaga et al., 1984; Mayer, 1982a; 1982b; Bale and Morris, 1981). Fox and Wofsy (1983) showed that the flocculation mechanism was second order with a rate co-efficient proportional to the square of salinity.

Matsunaga *et al.*, (1984) and Mayer (1982a) found the reaction to be two stage with an initial fast step followed by a slower temperature dependent reaction. The presence of particles from the turbidity maximum in the low salinity region also enhances the rate and extent of the Fe precipitation (Aston and Chester, 1973).

The precipitation of dissolved Fe onto particle surfaces produces fresh coatings of amorphous Fe oxides which can occur as discrete microscopic particles of Fe oxide adsorbed on or in the particle surface (Torres-Sanchez *et al.*, 1985). Amorphous Fe oxides have both large specific surface areas and large potential for the adsorption of both trace metals and dissolved nutrients (Crosby *et al.*, 1984; 1983; Marsh *et al.*, 1984; Millward and Moore, 1982; Swallow *et al.*, 1980). The particle composition is further modified by fresh coatings of organics especially macromolecular humics that precipitate from the dissolved state during mixing between river water and saline estuary waters. These coatings affect the particle surface, especially in terms of adsorptive capacity. However the highly complex nature of the humate materials has frustrated attempts to resolve the chemical composition which is required if the contribution of this component to particle make-up and behaviour is to be fully investigated.

In conclusion it is possible to build up a picture of the nature and composition of estuarine particles. The essential components are an underlying crystalline phase which is overlain by fresh coatings of precipitated materials. The crystalline phase comprises a mixture of aluminosilicate clays, (the types and abundance of which are dependant on the geology and soils of the catchment); quartz grains,

reworked soil particles, and iron oxide mineral phases. These are

coated with organic materials, especially flocculated humics and

cell secretions (mucus). Fecal pellets and the calcareous shells of

plankton may also become incorporated into the particle aggregate

which is held together by the organic coatings. In addition,

flocculation of colloidal Fe and Mn oxides onto particle surfaces

occurs continuously as Fe and Mn colloids are brought into the

estuary by the river.

The inhomogeneity of the particle make-up means that the solid-

solution interface between the particles and the water column is

very complex and sorption processes that take place at this phase

discontinuity will be very variable. This aspect and its

relationship to estuarine chemistry will be discussed in the next

section.

1.3.2. SURFACE PROPERTIES.

The influence of estuarine particles on the distribution of

nutrients and trace metals in the water column has been widely

reported (Li et al., 1984b; Readman et al., 1984; Sundby et al.,

1984; 1981; Morris et al., 1981; Moore et al., 1979; Morris and

Bale, 1979). Most chemical reactions that occur in natural waters

take place at phase discontinuities. Of interest in this study is

the liquid-solid interface, where crystallization and precipitation

reactions and sorption processes involving cations, anions, and

weak acids can occur (Stumm and Morgan, 1981). In the estuarine

environment, particle composition and the aqueous phase are complex

and a number of additional processes are thought to be important.

These include adsorption through ion-exchange, hydrophobic interactions with the particle surface, co-precipitation with Fe/Mn oxyhydroxide coatings, complexation with organic substances (already associated with the particle surface), incorporation of the adsorbate species into mineral lattices and organisms, and flocculation of colloids during the mixing of sea and river water. (Moore and Millward, 1988; Anderson *et al.*, 1985; Cameron and Liss, 1984; Mayer, 1982a; Olsen *et al.*, 1982; Duinker, 1980; Gearing, 1980; Gibbs, 1977; Burton, 1976; Burton and Liss, 1976; Sholkovitz, 1976; Edzwald *et al.*, 1974). All these processes are mediated by the occurrence and distribution of electrical charges at the solid solution interface. Due to the heterogeneous nature of estuarine particles, little direct evidence about the nature of these surfaces has been obtained apart from a few surface charge and surface area measurements (Glegg *et al.*, 1987; Newton and Liss, 1987; Titley *et al.*, 1987; Martin *et al.*, 1986; Hunter and Liss, 1982; 1979). More comprehensive studies have been undertaken on single component solid phases, such as pure clays and synthetic Fe oxyhydroxides, and these will be reviewed together with information on natural particles in the following sections.

1.3.2.1. Surface Charge.

The concept of the electrical double layer is now a widely accepted theory for explaining the behaviour of many colloids and suspended particles in natural waters (Stumm and Morgan, 1981). The electrical double layer is induced as result of charge imbalances at the particle surface which can arise through a number of processes. The surfaces of clays can aquire a charge as a result of isomorphous

substitutions of cations within the clay lattice for Al. If cations with less valency than Al are involved, (e.g Mg) then a charge imbalance is set up in the clay lattice. A pure clay lattice with no imperfections would be electrically neutral, and therefore the magnitude of the imbalance in the charge distribution will depend on both the number of substitutions made per unit area, and the valency of the cations involved. As most cations involved in substitution will be of lower valency than Al, the predominant charge imbalance produced in clay lattices will be negative. Additionally charge imbalances can arise at the surfaces of sheared crystals.

A second mechanism for the production of a charged surface may arise from chemical reactions at the surface. Solid surfaces such as Fe oxides contain ionizable functional groups, e.g. OH, $COOH$, OPO_3H_2. The surface charge will depend on the degree of ionization and the pH of the medium. Oxides and hydroxides exhibit amphoteric behaviour, that is the surface charge can change from positive at low pH to negative as the pH of the media increases. Organic substances can behave in a similar fashion, with the charge arising from protolysis of functional amino and carboxyl groups. The pH dependence of the surface charge means that at some intermediate pH the surface charge will theoretically be zero; the so-called isoelectric point (Stumm and Morgan, 1981).

Surface charge on particles can also arise from adsorption of a surfactant ion. In the natural environment adsorption of organic matter onto particle surfaces during mixing with seawater is commonly observed (Loeb and Neihof, 1977; Neihof and Loeb, 1974; 1972), and the charge of the surface altered (Hunter and Liss, 1982; Davis and

17

Leckie, 1978).

The surface charge produced by these mechanisms is predominantly negative, and when in contact with the aqueous phase attract a layer of counter-ions. These are distributed diffusely through the liquid as a result of thermal motion, but remain near to the charged surface as a balance between electrostatic and thermal forces is attained. Further adaptations of this model of the electrical double layer have been developed, for example that of Stern (1924) who divided the counter-ion layer into two, the first consisting of a layer of ions specifically adsorbed at the surface forming the compact Stern layer, and the second forming a more diffuse layer (Stumm and Morgan, 1981).

Ions involved in the counter-ion layer in the electrical double layer readily exchange for other ions. This process favours the exchange of bivalent ions such as Ca^{2+} for monovalent species, such as Na^+. The exchange of cations through the electrical double layer is an important adsorption process especially at the surfaces of clays where it is thought to be the main adsorption process (Van Olphen, 1965). However the presence of iron oxides on the surfaces of sediments which have a much greater adsorptive capacity than clays overshadow this adsorptive process (Berger *et al.*, 1984; Duinker, 1980; Aston and Chester, 1973).

The exchange of ions with different valencies in the electrical double layer also has an impact on the physical surface properties of the clays, especially the extent of swelling in expanding clays such as montmorillonite (Stumm and Morgan, 1981).

18

While it is relatively simple matter to describe the surface
chemistry of individual solids in isolation, the highly complex
nature of natural particles makes quantification of their surfaces
much more difficult. Additionally, adsorption processes at the
solid-solution interface are modified by the presence of a range of
ions which compete for surface sites within the electrical double
layer or on the particle surface. In addition, the presence of
complexing organics especially humics which hold dissolved species
in solution, and the speciation of the ions involved in adsorption
can cause complex sorption behaviour at the solid-solution interface
(Bourg, 1987; 1983; Mouvet and Bourg, 1983; Florence, 1977).

Dissolved and particulate organic materials in natural waters are
thought to be especially important in the control of solution
chemistry. Humic materials interact with clay surfaces (as surface
coatings), metal ions and metal hydroxides. During exposure to sea
water for example, most solid phases develop coatings of organic
materials (Loeb and Neihof, 1977; Neihof and Loeb, 1974; 1972) and
these produce a net negative charge on all particle surfaces
irrespective of the original charge (Hunter and Liss, 1982). These
uniform organic coatings on the surfaces of the particle matrices
can dominate the adsorptive properties of the sediment under natural
conditions.

In addition to the role of organic macromolecules, the formation of
hydrous metal oxides coatings of low solubility on clay surfaces
produces a pH dependent surface charge and may encourage the
separation of alumino-silicate sheets in the clay lattice (Oades,
1984). Theoretically this could increase the available surface area

by as much as 2 orders of magnitude. The modification of the
sorptive properties of clays by these processes is believed to be of
significance in the estuarine environment (Berger *et al.*, 1984;
Hamilton-Taylor and Price, 1983; Eisma *et al.*, 1978; Sholkovitz,
1976; Aston and Chester, 1973).

1.3.2.2 Surface Areas and Porosity.

At present, systematic examination of natural particle surfaces has
been limited to surface ion exchange capacities and the role of
organic coatings on surface charge (Hunter and Liss, 1982; Loeb and
Neihof, 1977). Although this aspect is important other features,
especially the distribution of sites on the surfaces of the
particles are key parameters for the mechanisms of adsorption of
dissolved species. At present, surface features on estuarine
particles such as surface areas and porosities have been largely
ignored, although porosity for example may be an important factor in
the intercalation of ions. Recently work has been carried out on
estuarine particles (Glegg *et al.*, 1987; Titley *et al.*, 1987; Martin
et al., 1986; Elbaz-Poulichet *et al.*, 1984); coastal water particles
(Nyffeler *et al.*, 1984) and soils (Madrid and De Arambarri, 1985;
Cabrera *et al.*, 1981).

Work with clay structures reveals that clay platelets can form an
open cardhouse structures during flocculation. Mixtures of quartz
and kaolinite suspensions produce open structures through strong
interactions between the edges of the clay surfaces and quartz
grains, although these are comparatively fragile (Williams and
James, 1978; Smart, 1966)(see Figure 1.2). These structures are
stabilized by the presense of adsorbed organic materials and metal

20

Zn Intercalation

1nm   (Zn) $\updownarrow$0·18nm

$\updownarrow$3·5nm

20nm
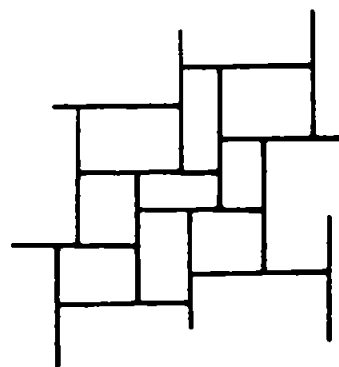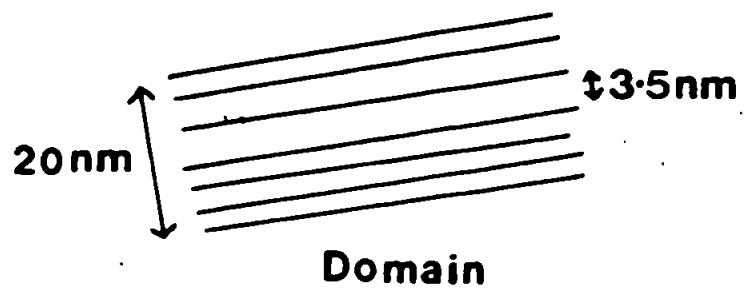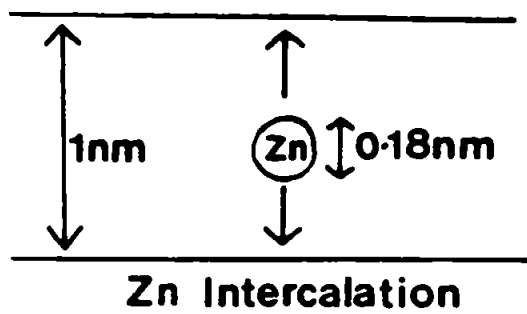
Domain

Card house floc

1μm
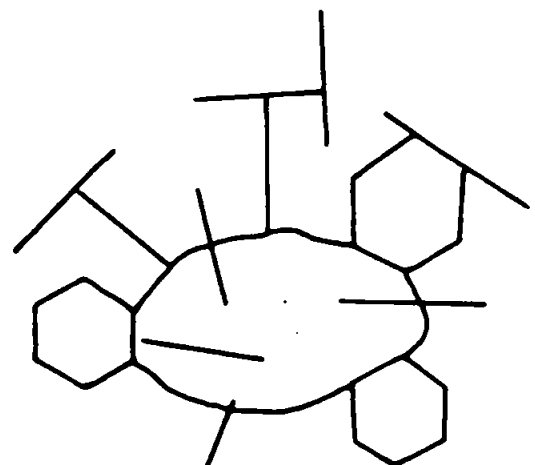
Pin cushion floc

Figure 1.2. Morphological features of clays. (From Glegg, 1987)

Top: Intercalation of a Zn ion between aluminosilicate sheets. Dimensions of the domain structures are shown.

Bottom: Larger morphological features created during natural flocculation processes.

21

oxides (Quirk, 1978). In the estuarine environment organic materials are implicated in the stabilization and aggregation of sedimentary particles (Bale, 1987). During the constant resuspension and depositional processes of sediments in estuaries, these open structures become re-ordered resulting in aggregation and consolidation of particles. The substitution of Na$^+$ ions with large hydration spheres for bivalent cations in the electrical double layer around clay surfaces occurs in saline waters and this produces greater pressures in the interlamellar spacings of expending clays. The larger sphere of hydration associated with Na$^+$ ions causes greater swelling pressures within the clay lattice which will also consolidate the microstructures of the clay surfaces (Stumm and Morgan, 1981). This description provides a view of the gross morphology of estuarine particles; which are essentially freshly flocculated clay particles and platelets arranged into an open structure by facial interactions with quartz. In the low salinity region where precipitation of new solid phases occurs, these particles are very fragile (Bale *et al.*, 1984). However during cycling of the sediment up and down estuary and the effects of varying salinities, the particles could consolidate and loose their open structure and reduce both surface area and the availability of surface sites for adsorption processes. Adsorption of ions at the particle surface would therefore be affected by these processes. However the scale of these processes occur in the 0.1-10 nm size range, and the observable consolidation processes, especially with respect to particle size are several orders of magnitude greater. Therefore analysis of microscale features such as surface areas and porosities in the nanometer size range is desirable as ions which

have dimensions of <0.5 nm can produce the two stage uptake

profiles frequently observed in adsorption processes (see Figure

1.3).

Surface area is a key element of particle surfaces as it provides

a description of the potential that a surface has for adsorption.

Measurement of surface area is not straight forward, the results

obtained being method dependent (Adamson, 1982). Essentially, the

concept of absolute surface area is nonsensical as it is

theoretically possible to analyse a surface in greater and greater

detail until the atomic level is reached. However, if consistent

methodology is chosen, surface area results can be compared to

provide inter-particle comparisons. Van den Hul and Lyklema (1968)

demonstrated this by determining the surface area of AgI using dye

adsorption, negative adsorption, and BET N_2 gas adsorption

techniques. The results obtained were different by an order of

magnitude, but trends in the surface area between different particle

sizes were comparable (see Table 1.1).

BET, N_2 gas	Negative Adsorption	Particle Size	Dye Adsorption	(Neg. Ads.)/BET
0.45	1.5	0.25	0.87	3.2
0.38	1.3	0.18	0.61	3.8
0.52	1.6	0.32	0.98	3.1
0.30	0.9	0.22	0.65	3.2
0.97	3.3	0.45	2.18	3.6
1.99	5.5	--	2.14	2.8

Table 1.1
Surface areas (m^2/g) of AgI samples determined by a variety of
methods (Van den Hul and Lyklema, 1968).

23

Amount Adsorbed

Slow Internal
Adsorption –
"Tunnelling"

Fast Surface
Adsorption

Time

$$S + X \xrightleftharpoons[k_{-1}]{k_1} SX \xrightleftharpoons[k_{-2}]{k_2} S'X$$
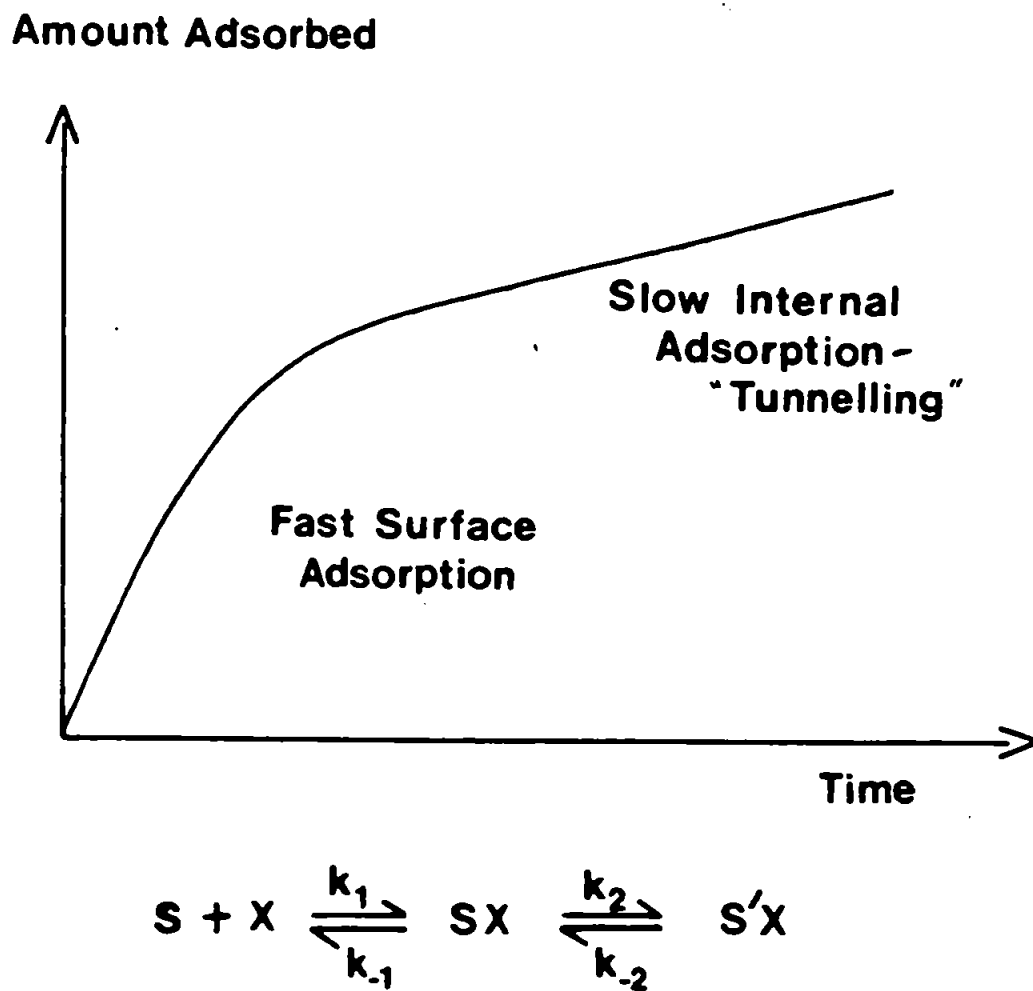
Figure 1.3. Simplified adsorption profile, showing initial fast surface adsorption followed by more persistent uptake, associated with diffusion of ions into the particle matrix.

Determination of the surface areas of natural solids *in situ* would be preferable to avoid unnecessary changes to the particles surfaces. However, no reproducible techniques for *in situ* measurement of surface area are available at present (Crosby, 1982; Gregg and Sing, 1982; Van den Hul and Lyklema, 1968) and methods that are available do not allow for the measurement of porosity.

In the absence of a suitable technique for measuring the surface area of natural particles, the BET nitrogen adsorption method was adopted. This technique is the standard industrial method for assessing surface area of solids and powders (Adamson, 1982; Gregg and Sing, 1982), and it is used as a yardstick against which all other surface area determinations are compared. The small size of the N_2 gas molecules provides detailed information about surficial features in the size range 1-50 nm. Work already undertaken in this laboratory shows that the BET surface area determination method on dried solids gives consistent information about particle surfaces (Glegg, 1987; Glegg *et al.*, 1987; Titley *et al.*, 1987; Marsh *et al.*, 1984; Crosby *et al.*, 1983; Marsh, 1983; Crosby, 1982). The results of studies on natural particles are also in agreement with those reported by other workers, for example, Donard and Bourg (1986) Martin *et al.*, (1986).

Examples of the surface areas obtained using these methods are shown in Table 1.2.

Sample	BET Surface Area, m^2/g	Reference
Amorphous Iron Oxide	200-350	Glegg, 1987; Crosby et al., 1983; Crosby, 1982; Borggaard, 1983.
Tamar Estuary Suspended Sediment	8-22	Glegg et al., 1987; Titley et al., 1987.
Gironde and Loire Estuaries Suspended Sediment	8-40*	Donard and Bourg, 1986; Martin et al., 1986.
Narragansett Bay Sediment	12.9	Nyffeler et al., 1984
San Clemente Basin Sediment	10.0	Nyffeler et al., 1984

*Ar gas used.
Table 1.2
Surface areas of Fe oxides and sediments from this laboratory and from the literature.

Use of the gas adsorption technique on solids also yields qualitative and quantitative information about the porosity of the surface which would not be obtainable from the wet solid and it is also possible to investigate the role of surface coatings (especially organics and hydrous metal oxides) on surface area (Glegg et al., 1987; Titley et al., 1987; Martin et al., 1986).

Investigation of the porosity of the particle surfaces is a key factor in understanding the adsorptive properties of particles (Glegg, 1987; Rasmuson, 1986). Additionally the gas sorption data can be used to obtained pore size distributions within the particles (Lippens et al., 1964; Cranston and Inkley, 1957). These features have been implicated in the so-called two stage uptake mechanism often observed during sorption experiments (see Figure 1.3).

Work with soils has shown the importance of both the pore size
distributions and the pore shapes on adsorption of ions from
solution especially dissolved phosphate (Bolan, 1985; Madrid and De
Arambarri, 1985; Barrow, 1983). However investigation of these
mechanisms in the estuarine situation has only recently started
(Glegg, 1987; Li et al ., 1984a). The importance of porosity in
adsorption mechanisms was shown using synthetic Fe and Mn oxides and
dissolved phosphate. Phosphate was strongly adsorbed by the
amorphous Fe oxides, but uptake was reduced when the amorphous
surface became more crystalline and lost both surface area
and porosity (Crosby, et al., 1984; 1983; Crosby, 1982; Crosby et
al., 1981). Other work showed that dissolved phosphate may become
incorporated in the coagulation products of goethite particles
(Anderson et al., 1985). The high degree of association of both
trace metals and nutrients with hydrous metal oxides supports
observed sorptive behaviour of phosphate and trace metals (Loring,
1982; Luoma and Brian, 1981; Tessier et al., 1980). The uptake of
dissolved phosphate onto estuarine particles may be important as the
"Dissolved Transport Index" determined by Martin and Maybeck (1981)
from an analysis of World Rivers showed that only 1-10% of phosphate
is transported in the dissolved phase. Thus, estuarine transport of
phosphorus occurs in the particulate phase. It is essential to know
where the phosphate ions are located on particles and their
aggregates and what proportion of the phosphate is biologically
available.

Work by Lijklema (1980), showed that the adsorption of phosphate on
Fe oxides exhibits a hysteresis effect with reduced desorption of
phosphate back into solution following the initial adsorption

27

process. This is thought to be related to the diffusion of phosphate ions into the internal spaces within the particles, the delayed desorption occurring as phosphate diffused out of the pores. Madrid and De Arambarri (1985) showed that the uptake of phosphate from solution onto Fe mineral phases was controlled by the accessibility of surface sites and the occurrence of microporosity into which phosphate ions could diffuse during the 'slow' continuing uptake phase as shown in the reaction scheme in Figure 1.3. Thus microscale surface features on particles in estuaries are likely to be of importance in the biogeochemical cycling of phosphate.

1.4 ESTUARINE ENVIRONMENTS STUDIED.

The surface properties of natural particles from three estuarine environments were investigated. The estuaries chosen for major investigation were the Tamar and Restronguet Creek, both in South West England. In addition, particles from the Fe rich Keithing Burn and from the Mersey Estuary were also examined.

1.4.1 THE TAMAR ESTUARY

1.4.1.1. Background

The Tamar Estuary is a drowned river valley or "ria" (Pritchard, 1967) in the south west of England. It rises at Alfardisworthy on the North Coast of Cornwall (see Figure 1.4) and runs south to Plymouth. The River and Estuary is 100 km in length of which 32 km is tidal, and the extreme limit of the tidal intrusion reaches Weir Head at Gunnislake. The catchment of the Tamar River is about 917 km^2, of this most is agricultural land with low population density. Industrial discharges to the system are limited to run-off from farmland (fertilizers and occasional silage spills) and discharges of domestic wastes, mainly sewage. The latter predominate around the City of Plymouth (Population $\approx$ 250,000) which is sited at the mouth of the Estuary and this urban area is responsible for some limited industrial discharges. The Tamar Valley is "mineralized" and there is a history of mining in the area which generated spoil heaps containing heavy metals. These are still very much apparent around the upper reaches of the Estuary.

The Tamar Estuary has two main tributaries, the Tavy and Lynher

29

N

**Atlantic
Ocean**

River Tamar

Devon

Gunnislake

Tavy

Lynher

Cornwall

Plymouth

**English
Channel**

0   8   16

scale km
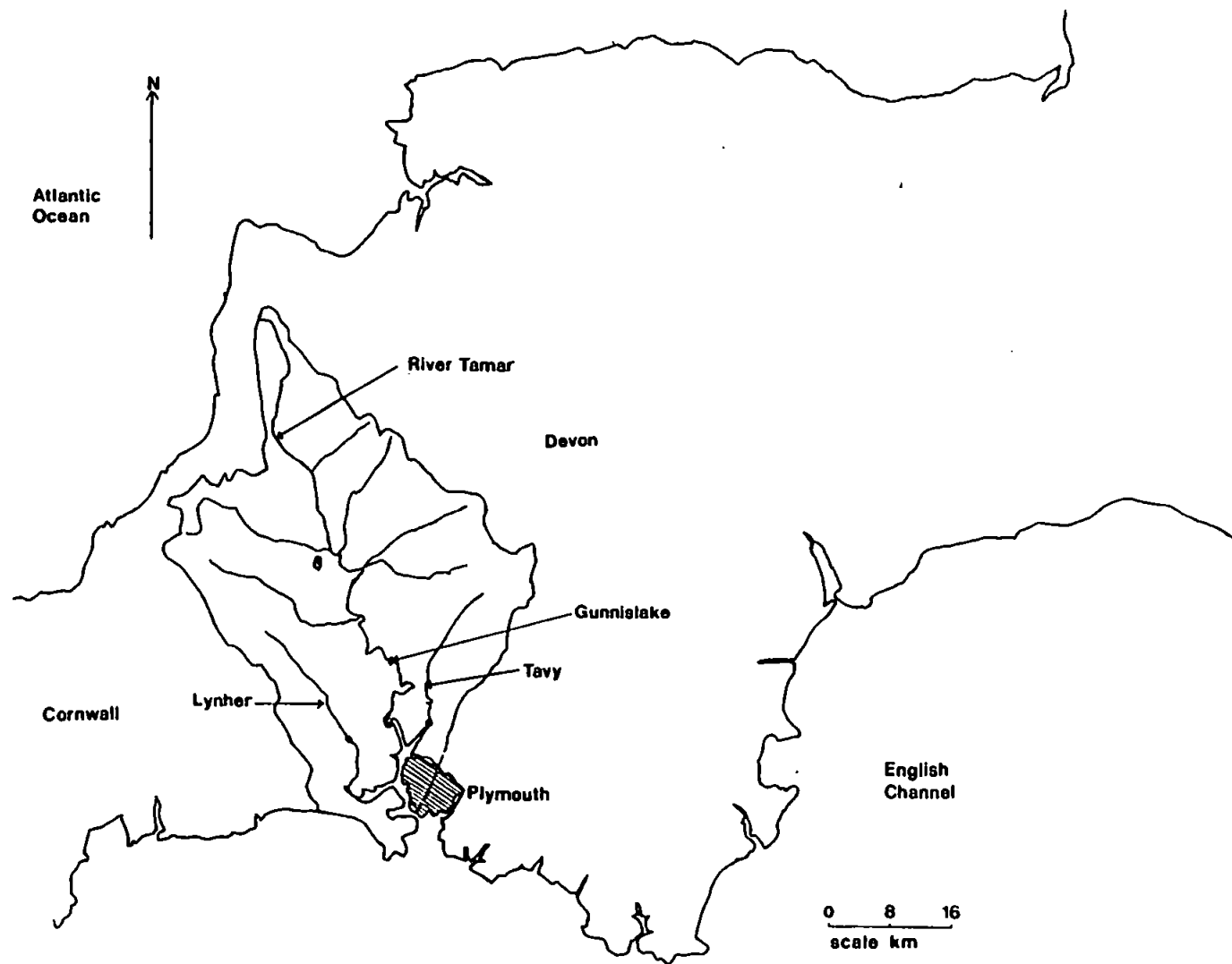
Figure 1.4. The Tamar Estuary, River and Catchment Area.

Rivers which drain into the Estuary from the east and west sides
respectively (Figure 1.4). These two tributaries each make
contributions of about 20-30% of the flow of the Tamar River itself
(Uncles *et al.*, 1983). Both of these tributaries drain mainly
agricultural land although their subcatchments are mainly higher
moorland. Thus much of the natural run-off contributing to the
fresh water discharge first passes through acidic peaty soils and
will carry an abundance of dissolved humics and complexed trace
metals. All the main rivers within the catchment are described as
"clean" by South West Water and therefore have potential as sources
of water supply. The principal hydrodynamic features of the Tamar
Estuary are shown in Table 1.3.

Annual Rainfall in Catchment 1985-1987 (mm)	River Discharge (Weir Head) 1985-1987 (m^3/s)	Tidal Ranges Neap-Spring (m)	Flushing Time (Whole Estuary) (Days)
1000-1200	5-300 (Mean 21.3)	2.2-5.5	7-12

Table 1.3
Important hydrodynamic parameters in the Tamar Estuary.

The catchment is characterised by high rainfall which produces a
quick response in river flow, with short lived peak discharges
exceeding 300 m^3/s. This highly variable discharge has a
substantial effect on the flushing time of the estuary especially in
winter when high flows reduce the flushing time.

1.4.1.2 Geochemical Characteristics of the Tamar Estuary.

Over the past two decades the Tamar Estuary has been characterised
in terms of hydrodynamic and chemical behaviour and these have been

interlinked (Morris *et al.*, 1986). Hydrodynamically, the Estuary is partially to well mixed, with the majority of the estuarine transect being partially mixed (Uncles *et al.*, 1985). Tidal behaviour within the estuary is asymmetric especially in the upper reaches where frictional effects between the in flowing tide and the bed are at their greatest (Uncles *et al.*, 1985; George, 1975). The flood tide is therefore of greater velocity but shorter duration than the ebb. This effect is of great significance for the mobilization and cycling of both suspended and bed sediments within the estuary as described in Section 1.2.2.

Bed sediments in the lower estuary (20-30 km below Weir Head) are typically intertidal mudflats which are well compacted and gently sloping. In the mid-estuarine region (8-20 km below Weir Head) the mud banks are steeper and the sediments more fluid and are susceptible to resuspension by tidal flow. The asymmetrical nature of the tidal currents in the Tamar Estuary especially the greater flood tide velocities result in extensive resuspension of these fluid mud banks to create a population of suspended particles that contribute to the turbidity maximum in the Estuary (Bale *et al.*, 1985).

Within the mid-estuarine zone and in the upper reaches of the Tamar Estuary, the tidal channel narrows and becomes canalized in parts and this causes a funnelling effect that increases both the tidal range and the current velocity. Dissipation of the tidal energy by friction with the estuarine bed encourages further resuspension of the more fluid bed sediments (Bale *et al.*, 1985; Allen *et al.*, 1980; Eisma *et al.*, 1978). In the Tamar Estuary a well developed

32

turbidity maximum is usually created during the spring tides when fresh water flow is low. Under these conditions tidal currents produce a net landward transport of sediments.

During late autumn and winter when run-off is much higher, sediments are transported back down estuary to localized depositional regions in the mid-estuary (Bale *et al.*, 1985). During the winter months, suspended solids from the river contribute substantial quantities of new material to the sediment budget. Materials passing through the low salinity region of the estuary from up estuary of the saline intrusion during the high runoff winter months comprise fresh riverine material and recycled estuarine sediment in the proportion 1:1.6 (Bale *et al.*, 1985).

The particle population within the Tamar Estuary is composed of crystalline solid phases such as quartz grains and iron oxides; haematite, lepidicrocite and goethite as well as a number of clay phases, especially kaolinite, muscovite, illite and chlorite (Glegg, 1987). These are supplied by the erosion of soils within the catchment and are therefore dependent on the underlying geology of the region. In addition to these lithogenous phases, runoff from the land brings detrital organic matter, especially small fragments of leaf matter, twigs and other remnants of vegetation. These solid phases are coated in the low salinity region of the estuary with flocculating colloidal species, especially Fe oxides and humic materials (Bale and Morris, 1981). *In situ* activity by bacteria can result in particle coatings of organic secretions or bacterial colonies themselves (Plummer *et al.*, 1987). Biological activity within the water column and mudbanks especially detrital feeding may

33

result in particles being repeatedly coated with mucus or cleaned of it. Thus the suspended particles are highly complex and variable in nature and are continually subject to modifying processes.

The occurrence of solid phases suspended in the water column especially in the chemically active low salinity region is of great importance for geochemical cycling, transport and retention of trace dissolved species. An appreciable proportion of Fe, Mn and other trace metals is scavenged by suspended particles in the high turbidity low salinity region of the Tamar Estuary (Ackroyd et al., 1986; Morris, 1986; Morris et al., 1986; Ackroyd, 1983; Morris et al., 1982b; Bale and Morris, 1981).

Assessment of the adsorptive capacity of particles in the water column for dissolved trace metals and nutrients is usually undertaken by selective chemical leaching procedures such as Tessier et al., (1980), or Chester and Hughes (1973) which give an idea of the trace metal content of the sediments. The geochemical composition of sediments from the Tamar Estuary are shown in Table 1.5.

Fe, mg/g	Mn, mg/g	Cu, mg/g	Zn, mg/g	As, mg/g	C, %*
21-49	0.1-1.5	0.2-0.55	0.22-0.6	0.03-0.24	4.7-7.5

*From Glegg, 1987.
Table 1.5.
Heavy metals and carbon content of sediments from the Tamar Estuary.
Samples digested with aqua regia/HF (Bland et al., 1982).

These approaches remove trace metals associated with various phases which are operationally defined; e.g loosely bound, bound to organics, bound to Fe and Mn oxides. However these approaches do not define the basic adsorptive processes that take place at the particle surface, and are far removed from the natural conditions of pH, and salinity. It is generally acknowledged that the basic sorption process takes place either through ion exchange or by complexation with OH groups on the particle surface (Olsen et al., 1982). However at present no systematic study of the sorptive capacity of particles in the water column has been undertaken. Furthermore the nature of the particle surface, such as surface area and surface roughness are also ignored in most particle sorption studies. The physical nature of the particle surface is also implicated in the sorptive process, as the dissolved species must diffuse from the surrounding water to the solid interface and then diffuse through the porous network of the aggregate before the sorption process itself can take place (Rasmuson, 1986).

Some evidence of intra-estuarine variability of the reactivity of particle surfaces in the Tamar Estuary has been reported (Bale and Morris, 1987; Bale et al., 1984). This work revealed a substantial decline in particle size in the turbidity maximum which is thought to be related to increased tidal shear forces in the high turbidity region causing disaggregation of particles. The decline in particle size suggests that the specific surface area of the particles should be larger giving them greater adsorptive capacity. However this is an indirect measure of the surface area of the particles and it does not provide any description of the nature of the particle surface.

Work by Titley *et al.*, (1987) showed that the BET surface area of
particles in the Tamar Estuary were in the range 8-22 m²/g.
Furthermore the surface areas of the particles showed a high degree
of intra-estuarine variability, and in addition much of the surface area
detected is located within pores of 1-30 nm diameter.

These results are similar to those observed by Martin *et al.*, (1986)
and Donard and Bourg (1986) in the Loire and Gironde estuaries (see
Table 1.2). The surface area values obtained are 2 orders of
magnitude higher than those calculated from particle size and are
thought to be related to the chemical composition of the sediment,
especially the relative abundance of Fe oxides and organic carbon
coatings. The latter have been implicated in controlling the
surface charge of particles in the water column and are thought to
be of importance in mediating the sorptive capacity of the particle
surface (Hunter and Liss, 1982).

Given the data already available for the Tamar Estuary, especially
with respect to the hydrodynamics, geochemistry, and particle
characteristics, this system is ideal for a study of particle
microstructures.

1.4.2. RESTRONGUET CREEK.

Restronguet Creek provides a contrasting environment to the
Tamar Estuary. It is located 50 miles West of the Tamar (see Figure
1.5) and drains into Carrick Roads which is a drowned valley.
The chemical characteristics of the system are dominated by high
inputs of Fe and other trace metals as a result of the highly
mineralized nature of the catchment. This area was extensively mined

36
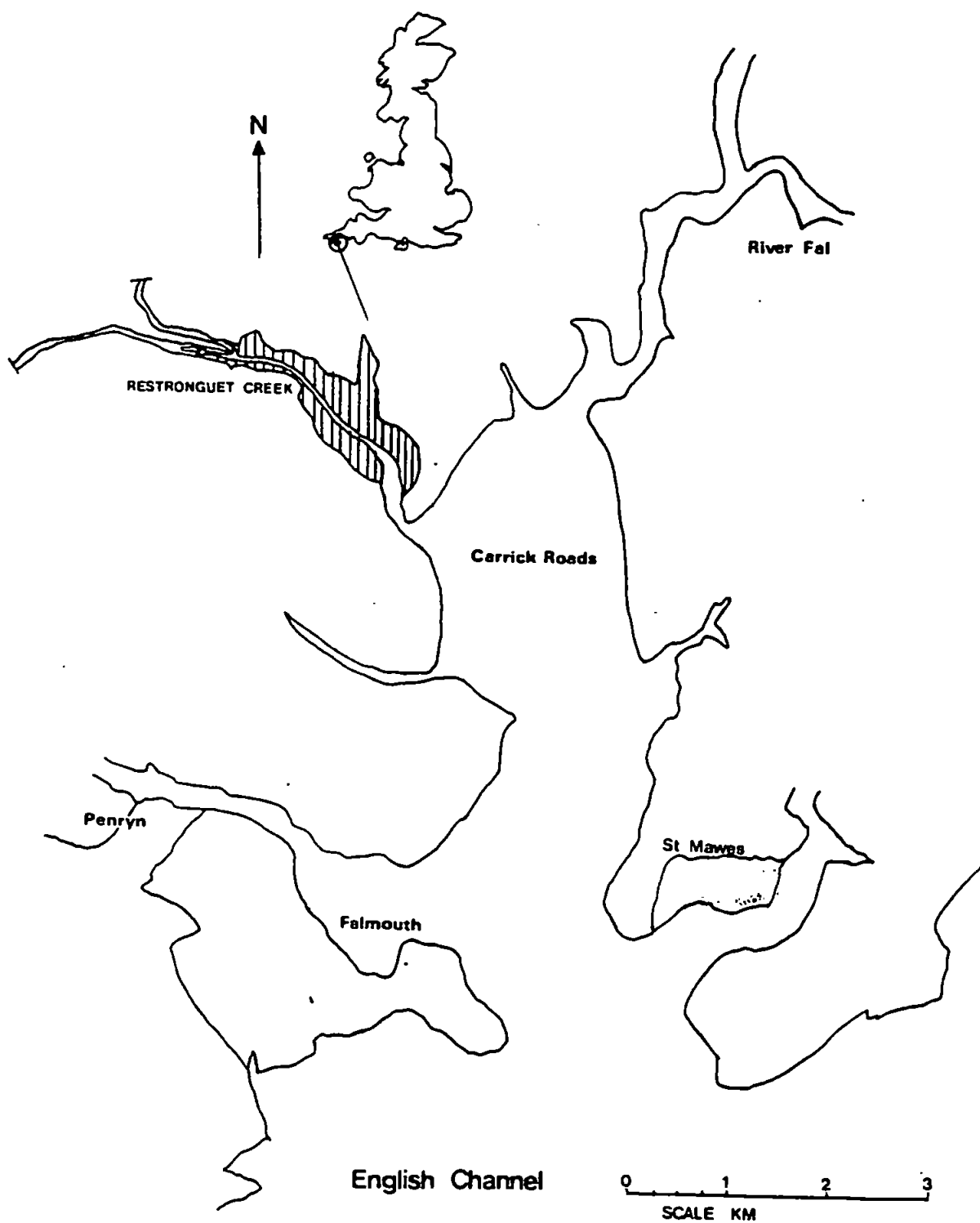
Figure 1.5. Location of Restronguet Creek.

Labels within figure: N, River Fal, RESTRONGUET CREEK, Carrick Roads, Penryn, St Mawes, Falmouth, English Channel, SCALE KM, 0, 1, 2, 3

in the past and acid mine streams contribute to the total flow of
the Carnon River. As a result the river system has an unusually low
pH (occasionally <4) and low carbon content (1-2%)(Johnson *et al.*,
1986; Millward and Marsh, 1986). The principal features of this
system are shown in Table 1.6.

River Carnon			Restronguet Creek		
River Flow m³/s	Fe, mg/l	Total Organic Carbon mg/l	Fe, mg/g	Cu, mg/g	As, mg/g
0.5-2.0	21.2	2.0	Upto 150	Upto 40	Upto 30

Table 1.5
Hydrodynamic and chemical features of the Carnon River and its
estuary (Johnson, 1986).

The river flow is about 10 times less than the Tamar and the
estuary itself is 1/6 the length of the Tamar Estuary. The river
waters brings approximately 3000 kg of Fe per day into the estuary
and the sediments in the system are orange from precipitated Fe
oxyhydroxides. Such oxides provide a relatively abundant surface
area for adsorption processes (Johnson, 1986).

1.5. AIMS OF PRESENT WORK

The overall aim of this work is to investigate the surface areas and porosities of suspended solids and sediments from U.K estuaries, (mainly the Tamar Estuary and Restronguet Creek) and to undertake inter and intra-estuarine comparisons of the results. Investigation of composition and its relationship to the microstructural features was also undertaken, and the influence that the surface morphology of the particles has on the sorptive behaviour of dissolved phosphate was investigated.

The objectives of the study were as follows:

1) To develop a suitable preparation technique capable of examining particle microstructures with minimum disruption to the particle matrix.

2) To determine the reproducibility of the technique on a range of solids and to compare the results with those from other laboratories to assess whether the technique is suitable for making comparisons between samples.

3) To collect samples from the whole hydrodynamic regimes of the estuaries and to carry out microstructural examination of the solids.

4) To determine the carbon and non-detrital Fe and Mn contents of the estuarine particulate matter in an attempt to isolate the phases reponsible for the microstructural features of the surfaces.

5) To investigate the sorptive behaviour of dissolved inorganic

phosphate using natural particles and natural and simplified media, as a function of salinity, turbidity and initial phosphate concentrations.

6) To develop a conceptual model of the variability of the particle microstructures and the chemical reactivity of the particles in estuarine systems.

CHAPTER TWO

TECHNIQUES AND METHOD DEVELOPMENT

This chapter gives details of the apparatus and methods used to study the surface areas and porosities of estuarine particle surfaces. The approach taken to model the sorptive behaviour of dissolved phosphate under simulated natural conditions is also described.

Throughout this chapter and the rest of the work extensive references will be made to "surface area" measurements determined by two methods:

(i)Brunauer, Emmett and Teller (1938), abbreviated to BET;
and

(ii)Cranston and Inkley (1957), abbreviated to C&I.

Both measures of surface area yield method specific results (as opposed to an absolute measure) which depend on the sample preparation, the adsorbate gas used and the theory applied. Therefore throughout the text the term "surface area" will refer to a BET determined "specific surface area" (using nitrogen gas at 77°K) unless otherwise stated.

The chapter is divided into four main sections: 1) The methods used for microstructural examination of estuarine particles; 2) Sample collection and preparation; 3) The methods used to investigate the role of particle coatings on particle microstructure and 4) The methods used to model the sorption behaviour of dissolved phosphate.

2.1 MICROSTRUCTURAL EXAMINATION OF ESTUARINE PARTICLES

2.1.1 NITROGEN GAS SORPTION STUDIES

2.1.1.1 The Vacuum Microbalance

The apparatus used for determining surface areas and porosities was the gas sorption balance constructed in 1974 and described by Carter (1983). The system utilises a CI Microforce Microbalance (Mark 2C) from CI Electronics Ltd, with a maximum weighing capacity of 1g and repeatability of ±0.5 µg. The balance head consists of an electronic bridge circuit maintained in continuous balance by a servo system enclosed within a vacuum flask designed to work at pressures down to 10^{-6}Torr. The balance arm carries a shutter which is positioned between a lamp and two silicon photocells. The shutter blocks the light until a change in weight on the arm causes a movement affecting the relative illumination of the photocells which induces a weight proportional current. As a result the apparatus has a rapid response (<100ms) and is very sensitive to slight weight changes (0.5%), but insensitive to external vibration. Electrical output from the balance is fed to a compatible CI Instruments analog control unit with five weight ranges selected by direct switching. Stabilized power supply and electronic tare (uncalibrated) are included. The analog unit has weight ranges: 0-1 mg, 0-2.5 mg, 0-10 mg, 0-25 mg, and 0-100 mg and the first three ranges were the most frequently used. The balance head vacuum unit was attached by taps and glass tubing to a two stage rotary pump, a mercury manometer and a gas reservoir and cylinder. Figure 2.1 shows the complete vacuum system arrangement. The experimental procedure on the apparatus was

42

Mercury
Manometer

Optical Balance

To pump

Dosimeter

Dewar Flask

Dewar Flask

Cold Trap

Gas Reservoir
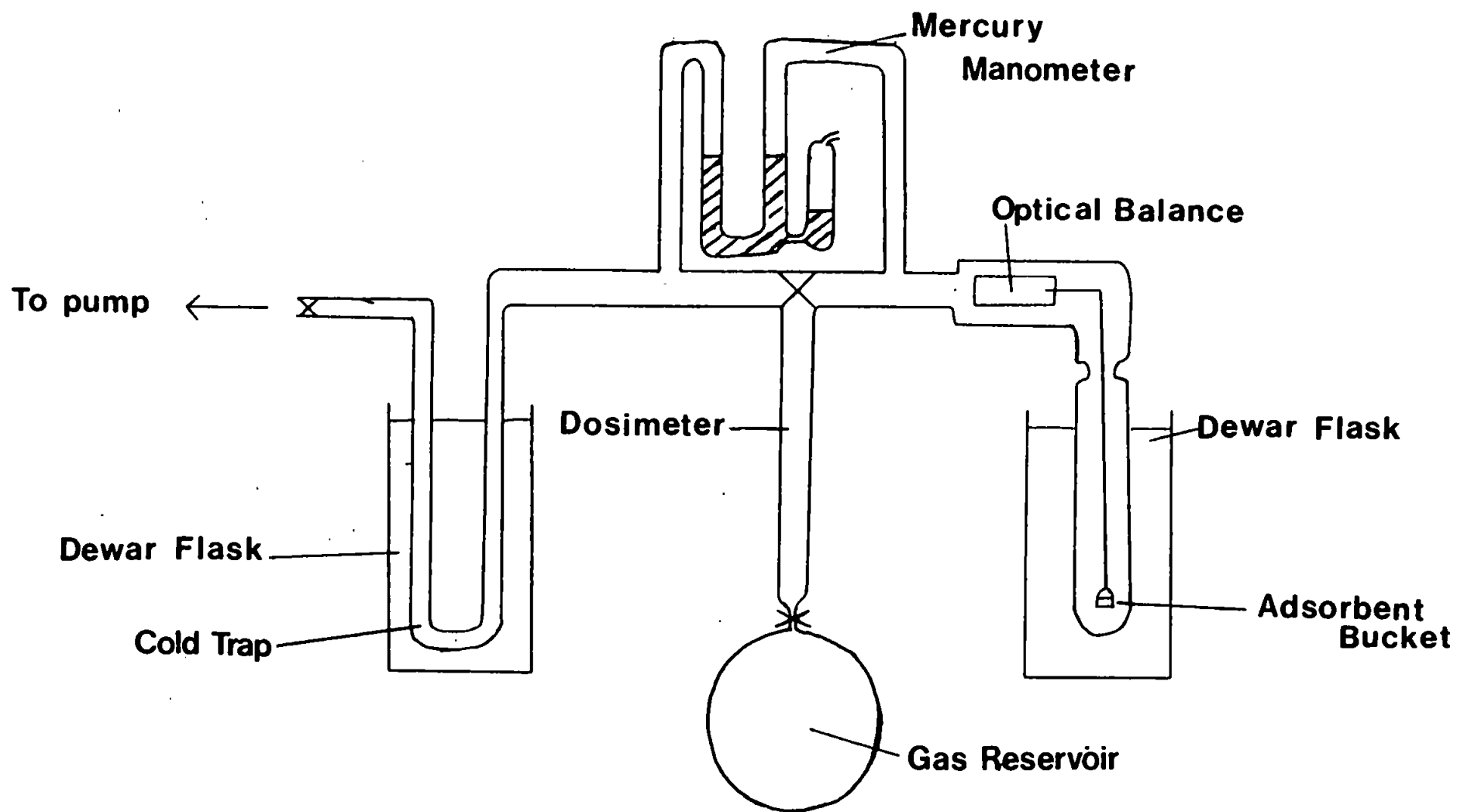
Adsorbent
Bucket

Figure 2.1: Main components of the vacuum microbalance system.

as follows:

Approximately 0.2g of sample was weighed out into the adsorbent bucket, and suspended from the optical balance by a 27 cm long fine Pyrex fibre. The apparatus was then sealed and evacuated using a two stage pump to a pressure of 10^{-3}Torr. Degassing of the sample (i.e. loss of adsorbed moisture and volatiles) registered as a weight loss over time. Degassing was encouraged by immersing the cold trap in a Dewar flask of liquid nitrogen (see Figure 2.1). Outgassing continued until the observed weight-loss became minimal; (usually between 0.5 and 5h). True sample weight (i.e. less weight lost on outgassing) was noted; the balance zero set and the adsorbent bucket (with sample) was immersed in a Dewar flask of liquid nitrogen such that the bucket was at least 15 cm below the coolant surface thereby keeping sample temperature at 77-78°K (Glasson and Linstead-Smith, 1973).

For BET surface area determinations (up to relative pressure $P/P_0=0.3$), "White Spot" nitrogen gas (>99.9% pure, Air Products) was allowed into the balance in doses of 30-50 mmHg and the system allowed to attain equilibrium, after which partial pressure of nitrogen and gravimetric uptake were recorded. At least five readings in the BET region were taken; but once above the BET range i.e. $P/P_0>0.3$, gas dosing of the sample was undertaken with steps of 50-100 mmHg. Equilibrium was established at each point (0.5 to 2h) and the end point was reached at the apparatus limit - about $P/P_0=0.96$. Desorption then proceeded in similar steps with a maximum of ten readings being taken and observed equilibrium times of up to 2h. Corrections for buoyancy effects on the sample, the adsorbent bucket, microbalance beam and Pyrex fibre (and

counterweights when used) were included in the BET surface area

calculation as described in the following section.

2.1.1.2 Surface Area Theory

When a disperse solid is exposed in a closed space to a gas or

vapour at a definite pressure, the solid begins to adsorb the gas.

The amount of gas adsorbed onto the solid will depend on the

pressure, temperature and the nature of the gas as well as the

character of the solid surface and the adsorption process taking

place i.e. chemisorption, physisorption or a combination of the two.

Gas adsorption isotherms on solid surfaces can be obtained (Figure

2.2) and interpreted to give qualitative and quantitative

information about the solid surface (Gregg and Sing, 1982). Five

types of adsorption isotherm were initially identified by Brunauer,

Deming, Deming and Teller (1940), now more often referred to as the

BET classification (Brunauer et al., 1938). These different

adsorption isotherms types (e.g. Figure 2.2) can be interpreted to

obtain a surface area measurement by use of available theory, such as

the BET model (equation 2.1).

$$\frac{p}{q(p_0-p)} = \frac{1}{X_mC} + \frac{C-1}{X_mC}.\frac{p}{p_0} \qquad \text{Equation 2.1}$$

where   q = mass of adsorbate/unit mass of sample;
        p = pressure of adsorbate gas;
        p_0= saturation pressure of adsorbate gas;
        C = energy constant, dependent on the nature of the
            adsorbate-adsorbent system;
        X_m= monolayer capacity (mg adsorbate/g sample).

This equation is an extension of Langmuir's interpretation to include

multilayer adsorption (Gregg and Sing, 1982), and provides a method
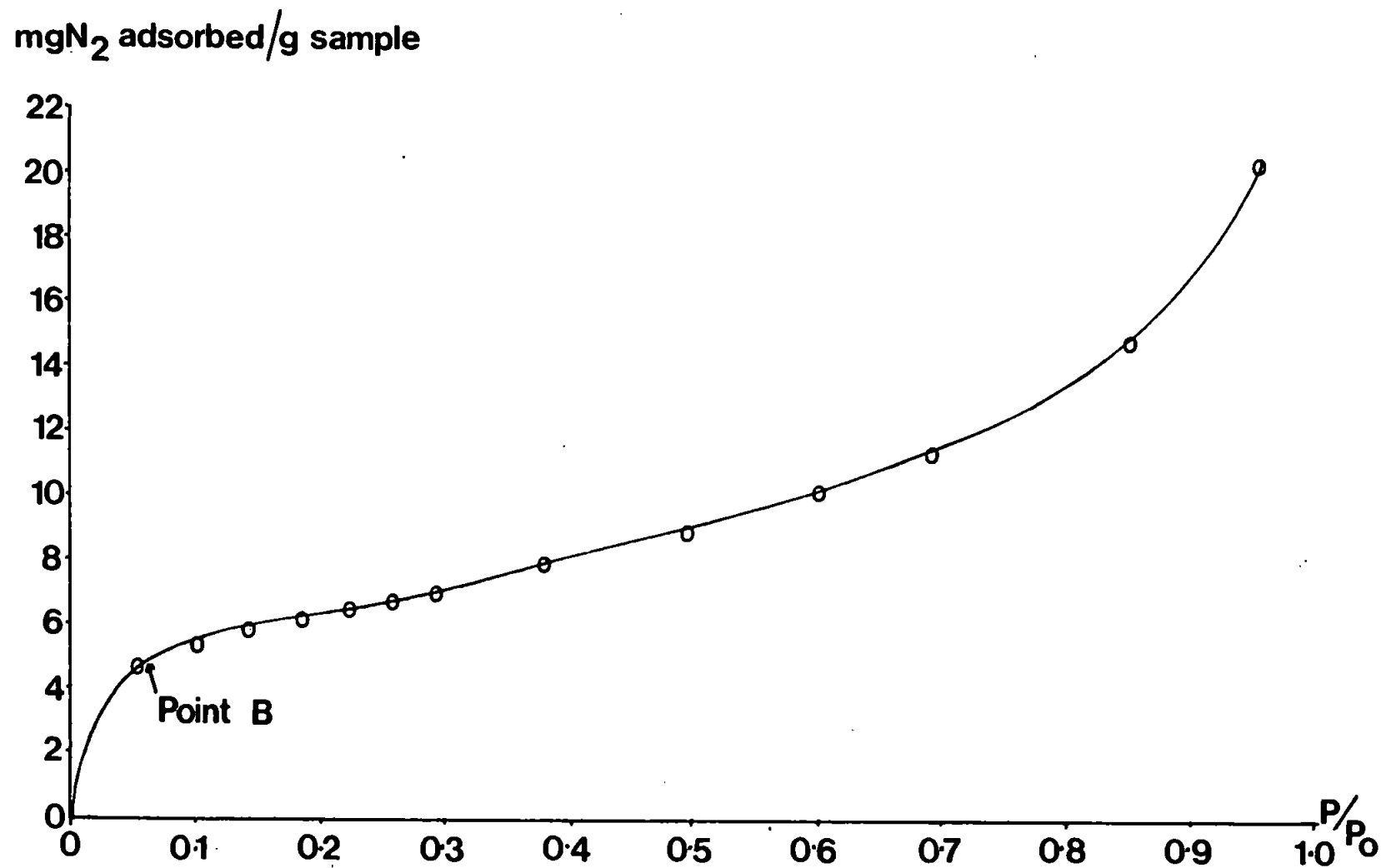
Figure 2.2: Typical N_2 gas adsorption isotherm obtained on Tamar Estuary sediment. The approximate region of point B is shown.

of calculating the monolayer capacity (X_m) which is defined as the quantity of adsorbate which can be accommodated in a completely filled single layer of molecules on the adsorbate surface. The monolayer capacity is proportional to the surface area of the particle surface, and therefore the BET model can be used to obtain a specific surface area measurement. The method however includes a number of important simplifying assumptions, which are detailed in the literature (Mikhail and Robens, 1983; Adamson, 1976) and these may limit the application of this model.

Nonetheless the BET technique is a widely used practical method of measuring surface area; and using nitrogen as the adsorbate is accepted as a standard technique (Adamson, 1976; Ponec *et al.*, 1974). If the data are plotted as $P/q(P-P_0)$ against P/P_0 (see Figure 2.3) the graph will have a slope of $\frac{C-1}{X_mC}$ and an intercept of $\frac{1}{X_mC}$. It can be shown that:

$$\frac{1}{X_m} = \frac{C-1}{X_m} + \frac{1}{X_mC} \qquad \text{Equation 2.2}$$

Therefore using the two values obtained; X_m may be calculated. Adsorption specific surface area (S_A)(in m^2/g) is related to X_m by the equation:

$$S_A = \frac{X_m \cdot N_A \cdot A_m \cdot 10^{-15}}{M_r} \qquad \text{Equation 2.3}$$

where M_r = relative molecular mass
        N_A = Avagadro's constant
        A_m = area occupied by one adsorbate molecule.

The A_m value for nitrogen gas that gives a consistent surface area for a range of solids is 0.162 nm^2 (Adamson, 1976). This value is close to that calculated from the liquid density of nitrogen at
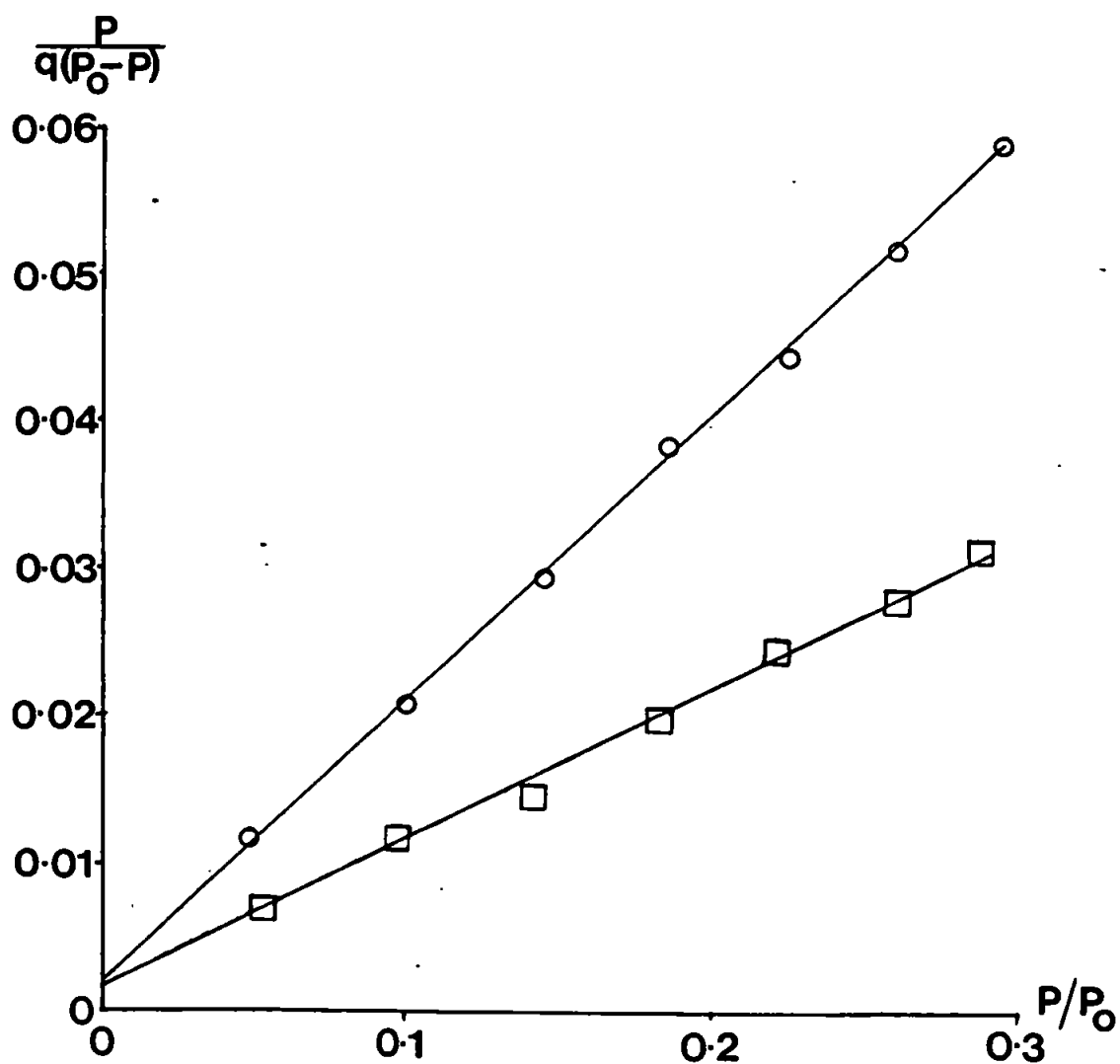
Figure 2.3: A plot of P/q(P$_0$-P) versus P/P$_0$ for determination of BET surface area.

(□): Restronguet Creek sediment, surface area 32.8 m^2/g.

(○): Tamar Estuary sediment, surface area 17.8 m^2/g.

its boiling point, which improves the validity of the A_m value estimate at the sample temperature (77°K). Substituting the values for M_r, N_A and A_m into equation 2.3, yields equation 2.4 which can be used to calculate the BET surface area (m²/g).

$$S_A = 3.485 \cdot X_m \qquad \text{Equation 2.4}$$

The data obtained on samples using the vacuum microbalance (described in Section 2.1.1.1) were plotted as shown in Figure 2.3, and linear regression analysis of the data was carried out on the Prime 950 mainframe computer, using the Minitab statistical package. For all data sets the least square regression values exceeded 90%; (usually >98%) showing the good linearity of the data in the BET range of partial pressures (0.05-0.3)(Figure 2.3). The adsorption energy constant "C" may also be calculated from the monolayer capacity and the intercept for inclusion with BET surface area results (Sing, 1982). The intercept on the "y" axis is usually small (<0.01) and slight changes in the absolute value produces widely varying values of "C" – usually in the range 10-100. Values of "C" in this range and the satisfactory application of the BET model up to $P/P_0=0.3$ corresponds to surface coverages of between one and two layers of nitrogen (Mikhail and Robens, 1983). The application of this method on dried estuarine samples will be discussed in Section 2.2.2.

2.1.1.3 Investigations of Particle Porosity

While surface area is determined upto partial pressures of 0.3, full adsorption/desorption isotherms with hysteresis loops enable porosity characteristics to be evaluated (Gregg and Sing, 1982).

The surfaces of all particles feature roughness and porosity to some degree, and these surface irregularities can be detected by characteristic gas adsorption isotherms at low temperatures. The five main types of adsorption isotherms have been identified by the BET classification (see Figure 2.4), and reveal qualitative information about the particle surfaces. These isotherms can be augmented by observing the desorption of gas from the solid surface. A characteristic hysteresis effect is frequently observed, where for some or all of the isotherm the desorption limb remains higher than the adsorption limb. The shape and the opening and closure of the hysteresis loop provides some assessment of pore shapes and size distributions. The forms that the hysteresis loops take can be divided into two broad categories; those where the desorption branch rejoins the adsorption limb at some lower pressure; and an open loop where a measurable amount of gas is irreversibly adsorbed, as shown in Figure 2.5 (Mikhail and Robens, 1983). Hysteresis loops and gas adsorption isoterms reveal qualitative and semi-quantitative information about pore sizes and shapes; and have led to the IUPAC classification of pore sizes (Gregg and Sing, 1982):

Micropores $<2nm$ diameter
Mesopores $2-50nm$ diameter
Macropores $>50nm$ diameter

Most solid surfaces would be expected to have pores in all these size ranges with a variety of shapes. During the adsorption phase, the isotherms produced depend on the filling of micropores; followed by multilayer adsorption and the more gradual filling of meso and macropores with capillary condensation of the adsorbing gas within some pores. Refining of the qualitative descriptions of porosity
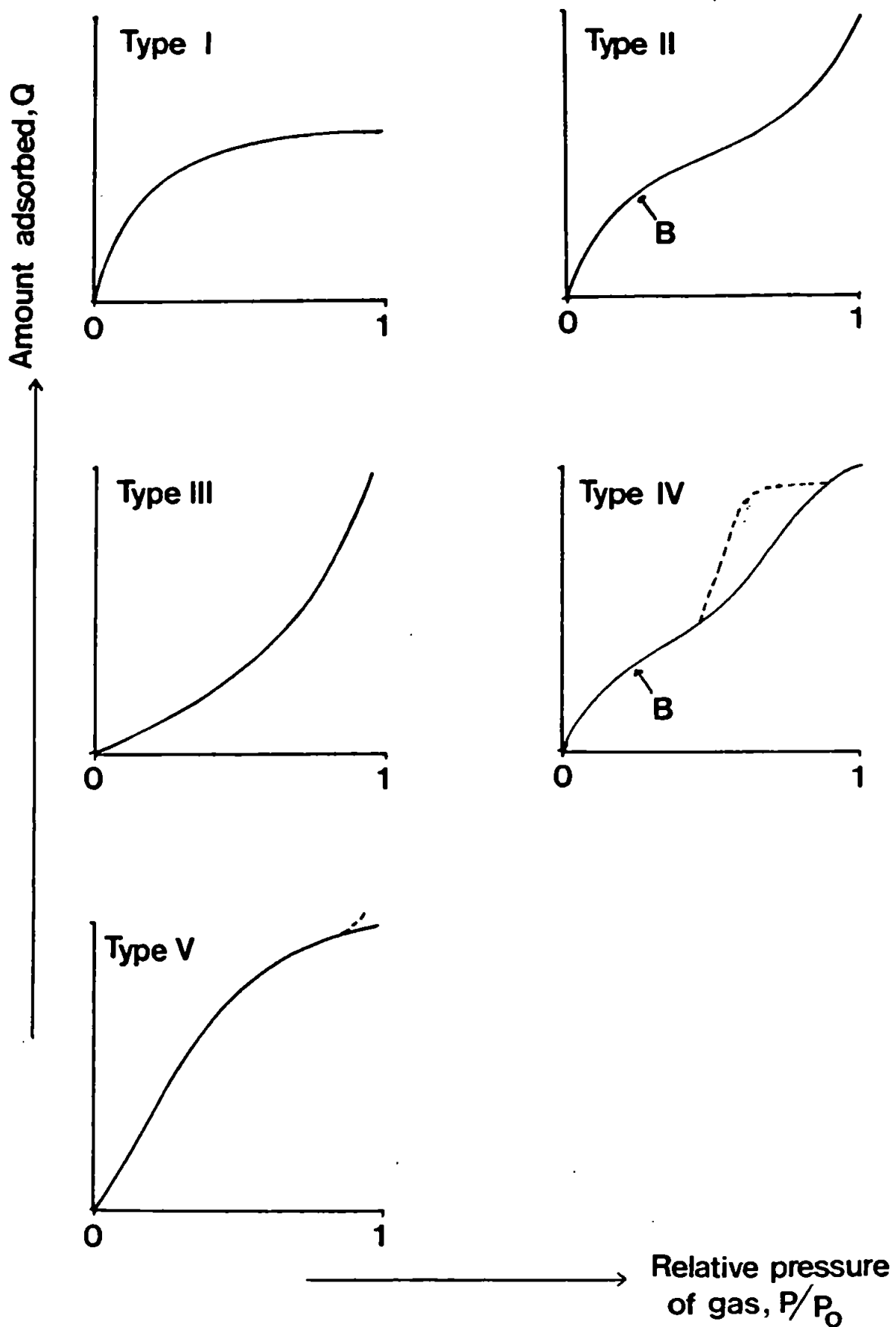
Figure 2.4: The five types of adsorption isotherms identified by Brunauer, Deming, Deming and Teller (1940). Estuarine solids are type II.
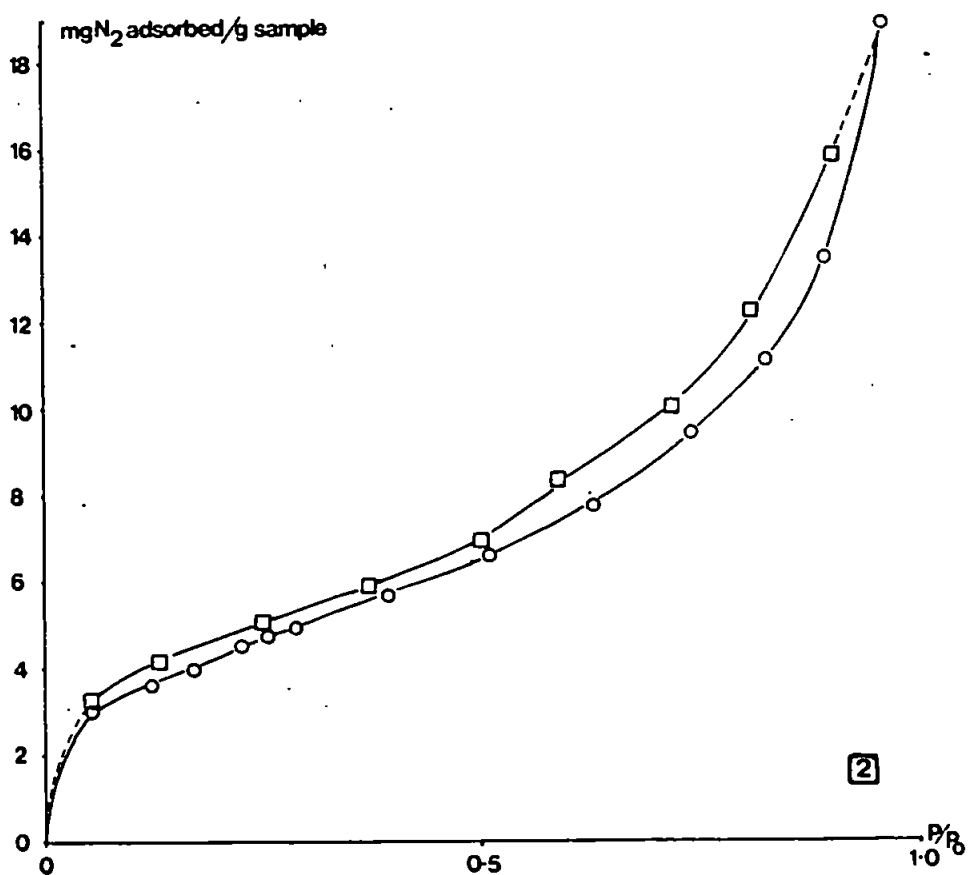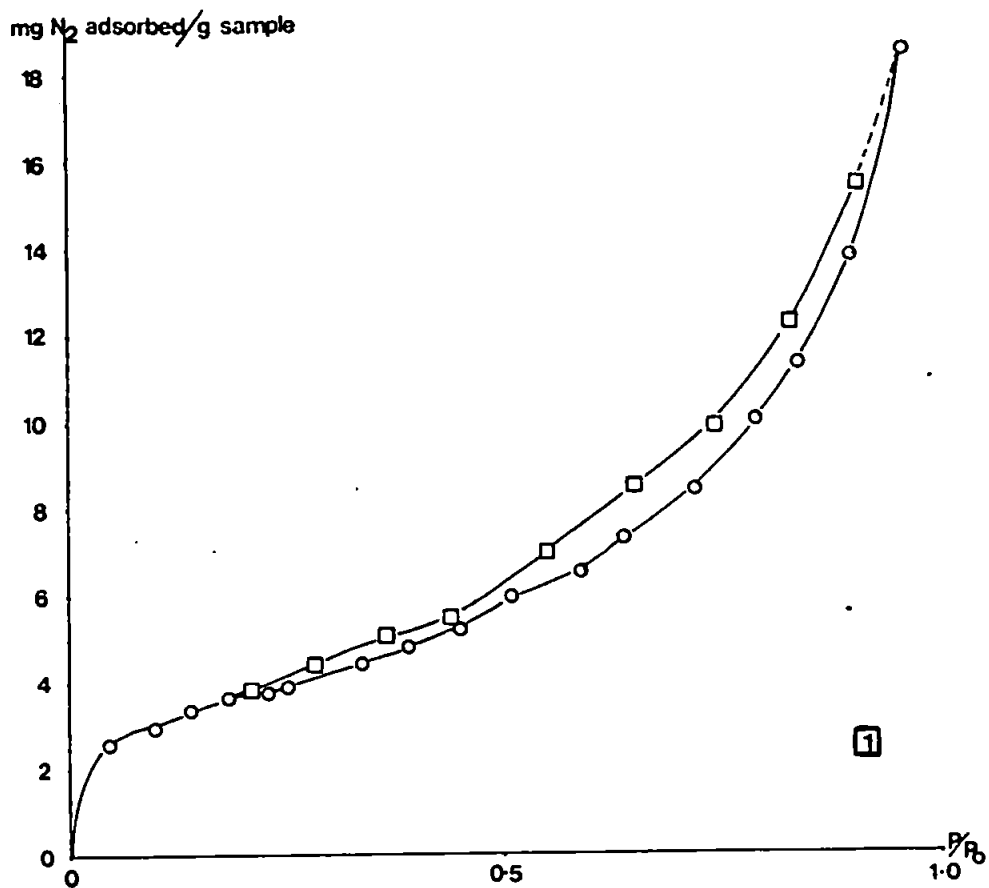
Figure 2.5: Two main hysteresis loop types. 1) Desorption branch rejoins
adsorption limb at low pressure. 2) Open loop.
Suspended solids from Tamar Estuary.

52

provided by the hysteresis loops is possible by use of the Kelvin equation:

$$Ln(P/P_0) = -[(2Vj/rRT)] \qquad \text{Equation 2.5}$$

where V = molar volume of adsorbing gas
       j = surface tension of the condensed gas
       r = pore radius
       R = universal gas constant
       T = temperature in °K

Taking V as 34.68 cm^3/mol; and j as 8.72*10^{-7} J/cm^2 (values for nitrogen at 77°K) allows pore radii to be calculated, an example is shown in Figure 2.6 (Gregg and Sing, 1982). De Boer (1958) and Barrer *et al.*, (1956) devised qualitative descriptions of pore shapes to fit the hysteresis loop types observed (Figure 2.7) and in this study both methods are used to obtain qualitative and semi quantitative information on the porosity of the particle surfaces. Many samples in this study exhibited open loop hysteresis curves where some nitrogen gas was adsorbed irreversibly e.g. Figure 2.8. These are generally ascribed either to nitrogen molecules becoming strongly held in micropores with similar radii to the molecules themselves (0.2-0.4 nm) or to irreversible changes in the solid adsorbent itself, such as swelling of flexible reticules caused by the penetrating nitrogen adsorbate molecules. The qualitative data obtained on particle microstructures using the methods described can be supplimented by quantitative information on porosity, using the Cranston and Inkley (1957) method for determining pore structures. This method yields pore size distributions, and specific surface area data largely independent of BET measurements. Furthermore the method can be applied to either the adsorption
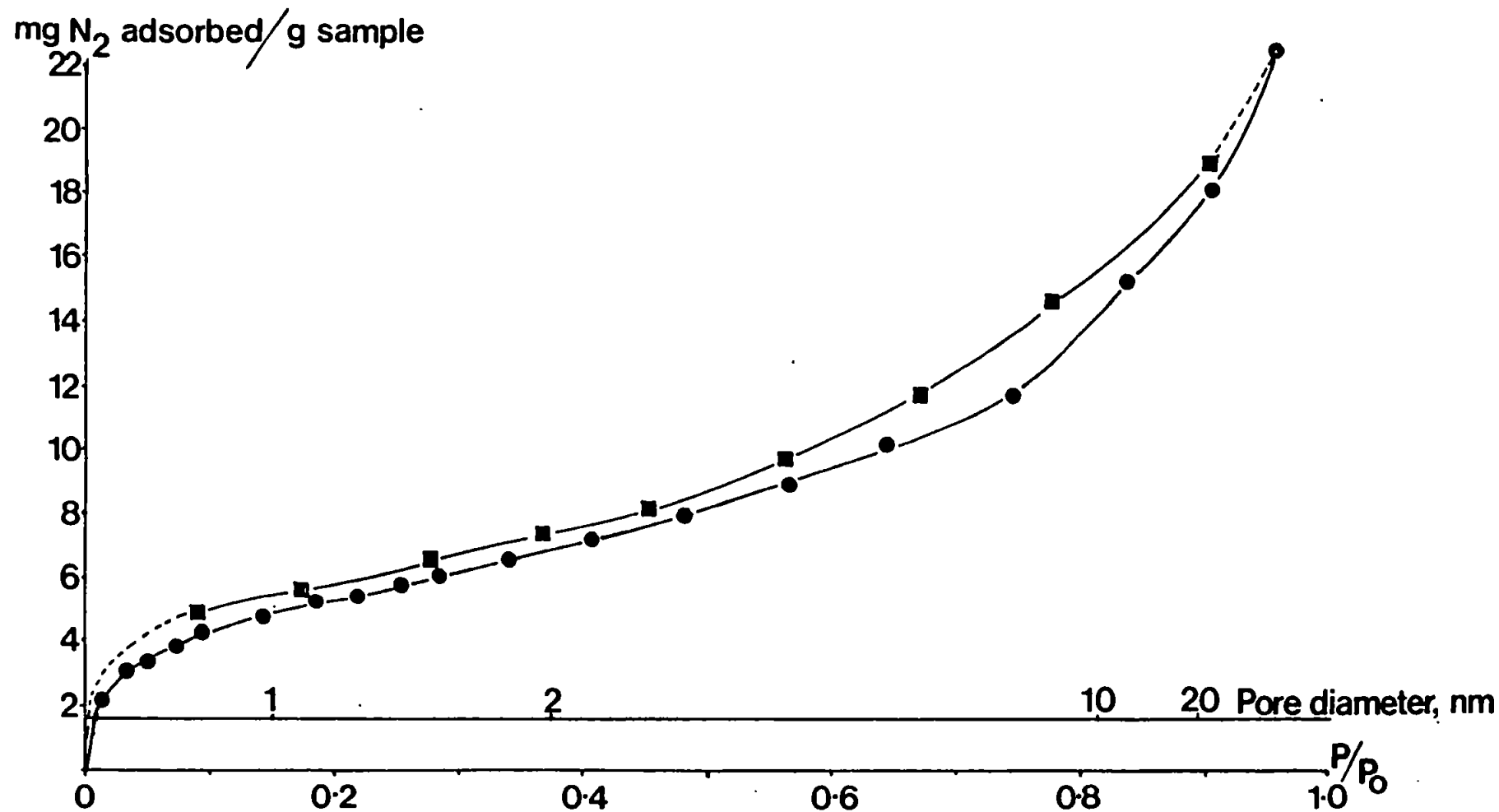
Figure 2.6: Full adsorption/desorption isotherm showing hysteresis loop for a Tamar Estuary sediment. Pore diameters calculated using the Kelvin equation (section 2.1.1.3.) are shown. ●-Adsorption;■-Desorption.
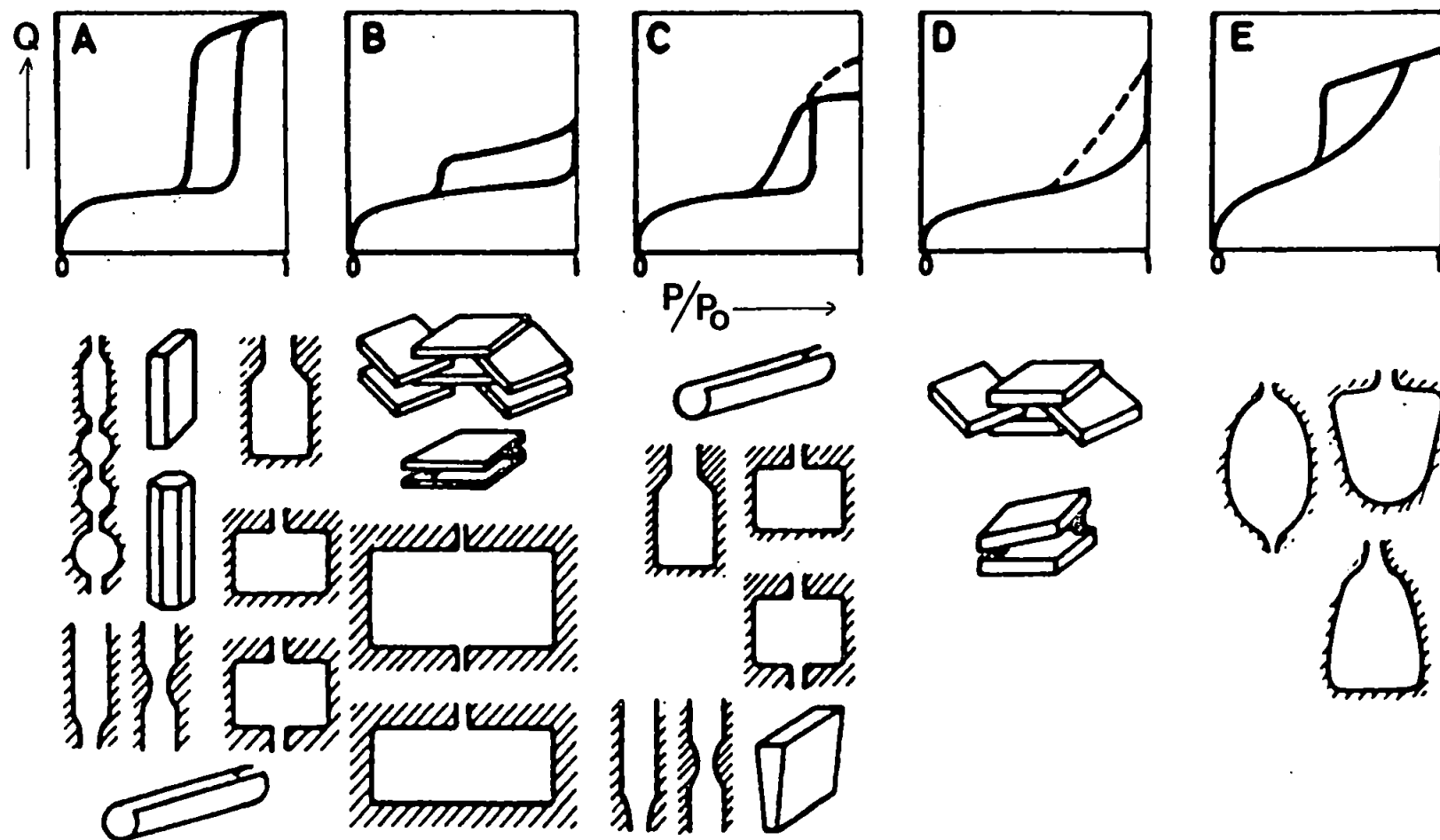
Figure 2.7: Types of isotherms for porous materials (de Boer 1958). Types A,B, and E are the most important. Type A: mostly cylindrical, both ends open; type B: mostly slit shaped; type E: "ink bottle".
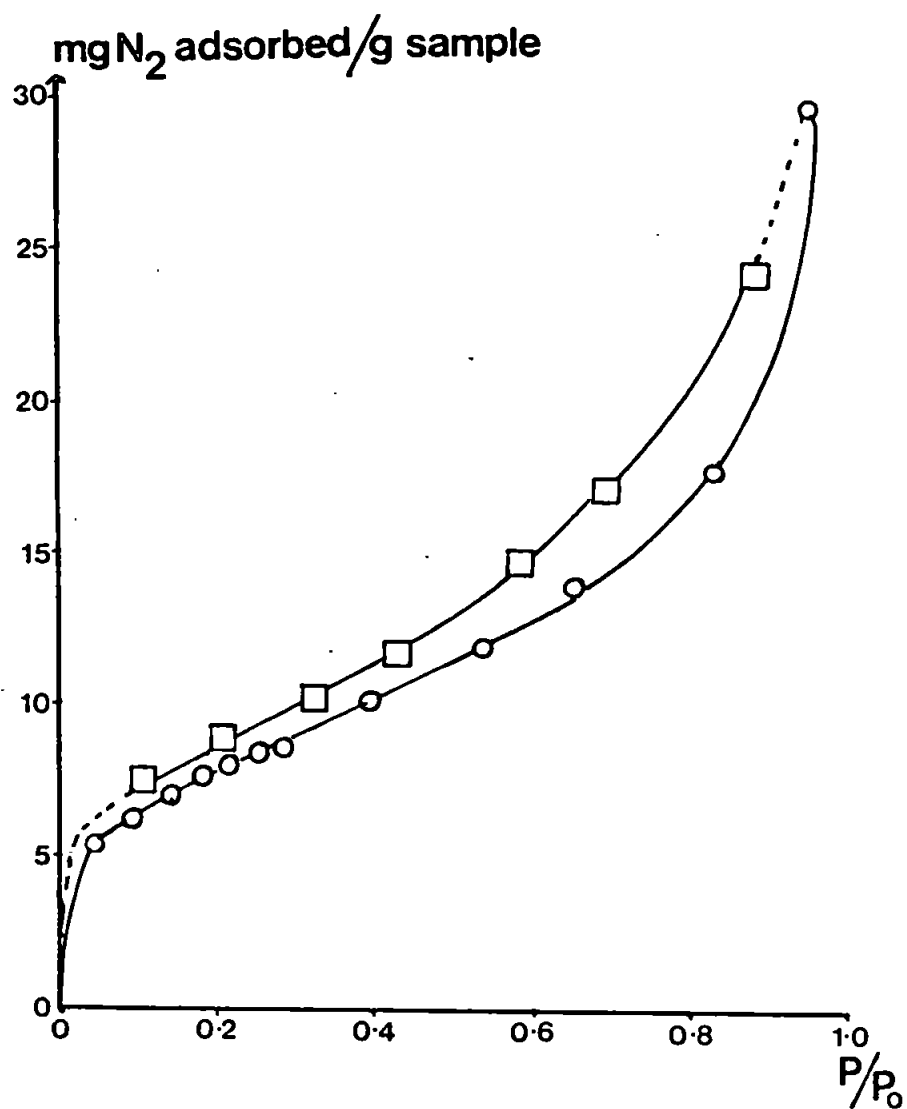
Figure 2.8: Open hysteresis loop indicating the presence of micropores.
Restronguet Creek sediment sample. O-Adsorption; □-desorption.

or desorption branch of the isotherm unlike most other techniques

which utilise only the desorption limb.

The method is based on a model surface that is assumed to have pores

in the size range 1-30 nm, and it assumes that the surface area in

pores >30 nm diameter is negligble. Over a finite increase in

pressure of gas from P_r to $P_{(r+\delta r)}$, pores in the size range r to

r+δr will be being filled with gas. At pressure P_r pores of radius

r are just about to fill with condensate and at $P_{(r+\delta r)}$ pores of

radius r+δr will just be filled. During this pressure change

smaller pores are already filled, while in the larger pores the

thickness of the adsorbed layer on their walls increased from t_r to

$t_{(r+\delta r)}$. At the limiting case where δr tends to zero equation 2.6

can be written:

$$v_r\,dr = \frac{(r-t_r)^2 V_r\,dr}{r^2} + dt \int_r^{\infty} \frac{2 V_r\,(r-t_r)\,dr}{r^2} \qquad \text{Equation 2.6}$$

where $V_r\,dr$ is the volume of pores over the size range r to r+dr
$v_r\,dr$ is determined experimentally,
and r, t_r, dr and dt are all pressure functions which can
be evaluated.

Integration of equation 2.6 over small finite ranges of radii

allows the calculation of pore volumes over small radii changes.

The method was applied as described in the original work using the

tables of values given. Calculation was terminated when a negative

value for pore volume was obtained. Data from both adsorption

and desorption branches were used, surface area values calculated

from each of these were compared with the BET result for the sample

and the data that showed best agreement was chosen as the better

representation of the particle porosity. Due to the extensive

calculation procedure involved, a computer programme (see appendix 2)

was written in BBC Basic using the tables of constants given in the

original C&I model. The programme was validated using the original

data (Cranston and Inkley, 1957) from the worked example given (from

sample A; silica alumina; heat deactivated) which was compared with

the programme output. Differences were observed toward the end of

the calculation, the surface area result obtained from the programme

being 6.7% higher than the original example. This difference can be

ascribed to the number of calculation steps (148) which go to

produce the cumulative result. The microcomputer can hold nine

significant figures whereas the original workers probably used three

or four. The cumulative nature of the calculation is responsible

for the gradual deviation of the C&I results from those obtained on

the computer. Thus the five extra significant figures held in the

computer have an incremental effect which becomes noticable toward

the end of the calculation and generates the observed differences.

The computer programme was used throughout the study for determining

pore size distributions because it enabled large numbers of

consistent calculations to be completed which would otherwise have

been impossible. The extensive quantities of data generated by the

technique were plotted as either pore size distributions or log

normalized plots. Figure 2.9 shows the results of a typical

analysis for an estuarine suspended solid. The principal use of the

output was to enable comparisons to be made between samples rather

than to yield absolute information on particle microstructure.

Statistical comparisons were made between data obtained on samples

used in interlaboratory studies and were also used to assess sample
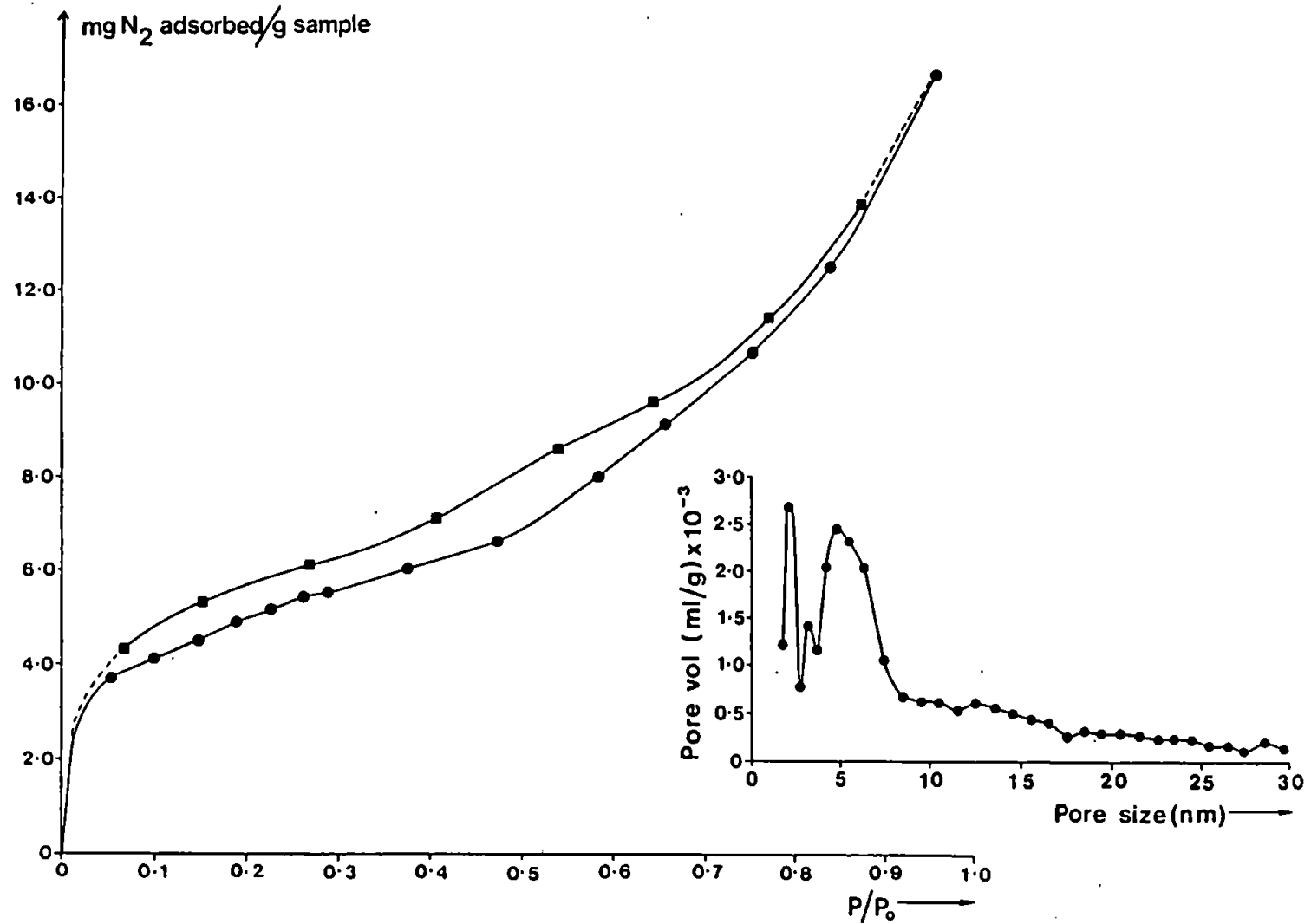
Figure 2.9: Hysteresis loop obtained on Tamar Estuary sediment sample. Cranston and Inkley (1957) pore size analysis of this isotherm is shown (inset).●-Adsorption;■-desorption.

preparative methods, and to compare various environmental samples.

2.1.1.4 Standards and Calibrations

During this study, a series of standards were run to enable
calibration of the vacuum microbalance system using graphitized
carbon black solid samples of known surface area (N.P.L.
Laboratories). One of these, sample M11-01 was examined repeatedly
because of the closeness of the surface area (11.1±0.8m^2/g) to the
natural samples under investigation (Table 2.1). Many graphitized
carbons feature energetically homogeneous surfaces that can affect
the linear range of the BET equation (Sing, 1982). The linear range
of the BET equation for each sample and the energy constant "C" are
included in the table. Two comparisons are shown, firstly the non-
linear regression technique of Dr. Kinniburgh (British Geological
Survey, Wallingford). This method identifes the monolayer capacity
"point B" on the adsorption isotherm (see Figure 2.2) independently
of the BET linear plot, and so provides a good check on the results.
The results of Glegg (1987) on the same samples using the same
apparatus are also included; together with the non-linear method
results on the same samples. The results show good agreement
between the measured data using the linear regression method and the
standard value, the agreement being acceptable on both M11-01 and
M11-02. The non-linear regression method results for M11-01
differed more substantially from the standard value, they were
higher and had a larger co-efficient of variation (12.3 m^2/g ±12.2%)
than those obtained using the linear regression method (11.9 m^2/g
±8.4%). The non linear regression method appears to provide little

| | This work[a] | | | | | Glegg, 1987[a] | |
Material	Standard value m^2/g	Surface area m^2/g	Linear range P/P_0	BET "C" value	Non linear surface area m^2/g	Surface area m^2/g	Non linear surface area m^2/g
M11-01	11.1±0.8	12.3	0.1-0.3	27.3	12.0	9.2	11.1
Carbon		10.6	0.1-0.3	38.6	10.4	9.7	12.1
black		12.9	0.1-0.3	241.2	13.7	9.3	11.7
FT-G		11.8	0.1-0.3	86.6	11.6	9.7	10.6
2700		12.9	0.05-0.3	184.6	13.8	9.4	--
		10.8	0.05-0.3	--	--	-	--
MEAN	11.1±0.8	11.9±1.0	----	--	12.3±1.5	9.5±0.2	11.4±0.7
M11-02	71.3±0.3	67.9	0.05-0.3	610	--	66.2	--
Carbon							
black							
3-G							
(2700)							

[a] Outgassed at room temperature. Nitrogen gas adsorbed at 77°K

Table 2.1
Results of calibrations undertaken on standard samples of known surface area using linear and non-linear regression analysis.

advantage over the linear approach either on these standards or on sediment samples (Glegg, 1987); therefore its application was not extended beyond the standards in this study.

2.1.2 X-RAY ANALYSIS

To establish information on estuarine particle compositon and the potential role this has on surface area, X-ray diffraction analyses were carried out on key samples before and after removal of hydrous oxide coatings. The instrument used in the study was a Philips P1710 Xray Diffractometer with a copper K (α) source lamp. The samples were ground in an agate pestle and mortar and then <0.1g of sample was mounted on a silicon slab ready for analysis. Interpretation of the trace produced was aided by the use of

A.S.T.M. powder diffraction cardfile (Smith, 1960).

2.1.3 LASER PARTICLE SIZE ANALYSIS

Laser particle size analysis was carried out on samples from two axial surveys in the Tamar Estuary, using a Malvern Instruments 2200 particle sizer system, as described by Bale *et al.*, (1984). Discrete samples (250 ml) of suspended solids were collected and analysed within 24h of collection. The system uses a laser to produce a Frauhofer diffraction pattern, which is scanned 25 sec^{-1} and the results fed to a microcomputer (McCave *et al.*, 1986). The laser was initially aligned using a distilled water blank. The amount of light passing through was maximised using horizontal and vertical controls, and the obscuration set to read 100%. Standard glass beads of 11.3 μm diameter with a standard deviation of 15% were used to calibrate the system. Aliquots of the estuarine samples were put into the cell and kept in suspension by a stirrer. More turbid samples required dilution to reduce excess obscuration. Results of the scanning were collected in a micro-computer and the particle size distributions in the range 1.9-188 μm were calculated and printed out as a 15 element histogram. Mean particle sizes and standard deviations were calculated from the data using grain size statistics (Folk, 1966).

2.1.4 EXAMINATION BY SCANNING ELECTRON MICROSCOPE

Visual inspection of Scanning Electron Micrograph magnifications of estuarine particulate matter was undertaken to provide a qualitative insight into the particle morphology, size and composition. A systematic study was not undertaken due to the laborious nature of

the examination which would be required because of the inhomogeneous nature of the samples. Particles selected for investigation were suspended solids from the iron rich Restronguet Creek; and bed sediment from the Tamar Estuary. Substantial chemical and physical data had already been obtained on the samples; including surface area, Fe and Mn oxide content and carbon and nitrogen concentrations. After collection the samples were filtered and dried as outlined in Section 2.2.2 before preparation for examination by electron microscope. The dried solid was lightly and evenly sprinkled onto double sided adhesive tape, mounted on aluminium stubs and coated with a thin layer of gold (12-15 nm thick) in a Polaron E1500 vacuum coating unit. Samples were examined and photographed through a J.S.M. T20 Scanning Electron Microscope at a range of magnifications (20-2000 times).

2.2 SAMPLE COLLECTION AND PREPARATION

2.2.1 COLLECTION OF SEDIMENT AND SUSPENDED SOLIDS

Samples were collected from the Tamar Estuary, Mersey Estuary,
Restronguet Creek and Keithing Burn during about 20 surveys. The
surveys were carried out in a variety of shallow draughted vessels
and in some cases, sediment samples were collected from the side of
of the estuary during littoral surveys. Surveys using the I.M.E.R.
vessel "Tamaris" had a number of advantages including an onboard
continuous monitoring system for master variables (temperature,
salinity, pH, oxygen and turbidity)(Morris *et al.*, 1982). In all
other cases, salinity and temperature were monitored using an M.C.5
T/S Bridge. Suspended solids were collected in polyethylene carboys
of 10, 25 or 50 litre capacity, as part of an axial survey of the
estuary over a representative salinity range. Discrete samples of
between 10 and 50 litres were collected (depending on turbidity) to
isolate a minimum of 1g of dried sediment. Separate water samples
(250 ml) were simultaneously abstracted for gravimetric turbidity
assessment and laser particle size analysis. The large volume
samples were filtered as soon as possible after collection; either
in the field or on return to the laboratory. The filtration unit
consisted of perspex tubing (I.D. 140 mm) which could hold eight
litres of water and accommodate filters 142 mm in diameter
(Sartorius or Millipore membrane; 0.45 μm pore size) on teflon
filter supports. The system was gas tight and filtration was induced
by increasing the air pressure over the sample by about 1
atmosphere. On completion samples were washed with deionized water
to remove salt from the particles.

Surface sediments were also collected for analysis either using a gravity corer or by surface scrape of the top two centimetres of exposed sediment. Sediment cores were segmented into two centimetre bands; fractionated across a 45 μm sieve (with backwashings) and each fraction filtered and washed with deionized water. Sediments collected by surface scrape were treated similarly, or separated by grain size across a range of microplate laboratory test sieves (Endecotts Ltd.).

2.2.2 SAMPLE PREPARATION TECHNIQUES

2.2.2.1 Interlaboratory Studies

In order to observe the effects of different sample preparation methods on the microstructures of particle surfaces a series of interlaboratory studies were undertaken. The vacuum microbalance in this laboratory was compared with the volumetric apparatus of Dr Reid (English China Clays, St Austell), Mr Roberts (University of North Wales) and Dr Bryant (Swansea University). A variety of samples were compared to allow both comparisons between two different types of apparatus (i.e. gravimetric and volumetric) and also to observe the effects of different drying methods on a range of inhomogeneous samples. Table 2.2 shows the study undertaken with English China Clays, using their automated Carlo Erba Sorptomatic 1822 Volumetric surface area method. The samples were passed to Dr Reid wet and were dried by his methods. These results show fair agreement of the data between the volumetric apparatus at the E.C.C. Laboratory; and the gravimetric unit at the Polytechnic. Results on estuarine sediment are especially good (within 8%) and overall agreement on these

65

samples was about 10%. A second study was undertaken with the
University of North Wales using their volumetric apparatus. Two samples,
one of manganese/zinc nodules accreted in a disused mine and one of
deposits from a hydroelectric aquaduct in mid Wales were used in the

Sample	Outgassing time, h.	Outgassing temp.,°C.	E.C.C. result m^2/g	Plymouth result m^2/g
Ochreous mine stream sediment	18 18	25 80	189.2 186.2	164[a]
Poorly crystallised lepidocrocite	18	25	130.4	121[a]
Fe(III)-derived precipitate	18	25 .	252.8	234[a]
Suspended solids from turbidity maximum in Tamar	18 48	25 25	21.0 21.0	22.7

[a]Values determined in Crosby *et al.*, 1983.

Table 2.2
Interlaboratory comparison of surface areas. This table gives the
drying conditions carried out at the E.C.C. Laboratories.

comparison. BET surface areas, adsorption/desorption isotherms and

Cranston and Inkley (1957) t-plot pore size distributions were

obtained for both samples, and the results are summarised in Table

2.3. Samples analysed in North Wales were air dried and degassed

for 24 hours at room temperature to better than 10^{-3}Torr. Samples

supplied to Plymouth were partly dried and were completed under

vacuum, before being analysed by gas adsorption. Neither of the two

samples is ideal for interlaboratory comparisons because of the

inhomogeneous nature of the surface, and this is apparent from the

differences observed, with the Mn/Zn nodules producing substantially

66

different results. This sample seems to have been substantially affected by the different finish to the drying procedure. Agreement of BET surface area measurements on the aquaduct deposits was substantially better with differences of about 14%, which implies that the sample is less inhomogeneous in nature and that the different preparation approach has had less impact on the surface. A fuller investigation of the gas adsorption isotherms obtained on both samples using the two different apparatus sets was carried out using the Cranston and Inkley (1957) t-plot method. Table 2.3 shows the C&I surface areas obtained on the samples, and for the Mn/Zn nodules agreement between the two laboratories is poor. These

Mn/Zn nodules	Plymouth result m²/g	North Wales result m²/g	Differences %
BET surface area	123.3	76.6	38
C&I surface area	171.7	72.8	58
C&I:BET ratio	1.39	0.95	--
Aquaduct deposit	Plymouth result m²/g	North Wales result m²/g	Differences %
BET* surface area	84.8	116	27
Mean surface area⁰	109	127	14
C&I surface area	88.2	111	21
C&I:BET* ratio	1.04	0.96	--

*Result compatible with C&I surface area
⁰Mean of two results

Table 2.3
Surface area determinations by BET model and C&I analysis of Mn/Zn nodules and aquaduct deposits.

differences are caused by changes in pore shapes and size distributions, and the assumptions made in the Cranston and Inkley paper. A comparison between BET surface areas and C&I results is recommended to improve validation of the data and the ratios obtained are shown in Table 2.3. The results on the Mn/Zn nodules indicate that the main problem lies with the sample analysed in this laboratory. This suggests that the difference in the completion of sample drying has affected the Mn/Zn nodule microstructure (especially pore shapes) significantly. However these differences in microstructure are not apparent from an examination of the full adsorption/desorption isotherms which generally show good agreement (see Figures 2.10 and 2.11); although the plots for the Mn/Zn nodule reveals substantial differences in terms of the absolute amounts of nitrogen adsorbed. Opening of the hysteresis loops occurs immediately after the commencement of desorption, and closure was either approached or took place at P/P_0 values of 0.45, although the aquaduct deposit (Plymouth Laboratory) shows some low pressure hysteresis. The desorption limbs all show complete reversal (hysteresis loop closure) which implies that none of the micropores have restricted openings: although the larger pores are possibly "ink bottle".

Results from C&I analysis of the isotherms are summarized in Tables 2.4 and 2.5. The data reveals an overall fundamental difference between the Plymouth data and the results from North Wales: the samples that had been air dried and degassed for 24 hours featured pore size distributions with >25% of total pore volume in pores <2nm diameter. The samples dried under vacuum favoured pores in the size

68
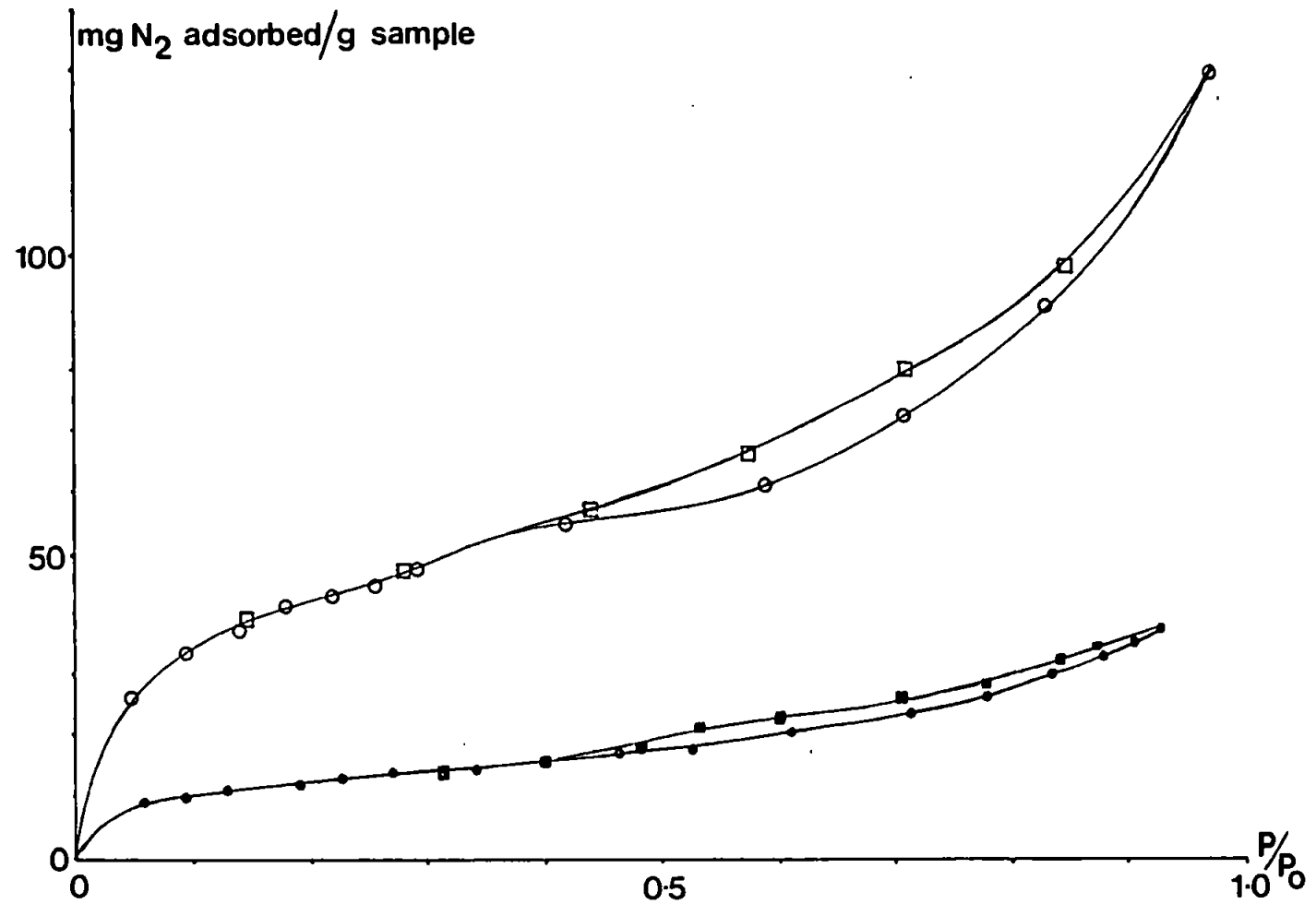
Figure 2.10: Hysteresis loops obtained on Mn/Zn nodules by gas adsorption experiments. O-Adsorption; □-desorption, (Plymouth laboratory); ●-adsorption; ■-desorption, (North Wales laboratory).
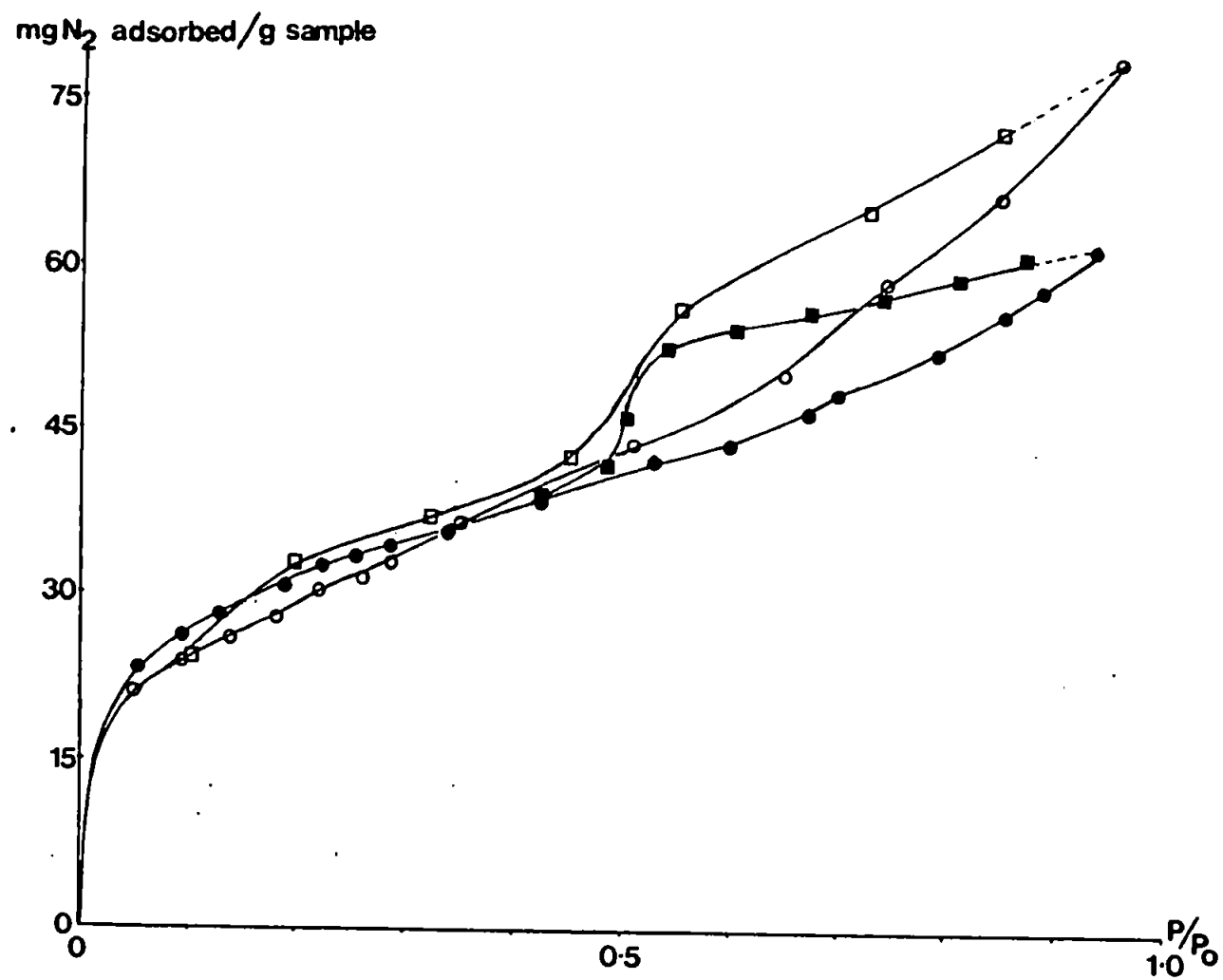
Figure 2.11: Hysteresis loops obtained on aquaduct deposits by gas sorption experiments. O-Adsorption; □-desorption, (Plymouth laboratory); ●-adsorption; ■-desorption, (North Wales laboratory).

Pore size (nm)	Plymouth results				North Wales results			
	Surface area m^2/g	% of total	Pore vol. ml/g $*10^{-3}$	% of total	Surface area m^2/g	% of total	Pore vol. ml/g $*10^{-3}$	% of total
<2	72.5	42.2	25.2	15.2	45.2	62.0	15.1	25.6
2-5	61.6	35.9	48.9	29.4	15.2	20.9	12.6	21.4
5-10	24.9	14.5	41.9	25.2	7.7	10.6	13.3	22.5
10-20	10.1	5.9	34.9	21.0	3.8	5.2	12.7	21.6
20-30	2.6	1.5	15.2	9.2	0.9	1.2	5.2	8.9

Table 2.4
Cranston and Inkley data on Mn/Zn deposits, showing surface area and pore size distributions from Plymouth and North Wales; calculated on the microcomputer obtained from N_2 gas adsorption/desorption isotherms at 77°K (section 2.1.1.3).

Pore size (nm)	Plymouth results				North Wales results			
	Surface area m^2/g	% of total	Pore vol. ml/g $*10^{-3}$	% of total	Surface area m^2/g	% of total	Pore vol ml/g $*10^{-3}$	% of total
<2	12.8	14.5	5.5	5.6	59.7	53.6	20.5	25.2
2-5	52.1	59.0	40.9	41.3	37.2	33.3	28.1	34.4
5-10	17.4	19.7	30.0	30.3	10.6	9.5	17.9	21.9
10-20	4.8	5.5	16.2	16.3	3.0	2.7	9.9	12.1
20.30	1.1	1.2	6.4	6.5	0.9	0.9	5.3	6.4

Table 2.5
Cranston and Inkley data on aquaduct deposits, showing surface area and pore size distributions obtained in the Plymouth laboratory and at North Wales from N_2 gas adsorption/desorption isotherms at 77°K.

ranges 2-5 and 5-10 nm. This skew in the pore size distribution is also apparent from the mean pore diameters calculated from the Cranston and Inkley pore size distributions.

	Plymouth result	North Wales result
Mn/Zn nodule Mean pore size (nm)	8.21	7.92
Aquaduct deposit Mean pore size (nm)	7.49	6.35

These show that the mean pore sizes for both samples dried at Plymouth are significantly larger. This interlaboratory study has highlighted a number of areas that require attention when estuarine particles are investigated using the gas adsorption technique. The main area of study will be to find an appropriate and consistant method for sample preparation.

The inhomogeneous nature of the samples used in this interlaboratory study present problems similar to those likely to be encountered when dealing with estuarine samples which are known to be composed of a wide variety of solid phases.

Statistical comparisons between the data obtained from the two laboratories was undertaken by multiple regression analysis of the C&I data, which was carried out on the "Minitab" statistical package on a "Prime" mainframe computer. Best fit regression equations on Log-normalized plots of pore size (A) versus pore volume $(ml/g*10^5)$,(from the C&I method; see Figures 2.12, 2.13 and 2.14) were used for statistical comparisons by comparing the individual regression lines with the pooled data (Draper and Smith, 1981). The comparisons made in this way on the Mn/Zn nodule data and the
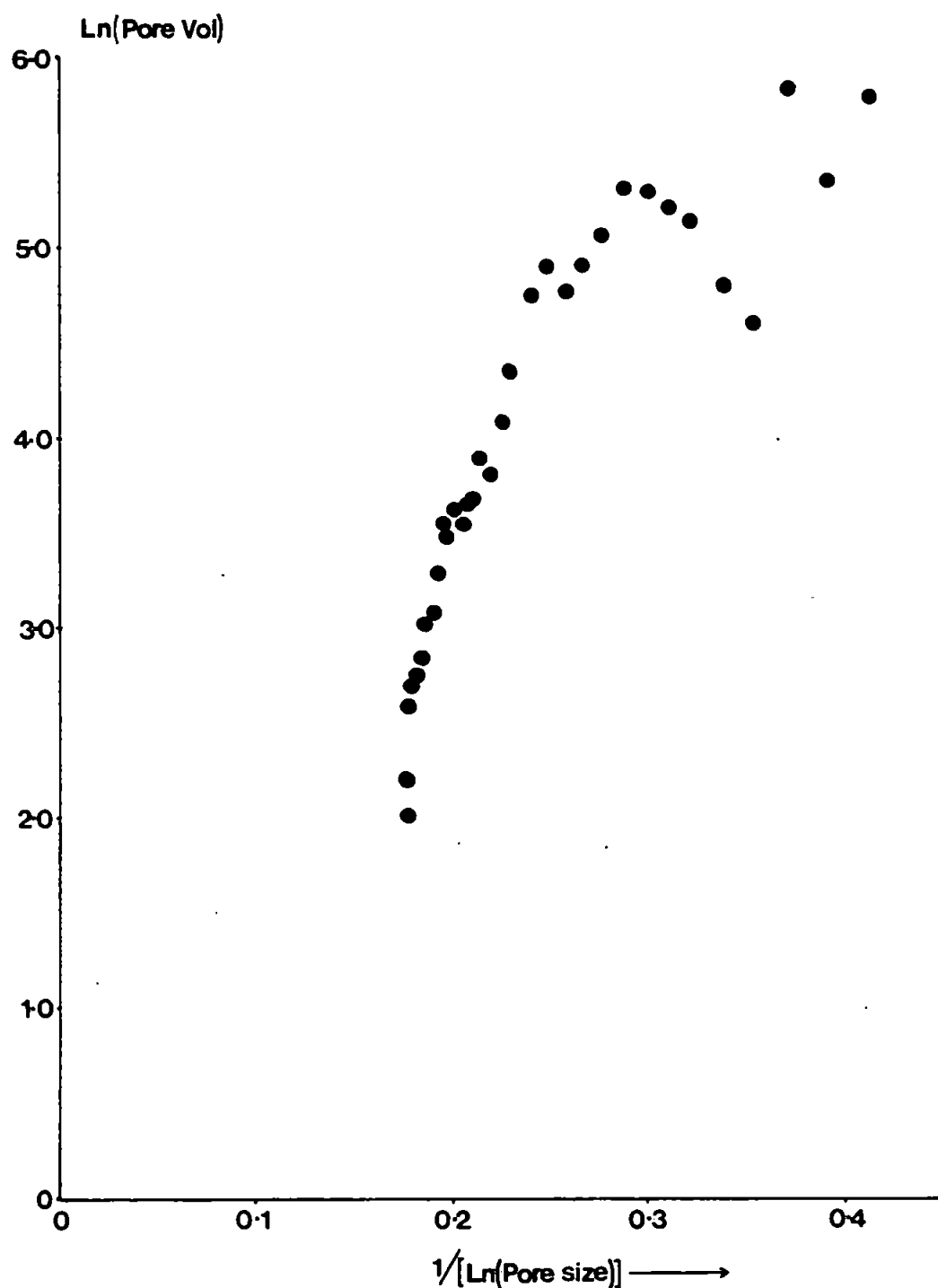
Figure 2.12: Plot of ln(pore volume) versus 1/[ln(pore size)] using Cranston and Inkley's method.

(From the hysteresis loop obtained on the aquaduct deposit, Plymouth result (figure 2.11)).
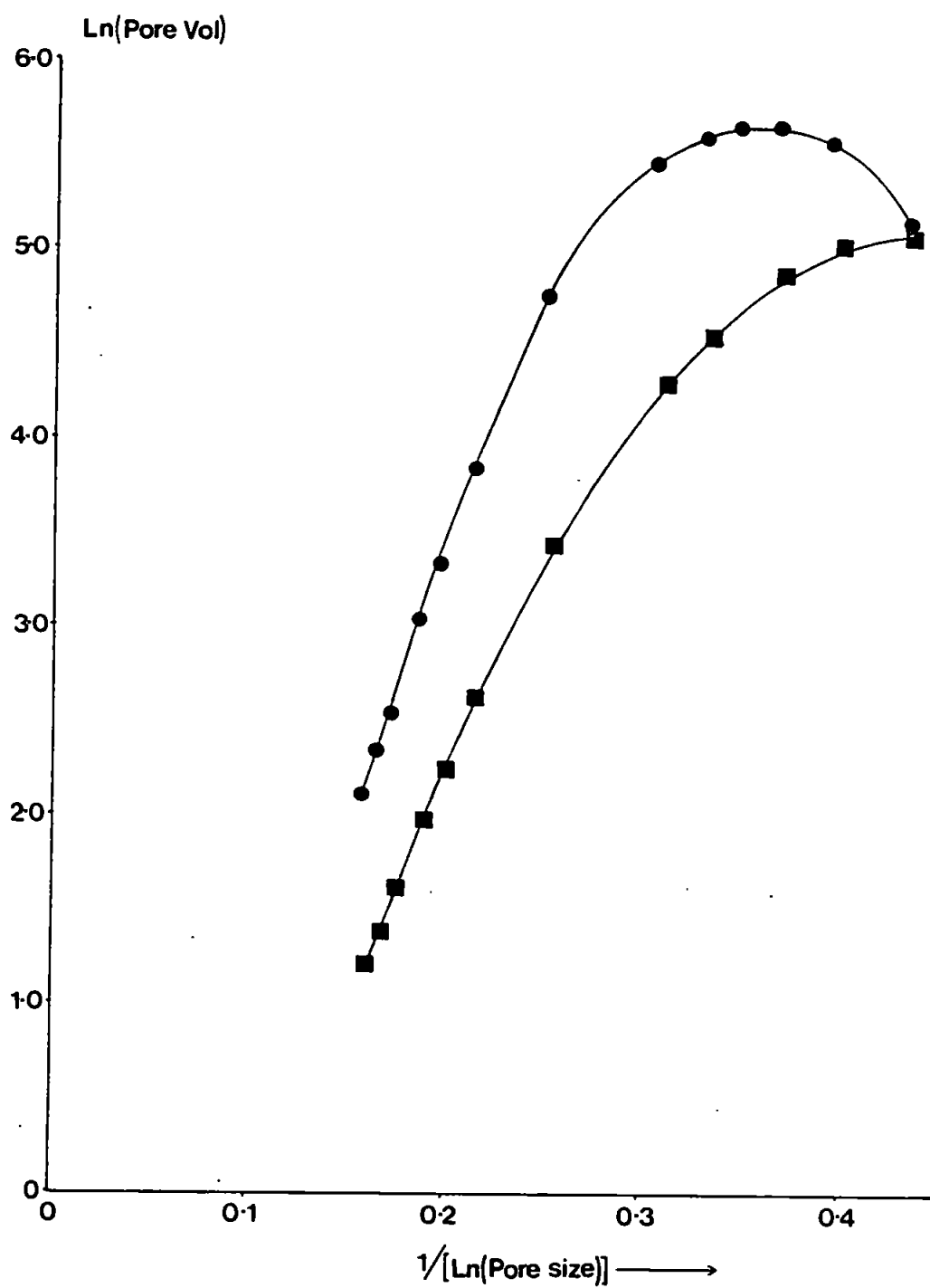
Figure 2.13: Best fit regression lines obtained from the log-normalized plots of pore size distributions.

(Mn/Zn nodule results; ●Plymouth laboratory, ■North Wales laboratory).

74
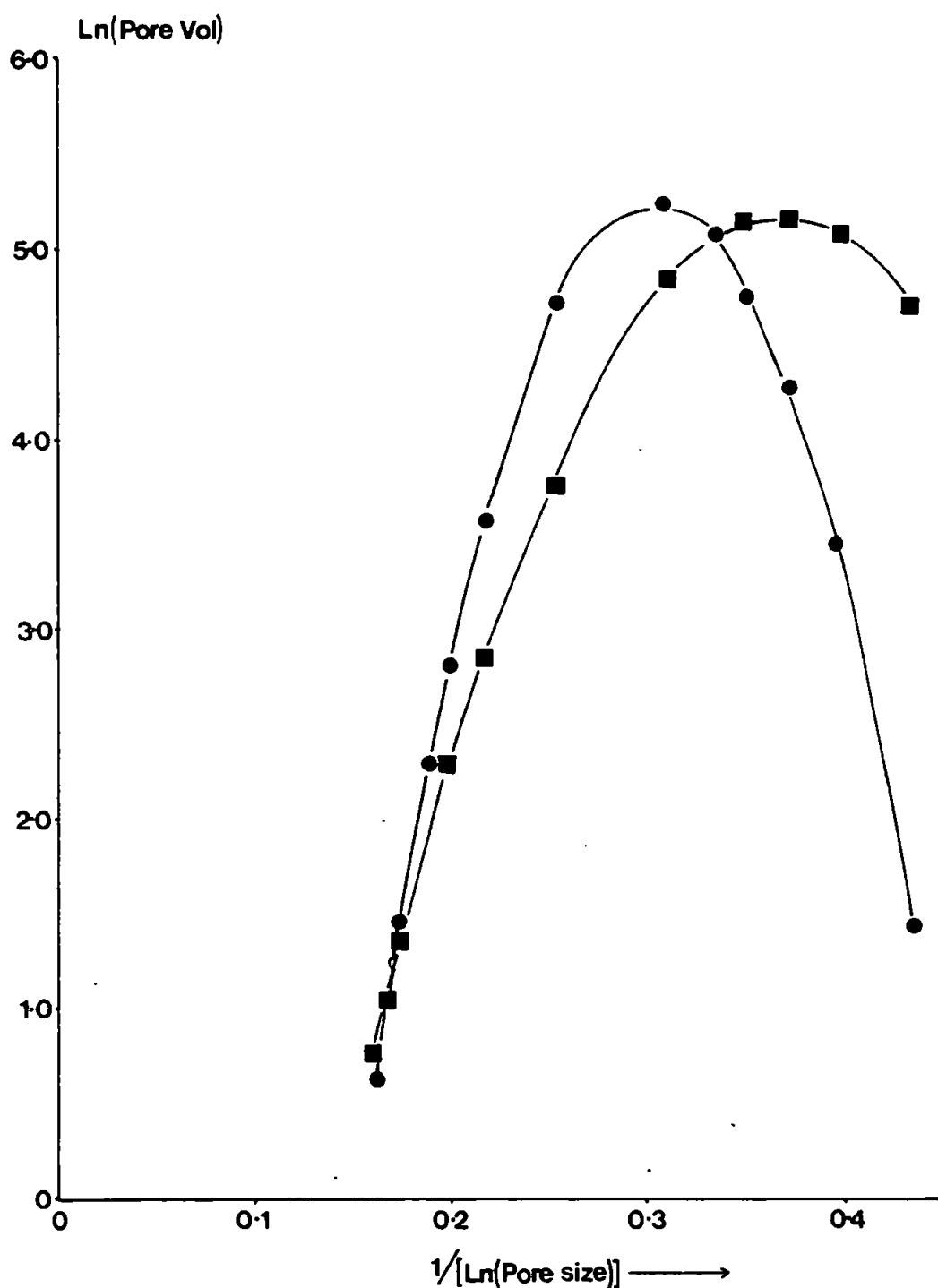
Figure 2.14: Best fit regression lines obtained from the log-normalized plots of pore size distribution data.

(Aquaduct deposit results; ●-Plymouth laboratory, ■-North Wales laboratory).

aquaduct deposits revealed significant statistical differences and the regression line plots showed that the samples analysed in North Wales had pore size distributions skewed in favour of smaller pores. These effects are a product of both the inhomogeneous nature of the sample and also the inconsistent preparation method employed. Due to these observed effects and support in the literature for these findings on drying methods, a comprehensive review of preparation methods on estuarine samples was undertaken (see Section 2.2.2.2). A final interlaboratory study was carried out on two samples of Welsh Anthracite (<10 μm particle size) supplied by the Department of Chemical Engineering at Swansea University. This allowed another comparison between the vacuum microbalance system at Plymouth and a different volumetric unit (Table 2.6).

DIRECTLY DRIED ANTHRACITE						SOLVENT DRIED		
Plymouth results				Swansea results		Plymouth results		
BET SSA m²/g	BET 'C'	C&I SSA m²/g	C&I:BET	BET SSA m²/g	BET 'C'	BET SSA m²/g	C&I SSA m²/g	C&I:BET
85.5	34.0	84.9	0.99	135.5	12.3	120.0	102.9	0.86
139.0	6.8			136.2	11.8			
132.0	9.8			111.0	13.0			
82.5	12.1							
Mean 109.8 ±29.9	Mean 15.7	---	----	Mean 127.2 ±14.9	Mean 12.4			

Table 2.6
BET surface areas and Cranston and Inkley data on two anthracite samples; showing results from the two laboratories.

The two samples were known to be inhomogeneous, and to have an extensive micropore network. The samples had been prepared in two ways to observe the effects of different preparative methods on highly microporous solids. One sample had been vacuum dried directly; in the other water had first been exchanged for a solvent (methanol) and then dried under vacuum.

The data shows fair overall agreement between the two laboratories on the water dried anthracite sample, the differences are about 14%, which is similar to the interlaboratory comparison with North Wales (on the aquaduct deposit) and with the E.C.C. laboratories on estuarine and iron oxide samples. The heteorogeneous nature of the anthracite surface and the microporous network present within the solid matrix caused some difficulties during analysis. During the nitrogen adsorption phase, a slow approach to equilibrium was observed with persistent gradual uptake of gas onto the surface which continued for a number of hours. This effect was probably generated by the persistent slow diffusion of nitrogen gas into the extensive micropore network. The full adsorption/desorption isotherms on the two samples dried by the different methods are shown in Figures 2.15 and 2.16. Both samples exhibit adsorption isotherms that are initially very steep followed by a more limited uptake as P/P_0 approaches 1.0, this isotherm shape confirms the highly microporous nature of the two solids. The desorption limb shows no release of nitrogen until the partial pressures dropped below 0.1 which implies that the pores are so shaped as to inhibit nitrogen release from the surface. Cranston and Inkley t-plot analysis on the two samples (from adsorption isotherms) is summarised in Table 2.7. The data shows that the pore size

77
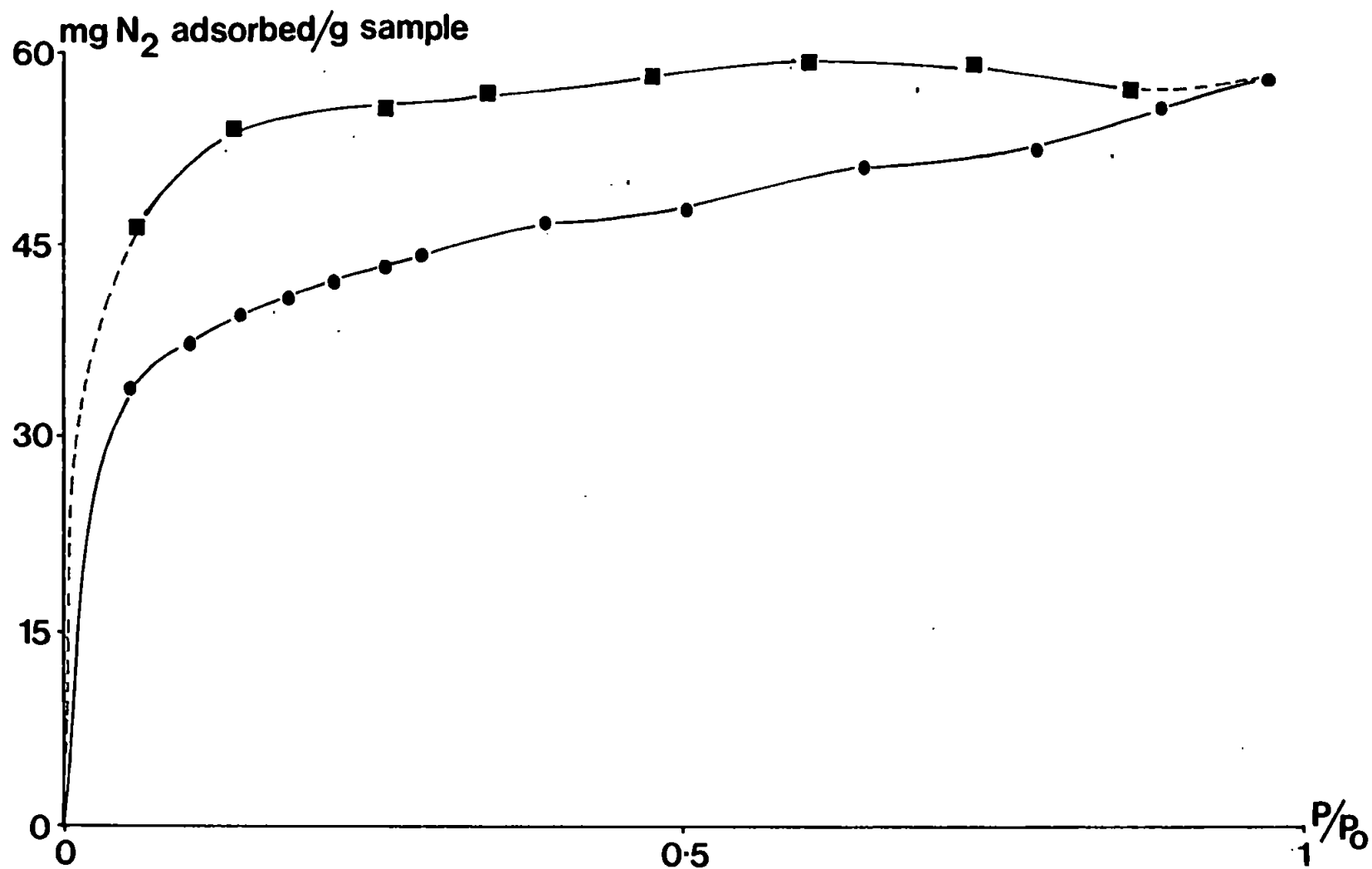
Figure 2.15: Hysteresis loops obtained on solvent dried anthracite by gas sorption experiments. ●-Adsorption; ■-desorption.
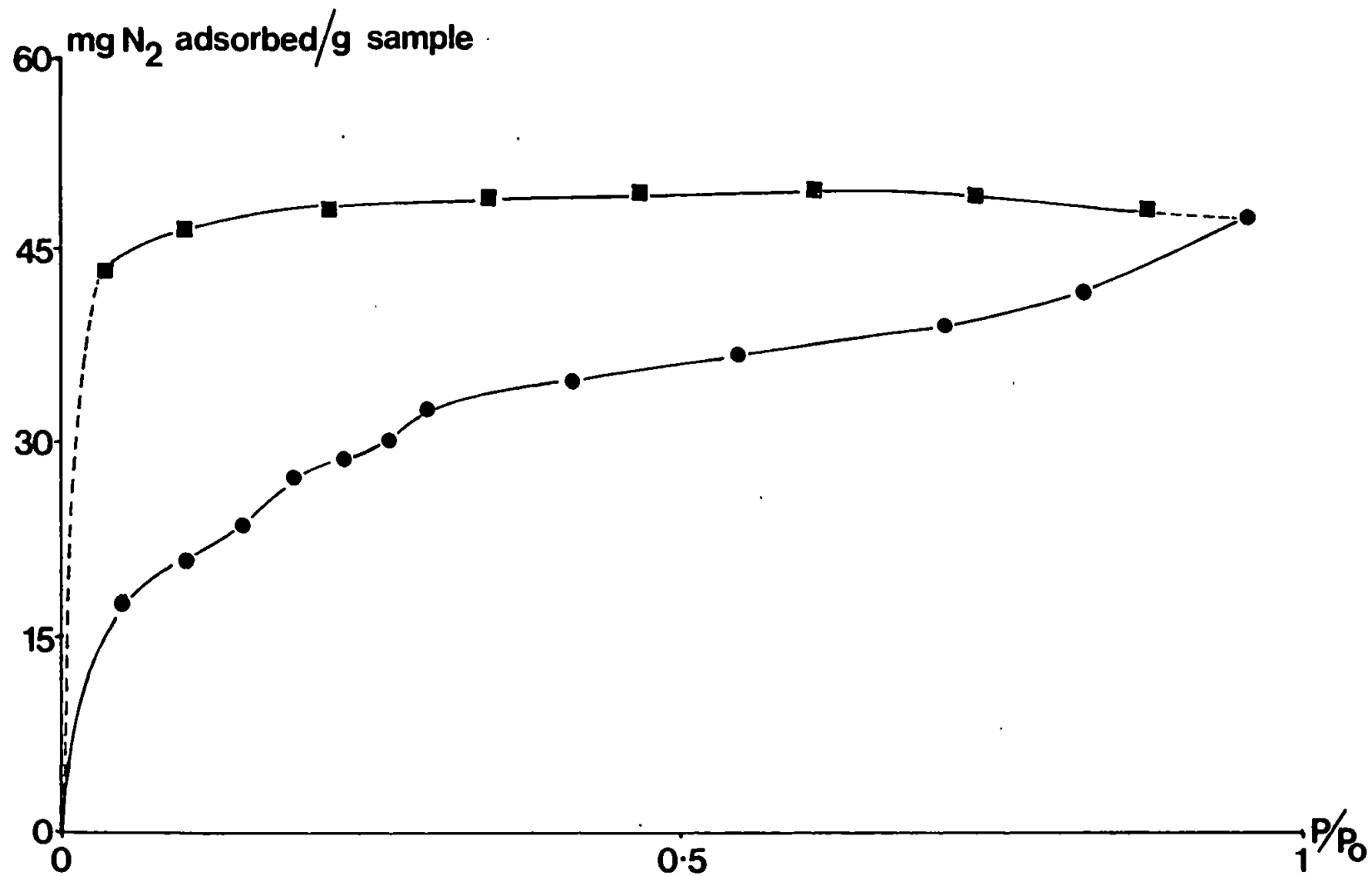
Figure 2.16: Hysteresis loop obtained on directly dried anthracite, by gas sorption experiments. ●-Adsorption;
■-desorption.

distributions of the two samples are similar, with >75% of pore volume in the size range <5 nm confirming the microporous nature of the solid surface. The pore size distribution of the sample dried after solvent exchange has a pore size distribution skewed more in favour of micropores (<2 nm) than does the directly dried anthracite sample.

Pore size (nm)	Direct Dried Anthracite				Solvent Dried Anthracite			
	Surface area m^2/g	% of total	Pore vol. ml/g $*10^{-3}$	% of total	Surface area m^2/g	% of total	Pore vol. ml/g $*10^{-3}$	% of total
<2	28.7	33.8	12.9	21.2	61.6	59.8	22.3	36.4
2-5	50.9	60.0	33.4	55.0	35.5	34.5	25.1	40.9
5-10	3.1	3.6	4.9	8.1	3.7	3.6	6.3	10.3
10-20	1.6	1.9	5.9	9.7	1.9	1.9	6.3	10.2
20-30	0.6	0.7	3.7	6.0	0.2	0.2	1.4	2.3
	Direct dried anthracite		Solvent dried anthracite					
Mean pore size	5.49 nm		4.46 nm					

Table 2.7
Pore size distributions and specific surface area results on Welsh Anthracite dried by two methods.

This difference in size distribution caused the average pore sizes of the two samples to be significantly different; the solvent exchanged sample had a smaller mean pore diameter of 4.46 nm compared to the directly dried sample (pore diameter 5.49 nm). This can be ascribed to the different surface tension effects of methanol and water on the pore structure during the phase change from liquid to gas. The greater surface tension forces associated with water

vapourisation from the pores caused structural changes; mainly aggregation of micropores to small mesopores.

In conclusion, the ability of the vacuum microbalance system to consistently and precisely assess the microstructures of particle surfaces was considered. The standard graphitized carbons of known surface area were reproduced consistently by the apparatus (Section 2.1.1.4), overall agreement was within 10%. Interlaboratory studies compared the system with three different volumetric apparatus, all completely independent of each other and using different inhomogeneous samples. The gravimetric unit produced fairly consistent results, which were lower than the volumetric units by 10-20%. These experiments also highlighted the need for consistency in sample preparation and the problems likely to be encountered on inhomogeneous samples. The observed effects of even slightly varying preparation methods on micro and smaller mesopores on particle surfaces warranted the fuller investigation of sample drying techniques reported in Section 2.2.2.2.

2.2.2.2 Comparison of Drying Techniques for Natural Samples

The principal drawback of the gas sorption technique on estuarine samples is that *in-situ* measurements cannot be made and the solid has to be isolated and then dried prior to analysis. Any drying process disrupts the particle surface because the evasion of water from within the microstructure generates localized forces (e.g. surface tension effects), which can affect surface features such as pore shapes and pore size distributions. An *in-situ* method that can assess surface features of this kind with particles still

in the wetted state would be an ideal approach as the results could be easily applied to the environment. A number of methods are available for the *in-situ* measurement of surface area on wetted particles, using either dye or negative adsorption techniques (Crosby, 1982; Van den Hul and Lyklema, 1968; Gregg, 1967). Work by Glegg, (1987) compared BET surface area measurements with a dye adsorption approach on Tamar estuarine particles and the results are shown in Table 2.8. The dye adsorption areas are between 6 and 9 greater than the BET values. The differences observed between the two approaches are compatible with those found by Van den Hul and Lyklema (1968), but the fact that the dye adsorption approach gives higher values does not make it any more correct.

BET surface area m^2/g	Dye surface area m^2/g
23.1	146
16.5	127
14.6	133
11.5	106

Table 2.8
Comparison of BET surface areas with dye adsorption surface areas using Tamar estuary sediment samples.

There are a number of problems with *in-situ* measurements, including the large molecular area of the dye molecules (at least five times that of the nitrogen gas used in the BET technique), which means that microscale surface features would not be penetrated by the adsorbing molecules and therefore would pass undetected. Dye molecules can form micelles in solution in preference to adsorption and may also change their orientation during the adsorption process to lie flat at lower concentrations and then end on as the

concentration is increased. The reproducible determination of monolayer capacity is made more difficult. Furthermore the area occupied by the dye molecules can vary depending on the nature of the surface under investigation. Gregg, (1967) suggests that the dye adsorption approach should be used as a secondary method on particles where the surface area has already been assessed in some other way. Solution adsorption techniques currently available are unable to assess particle porosity; the only reliable method is by gas adsorption. Everett (1982) has suggested that there should be attempts to unify the theories of gas-solid adsorption with those of liquid-solid adsorption, although at present such unification is a long way off.

The approach taken in this study has been to utilise the gas adsorption approach to obtain a method specific result; which is then interpreted in terms of the sample preparation technique. Selection of a suitable drying method was based on the need for good reproducibility, and minimal disruption to the particle microstructure. Development of a consistent technique for particle preparation prior to analysis is essential as even subtle differences in approach can substantially affect the results (see preceding section and Aylmore, 1977). The problem of selecting an appropriate drying technique was addressed using both natural solids and pure kaolinite samples. Three ways of sample preparation were considered.

1) Air drying at 50°C or ambient temperature;

2) Critical point drying; in which ethanol was gradually exchanged
    for the water associated with the sediment, by exchange washing
    with mixtures of increasing ethanol concentration. The ethanol
    was then exchanged for carbon dioxide and the solid dried in a
    commercial critical point drier (Tousimis Research).

3) Freeze-drying; with the samples prefrozen to -18°C followed by
    vacuum freeze drying at low temperatures (Edwards High Vacuum).

Air drying involves the passage of a gas/liquid interface through

the specimen, with large surface tension forces causing severe

distortion of the pore structures, morphology and ultrastructure of

soft materials which have a high water content (Tippkötter, 1985;

Egashira and Aomine, 1974). Samples dried in this way may shrink and

coagulate to produce a hard solid mass from which it is difficult to

obtain a representative sample, unless it is first ground to a

powder. The work of Glegg, (1987) on the effects of different drying

techniques on BET surface areas of Tamar estuary sediment (10

replicate analyses) revealed that air drying produced smaller

surface areas with a larger co-efficient of variation (9.9 m²/g

±14.5%) than did freeze drying (12.6 m²/g ±10%).

Critical point drying is an alternative method to both air and

freeze drying and would appear to overcome the problems associated

with air drying. At the critical point there is no liquid/gas

interface and so disruptive surface tension effects are minimal.

This technique was designed to preserve the 3-dimensional hydrated

morphology of certain biological materials (Boyde and Jones, 1974;

Cohen, 1974) but it was found to be unsatisfactory for the drying

of clay soils (Greene-Kelly, 1973). Two major problems occurred

when the method was applied to estuarine solids. Firstly, some of

the surface organic material is ethanol soluble and was extracted

into the solvent during the initial exchange procedures; the

solution being coloured brown and then yellow/green from organic

matter and pigments. The second major problem was incomplete

exchange of ethanol for water and then carbon dioxide before drying. Water may be strongly held in micropores at the solid surface or in the interlamellar spacings between the aluminosilicate sheets of clays (Stul and Bock, 1985). Difficulty was experienced in attempting to dry samples of sediment and pure kaolinite, both ethanol and water were present at the end of the drying process, and these samples had to be completed under vacuum.

The third technique investigated was freeze drying; which is a method that may be employed on samples where observations of ethanol or acetone soluble components is desired. During drying, particle held water sublimes directly from the solid to the gas- therefore no liquid/gas interface passes through the structure; the reticular nature of the solid should be preserved, and sample shrinkage reduced (Keng *et al.*, 1985; Greene-Kelly, 1973).

A series of experiments were under taken to compare the results obtained on samples dried in the ways outlined above (Table 2.10). Because of the difficulties associated with critical point drying only a limited number of studies using this method were undertaken. The results obtained confirm that two undesirable processes occur during the critical point drying process on the estuarine samples. Firstly removal of surface organic material during the ethanol exchange process exposes Fe/Mn coatings with higher surface areas, in a process similar to that ocurring during sample oxidation with hydrogen peroxide (Glegg, 1987). Furthermore a chemical reaction between the ethanol and the clay lattices of the particles or the larger domain structures causes an opening out of the structure and exposes a greater surface to the adsorbing nitrogen

molecules.

Drying method	BET surface area m^2/g	
	High salinity	Low salinity
Air dried	4.6*	9.8@
Freeze dried*	7.0	13.1
Critical point dried	13.4	18.5

Air dried at *room temperature; @50°C.
*Prefrozen at -18°C.

Table 2.10.
Surface area results on samples of estuarine sediment dried in different ways.

This second effect was investigated using a pure kaolinite sample (Supreme China Clay; 100% kaolinite). The sample was subdivided into four, one portion retained dry and the other three portions wetted in distilled water for 24 hours, before being dried by various methods. The results Table 2.11. show that the wetting and re-drying processes produce an increase in surface area over the original dried solid. The critical point dried solid showed the largest increase which supports the hypothesis that a chemical reaction is occuring between the ethanol and the domain structure within the clays and exposing more surface to the sorbing N_2 molecules. In this study analysis of chemically unaltered particles is preferred, thus freeze drying was selected in preference to the critical point drying method.

Sample	BET surface area m^2/g
Dry Kaolinite (retained dry)	10.0
Freeze dried*	11.5
Freeze dried[e]	11.8
Critical point dried	13.6

Initially frozen at *-18°C; [e]-196°C.

Table 2.11
Surface area of kaolinite samples dried by different methods.

Investigations were carried out into the action of freeze drying on both clays and natural samples to improve the understanding of preparation methods on particle structures, because although during the freeze drying process water sublimes directly from solid to vapour without causing surface tension effects; some artefacts may be generated during the initial freezing process. The method has been thoroughly criticized by Greene-Kelly (1973), the main problem appears to be the passage of the solid/liquid interface through the the sample during freezing. For samples dispersed in water a slow freezing rate (e.g. freezer at -10°C) causes a gradual solidification process from the outside in and migration of particles ahead of the solid-liquid interface is sometimes observed (Rowell and Dillon, 1972). Furthermore, at these relatively high temperatures, minute ice crystals are created within the particle structure causing crystalline pressure on the surrounding matrix

(Keng *et al.*, 1985). Rapid freezing at very low temperatures (e.g.
in liquid nitrogen) may inhibit these formations as can the addition
of polar compounds such as glycerol or dimethyl-sulphoxide (DMSO)
(Greene-Kelly, 1973; Keng *et al.*, 1985). In this study the basic
freeze drying process was used but with variations to the sample
freezing process as outlined below.

i)   Freezing samples dispersed in water at -18°C prior to freeze
     drying;

ii) Freezing samples rapidly in liquid nitrogen at 77°K, and then
     storing at -18°C prior to drying;

iii) Adding a cryoprotective agent (DMSO) to the aqueous suspension
     before rapid freezing in liquid nitrogen at 77°K, followed by
     storage at -70°C prior to drying.

BET surface areas, and porosity studies (by Cranston and Inkley's
method) were carried out on the samples and the pore size
distributions were compared statistically to determine if any
significant differences had been generated as a result of the
different preparative methods employed. Samples of estuarine
sediments and a sample of Supreme China Clay were used in these
preparation experiments. The Supreme China Clay sample was prepared
by subdividing it into three aliquots, one of which was retained dry
and one was soaked for 24 hours in distilled water (to encourage
complete wetting) prior to freezing at -18°C and freeze drying. The
remaining portion was soaked for 24 hours in a DMSO/H$_2$O solution
(30:70 v/v DMSO:H$_2$O), before being fast frozen in liquid nitrogen
and then stored at -18°C prior to freeze drying. However this
storage temperature was not low enough and the DMSO/H$_2$O solution
thawed and had to be transferred to a freezer at -70°C. During the
freeze drying process the sample again melted before the sublimation

88

process was complete. The solution composition was varied to 10/90 DMSO:H_2O (v/v) in an attempt to increase the freezing point of the mixture although the reduced DMSO concentration would have less cryoprotective effect (Keng et al., 1985). This sample was successfully freeze dried and the surface area data obtained on these samples is shown in Table 2.12.

Sample: Kaolinite	BET surface area m^2/g	C&I surface area m^2/g
Retained Dry	9.4	9.0
Freeze dried*	13.0	18.1
DMSO treated & freeze dried[e]	14.3	17.2

*Prefrozen and stored at $-18^{\circ}C$.
[e]10:90 DMSO:H_2O solution; prefrozen at $-196^{\circ}C$.

Table 2.12
Surface area data from kaolinite samples prepared by two variants of the freeze drying process.

The drying experiments on kaolinite reveal that the freeze drying process increases the surface area of the sample, presumably by opening up the "cardhouse" structure or by affecting the domain ultrastructures. Rapid freezing at $77^{\circ}K$ prior to drying causes a substantial thermal shock to the sample which may also affect the ultrastructure (Keng et al., 1985) and the surface area is increased as a consequence, this is shown in Table 2.11. The rewetting and then drying of the kaolinite sample produced an increase of 15-35% (Tables 2.11 and 2.12) over the original dry sample. The sample protected by the DMSO also had a substantially increased surface

area, the result here probably being generated by the interaction
of the DMSO molecules with the clay layer structure. Cranston and
Inkley surface area results also show a similar trend in the data
with a 100% increase in surface area over the original dried sample
occuring for the rewetted and freeze dried clay. Full
adsorption/desorption isotherms on these samples were obtained and
interpreted using Cranston and Inkley's model and the results are
summarised in Table 2.13. The main feature of these data concerns
the appearance of micropores in the freeze dried samples as a result
of the reordering of the domain and cardhouse structure. This
reopening of micropores appears to account for the observed

Sample	Pore size (nm)	C&I Surface area m^2/g	% of total	Pore vol $(ml/g*10^{-3})$	% of total
Dry kaolinite sample mean pore size 8.53nm	<2	0	0	0	0
	2-5	5.55	61.5	4.39	32.6
	5-10	2.18	24.6	3.78	28.0
	10-20	0.97	10.7	3.41	25.3
	20-30	0.33	3.6	1.90	14.1
Freeze dried kaolinite mean pore size 8.00nm	<2	8.23	45.6	3.22	19.3
	2-5	6.45	35.7	4.88	29.2
	5-10	1.96	10.8	3.31	19.8
	10-20	1.18	6.5	3.89	23.3
	20-30	0.25	1.4	1.43	8.6
DMSO trea-ted freeze dried kao-linite mean pore size 8.56nm	<2	6.05	35.1	2.51	13.9
	2-5	7.09	41.1	5.24	28.9
	5-10	2.63	15.3	4.64	25.6
	10-20	1.14	6.6	3.81	21.0
	20-30	0.33	1.9	1.91	10.6

Table 2.13
Pore size distributions, specific surface area data and mean pore
sizes for the dry kaolinite and the two freeze dried samples.

increases in surface area; if the surface areas and pore volumes
associated with pores of <2 nm are removed from the data on the
freeze dried sample and from the DMSO protected sample then the
results for all three clays become very similar (Table 2.14).
Plots of the data are shown in Figure 2.17. Statistical
comparisons of the pore size distributions of the three samples by
regression analysis was undertaken. Initially, the data obtained in

Sample	C&I surface area m^2/g	Pore volume ml/g
Dry kaolinite	9.0	$13.48*10^{-3}$
Freeze dried kaolinite	9.8	$13.51*10^{-3}$
DMSO & freeze dried	11.2	$15.60*10^{-3}$

Table 2.14
Surface areas and pore volumes for the three samples when pores
<2 nm are ignored.

the micropores (<2 nm) of the two freeze dried samples were not
included in the comparisons. Using the F-statistic calculated from
the regression analysis data, comparisons of the individual data
sets with the pooled data (Draper and Smith, 1981) revealed that
there were no significant differences between the three samples.
When the micropore data was included in the comparison, however, the
F-test on the data sets revealed statistically significant
differences in the data. This clearly shows that the rewetting and
drying process generates micropores (pores <2 nm) by altering the
domain and cardhouse structure. The resultant pore size
distributions (especially in the micropore size range) are highly
dependent on the sample preparation method which confirms the
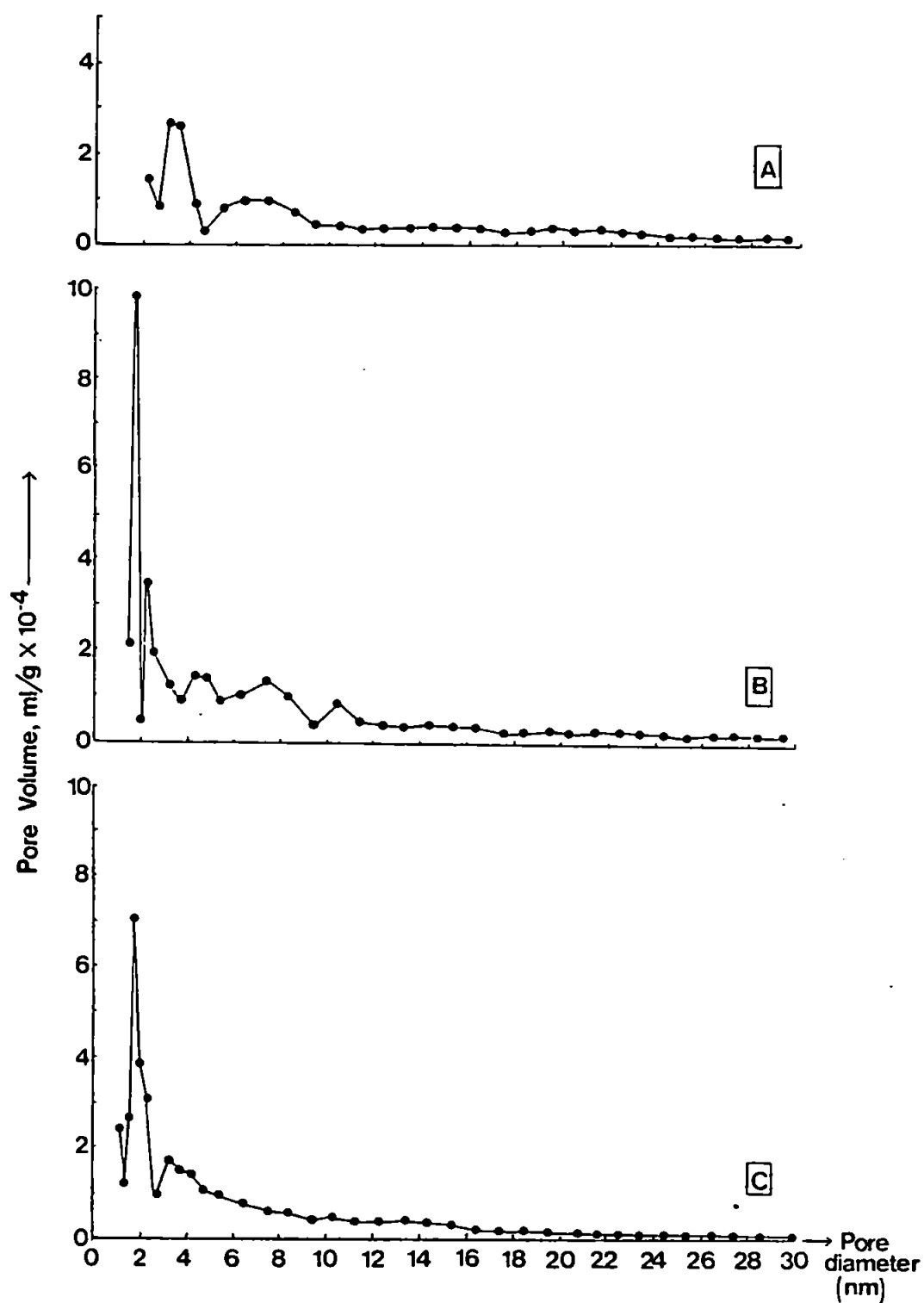
Figure 2.17: Plots of pore volume versus pore diameter calculated using the method of Cranston and Inkley (1957). A] Kaolinite (retained dry); B] kaolinite protected by DMSO; C] kaolinite freeze dried without protection.

observations already made (in the preceding section) on various samples. The addition of DMSO into the solution results in a significantly different pore size distribution compared with samples freeze dried without.

These experiments were extended to compare the straight freeze drying of estuarine sediments with sediments that had been protected with DMSO prior to freezing. The surface area results are shown in Table 2.15.

Sediment sample	BET surface area m²/g	
	Freeze dried	DMSO treated freeze dried
Suspended solids	19.6	19.7
from low salinity	12.6	15.0
region of Tamar	17.8	17.2
Bed sediment	5.0	5.7

Table 2.15
BET surface areas of sediment collected in the Tamar estuary either directly freeze dried or protected by DMSO and freeze dried.

Cranston and Inkley (1957) pore size analyses were carried out on the samples and the log normalized data compared statistically by multiple regression analysis. Surface area data for the samples is shown in Table 2.16 and the pore volume data plotted in Figures 2.18 and 2.19. The data in Table 2.16 show that for straight freeze dried samples most of the surface area is found in pores of <10 nm, which suggests that the drying method may preserve smaller pores and prevent aggregation into larger pores. Aliquots of the same samples
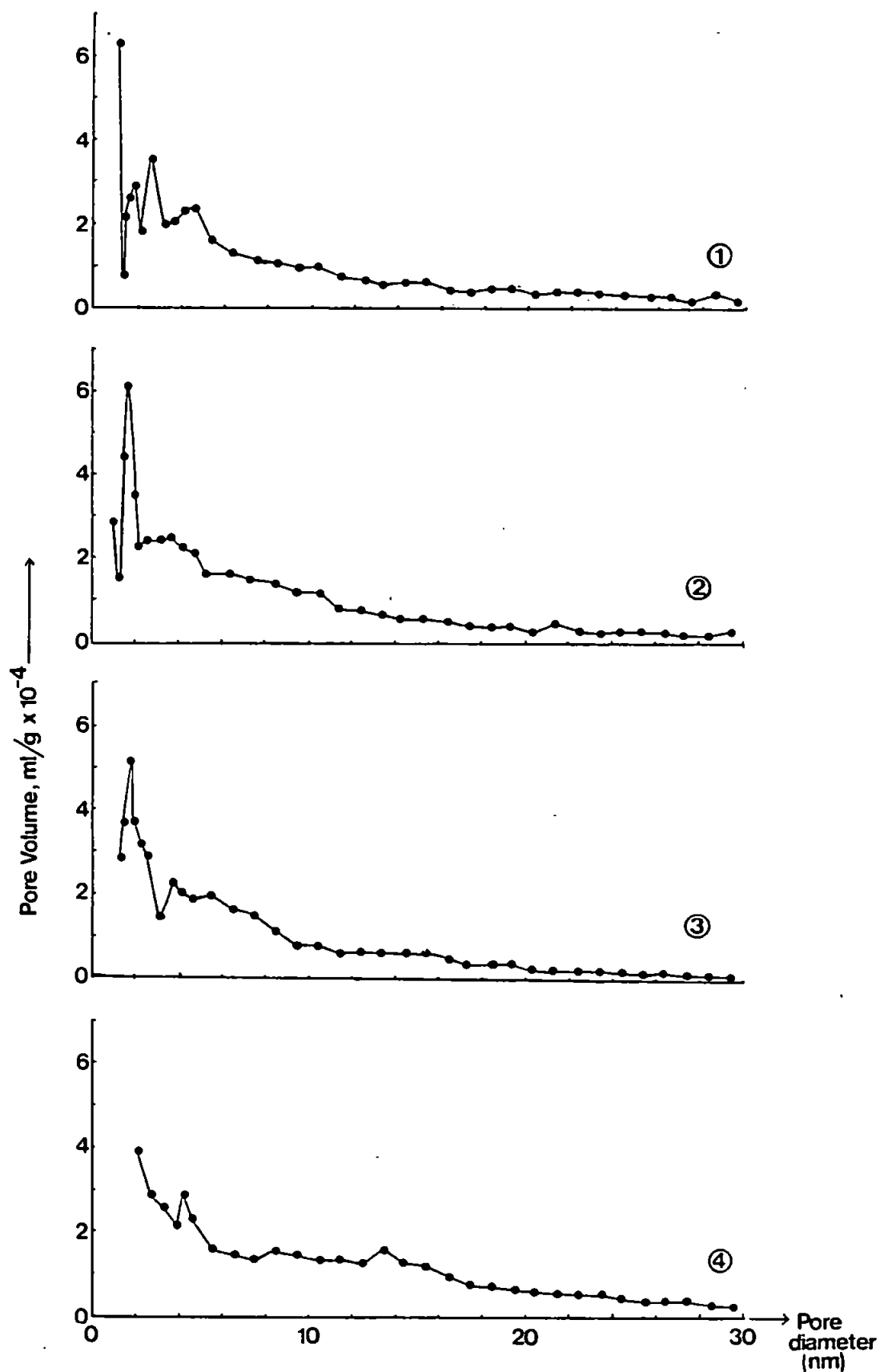
Figure 2.18: Plots of pore volume versus pore diameter calculated using the method of Cranston and Inkley (1957). Suspended solids from the Tamar estuary. 1) Freeze dried directly and 2) DMSO protected (same sample); 3) freeze dried directly and 4) DMSO protected (same sample).

94
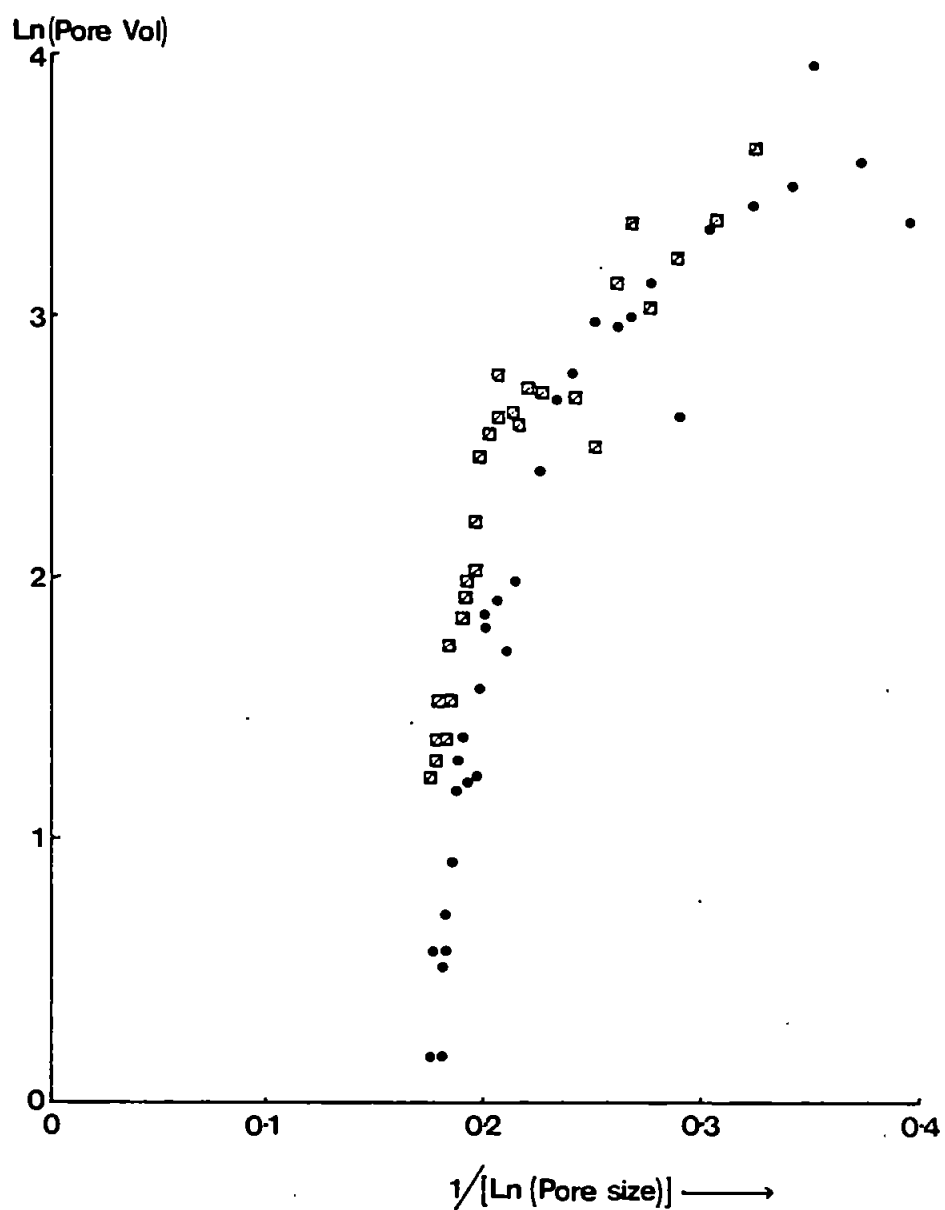
Figure 2.19: Plots of log normalized data from figure 2.18 (3&4).
●-Freeze dried directly; ▨-DMSO protected.

that were dried using DMSO as a protecting agent have surface areas

that show a marked skew in favour of larger pores with two of the

samples having no micropores. In all cases the cryogenically

protected samples have larger mean pore sizes than their equivalent

straight freeze dried samples. Statistical comparisons on the

samples dried by the different methods show that significant

differences are generated by the two preparative methods in three of

the four experiments.

Sample	Pore size nm	C&I Surface area m^2/g			Bed sediment
		Supended sediments from low salinity region of Tamar			
Freeze dried direct	<2	7.6	10.6	8.6	2.7
	2-5	8.6	5.4	8.5	2.5
	5-10	4.1	3.0	3.4	1.1
	10-20	1.6	1.1	1.7	0.6
	20-30	0.4	0.3	0.5	0.2
DMSO treated freeze dried	<2	0.0	0.0	9.7	0.0
	2-5	10.6	7.9	8.6	1.6
	5-10	4.2	3.3	4.3	1.2
	10-20	3.3	1.8	2.0	0.8
	20-30	0.8	0.5	0.5	0.2
Mean pore size nm freeze dried direct		8.51	8.00	8.11	9.91
Mean pore size nm DMSO freeze dried		9.77	10.69	8.97	12.21

Table 2.16
Surface area distributions in relation to pore size for
various samples of Tamar estuary sediment dried using two
freeze drying methods.

Plots of the log normalized data show that the reason for the differences is the skew in the pore size distributions favouring the larger pores in those samples prepared for freezing with DMSO, and this finding is consistent for all four data sets.

In conclusion, the method selected for drying of the sediments is of great importance as it is a key controlling influence on surface area and on pore size distributions. A number of approaches were examined, using pure clays and sediments, and these showed that some drying methods had a chemical effect on the particle composition, such as removal of surface organics or interactions with clay components. Tamar estuary sediment is compositionally inhomogeneous, and it is desirable to observe the contribution made to the surface microstructure by all the components in an unaltered form. Therefore drying methods that caused chemical changes to the particle surface were avoided. The principal physical effect on the particle surface by the drying methods investigated was on micropores and the smaller mesopores (pores <10 nm). Despite the critisms of freeze drying in the literature this method was selected because it caused no chemical effects on the particles, and the samples produced were finely divided and easy to obtain sub aliquots from. Work by Glegg, (1987) showed that consistent results could be obtained using the method on estuarine solids. This section also showed that attempts to protect the samples during the freezing process with DMSO produced consistently different pore size distributions which favoured larger pores, compared with straight freeze dried samples. As both techniques were self consistent and due to the logistical problems associated with use of DMSO it was decided to pursue direct freeze drying as the preparative method.

The reproducibility of the approach on samples will be considered in section 2.2.2.3. This section shows that all results obtained will be relative values and should be interpreted in terms of the preparative method employed.

2.2.2.3 Reproducibility of Microstructural Analyses on Estuarine Samples

The reproducibility of both BET surface area measurements and pore size distribution analysis was examined on freeze dried portions of estuarine sediment using the vacuum microbalance. Reproducibility studies were necessary because the particles under analysis were of highly variable composition; made up of quartz grains, aluminosilicate clays, Fe/Mn oxides, organic detritus and biogenic debris. Earlier work by Glegg (1987) on estuarine solids has shown that for ten replicate analyses of surface area on freeze dried estuarine solids the co-efficient of variation was ±10%. In this study, bed sediment samples were collected by surface scrape from the mid-estuarine region of the Tamar estuary; and fractionated across a 45 μm sieve (Endecotts Ltd). Both fractions were filtered across a membrane filter (0.45 μm pore size), washed thoroughly with deionized water to remove salt; and then freeze dried. Eight replicate analyses of surface area were then carried out on each portion and the results are shown in Table 2.17. The co-efficient of variation for the two samples is very low at ±5.1% for the <45 μm fraction and ±3.5% for the >45 μm size. The mean surface area results (10.36 and 10.67 m²/g) are significantly different (at 99.5% probability) from each other. These results show that fractionation

98

by sieve and freeze drying of natural samples give surface area results with excellent reproducibility and therefore can be used to make statistical inferences and comparisons with confidence.

Replicate analyses of porosity on estuarine samples was also undertaken using the C&I model. A surface scrape of settled sediment from the low salinity region of the Tamar estuary was collected and then resuspended (by rapid stirring) in two litres of distilled water held in a settling tube.

BET surface area m²/g	
<45 µm	>45 µm
10.40	11.20
10.33	10.96
9.70	10.63
10.43	10.14
10.24	10.86
11.43	10.91
9.70	10.26
10.34	10.38
10.59	10.49
---	10.94
10.36 ±5.1%	10.67 ±3.5%

Table 2.17
Results of replicate BET surface area analyses carried out on Tamar Estuary sediment.

The sediment was allowed to settle for five minutes and then the fine material still in suspension was abstracted and the coarser, denser material was left settled. Both portions were retained, filtered, and then frozen prior to analysis. BET surface area measurements and full adsorption/desorption isotherms were performed

on four separate aliquots of the fine fraction. This was to
determine the reproducibility of pore size distribution analyses on
freeze dried estuarine sediment, and also to provide a reference
estuarine solid which could be used to compare the surface area and
porosity of other samples with. Statistical analysis undertaken on
the replicated pore size analyses of the suspended sediment fraction
showed no significant differences between the individual aliquots.
The best fit regression line obtained from the pooled data (log-
normalized) of the four analyses is shown in Figure 2.20 and the
surface area distributions from the porosity are presented in Table
2.18.

Pore Size, nm	% of Total Surface Area	Total pore Vol, ml/gx10^{-3}
<2	7.9	23.6
2-5	58.2	--
5-10	22.3	--
10-20	9.1	--
20-30	2.5	--

Table 2.18
Surface area distributions within the pore network of the standard
estuarine solid.
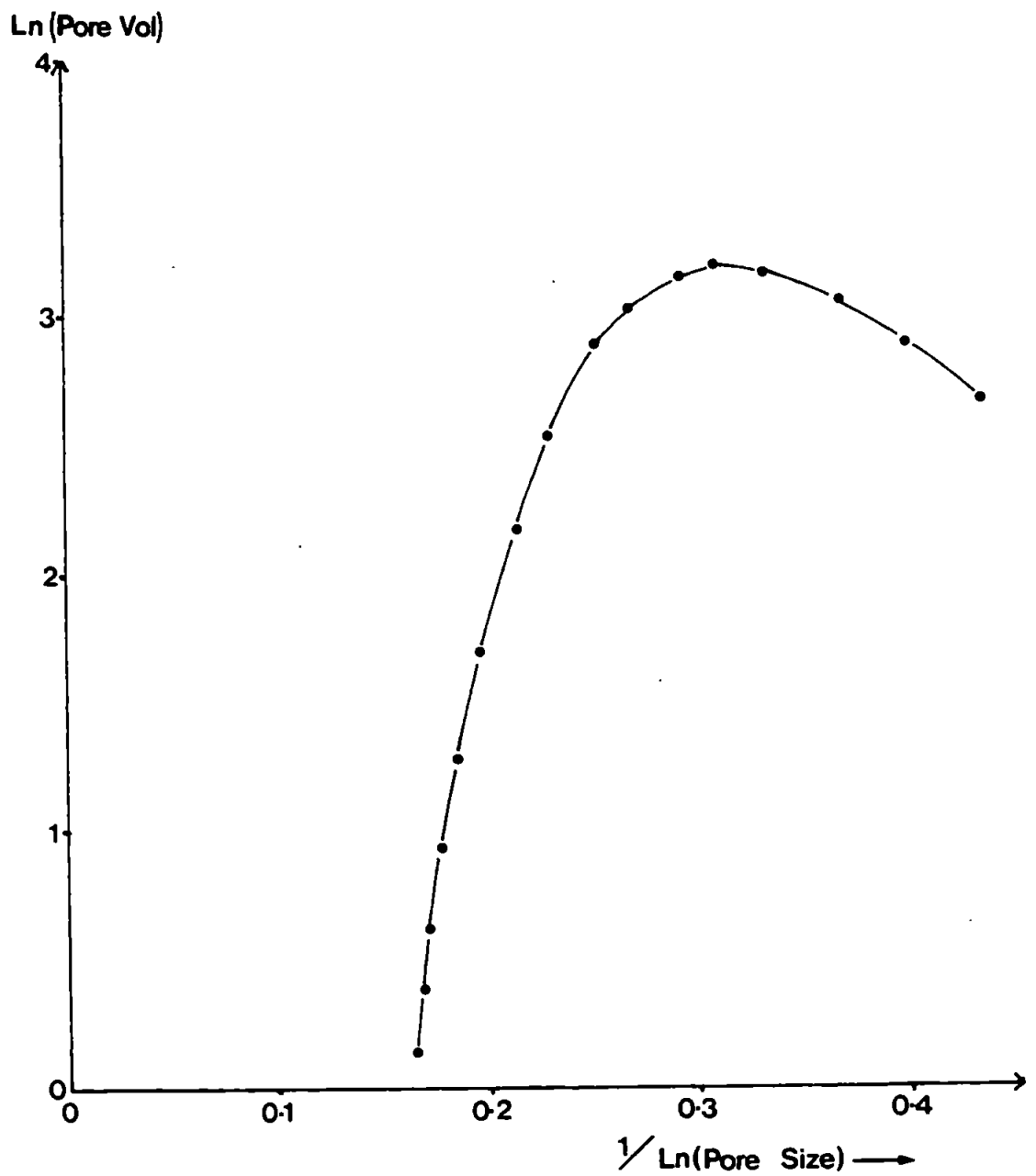
Figure 2.20. Best fit regression line through the pooled data
obtained from 4 aliquots of sediment from the Tamar Estuary.

2.2.2.4 Sample storage

The problem of aging of samples following collection and prior to analysis is addressed here. Two potential difficulties can arise and affect the results; firstly changes to particles following collection but prior to filtering, and secondly the aging of particles once freeze dried and ready for surface area analysis. During axial surveys of suspended solids in the Tamar, often bulk samples totalling 150 litres were collected, requiring some standing time prior to filtering. Glegg (1987) has shown that over a 48 hour period after collection suspended solids (from the Tamar) can lose 15-20% of their surface area due to aggregation processes taking place. In this work filtration of all samples was therefore completed within this time period. Following filtration, samples were redispersed in distilled water (40 ml) and stored frozen at -18°C. After drying samples were kept under partial vacuum in anhydrous conditions to minimize aging which can occur in humid atmospheric conditions. Water vapour in the atmosphere can adsorb onto the particle surfaces and through surface tension effects encourage particle aggregation and closure of micropores on the solid surface. Time trials showed slight loss in surface area of dried particles (5%) stored under vacuum for 45 days, and other experiments revealed that samples exposed to the atmosphere over longer time periods (upto 6 months) lost 30% of their surface area (Millward and Titley, 1985). In this study the aging effect was minimized by keeping the samples frozen prior to analysis and once dried samples were stored under vacuum in a dessicator and surface area determinations were completed within 7-10 days.

2.3 INVESTIGATION OF PARTICLE COATINGS

2.3.1 ORGANIC CARBON

2.3.1.1 Carbon Hydrogen and Nitrogen Analysis

Carbon, hydrogen and nitrogen (CHN) analyses were undertaken on a large number of samples collected from both Restronguet Creek and the Tamar estuary. The total CHN content was determined combustimetrically using an automated Carlo Erba Elemental Analyser, (Model 1106). Samples (2-8 mg) were combusted in a furnace under highly oxidising conditions, then reduced to nitrogen, carbon monoxide and water over hot copper metal before separation chromatographically. N_2 elutes first followed by CO and then water. Freeze dried aliquots of estuarine sediment were weighed out into acetone washed tin capsules on a Cahn Automated Electrobalance and then put into the carousel from which samples were automatically introduced into the furnace. Approximately 10 blanks and 20 standards of ultra-pure acetanilide (71.09% carbon, 6.71% hydrogen, 10.36% nitrogen) were included per 100 samples. Due to the inhomogeneous nature of the sediment and the small subaliquots used, at least five replicates of each sample were analysed during the runs, and the average value taken. The precision of the instrument is ±0.2% for carbon (Carlo Erba) and on freeze dried estuarine sediment Glegg (1987) showed that the co-efficient of variation on 10 replicate aliquots was ±2.7% for carbon, Freeze drying of samples prior to organic carbon analysis has received some criticism, due to the possibility of contamination by back diffusion of pump oil droplets into the drying chamber (Vazquez-Lopez et al., 1982). This possibility was investigated by comparing the

103

carbon content of Supreme China Clay (100% kaolinite) before and after freeze drying. The mean carbon content of four aliquots of clay prior to freeze drying was found to be 0.024%; following freeze drying the mean carbon content was 0.028%. Therefore it appears that contamination from this source is negligible. Calibration curves obtained from the standards included in the run were used to calculate the CHN content in the samples, and the results were then presented as a percentage by dry weight of sediment.

2.3.1.2 Removal of Organic Coatings by Hydrogen Peroxide

Oxidative digestion of organic carbon by H_2O_2 was undertaken to assess the role of carbon on particle microstructure. Initially 1g of sample was reacted with 30% v/v "AnalaR" grade H_2O_2 and 0.05M HCl (Tessier et al., 1979) at 80°C for 2h. Under these conditions excessive frothing and material loss occurred. Subsequent experiments used 6% v/v H_2O_2 solution over a 24h period to improve digestion efficiency, although it was found that even after this time interval some carbon remained (Glegg et al., 1987). After digestion samples were washed with distilled water, filtered and freeze dried. BET surface areas, pore size analysis and CHN measurements were made on the digested sediment and compared with untreated samples to assess the effects of organic carbon coatings on porosity. To determine the contribution made by disaggregation of particles on changes in BET surface area during H_2O_2 digestions, kaolinite samples of known surface area and carbon content were subjected to a hydrogen peroxide digestion, and the carbon content and surface area reassessed afterwards. The data obtained from this

104

will be included in the results section.

2.3.2 INVESTIGATIONS OF HYDROUS OXIDE COATINGS

2.3.2.1 Leaching methods and analysis

The leaching of hydrous oxide coatings of Fe, Mn and in some cases
Al was attempted in order to identify their role on particle
surfaces. The presence of fresh and crystalline Fe oxyhydroxides on
precipitated materials and soils have a significant effect on both
surface area and porosity (Marsh *et al.*, 1984; Crosby *et al.*, 1983;
Borggaard, 1982). Two leaching methods were used to isolate hydrous
oxide phases. The first used glacial acetic acid, and the second
involving a more selective approach used a solution of EDTA.
Extractions using the first method took place using a 10-20 ml
solution of 0.05M hydroxylamine hydrochloride in 25% (v/v) acetic
acid (Tessier *et al.*, 1979; Chester and Hughes, 1973) with
approximately 0.5g of sediment. Leaching was allowed to continue
for 15h before the solids were recovered by filtration, washed with
deionized water and frozen prior to surface area analysis. The
filtrate was collected in acid clean volumetric flasks for
determination of Fe, Mn and Al content by flame atomic absorption
spectrophotometry. The second extraction procedure used 0.1M EDTA
at pH >7.5 for 85 days (Borggaard, 1979; 1976), since this approach
can selectively remove amorphous iron oxides from soils. The
leaching solution was made up from 0.1M "AnalaR" grade EDTA (di-sodium
salt) and 5% "AnalaR" grade formaldehyde (BDH chemicals) in 1000 ml
of deionized water. The pH was manipulated into the appropriate
range by dropwise addition of NaOH. Leaching was allowed to proceed

105

for 85 days at approximately 1:50 solid:solution ratio. The solids
were recovered by filtration and washed with deionized water (pH>9)
prior to freeze drying and surface area analysis. The filtrate was
collected in acid cleaned volumetric flasks ready for analysis.
Triplicate procedural blanks were run as part of the the experiment
to ensure cleanliness and that no contamination occurred. The
filtrates from the leaching experiments were analysed using an
Instrumentation Laboratory Flame Atomic Absorption Spectrophotometer
(Model 151A) at wavelengths of 248.3 nm (Fe), 279.5 nm (Mn) and
309.3 nm (Al). An air-acetylene burner head was used for Fe and Mn
determinations and a nitrous oxide burner for Al. Calibration
curves were obtained for each element using standard solutions
prepared from "AnalaR" grade solid salts dissolved in acidified
distilled water. Samples were diluted as necessary to keep the
signal within the linear range of the calibration curves; these were
then used to calculate the metal concentrations in solution.
Background corrections for the Fe determinations (on the Flame
A.A.S) were initially made to ascertain whether significant interfe-
rences were occurring at the lowest wavelengths used (Fe; 248.3 nm).
Iron determinations were made on ten solutions without background
correction and then repeated with the correction. Statistical
analysis on the data revealed that the two sets of results were not
significantly different (Table 2.19), and in view of this and also
the added difficulty of carrying out analysis using background
correction on the Flame A.A.S. it was not employed in any other analyses.

One final study was undertaken to determine if the sieve
fractionation process employed on many estuarine sediment samples
was contributing to the leachable Fe/Mn content of the sediment.

The study was undertaken using 5 samples of pure kaolinite, which were divided into two aliquots. One of the aliquots was subjected to the acetic acid leaching method and the

Iron content mg/g	
With background correction	Without background correction
11.92 ±1.447	12.63 ±1.553

Table 2.19
Iron determinations on Tamar estuary sediment (mg Fe/g sediment) showing results obtained on a Flame A.A.S; with and without using background correction.

amount of Fe and Mn removed was determined. The other portion was wetted in distilled water and then passed through a 45 μm sieve (Endecotts Ltd). The clay particles were then leached using acetic acid and the amounts of Fe/Mn removed determined.

2.3.2.2 Iron and Manganese Oxide Precipitation Experiments

A series of studies were undertaken designed to investigate the role of Fe and Mn oxide precipitates on the surface area and porosities of estuarine particles. A buffered system of deionized water (25 litres) was made by the addition of 1.8g $NaHCO_3$ (per 10 litres) and air was bubbled through to establish a pH equilibrium system. The pH of this solution was then altered to 7 ±0.5 by addition of NaOH or HCl. Once the appropriate pH was established, dissolved Fe (50 ml; 0.05M $FeCl_3$ in acidified deionized water), was added to the buffered water and the Fe was observed to precipitate immediately.

The precipitate was allowed to age for 24h whilst still in the bulk

buffered water system. At set time intervals during this period

aliquots of the bulk solution were abstracted, filtered and

the filtrate was analysed for dissolved Fe content by flame A.A.S.

After 24h the bulk sample was filtered and the precipitate was

repeatedly exchange washed with acetone before drying prior to

surface area measurement and porosity analysis. The precipitation

experiment was repeated in the presence of dissolved Mn (at a range

of concentrations) which was introduced to the buffered water system

before the iron solution was added in order to observe co-

precipitation. The solid precipitate was recovered by filtration

for analysis after 24h aging.

2.4 PHOSPHATE SORPTION EXPERIMENTS

2.4.1 EXPERIMENTAL DESIGN AND ANALYSIS

2.4.1.1 Sample collection

Sorption experiments were carried out by introducing particles from

the Tamar estuary into a range of water types and observing the

changes of the water composition with time. Suspended solids were

collected from the low salinity, high turbidity region of the Tamar

and Humber estuaries. Samples of turbid brackish water (100 litres,

salinity ≤1% , turbidity 150-300 mg/l) were collected on three

occasions using polyethylene carboys pre-rinsed in deionized water

and in sample water. Suspended solids were recovered by pressure

filtration through Sartorius (0.45 μm pore size) membrane filters.

The filtered samples were carefully removed from the filter

membranes and resuspended in 1 litre of deionized water and stirred

for 2h until the solids were fully redispersed and homogenized. Aliquots of this solution (50 ml) were then abstracted into 20 polyethylene pots and stored at low temperature prior to use in the mixing experiments. This approach reduced the problem of turbidity variations in the mixing experiments caused by the difficulty of consistently abstracting the same amount of solid from the original bulk sample.

Natural waters in which the majority of the mixing experiments took place were collected from the low salinity regions of the Plym estuary and from Plymouth Sound. Samples were filtered immediately on return to the laboratory, using the pressure filtration unit (described in Section 2.2.1) and 0.45 μm membrane filters. The filtration gear was initially flushed through with deionized water and then a small amount of sample before filtration commenced. Samples were collected less than 96h before the start of mixing experiments; in each run 2.0 litres of water were used in both the reactor vessel and in the simultaneously run control. Up to 50% of water in the reactor vessel was removed in the "run"; the water being abstracted by syringe in 20 or 50 ml aliquots. Phosphate concentrations in the natural samples were generally in the range 1-100 μM/l, the highest values were in the low salinity regions of the Plym estuary. Sea water samples collected were spiked with orthophosphate ions to raise levels to nearer those encountered in the mid-estuarine sections of the Plym. Prior to the start of sorption modelling experiments the pH of the aqueous samples was controlled within the range 6-8 ±0.2 (as required) to observe the effects of different pH values on the sorption behaviour of phosphate. In some experiments, deionized water was used and a pH

buffering mechanism was established in these water samples as
described in section 2.3.2.2. The pH was then manipulated into the
desired range by dropwise additions of 5M 'AnalaR' HCl or NaOH.

2.4.1.2 Design of Mixing Experiments

The reactor vessels used to contain the mixing experiments were 2
litre acid cleaned Pyrex glass beakers, that had been pre-rinsed
with deionized water and sample prior to the experiment start.
Fresh sample was then introduced into the vessel and allowed to
equilibrate with the container for several hours (with continuous
stirring) before the mixing experiment commenced. Temperature and
pH were monitored continually prior to and during the sample runs.
A procedural blank was run alongside the mixing experiment to act as
a control to ensure cleanliness of the procedures and that any
contamination was detected. Individual 50ml aliquots of the frozen
particles (collected and prepared as outlined in Section 2.4.1.1)
were thawed out at ambient temperature and allowed to equilibrate
for several hours prior to introduction into the mixing vessel at
time t_0. Excess water from round the thawed particles was discarded
so that a minimal change in volume of water in the mixing vessel
occurred when the particles were introduced. A few minutes before
t_0, 3 subaliquots of sample were removed from the reactor vessel and
from the control to determine the starting concentrations. Samples
were abstracted using Millipore 20 ml or 50 ml syringes, and then
filtered through Millipore "Swinnex" 25 cm filter holders containing
0.45μm (pore size) membrane filters (Millipore or Sartorius).
Syringes and filter holders had been scrupulously cleaned prior to
use with 5M HCl followed by two rinses in deionized nanopure water.

110

Filter holders were assembled using gloves and the filters and seals located with acid cleaned tweezers. The assembled filter holders and syringes were stored in polythene bags and handled only with gloves or tongs. The open beakers in which the mixing experiments took place were covered over with polythene to prevent aerosol contamination. The mixing experiments were kept in continuous suspension using acid cleaned plastic coated magnetic stirrer bars and stirrer mounts. Transfer of heat from the mount to the reactor vessel was minimized by supporting the reactor vessels about 5 mm above the stirrer plate; the temperature of both mixing vessels was observed to vary about ±1.5°C.

At time t_0 particles were introduced into the reactor vessel and subsamples were removed in quick succession over the first 10 minutes to monitor any initial rapid reactions. Sampling frequency was gradually reduced with time and replicates at each time interval were taken when logistics allowed. Samples from the control reactor vessel were taken at 30 minute intervals initially so as not to interfere with the requirement for rapid sampling of the mixing vessel during the initial phase. Sampling frequency of the control was matched to that of the mixing experiment as the sampling frequency was reduced. The turbidity of the mixing experiments were assessed gravimetrically by abstracting (in triplicate) 100 ml aliquots of the suspension and filtering them through preweighed "Whatman" filters. The solids were oven dried at 50°C on the papers and reweighed. The mean turbidity of 15 mixing experiments was calculated and found to be 361 p.p.m. with co-efficient of ±20%, which shows reasonable reproducibility considering the difficulties

associated with work using particle suspensions. Phosphate concentrations in the abstracted filtered samples were determined by a colorimetric method.

2.4.1.3 Phosphate Analysis

The filtered 20 or 50 ml aliquots withdrawn from the reactor and control vessels were collected in acid cleaned glassware and then analysis was undertaken using the Molybdenum Blue complex single reagent method (Strickland and Parsons, 1972). The reagent was made up from "AnalaR" grade chemicals; ammonium molybdate, sulphuric acid, ascorbic acid and potassium antimonyl-tartrate; mixed together at the appropriate concentrations and in the required proportions. Reagent was added to the samples in the ratio reagent:sample 1:10 (v/v) and the colour was allowed to develop for 10 minutes (with slight warming). An LKB Spectrophotometer (Model 4051) was used to detect the absorbance of the coloured molybdenum complex at a wavelength of 885 nm (using 1 cm or 5 cm cells). Calibration of the system using a range of standards containing dissolved phosphate revealed the working linear range of the technique with the two cells. For most concentrations 1 cm cells were appropriate, and dilution of some Plym estuary samples were required to keep the absorbances within the linear range of the technique. Reagent blanks in nanopure deionized water (1:10 dilution, reagent:water v/v) were used to zero the spectrophotometer prior to analysis. The co-efficient of variation of the LKB spectrophotometer was found to be <1%, this being determined by 10 replicate analyses on the same reagent/sample mixture. Crosby (1982) showed that the co-efficient of variation of the complete method was ±6%. In this study the co-

efficient of variation of the complete analytical procedure was assessed using 10 aliquots of Ouse river water and found to be ±4.2%.

CHAPTER THREE

THE MICROSTRUCTURES OF BED SEDIMENTS IN ESTUARIES.

This chapter describes the microstructural features of bed sediments
collected from the Tamar Estuary and from Restronguet Creek.
Sediments from the iron rich Keithing Burn were also examined.
Keithing Burn is an example of an aquatic system that is dominated
by an acid mine stream, and it was chosen to assess the effect of
high Fe levels on the particle microstructures. This latter
investigation provided an opportunity to determine the relationship
between particle microstructure and surface charge and was carried
out jointly with P. Newton and P. Liss of the University of East
Anglia.

In Chapter 2 it was shown that the N_2 gas sorption method can be
used to assess the morphology of estuarine solids which have been
removed from their natural environment. It was also clearly
demonstrated that the method could be used to make inter and intra
estuarine comparisons of these properties provided the particles
were prepared in a consistent way.

In this Chapter the microstructures of bed sediments were
investigated using the methods described in Chapter 2. The work
concentrated on quantitative analysis of the surfaces of the
particles (surface areas and porosities) collected from the
intertidal mudflats in the two Estuaries. Chemical characteristics
of the sediment, especially coatings of Fe/Mn oxides and organic
matter were examined to isolate any relationships between these
coatings and particle microstructures.

3.1 RATIONALE

Initial examination of estuarine particles by scanning electron microscopy (S.E.M.)(see Plates 3.1-3.6), reveals that the particles are aggregates of smaller materials and are highly irregular in both size and shape. The particle surfaces appear extremely rough with an extensive pore network, and with increasing magnification the morphology of the individual components of the aggregates can be discerned. At very high magnification (>2000 times) there is a loss of resolution and many microscale features on the particle surface remain undetected. Furthermore, it is not possible to fully characterise the porosity observed under the microscope because of the tortuosity of the pores, which conceal many microscale features. The S.E.M. cannot therefore be used to observe pores in the nanometre size range.

The N_2 gas sorption method used in this work is able to resolve many of the features that normally remain undetected using an electron microscope. The small size of the adsorbate gas molecule (0.162 nm^2) allows probing of micropores, and the method yields quantitative information about surface area and porosity for pores in the size range 1-30 nm (Cranston and Inkley, 1957).

The porosity and internal surface area of the particles detected by both the electron microscope (see Plates 3.1-3.6) and the gas sorption method, may play a significant role in aquatic chemistry. Persistent uptake of dissolved species on to particle surfaces over long time scales has been reported, (Li *et al.*, 1984; Nyffeler *et al.*, 1984) which can be ascribed to the diffusion of ions through

115

PLATE 3.1:

An electron micrograph of a solid (resuspended on the outgoing tide)
collected from Restronguet Creek.

Salinity: 3.6 °/oo
Fe content: 30 mg/g, (Acetic Acid Leach). Fe:Mn ratio: 190.
BET surface area: 21.6 m^2/g

Magnification: 35

PLATE 3.2

Sample as above.

Increased magnification reveals the largest of the pores (30 μm) and
the highly irregular surface which suggests that aggregation is an
important process.

Magnification: 350
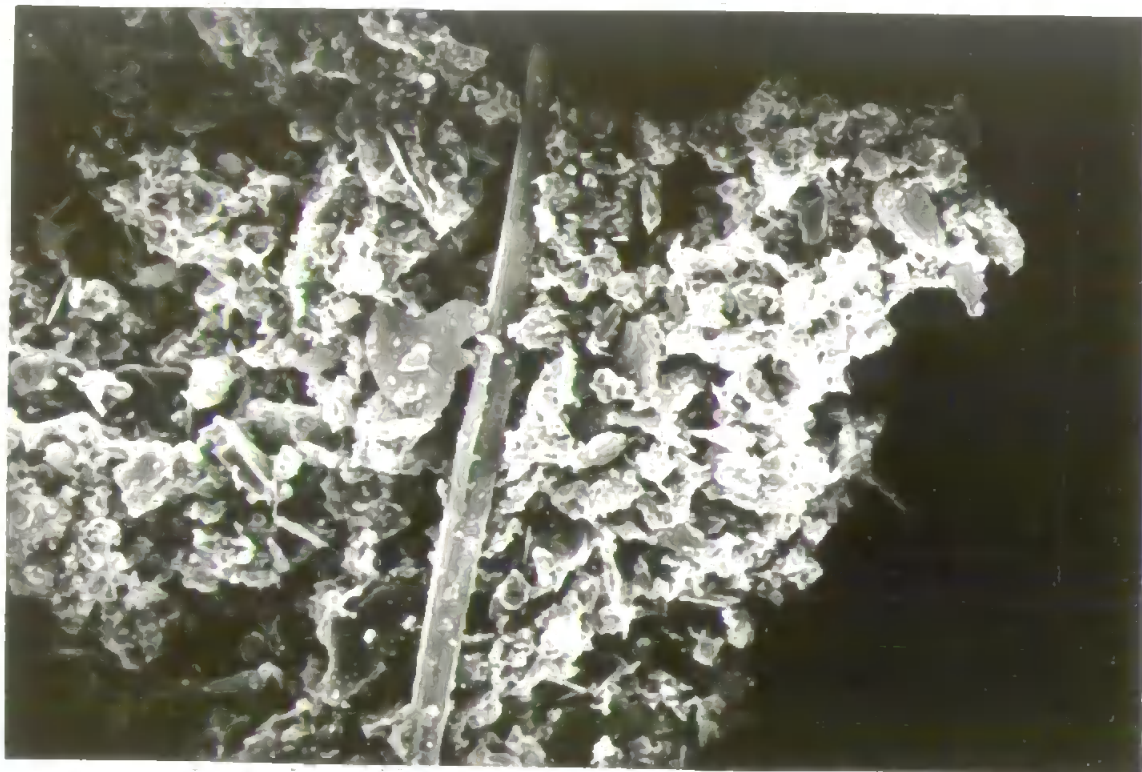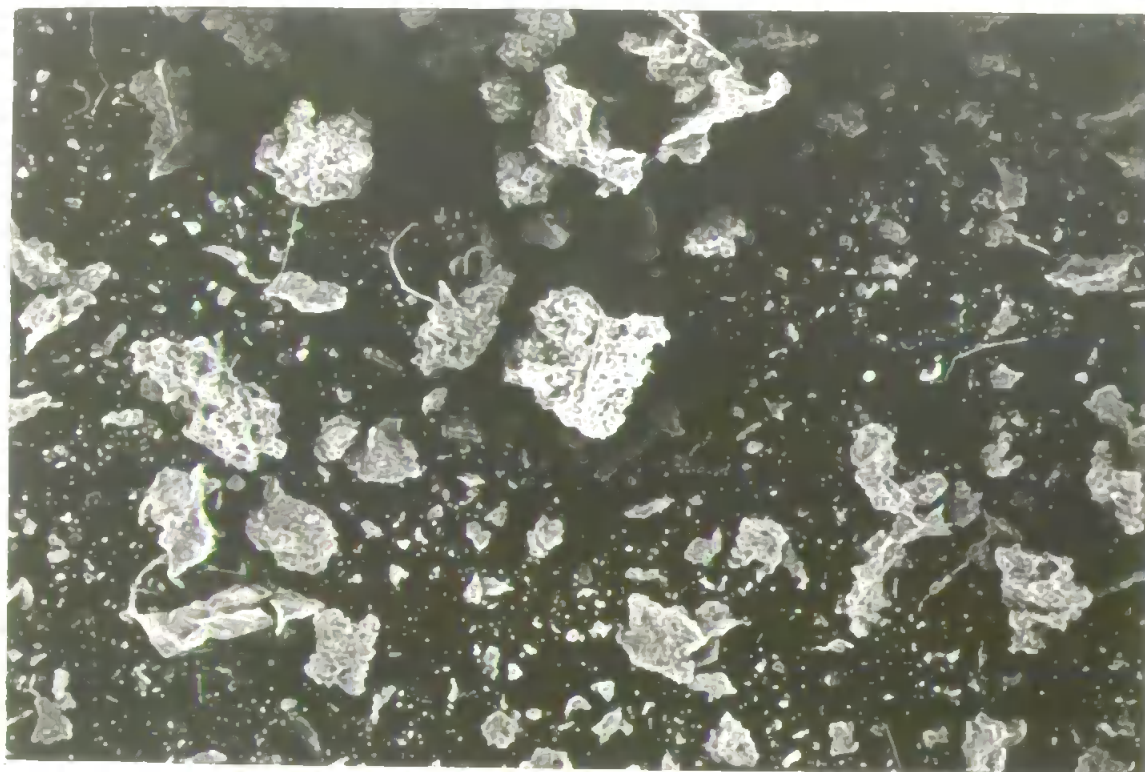
PLATE 3.3

Sediment from Restronguet Creek resuspended on the out going tide
shown in Plates 3.1 and 3.2. The electron microscope has closed in
on the central rod like structure visible in Plate 3.2. The BET
method is able to assess structures 1/1000 of the size of those
resolved at this magnification.
Platey clay-like structures are visible as are minute accretions
presumably of Fe.

Magnification: 2000

PLATE 3.4

An electron micrograph of a sample of bed sediment from the Tamar
Estuary.
The sediment shown was separated through a nest of sieves and this
material has a grain size in the range 45-63 µm.
The large feature on the right of the photograph is probably a well
aggregated flocc of clay platelets. Pores of 0.5-1.0 µm diameter
are visible.
BET surface area 7.3 m²/g
Specific surface area from the grain sizes: 0.034-0.044 m²/g.

Composition: 2.78% Carbon; 0.25% Nitrogen; (C:N = 11.1)
           6.88 mg/g Fe; 0.65 mg/g Mn (Acetic Acid Leach)
           (Fe:Mn = 10.6)

Magnification: 1500

0   10 µm

0   10 µm

119
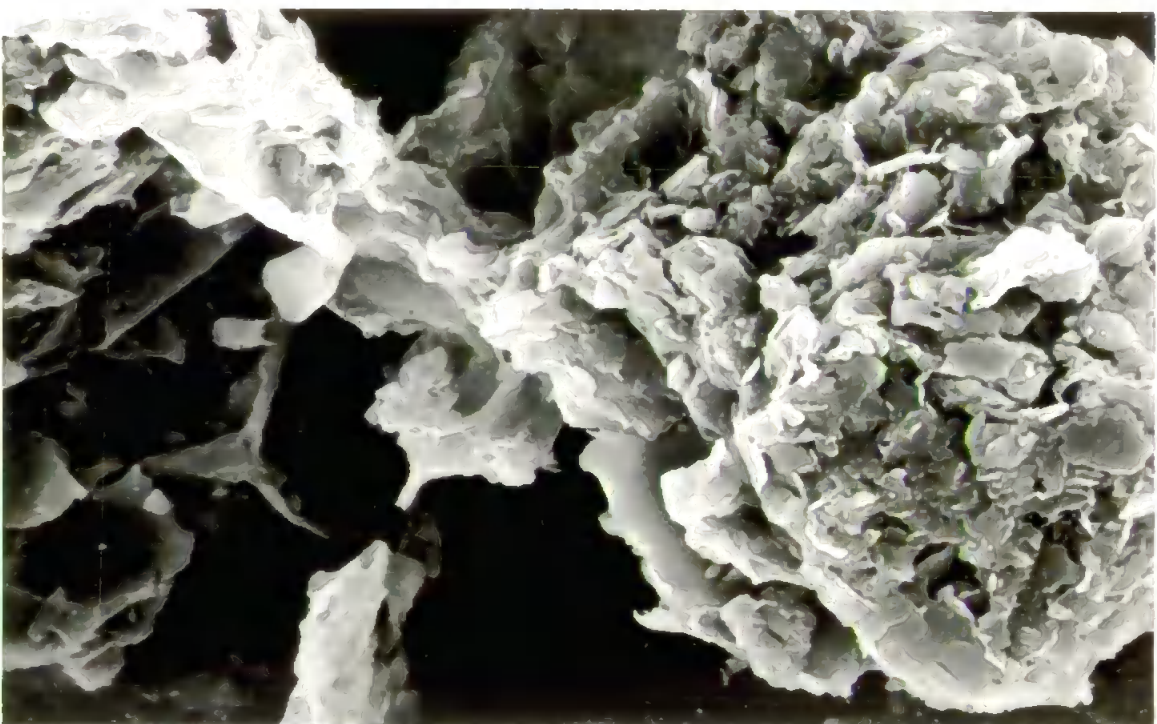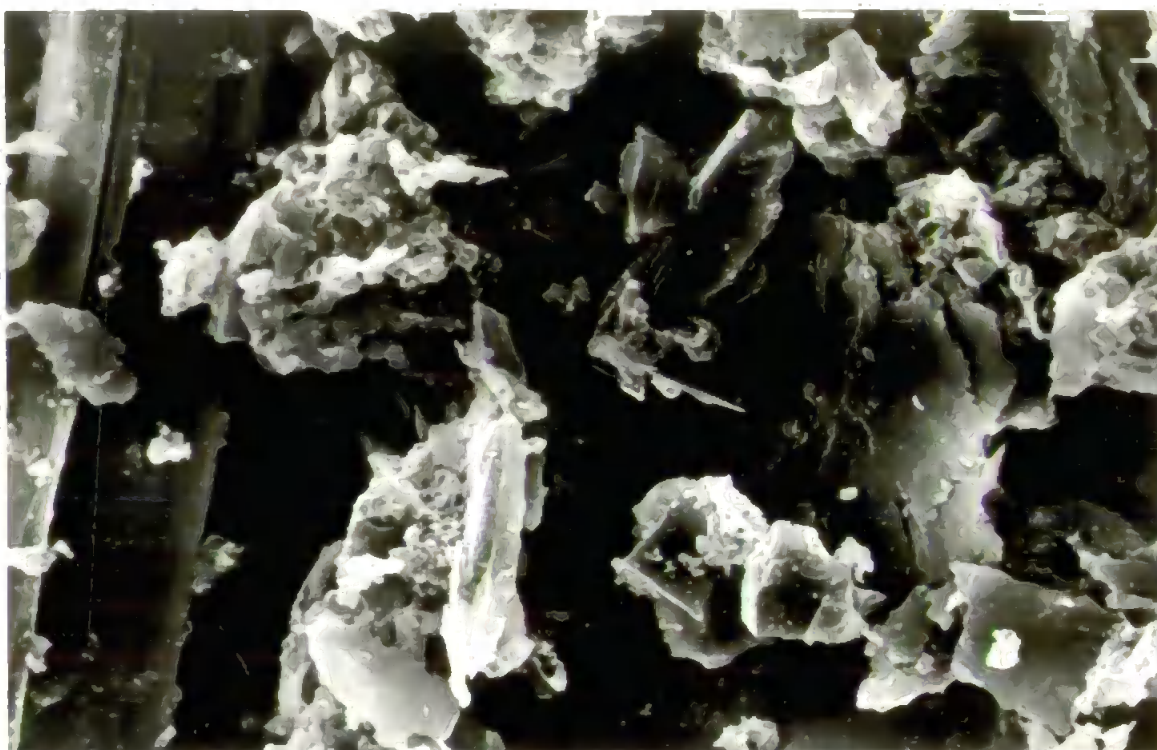
PLATE 3.5

An electron micrograph of bed sediment from the Tamar Estuary.
The sediment shown was separated through a range of sieves, this
fraction is in size range 63-125 µm.
Organic debris is apparent, in the bottom left hand corner is a fine
fibre, and top centre is a microscopic shell.
BET surface area 9.8 m^2/g.
Specific surface area calculated from the grain sizes: 0.024-0.034
m^2/g.

Composition: 3.82% Carbon; 0.282% Nitrogen; (C:N = 13.5)
            11.2 mg/g Fe; 1.3 mg/g Mn (Acetic Acid Leach) -
            (Fe:Mn = 8.7)

Magnification: 350

PLATE 3.6

An electron micrograph of bed sediments collected from the Tamar
Estuary.
Material collected was separated through a range of sieves.
Fraction shown is in the size range 125-180 µm.
In the top right of the photograph is a regular shaped solid,
possibly a particle of quartz. Centre left is an aggregate of clay
platelets.
BET surface area 10.6 m^2/g
Specific surface area calculated from grain sizes: 0.0167-0.024
m^2/g.

Composition: 10.9% Carbon; 0.64% Nitrogen; (C:N = 17.0)
            6.6 mg/g Fe; 1.4 mg/g Mn; (Acetic Acid Leach)
            (Fe:Mn = 4.7)

Magnification: 350

0 _____ 100 μm

0 _____ 100 μm

121
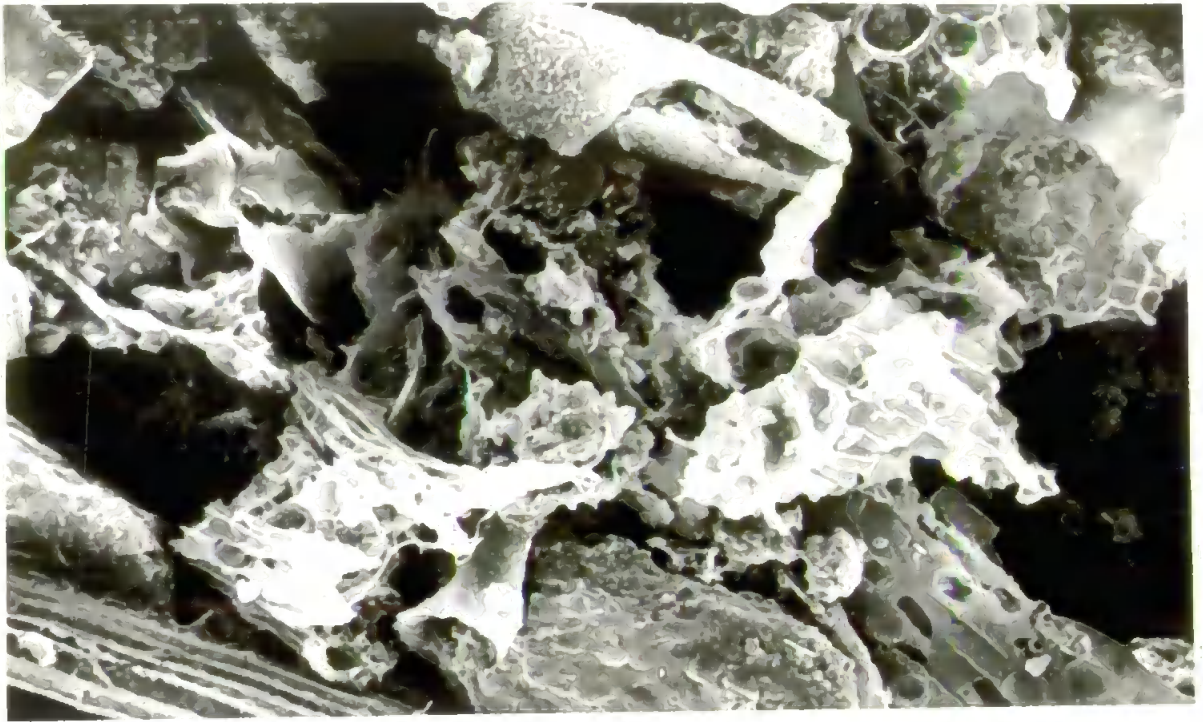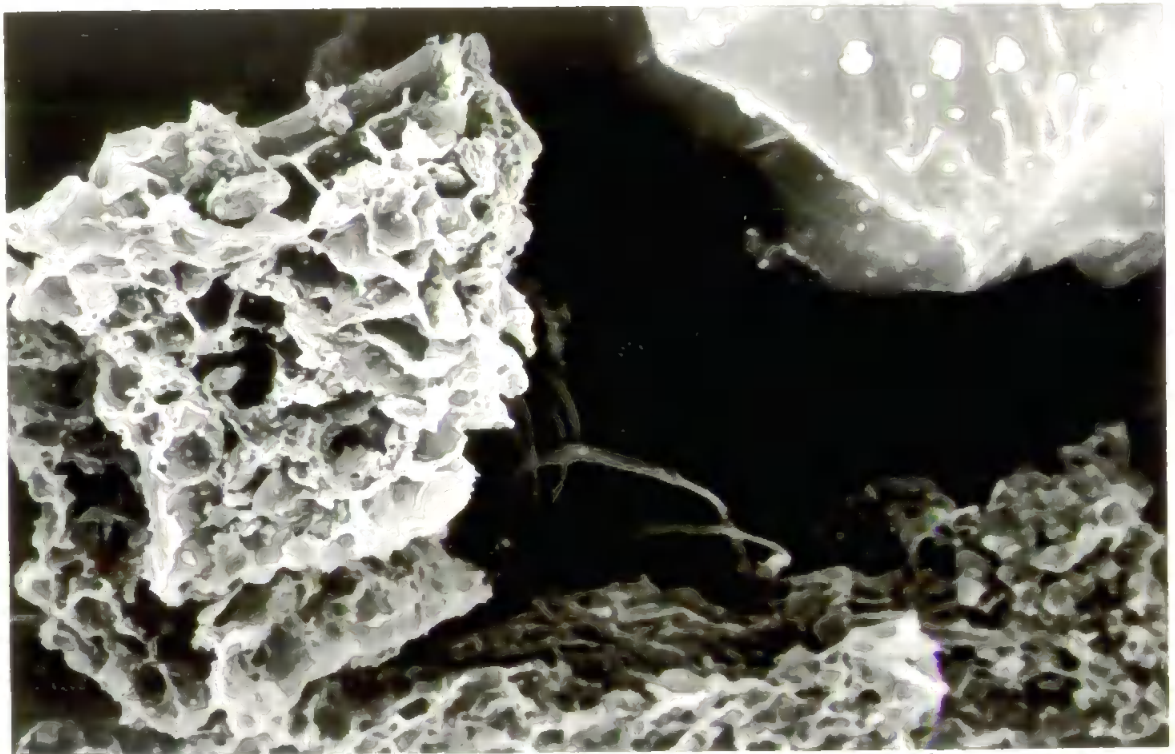
tunnelling into the meso and micropores of the particle matrix. A
substantial proportion of the total surface area of particles is
frequently located within these pores, and this internal surface is
thought to be the ultimate location of many dissolved species
adsorbed onto particles. Although efforts have been directed
towards understanding the role of particles in estuarine chemistry,
most work has centred on site specific adsorption mechanisms,
surface charge or complexation reactions e.g. Benjamin and Leckie,
(1981); Millward, (1980); Swallow *et al.*, (1980). At present
virtually no work has been done to assess the potentially large
internal surface areas that are associated with particle aggregates,
despite the qualitative evidence produced by electron microscopy,
and the impact these structures may have on sorption kinetics.

Specific surface area determinations are usually based on particle
size data, measuring only the external surface area. The results
obtained in this way are usually in the range 0.01-0.2 m^2/g (Glegg
et al., 1987) and are therefore assumed to be relatively unimportant
in determining the activity of particle surfaces. BET surface area
studies so far published are restricted to five estuaries, with
results ranging between 2.9 and 64 m^2/g. (Glegg, 1987; Glegg *et al.*,
1987; Titley *et al.*, 1987; Donard and Bourg, 1986; Martin *et al.*,
1986). The inter-estuarine variations in surface area observed may
be of great importance for understanding the unique chemical
behaviour encountered in all estuaries. Understanding the reasons
for the variation in particle surface area should therefore help
improve the overall understanding of chemical behaviour in
estuaries.

The gas sorption method desribed in Chapter 2 is a very powerful method in this respect as it can provide information about the contribution made by the individual components of the estuarine particles to the surface area and also the role played by natural coatings on particle surfaces such as iron oxides and organic materials. Estuarine particles are known to be a highly variable mixture of various materials, mostly of terrestrial origin; e.g. quartz grains, aluminosilicate clays, hydrous oxides of Fe, Mn, Al, organic matter (including solid plant matter and humics), and biogenic debris. Table 3.1 shows the BET surface areas of various

Material		BET Surface area, m^2/g.	Reference
Clays	Montmorillonite	800-840	Sposito, 1984
	Illite	93-132	Greenland and Quirk, 1962
	Kaolinite	10-75	This Work, Glegg 1987
			Weaver and Pollard, 1973
SiO_2	Quartz (SiO_2)	3.3	Martin *et al.*, 1986
	Borden sand (58% Quartz)	1.8	Curtis and Roberts, 1985
Humic Acids & Soils	Humic Acid	0.5-0.7	This Work, Glegg, 1987
	Sandy Loam Soil	35	Barrow, 1983a
	Urrbrae Soil	11*	Greenland and Quirk, 1962
	Athelstone Soil		
	<2μ, B horizon	50*	Greenland and Quirk, 1962
Fe/Mn Oxide	Haematite	36-44	Atkinson *et al.*, 1967, Madrid and De Arambarri, 1985
	Goethite	9-153	Schwertzmann *et al.*, 1985, Cornell and Schindler, 1987, Hingston *et al.*, 1972
	Lepidocrocite	14-121	Hingston *et al.*, 1972, Crosby *et al.*, 1983
	Fe Oxyhydroxide	140-300	Marsh *et al.*, 1984, This Work,
	MnOOH	400	Glegg, 1987

* H_2O_2 Treated before analysis
Table 3.1
BET surface areas of a range of materials important in estuarine particle composition.

materials contributing to estuarine particle composition.
The underlying matrix of the particles is probably composed of various clays, quartz grains, leached material from soil profiles (including humics), iron mineral phases such as goethite and hematite, and biogenic debris such as twigs and leaves in various states of decay. These materials are continually being brought into the estuary via river inputs and bank falls, and depending on the river flow may dominate the particle composition in the low salinity region of the estuary.

The specific surface area of the river-borne load might be expected to range between 3 and 50 m^2/g depending on the proportions of each phase present (see Table 3.1). At the fresh water-brackish water interface precipitation of amorphous Fe and/or Mn oxides (surface area 120-400 m^2/g)(Glegg, 1987; Crosby et al., 1984; Marsh et al., 1984) onto the particles should increase the surface area whereas coatings of precipitating organic complexes, and humics (surface area <1 m^2/g) may cover the more active Fe/Mn oxides and decrease the overall surface area. Careful removal of these coatings from the natural particles followed by surface area measurements can be undertaken to provide a further insight into the particle surfaces. This then demonstrates the potential power of the technique for assessing the activity of the estuarine particle surfaces.

Bed sediments in estuaries are thought to be important components for controlling the cycling of chemical species within the estuarine environment. In particular sediments can act as short and long term sinks for trace species including anthropogenic pollutants. Bed sediments can also release adsorbed species back into the water

column as the chemistry (e.g. redox conditions) of the sediments changes, as in the case of Mn (Morris *et al.*, 1982b). Trace species may also be partitioned at the sediment-water interface or released from sediments following their remobilization by tidal currents.

The sorption behaviour of dissolved species at the sediment-water interface requires further investigation as it is key to understanding the chemical behaviour and long term cycling including transport within the estuarine environment.

The sorptive behaviour of trace metals onto estuarine particles under natural conditions often feature two stage sorption kinetics, with an initial fast adsorption, followed by a slower more persistent uptake (Li *et al.*, 1984) and porosity at the particle surface is implicated in this mechanism. At present, work to assess the microscale features involved in these processes is limited to some surface area studies (Glegg *et al.*, 1987; Titley *et al.*, 1987 Donard and Bourg, 1986; Martin *et al.*, 1986).

Microstructural features on the surfaces of both suspended particles and bed sediments are likely to be of importance by their contribution to sorption processes, especially in terms of irreversible uptake. Given the importance of bed sediments as sinks for trace metals, surficial features on the particles that have the potential to cause the irreversible adsorption of trace species require assessing. This will therefore enable the role of bed sediments to be included in estuarine chemical models. Such a study is urgently required to improve the understanding of estuarine chemistry and the unique behaviour of individual estuarine systems.

3.2 BED SEDIMENTS IN THE TAMAR ESTUARY

3.2.1 SURFACE AREAS AND POROSITIES

Bed sediments in the Tamar were assessed for surface area and porosity by the collection of cores of material from the mid and fluvial regions of the Estuary. Surface scrapes of material were also taken from a variety of sites along the length of estuary.

The cores collected from the Tamar Estuary were segmented, separated across a 45 μm sieve and then freeze dried prior to surface area analysis. Figure 3.1 shows the results from a core collected in the mid-estuarine section. The grain size distribution throughout the core length was constant, approximately 77% of the material being <45 μm. The surface area of this fine material was 10.3 m²/g, and this was constant throughout the core length. Organic carbon may be involved in the surface coatings. In the fine fraction the organic carbon content decreased from 3.2 to 2.7% from top to bottom, suggesting that some carbon could have been mineralized in the deeper anoxic zone (i.e. below about 4 cm). These carbon values do not appear to vary enough to affect the overall surface area profile. However the coarse fraction (>45 μm) showed a consistent decrease in surface area with increasing depth, from 10.8 to 6 m²/g but this was not always accompanied by a systematic change in the carbon content which would be expected if the active surface and pores in the particles were being occluded by coatings of organic materials (Glegg et al., 1987). A closer inspection of the material at the bottom of the core showed evidence of remnants of terrestrial organic detritus, such as leaf matter, twigs and strands of grass
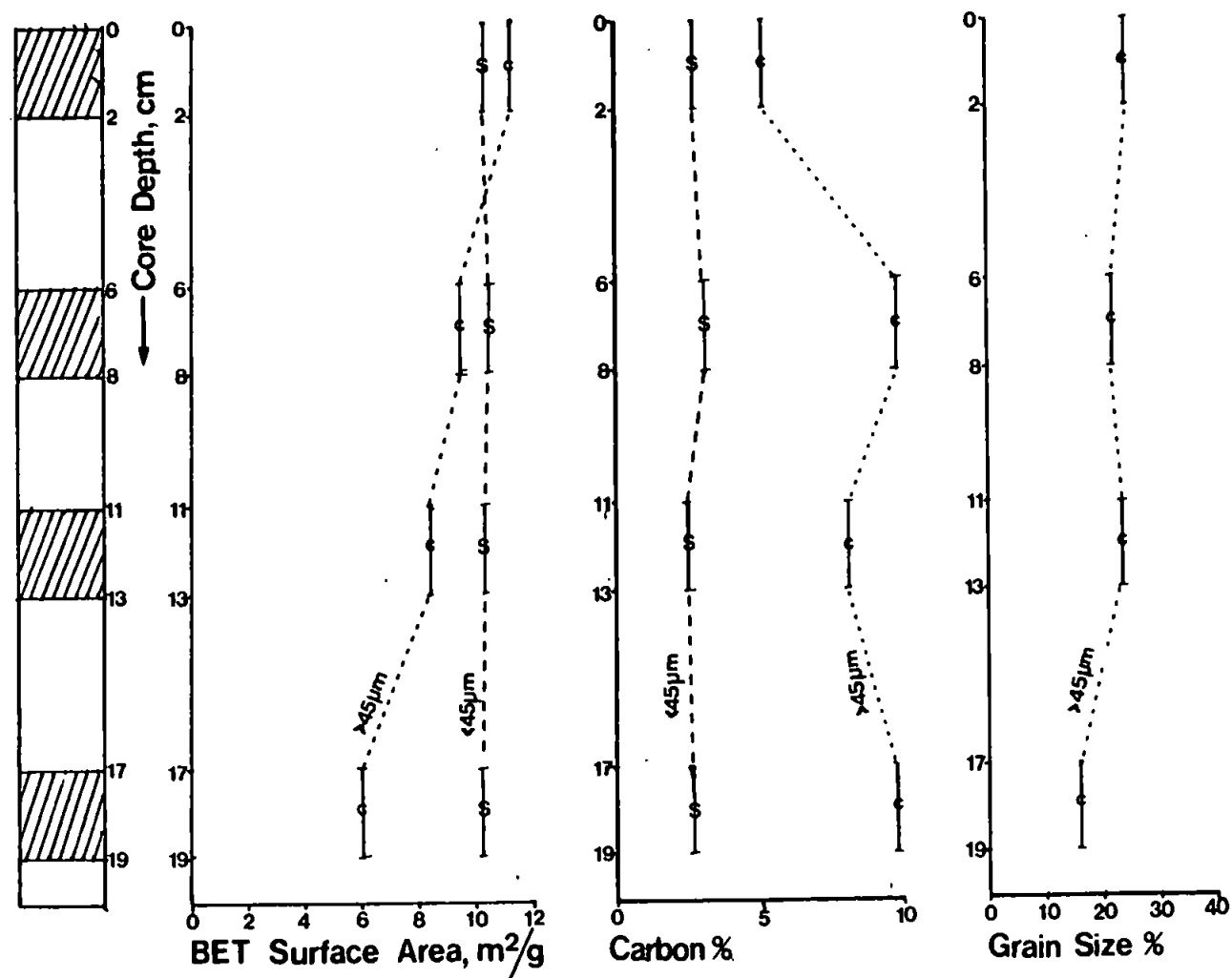
Figure 3.1. Surface areas, carbon contents and grain size distributions of bed sediments seperated across a 45 μm sieve.

which may have contributed to the low surface area of the sediment. Table 3.2 shows microstructural information obtained on a surface scrape of bed sediment material and suspended solids collected in the mid estuarine region.

Selected Samples from Mid-Estuarine Silt Minimum			
Characteristic	Bed Sediments (Surface)		Suspended Sediment
	<45 µm	>45 µm	
Surface Area, m²/g	11.2	9.8	14.2
Carbon, %	3.0	5.7	5.2
C:N	6.0	13.2	9.0

Table 3.2
Surface area and organic contents of sediments collected from the mid-estuarine section of the Tamar Estuary.

The data in Table 3.2 shows that the particle populations that make up the coarser and fine fractions of bed sediment and the suspended solids in the mid estuarine section are substantially different. This is surprising because it is often assumed that suspended solids in the water column are mainly composed of smaller fractions of bed sediment that have been resuspended by tidal action. The differences in surface areas observed between the bed sediments and suspended particles is in agreement with the higher values found by Glegg, (1987) and suggest that additional chemical processes such as flocculation are taking place that increase the surface areas of the suspended sediments.

A second core sample from the low salinity region of the Tamar Estuary was collected and prepared in the same way. The results

(Figure 3.2) are similar to the first core, approximately 80% of the material being <45 µm, with a constant surface area of 13.7 m²/g. The difference in surface area observed between the fine fractions of the two cores (13.7 and 10.3 m²/g; upper and mid estuary respectively) is real according to the analytical precision of the surface area method and can be ascribed to different physico-chemical processes at the two sampling sites in the estuary. Bed sediments collected from the low salinity region of the estuary are located in the up-estuarine silt maximum, (8-11 km down estuary of the weir) (Bale, 1987), whereas sediments collected from the mid estuarine region come from a region of silt minimum. The grain size fractions confirm this, with more material passing through a 45 µm sieve in the upper estuarine sediment ($\approx$ 83%) than in the mid estuarine region ($\approx$ 77%).

The coarser fraction (>45 µm) of the core from the upper region of the estuary showed a decline in surface area from 20 m²/g of the fluid mud near the surface, to 6 m²/g at about 30 cm depth, (see Figure 3.2) and this trend is again thought to be associated with carbon content in the sediment (Titley *et al.*, 1987). The overall surface area values of the sediment in this core are higher than in the core from the mid-estuarine section. This is probably because the sediment in the low salinity region is frequently resuspended during the tidal cycle and can exchange with the suspended material, which in this region of the estuary has larger surface areas (15-22 m²/g). The sediment collected in the mid-estuarine silt minimum was from a fairly quiescent region and was compacted (hence more aggregated) and anoxic below 4 cm suggesting that it had not been resuspended for some time. The core collected in the low salinity
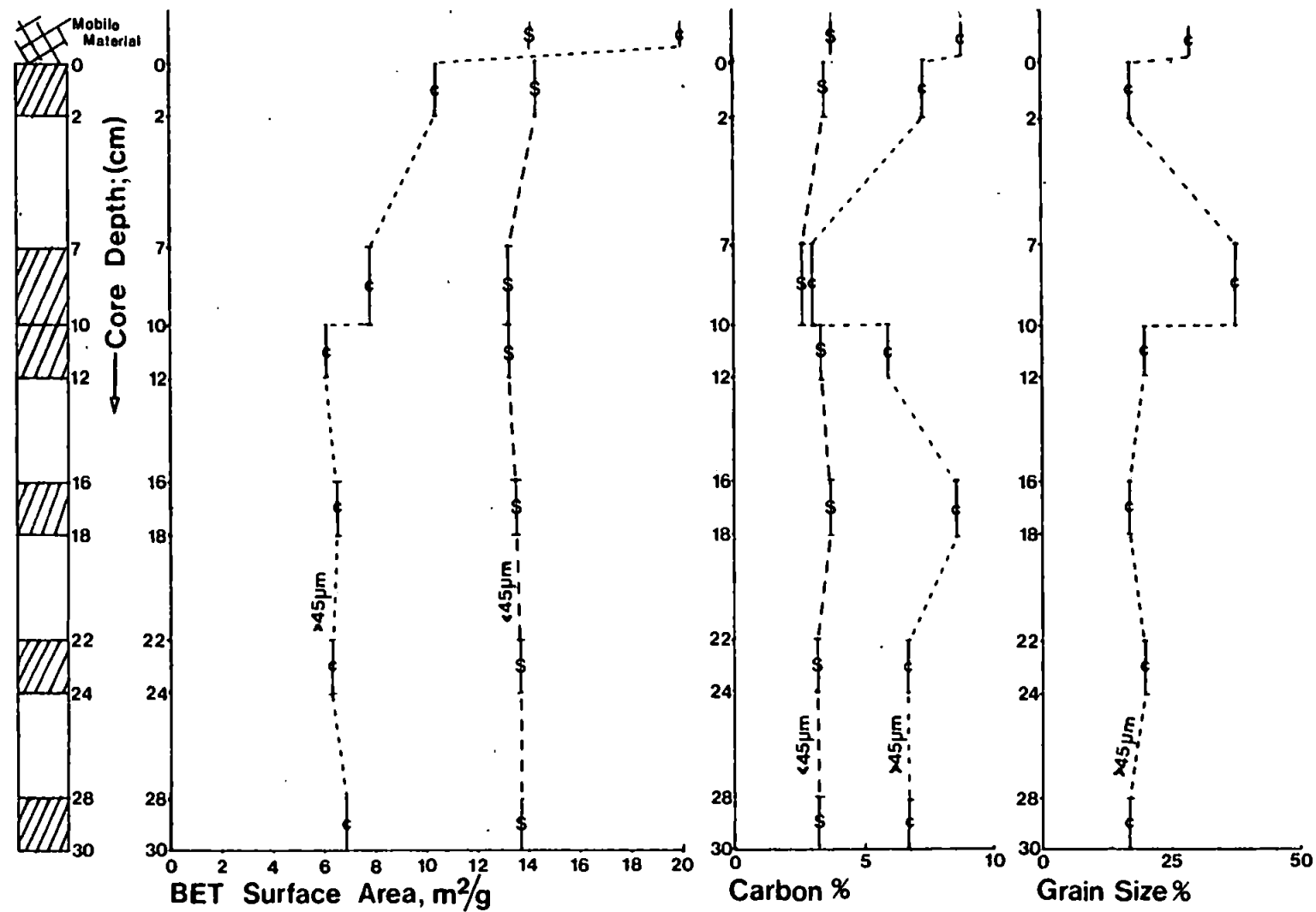
Figure 3.2. Surface areas, carbon contents and grain size distributions of bed sediments from the low salinity region of the Tamar Estuary. Samples were seperated across a 45 μm sieve.

130

region was less compacted and had no discernable anoxic layer and had probably settled out quite recently. Sediments from the mid-estuarine region represent material that is less frequently resuspended and therefore may become aged and more crystalline. Suspended solids collected from this region sometimes had surface areas in the range 10-15 m^2/g (although on some surveys the suspended sediments had higher surface areas $\approx$ 15-20 m^2/g) which is similar to those of the core and suggests that irregular exchange between the population of suspended particles and the bed sediment takes place. Freshly precipitated Fe oxides with high surface areas have been shown to lose a substantial proportion of this surface as they crystallize, and this process is probably important in this respect. This trend in the surface areas of bed sediments continues towards the marine end of the estuary. The surface areas of sediments collected on the surface of intertidal mud flats decrease to 5-7 m^2/g near the mouth of the estuary. This again corresponds to the lower surface area of suspended solids collected from this region, which were in the range 8-10 m^2/g.

Therefore it appears that the resuspension of bed sediment to become part of the turbidity maximum takes place and leads to the relationships observed between the surface areas of the bed sediments and suspended solids. The surface areas of bed sediments show a distinct trend which appears to be related to the position in the estuary, the salinity of the water located in the section and the tidal energy of the section. Tidal energy is highest in the low salinity region of the Tamar Estuary and frequently causes resuspension of sediments in this region. Injection of dissolved Fe

131

and Mn from the pore waters following resuspension of bed sediment encourages the formation of fresh oxide surfaces (Titley *et al.*, 1987). Thus sediments that are resuspended less frequently (and which are more compacted as a result) are recoated with fresh Fe and Mn oxides less frequently. The Fe and Mn oxides on the surfaces of these particles are therefore more likely to be aged and crystalline with lower surface areas and less porosity.

The porosity of sediments collected in the Tamar were assessed by adsorption-desorption isotherms and C&I pore size analysis. The hysteresis loops (see Figure 3.3 and 3.4) show a predominance of slit shaped pores in the size range 1-30 nm. Low pressure hysteresis is also apparent which suggests that microporosity is important. Cranston and Inkley pore size analysis of the sediments from the top and bottom of the core were undertaken to determine the availability and distribution of pores and surface area within the sediments. The C&I pore size distributions of the sediments from the top of the core are shown inset to the hystersis loops in Figures 3.3 and 3.4. The pore size distributions favour smaller pores (<10 nm) which is similar to the suspended sediments described in Chapter 4. A more detailed analysis of the porosity of the sediments was undertaken by statistically comparing the pore size distributions of the different fractions as described in Chapter 2. Pore volume data was simplified by multiplying by 10^5 and was then log-normalized. Pore sizes (in A) were log-normalized directly, and the data plotted as 1/Ln(Pore Size) against Ln(Pore Volume). Best fit (polynomial) regression lines were then obtained and statistically compared. Sediments isolated from the top of the low salinity core (separated through a 45 µm) sieve were compared with those obtained from the bottom of

132
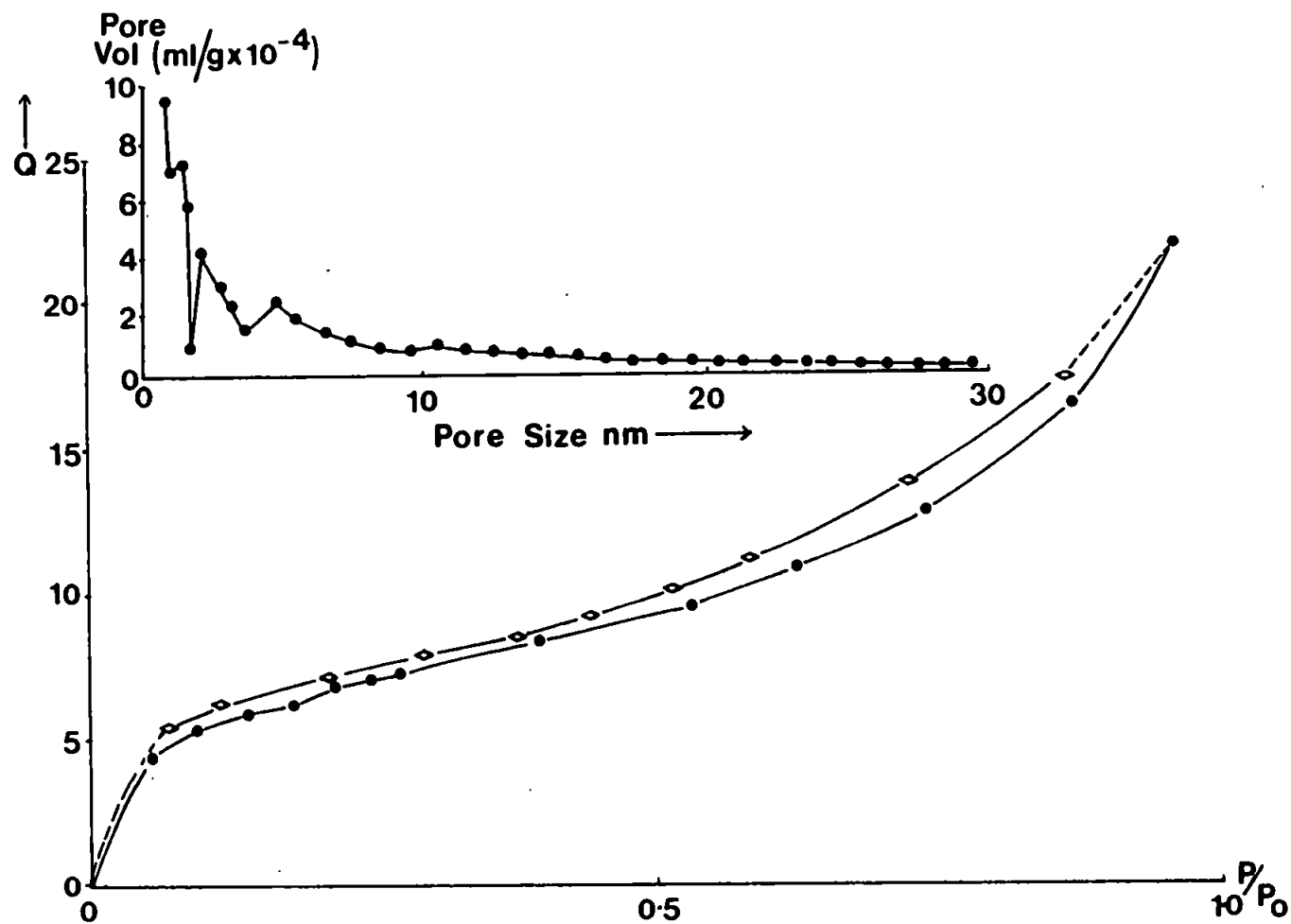
Figure 3.3. Hysteresis loop obtained on a sample of bed sediment from the top of a core from the low salinity
region of the Tamar Estuary (> 45 μm fraction). Inset is the C&I pore size distribution.
(●) - Adsorption. (◇) - Desorption.

133
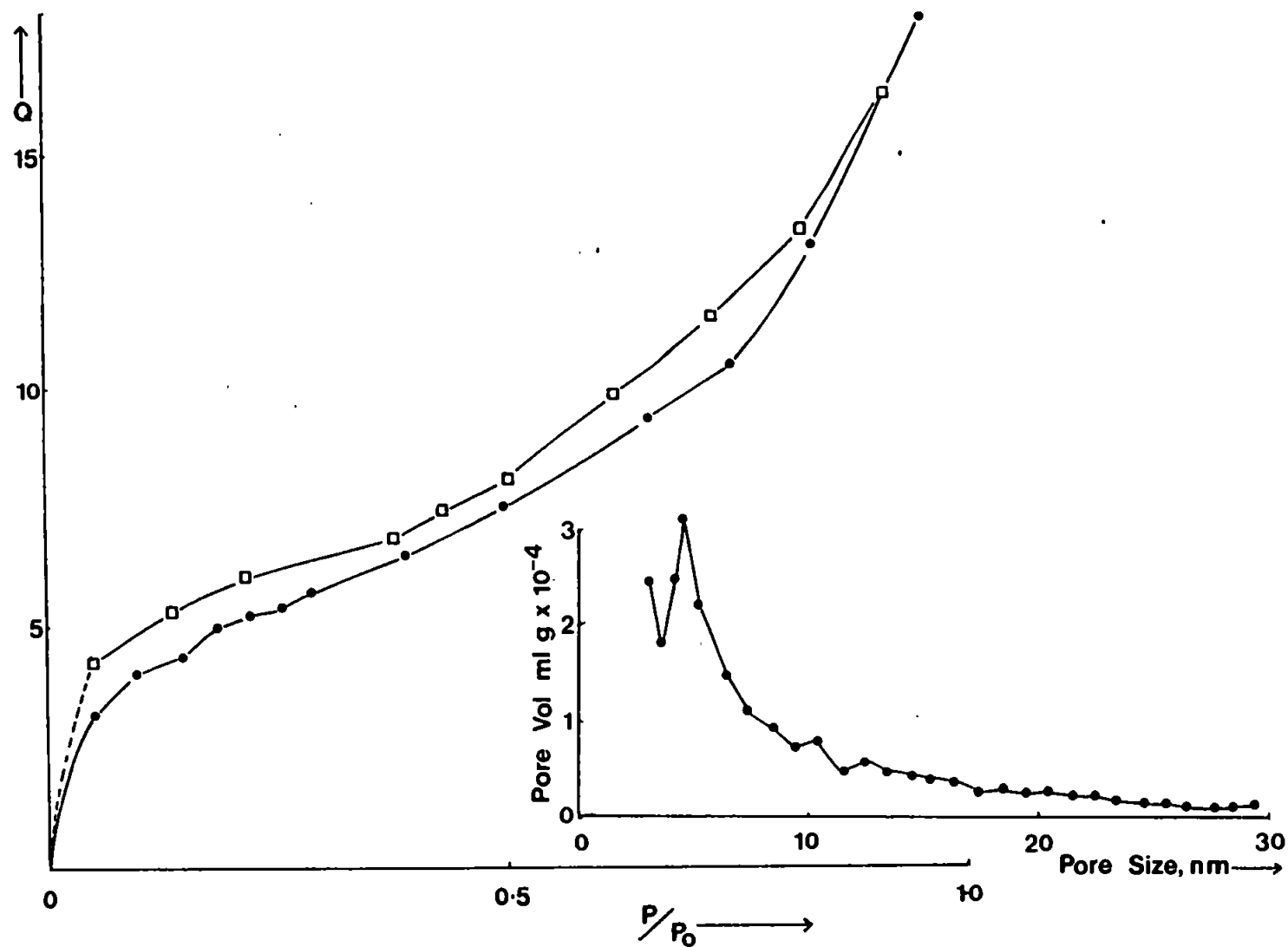
Figure 3.4. Hysteresis loop obtained on a sample of bed sediment from the top of a core from the low salinity region of the Tamar Estuary (< 45 µm fraction). Inset is the C&I pore size distribution. (●) - Adsorption. (□) - Desorption.

the core. The best fit regression lines are shown in Figures 3.5 (top of core) and 3.6 (bottom of core).

The best fit regression lines suggests that the sediments feature two distinct types of porosity. The fine sediments from both the bottom and top of the core have very similar porosities which might be expected as their surface areas and carbon contents are very similar. The pore size distributions show an increase in pore volume as pore diameter decreases. The pore volumes peak at pore diameters of about 2.5-3 nm, before showing a tendancy to decline through the still smaller size ranges. However it should be noted that the C&I pore model does not fit the data for these two samples below pore diameters of 2.5 nm and inferences below this are made from an extension of the regression line. In contrast to this the coarse material has pore volumes that continue to increase as the pore diameter decreases below 2 nm. The best fit regression lines suggest that much pore volume may be associated with pores <1 nm (i.e. interlayer spacing of clays). However it is impossible to investigate this more fully as the C&I model cannot be applied to the energetically complex regime found in pores <1 nm diameter. The different porosities of the two sediment fractions will potentially affect the mechanism of trace metal sorption. The coarse fraction, which is more microporous will tend to adsorb dissolved species much more slowly, because the availability of the surface areas will be reduced if they are located within micropores. However, the coarse fraction of the sediment will have the potential to go on adsorbing as ions diffuse into the pores. The fine fraction, which has a pore size distribution that favours larger

135
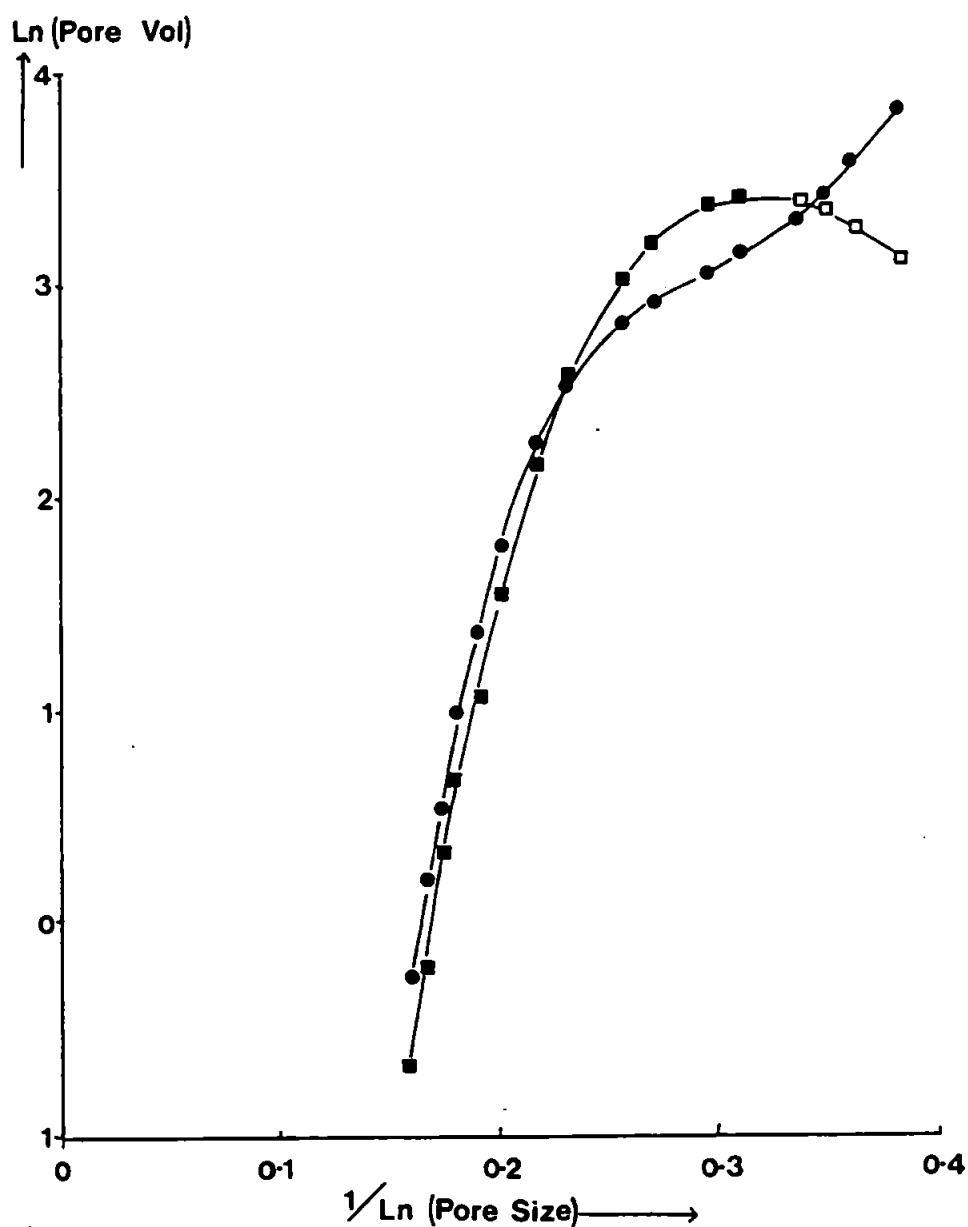
Figure 3.5. Best fit regression lines from the C&I distributions
of pore size. These were obtained on bed sediments
from the low salinity region of the Tamar Estuary.
Material from the top of the core is shown.
(■) - < 45 μm (Open squares represent an extrapolation).
(●) - > 45 μm

136
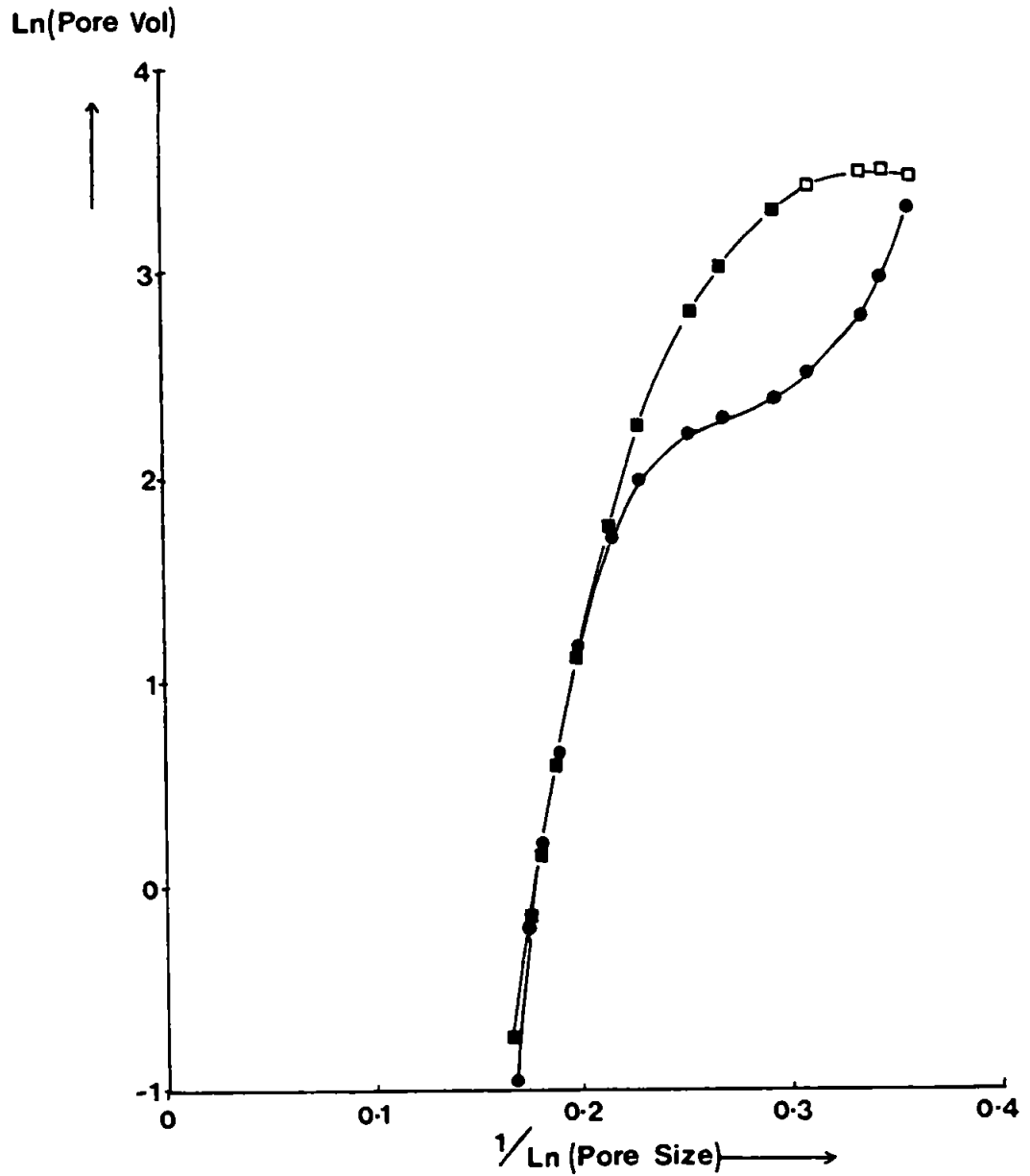
Figure 3.6. Best fit regression lines from the C&I pore size
distributions obtained on bed sediments from the low
salinity region of the Tamar Estuary.
Material from the bottom of the core is shown.
(■) - < 45 μm (Open squares are extrapolated data).
(●) - > 45 μm.

137

pores will have the potential to adsorb ions more quickly as the dissolved species will find the surface of the solid more readily accessible compared to the more microporous coarse fraction. However the potential for longer scale uptake of dissolved species will be less, as the micro-porosity of the particles in the fine fraction is limited.

The potentially large pore spaces can adsorb substantial quantities of dissolved species, and this diffusion process could be a mechanism by which dissolved ions become incorporated in the solid matrix. The microporosity observed in the coarse fraction of the sediments is preserved even at the bottom of the core although some pore volume is lost, presumably as a result of aging and increased crystallinity of the sediment. The loss of pore volume in this coarse fraction occurs largely in the micropore end of the size range, causing a change in the pore size distribution. It is possible that this crystallizing process may be important in the irreversible uptake mechanism. Ions that have diffused into the pores and had sorbed onto surface sites within the pore structure could become permanently trapped when the micropores close up during the reordering processes that accompany crystallization.

The surface areas distributions within the pores are of great importance as they represent potential sites for sorption reactions such as ion exchange. The surface area distributions within the pores of these sediments are shown in Table 3.3. From the data it can be seen that a substantial proportion of the surface area of all the sediment fraction is located in pores <5 nm. The coarse fraction of sediment taken from the top of the core has most surface

area in pores <2 nm which is in agreement with the pore size distribution which shows an abundance of micropores. The >45 μm fraction from the bottom of the core has no surface area in pores <2 nm in diameter. This does not agree with the best fit regression line data which suggests that an abundance of pores <2 nm diameter are present. The reason for this is probably due to the C&I model which does not fit the isotherm obtained on this solid below 2 nm pore diameter. However the general trend through the data obtained from the best fit line is for an increase of pore volume into the micropore size range.

Top of core (Mobile Sediment)			Bottom of core (28-30 cm).		
Fraction μm	Pore Diameter nm	% of Total Surface Area	Fraction μm	Pore Diameter nm	% of Total Surface Area
<45	<2	0.0	<45	<2	7.77
	2-5	46.97		2-5	63.11
	5-10	36.75		5-10	16.53
	10-20	13.11		10-20	9.97
	20-30	3.10		20-30	2.62
>45	<2	52.37	>45	<2	0.0
	2-5	29.43		2-5	59.73
	5-10	11.06		5-10	24.93
	10-20	5.67		10-20	12.89
	20-30	1.47		20-30	2.45

Table 3.3
Surface area distributions within the pore structure of sediments from a core taken from the Tamar Estuary.

3.2.2. INVESTIGATION OF CARBON AND HYDROUS OXIDES COATINGS.

Organic carbon and hydrous oxides of Fe and Mn are known to form coatings on particle surfaces (Grieve and Fletcher, 1977; Loeb and Neihof, 1977; Neihof and Loeb, 1974; 1972). Organic materials can control flocculation processes at the freshwater-brackish-water interface, where charge neutralization allows aggregation and flocculation of dissolved and suspended materials. (Morris, 1986; Cameron and Liss, 1984).

In this study the role of organic carbon and oxides of Fe and Mn for controlling the surface areas and porosities of sediments was assessed by combustimetric analysis of sediments to determine carbon content and acetic acid leaching to remove Fe and Mn oxides.

Careful removal of carbon from selected bed sediments using H_2O_2 was also undertaken as a way of determining the role of the carbon on the surface properties of the sediments. Titley *et al.*, (1987) showed that removal of organic carbon from the surfaces of suspended sediments resulted in an increase in surface area of all the sediments to a uniform value of about 26 m^2/g.

The surface areas of sieve fractionated bed sediments before and after H_2O_2 treatment to remove organic carbon are shown in Table 3.4.

Natural Sediments (Surface)			Oxidized Sediments	
Sieve Fraction	Surface Area m^2/g	% Carbon	Surface Area m^2/g	% Carbon
<45 µm	10.3	3.2	9.8	0.47
>45 µm	11.2	5.4	16.4	0.76
<63 µm	11.0	4.0	14.7	0.42
>63 µm	12.5	22.0	21.0	3.16

Table 3.4
Surface areas of sieve fractionated bed sediments collected from the Tamar Estuary before and after oxidation to remove organic carbon.

The data show that the coarse fraction of the sediments have higher surface area and more organic carbon associated with them, which is in agreement with the results obtained from the cores described in the previous section. Much of this organic carbon is tiny fragments of organic debris such as grass and twigs.

Oxidation of these sediments using H_2O_2 destroyed the carbon associated with these sediments and the surface area of the solids increased by 46-68 %. This is probably due to exposure of more active surface sites to adsorbing N_2 molecules which had been partly occluded by the organic matter. The fine fraction of the sediments (before oxidation) had lower surface areas and less carbon than the coarse fractions described, the core profiles showed that the carbon content of the sediment was fairly constant at all depths as was the surface area. Oxidation of the fine material with H_2O_2 had less effect on the surface areas of the sediments; a small decrease of 5.6% (<45 µm) and an increase of 34% (<63 µm) were observed. Thus fine sediments are affected to a lesser degree by the removal of carbon, which is reasonable given the lower carbon content present

initially. It can therefore be hypothesized that the presence of carbon on the sediments reduces the surface area, and that the initial carbon content is also important, higher starting concentrations result in bigger increases in surface area if the carbon is removed.

Removal of carbon is thought to expose more active sites with a higher surface area such as Fe and Mn oxides which had previously been covered (Titley *et al.*, 1987; Martin *et al.*, 1986). However it is also possible that the increase in surface area occurs as a result of either disaggregation of the particles into smaller components during carbon removal, or that the vigorous oxidization mechanism re-orders the underlying clay structure and results in an increase in surface area.

Bale (Pers. Comm.) showed that oxidation of sediments by H_2O_2 causes break-up of particles. However the change in particle size distribution is not sufficient to cause the increases observed. Re-ordering of the clay domain structure was investigated by treating a kaolinite sample with hydrogen peroxide before and after surface area measurements. The surface area of the clay increased after oxidation from 11.2 to 13.7 m^2/g. suggesting that some re-ordering of the domain structure of the clays is·taking place resulting in an increase in surface area. However the increase observed does not account for all the increase observed in the natural sediments. Alternatively, it is possible that removal of low surface area organic materials may result in an increased composite surface area simply because the organics themselves are removed and no longer contribute to the overall surface. However, the carbon content of

the sediment is usually <10% and therefore in sediments of surface area 10 m²/g, removal of organics with a surface area of 0.5 m²/g, should leave particles with a composite surface area of 11 m²/g, an increase of up to 10%.

Therefore it can be concluded that much of the increase in surface area observed in the coarse fractions of the sediments arises from exposure of underlying surface which has a higher surface area. This more active surface is probably associated with Fe and Mn oxide coatings which are known to have higher surface areas, often in the range 200-400 m²/g (Crosby 1982; This work).

The surface area variation observed in the coarse fraction of sediment cores from the Tamar Estuary and described earlier appears to be partly controlled by the variation in carbon content of the sediment. Carbon causes a reduction in surface area (Glegg et al., 1987), but the coarser sediments which have more carbon also have larger surface areas than the finer fraction (with less carbon). This is surprising, not only because of the lower carbon values, but also because smaller particles are generally assumed to have larger surface areas. To further investigate the surface areas and chemical composition of the bed sediments as a function of grain size, a surface scrape of sediment was separated through a range of sieves (mesh size 45-250 µm) and the surface areas and associated properties of each fraction were determined. The BET and geometric surface areas of these sediments are shown in Figure 3.7. The BET surface areas tend to show an increase in surface area with increasing grain size which is the reverse of what is generally assumed to happen, shown by the geometric surface areas
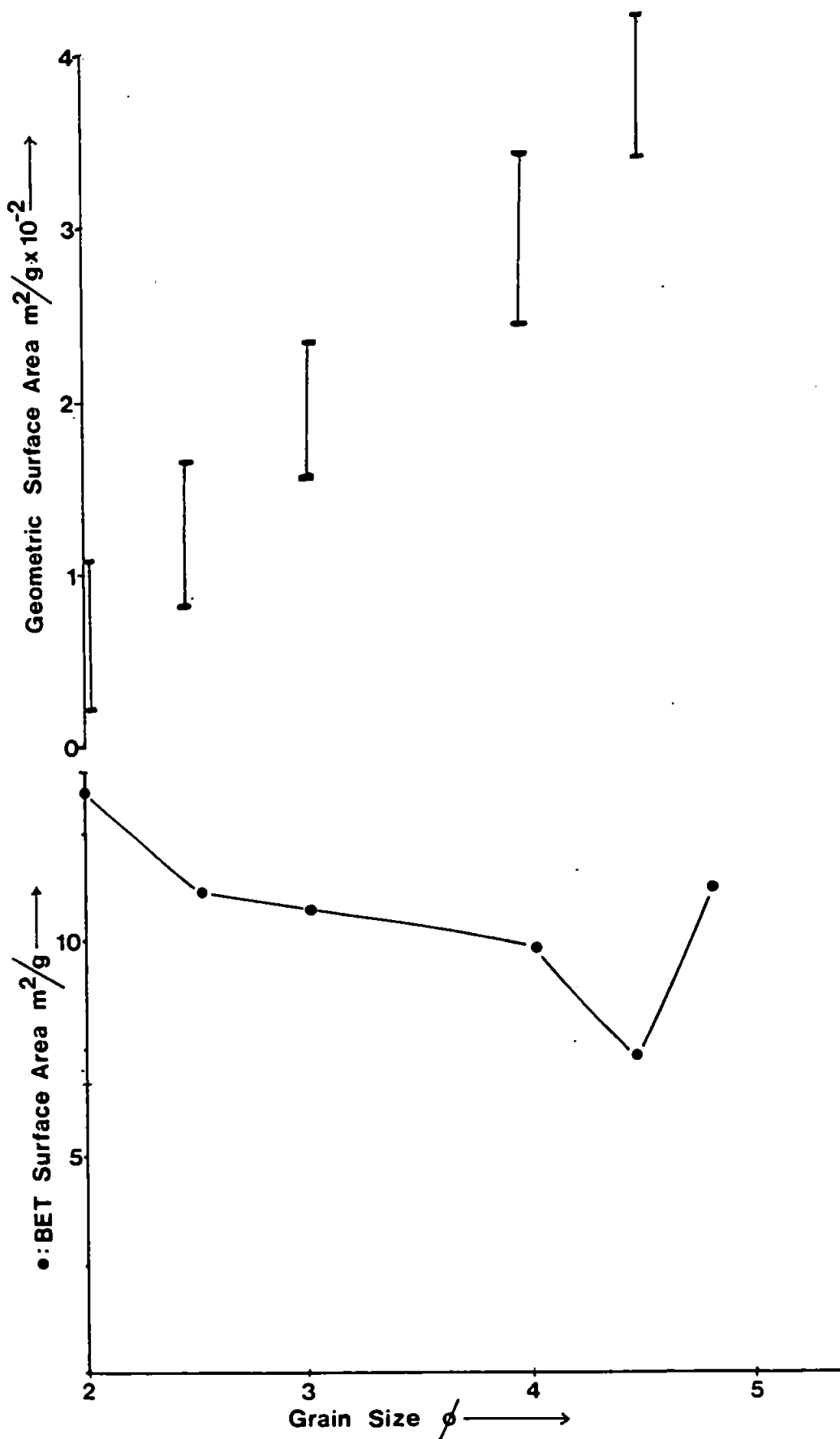
Figure 3.7. BET surface areas and geometric surface areas of bed sediment from the Tamar Estuary as a function of grain size.

which decrease as the grain size increases. Thus the surface areas

are apparently controlled by the surface properties of the

sediments, i.e. Fe/Mn oxides and carbon.

Each fraction of the sediment was leached with acetic acid to remove

non-detrital Fe and Mn oxides and the carbon content of the sediment was

also determined. The results of this are shown in Table 3.5.

Sieve Fraction μm	Surface Area m²/g	C %	N %	C:N	Fe, mg/g	Mn mg/g	Fe:Mn
<45	11.2	3.03	0.50	6.01	6.57	--	---
45-63	7.3	2.78	0.25	11.12	6.88	0.65	10.58
63-125	9.8	3.82	0.28	13.54	11.19	1.29	8.67
125-180	10.6	10.90	0.64	16.95	6.59	1.41	4.67
180-250	11.1	26.90	1.47	18.30	16.57	1.00	16.60
>250	13.4	30.70	1.65	18.60	27.20	0.82	33.30

Table 3.5
Surface areas and associated chemical data of sieve fractionated bed
sediment from the Tamar Estuary. (This material is also shown in
Plates 3.4-3.6)

The data in Table 3.5 show that the carbon content of the sediment

increases as the the particle sizes increase. This is because the

coarse material contains fragments of organic detritus, such

as leaves and twigs. The high C:N ratios of the material confirm the

presense of organics of low nitrogen content. Algal bimass has C:N

ratios of about 6.6:1 (Stumm and Morgan, 1981), therefore it is likely

that the larger organic particles are composed of leaf matter which has

an abundance of carbohydrate with higher C:N ratios (McClusky,

1981). The data also shows the distribution of Fe and Mn oxide

phases within the sediment. The Fe content of the sediment is

highest in the coarsest material which also has the largest surface

area (13.4 m²/g). This suggests that Fe oxide is playing an important role in controlling the surface area of the sediment. Removal of the Fe oxides from the coarsest fractions (180-250 and >250 µm) by leaching with acetic acid reduced the surface area to 8.4 m²/g (180-250 µm) and to an undetectably small value (<0.1 m²/g) for the >250 µm fraction. This last result is close to that of humic acid (surface area 0.5-0.7 m²/g) and confirms the importance of Fe/Mn oxide coatings which appear to be solely responsible for the surface area of this grain size fraction. It also appears that this fraction of the sediment is composed solely of organic debris and hydrous oxide coatings with no underlying crystalline matrix being present.

The Fe and Mn oxide coatings on sediments from the cores described in the preceeding section were assessed by leaching with acetic acid. The results of this together with surface area data are shown in Table 3.6.

<45 µm fraction					>45 µm fraction				
Core Depth cm	Surface Area m²/g	Carbon %	Fe mg/g	Mn mg/g	Core Depth cm	Surface Area m²/g	Carbon %	Fe mg/g	Mn mg/g
Mobile	14.1	3.9	11.5	0.44	Mobile	20.0	8.9	15.7	0.86
0-2	14.3	3.5	18.9	0.67	0-2	10.4	7.4	21.2	0.94
7-10	13.2	2.6	--	--	7-10	7.8	3.1	--	--
10-12	13.2	3.4	--	--	10-12	6.2	6.0	--	--
16-18	13.5	3.8	9.6	0.58	16-18	6.3	8.6	8.6	0.78
22-24	13.7	3.2	11.9	0.62	22-24	6.6	6.8	9.9	0.74
28-30	13.7	3.3	19.3	0.78	28-30	6.9	6.8	15.2	0.86

Table 3.6
Surface areas and associated properties of the coarse and fine fraction of an oxic core from the low salinity region of the Tamar Estuary.

The data show that the highest surface areas are generally associated with higher Fe concentrations; at the surface the coarse fraction with higher surface area has Fe concentrations of 19-21 mg/g, whereas the associated fine fraction has Fe concentrations of 11-19 mg/g. Near the core bottom the fine fraction has consistently higher Fe content than the coarse fraction, the latter also has lower surface areas. However the Fe concentrations in the fine fraction show considerable variability ranging between 10 and 19 mg/g of Fe, whereas the surface areas in the fine fraction are fairly constant. This suggests that Fe may not totally dominate the distribution of surface area but may be in competition with another component such as carbon.

The possibility of contamination of the sediments with Fe or Mn during the passage of the material through metal sieves was examined as a precaution. Samples of kaolinite were wet sieved using the same procedure as the sediments and then leached with acetic acid under the same conditions as the sediment. Samples that had not been subjected to the sieving process were also leached with acetic acid. It was found that the contribution of the steel sieves to the non-detrital Fe and Mn content of the kaolinite was negligible.

The roles of Fe and carbon coatings on the surface areas of sediments were also examined by studying the carbon poor, Fe rich Restronguet Creek (S.W. England)

3.3   BED SEDIMENTS IN RESTRONGUET CREEK

3.3.1 SURFACE AREAS AND POROSITIES

A range of bed sediments were collected from Restronguet Creek on a complete axial survey. Surface sediments were collected along the length of Restronguet Creek on an axial survey. The sediments were separated across a 45 µm sieve and then freeze dried prior to analysis. Sediments from Restronguet Creek were generally much coarser than those collected in the Tamar Estuary, with >50 % usually being retained by a 45 µm sieve whereas in the Tamar Estuary, 70-80% usually passed through.

The surface areas were found to range between 11.0 m^2/g in the saline region of the system to 42.0 m^2/g near the limit of saline penetration (see Figure 3.8). The surface areas of the finer fraction were consistently higher than the coarser material throughout the estuarine profile, ranging between 20 and 42 m^2/g. The coarser fraction had consistantly lower surface areas ranging between 11 and 37 m^2/g. It is clear from the data that surface areas of sediments from this iron rich system are considerably higher than those from the Tamar Estuary which ranged between 7 and 16 m^2/g.

A sediment core isolated from the estuary showed similar trends in surface area to data collected in the Tamar Estuary (see Figure 3.9). The grain size distribution of the sediment was reversed compared to the Tamar with about 70% of the material being >45 µm. Due to an analytical problem the carbon profile is not complete, but as was generally found throughout this estuary the carbon content

148
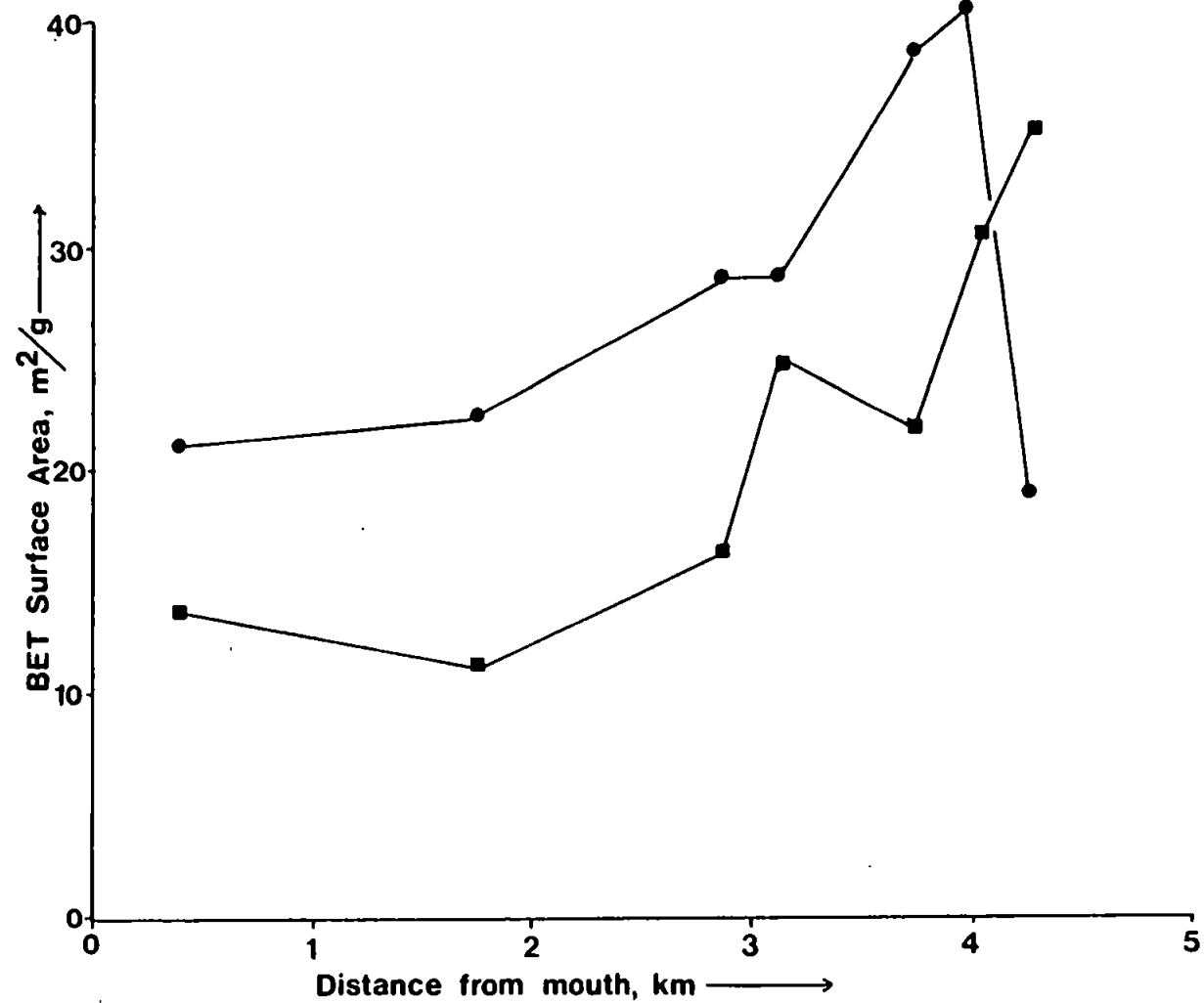
Figure 3.8. The surface areas of bed sediments from Restronguet Creek as function of distance up estuary. Sediment samples were separated across a 45 μm sieve. (●) - < 45 μm (■) - > 45 μm.
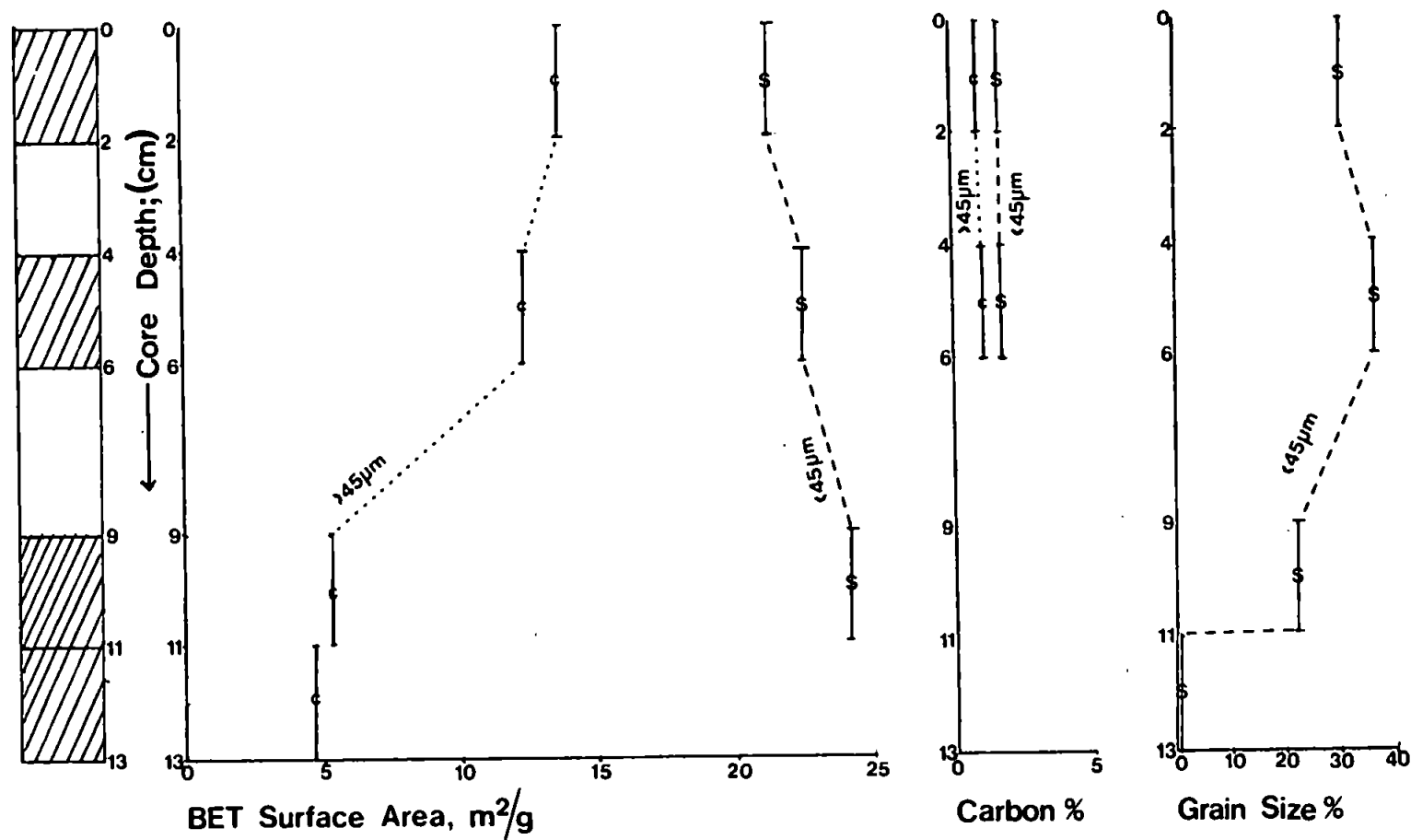
Figure 3.9. The surface areas, carbon contents and grain size distributions of a core of sediment from Restronguet Creek. The sediment had been separated across a 45 μm sieve.

was low (typically 1-3%). The fine fraction of the sediment (<45 μm) had BET surface areas in excess of 20 m²/g throughout the core. The surface area of the coarse fraction behaved in the same way as the Tamar sediments (i.e. declining with increasing depth) but in this case the particles at depth consisted of large coarse grained sandy materials with little evidence of organic detritus.

Porosity of the sediments was assessed using adsorption-desorption isotherms and C&I pore size analyses. The porosities of bed sediment fractions separated across a range of sieves (45-710 μm) were assessed. Hysteresis loops and the associated C&I pore size distributions are shown in Figures 3.10, 3.11 and 3.12. The hysteresis loops show low pressure hysteresis which suggests the presense of micropores. The C&I pore size distributions confirm the presense of pores of diameter 1-2 nm and upward. The coarser grains (125-180 and 355-500 μm) were more microporous than the fine material (<45 μm). The data was interpreted using best fit polynomial regression analysis and log-normalized data. The plots from these samples are shown in Figure 3.13. These reveal that material in the size band 125-180 μm was the most microporous with an overall distribution skewed in favour of the very smallest micropores. The finer sediments (grain size <45 μm) were less microporous, with a pore volumes favouring pore sizes of 2 to 3 nm. The surface area distributions obtained from this data are shown in Table 3.7. These confirm the pore size distributions; the fine fraction of sediment having no surface area within pores <2 nm. this is similar to the surface properties of sediments in the Tamar Estuary, and implies that adsorption processes onto the fine materials would be potentially faster because the surface is

151
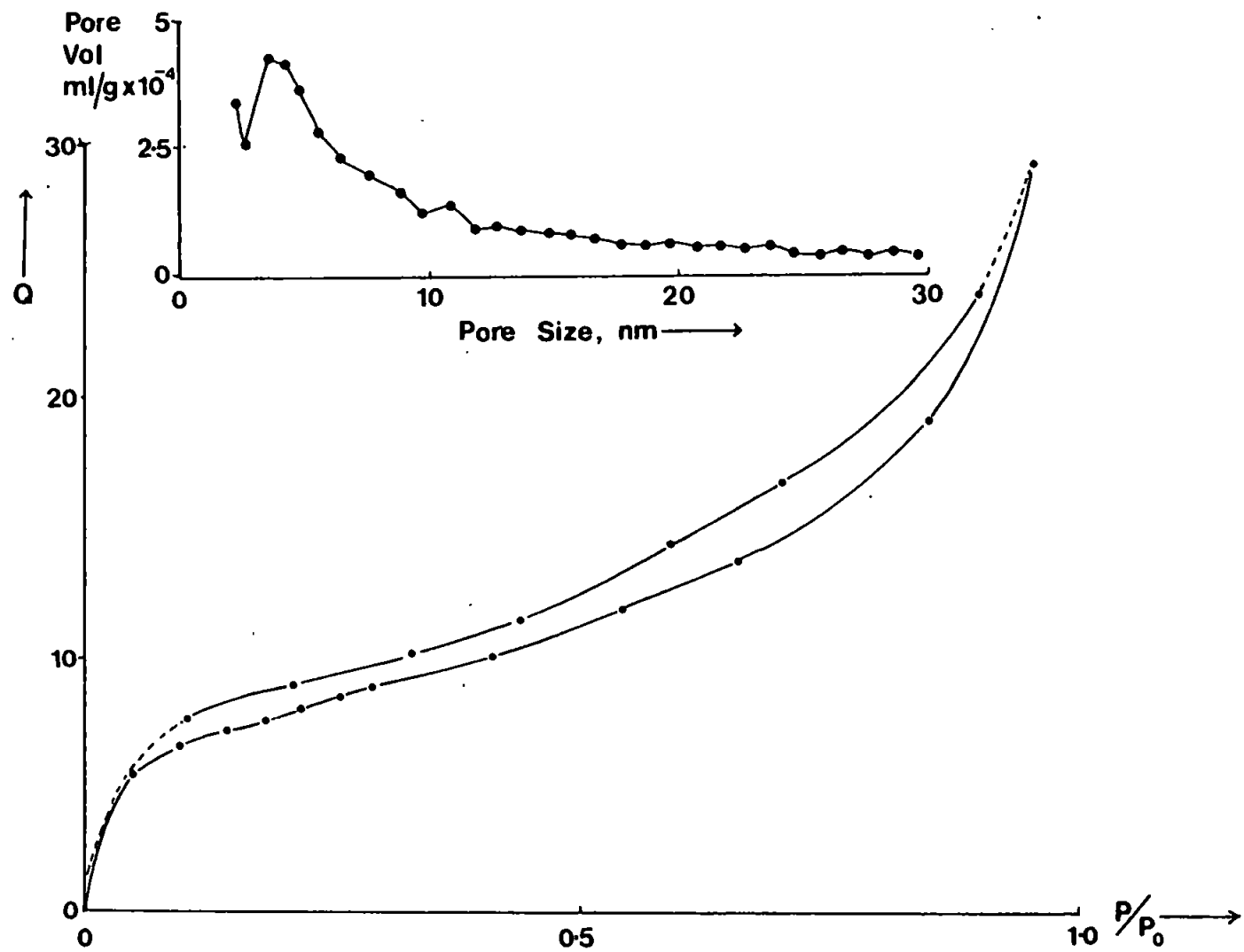
Figure 3.10. Hysteresis loop obtained from a sample of bed sediment from Restronguet Creek, (< 45 μm fraction) Inset is the C&I pore size distribution.
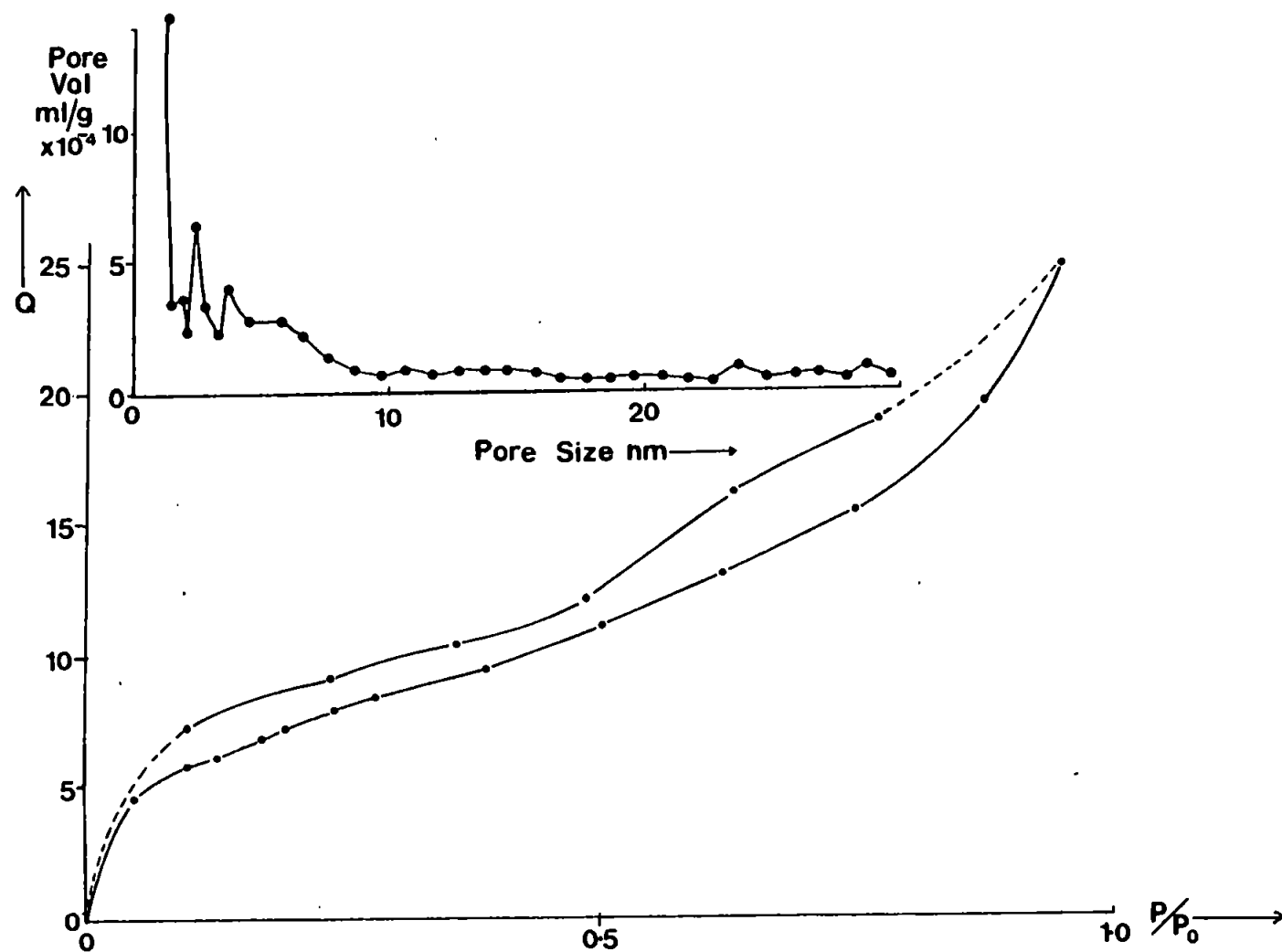
Figure 3.11. Hysteresis loop obtained from a sample of bed sediment from Restronguet Creek, (125-180 μm fraction). Inset is the C&I pore size distribution.
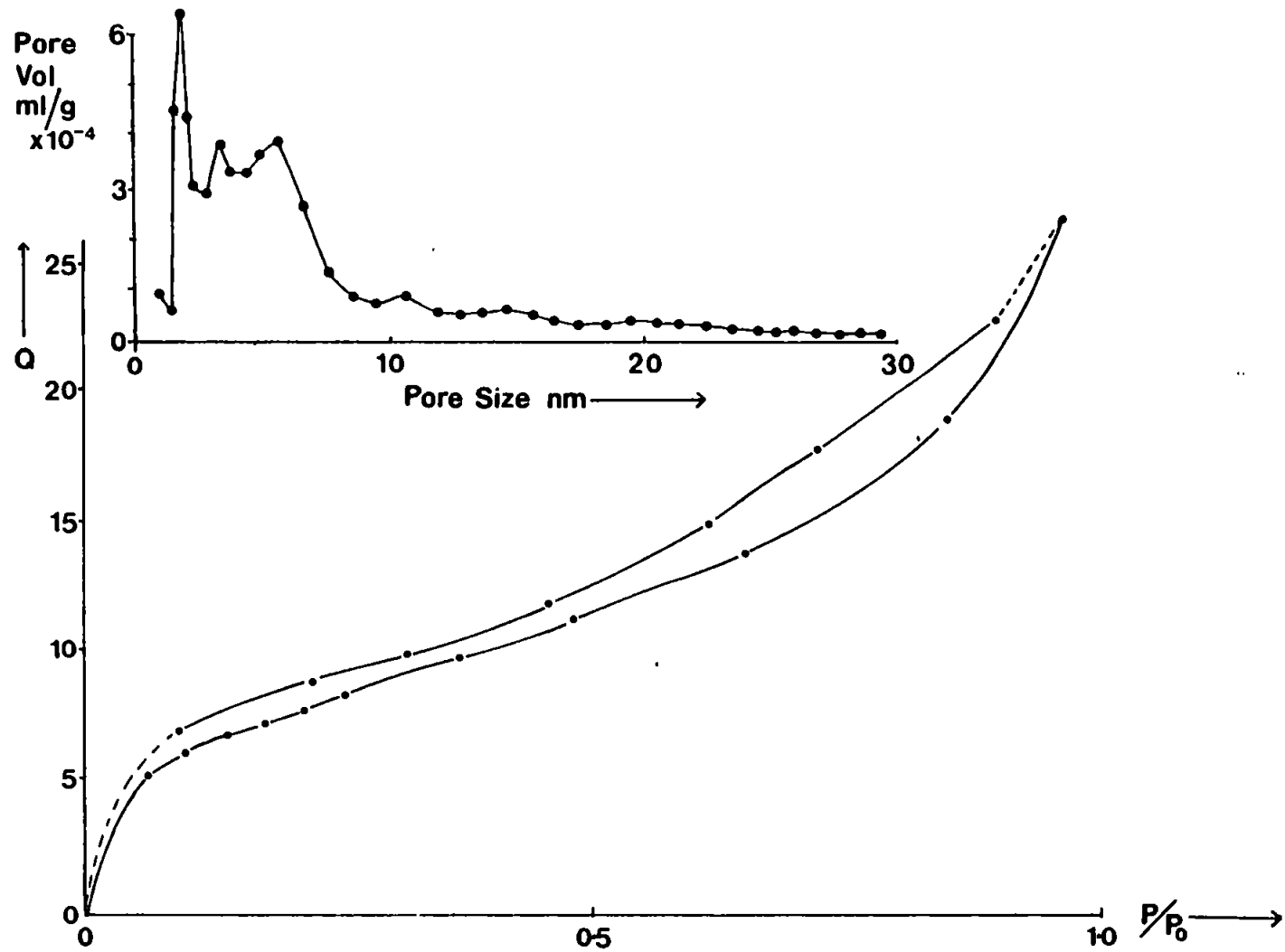
Figure 3.12. Hysteresis loop obtained from a sample of bed sediment from Restronguet Creek, (355-500 μm fraction). Inset is the C&I pore size distribution.
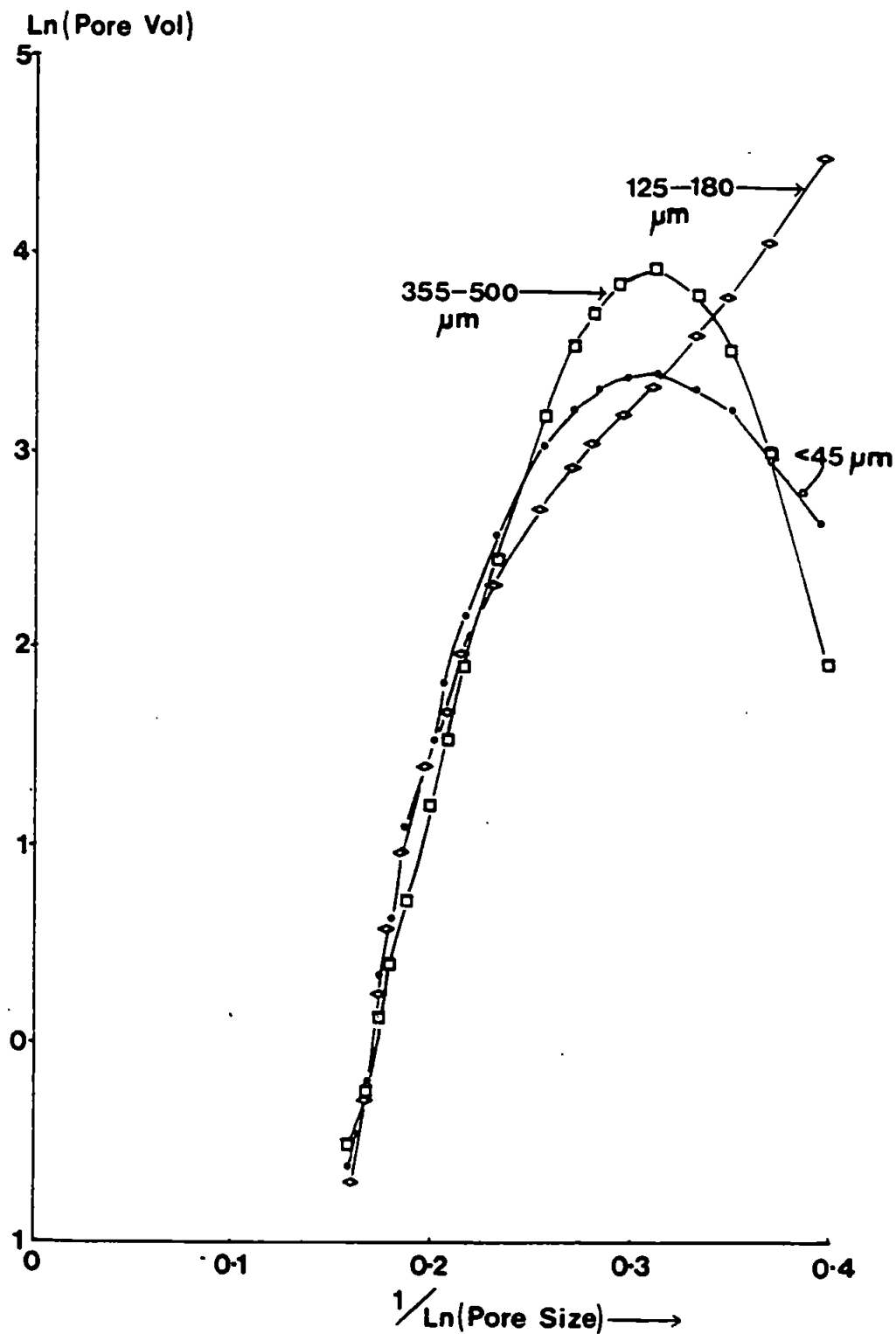
Figure 3.13. Regression lines fitted through the C&I pore size
distributions shown inset to Figures 3.10, 3.11 and 3.12.

relatively more accessible than in the coarser fractions of the sediment.

Sample	Pore Size nm	% of Total Surface Area	Carbon %	Iron mg/g
<45 μm	<2	0	2.84	26.2
	2-5	58.89		
	5-10	26.71		
	10-20	10.97		
	20-30	3.43		
125-180 μm	<2	38.49	7.40	15.4
	2-5	40.40		
	5-10	13.24		
	10-20	6.00		
	20-30	1.88		
355-500 μm	<2	29.15	7.20	--
	2-5	41.83		
	5-10	20.92		
	10-20	6.27		
	20-30	1.83		

Table 3.7
Surface area distributions within the pores of bed sediment fractions from Restronguet Creek.

3.3.2 INVESTIGATIONS OF ORGANIC CARBON AND HYDROUS OXIDE COATINGS.

Acetic acid leaches undertaken on the sediments from Restronguet Creek showed that the sediments were rich in Fe as compared to the Tamar Estuary, the Fe content varying between 10 and 77 mg/g. Combustiometric C/H/N analysis of the sediments showed that the sediments had low carbon values (ranging between 1 and 3.5%; see Table 3.8) in comparison to the Tamar. Thus particles in the Restronguet Creek are very different compositionally. Coatings of carbon and iron oxide have already been implicated as controlling

influences on surface area (Titley *et al.*, 1987; Martin *et al.*,
1986), and it appears that in the Restronguet Creek, the higher
surface areas of the sediments as compared with the Tamar Estuary
are a result of the contrasting composition of the sediments.

<45 µm			>45 µm		
Surface Area m²/g	Carbon %	Fe mg/g	Surface Area m²/g	Carbon %	Fe mg/g
19.2[1]	2.12	38.9	35.9	1.34	76.7
40.3[2]	3.54	23.0	30.2	3.89	29.8
39.0[3]	2.61	56.0	21.8	1.98	28.0
29.4[4]	3.35	38.7	16.2	1.16	30.9
22.5[5]	2.84	26.2	11.0	1.06	9.6
21.4[6]	1.74	35.8	13.7	0.94	30.9

[1]Head of estuary-[6]Mouth of estuary

Table 3.8.
Surface areas and chemical compositional data for Restronguet Creek
bed sediments.

The distribution of Fe in sediments within the Estuary are shown in
Figure 3.14. Generally the highest Fe values are associated with
the fine fraction of the sediments, and this correlates with the
distribution of surface area, the fine fraction of the sediments
have the highest surface areas. Iron values are also higher in the
low salinity region of the Estuary which is also where the highest
surface areas are found. The Mn content of the sediment is highly
variable with lowest values (0.025 mg/g) in the low salinity region.
This gives Fe:Mn ratios in the range 50-3000, the highest values
found in sediments from the head of the Estuary.

The core of material taken from the low salinity region of the
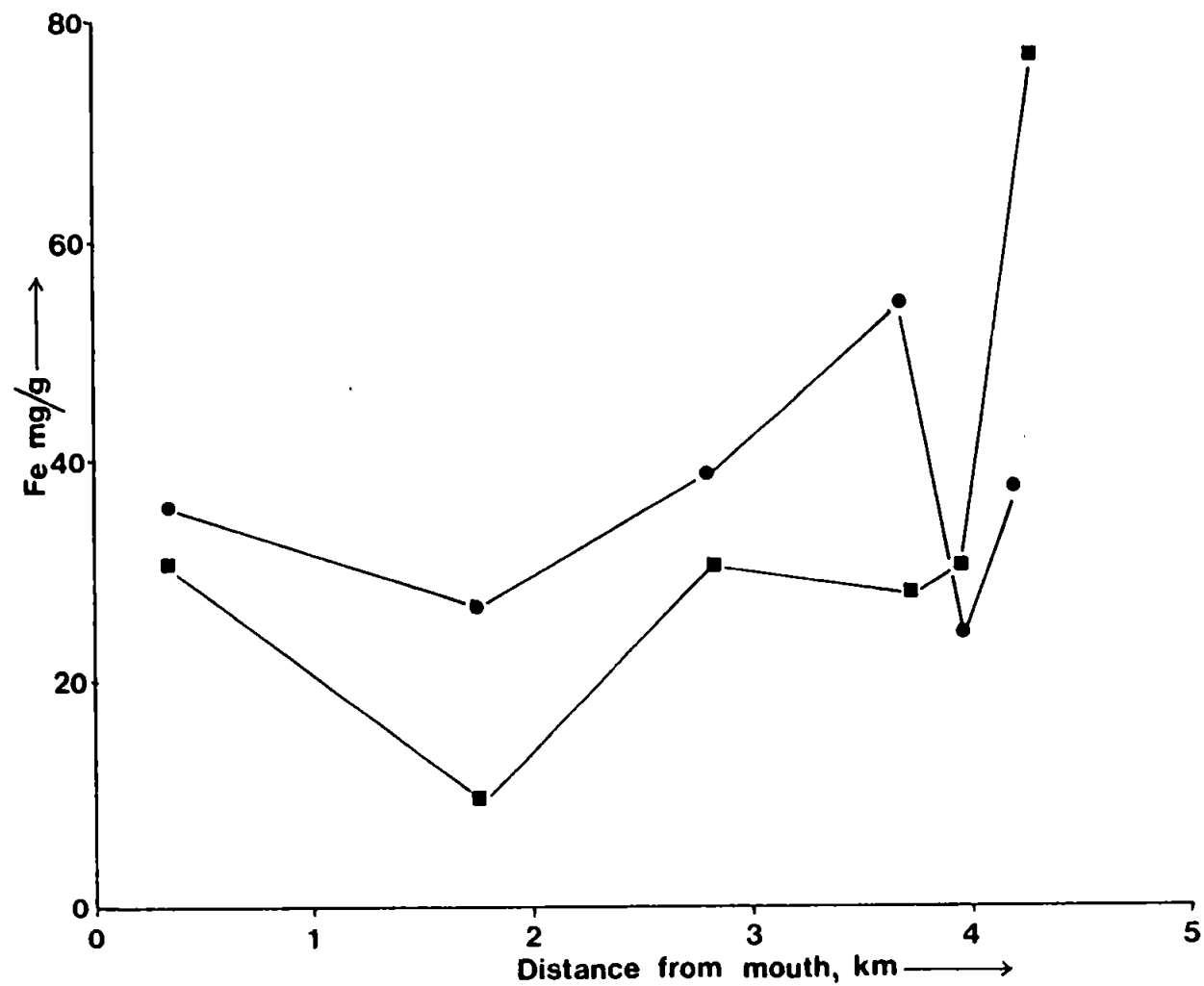
Figure 3.14. Acetic acid leached Fe content of bed sediments from Restronguet Creek, showing variation with position in estuary and grain size. (●) - < 45 μm, (■) - > 45 μm.

Tamar Estuary showed a relationship between leachable Fe and Mn content and the surface area patterns observed. The core taken from Restronguet Creek had similar trends in surface area to the core from the Tamar Estuary (Titley *et al.*, 1987), and the compositional data is shown in Table 3.9. The surface areas of the coarser fraction shows some degree of co-variation with the Fe content of the sediments.

Core Depth cm	<45 μm fraction				>45 μm fraction			
	Surface Area m²/g	Carbon %	Fe mg/g	Mn mg/g	Surface Area m²/g	Carbon %	Fe mg/g	Mn mg/g
0-2	21.4	1.74	35.8	0.55	13.7	0.94	30.9	0.65
4-6	22.6	1.78	24.8	0.11	12.4	1.10	16.1	0.85
9-11	24.3	--			5.4	--	3.1	0.05
11-13	No sed.	--	--	--	4.7	--	--	--

Table 3.9
Surface areas and associated properties of the coarse and fine fractions of a sediment core collected from Restronguet Creek (see Figure 3.9)

The coarser sediments were further investigated by fractionating the material across a range of sieves. Sediments collected from the Restronguet system are composed of larger particles, and so sieves of mesh size up to 710 μm were used to differentiate the particles.

Surface areas and chemical composition of the fractionated sediments are shown in Table 3.10.

Sieve Fraction μm	Surface Area, m²/g	Total Pore Vol. ml/gx10⁻²	Fe mg/g	Mn mg/g	Carbon %
<45	22.5	3.28	26.2	0.14	2.84
45-63	10.6	--	7.8	0.06	0.50
63-90	7.1	--	8.6	0.05	0.80
90-125	12.9	--	10.3	0.07	1.70
125-180	22.4	3.39	15.4	0.12	7.40
180-250	20.7	--	18.9	0.22	14.20
250-355	24.7	--	25.3	0.15	6.70
355-500	23.2	3.34	--	--	7.20
500-710	19.3	--	28.6	0.17	8.42
>710	18.2	--	27.8	0.15	10.90

Table 3.10
Surface areas and associated properties of bed sediment separated
through a range of sieves.

The results are similar to those obtained for Tamar Estuary sediment
with a distinct increase in surface area as the grain size
increases, which contrasts with the geometric surface areas. The
surface areas of these sediments are about twice those measured in
the Tamar Estuary. This is thought to be as a result of the high Fe
content of the sediment which are 20-40 % higher than the equivalent
fractions from the Tamar Estuary. The carbon content of the
sediments increases with increasing grain size which suggests that
larger fractions of detrital vegetation are being detained by the
sieves as was observed in Tamar sediments. Overall the carbon
contents of the sediments are about half the equivalent values from
the Tamar. Thus the higher surface area values in these
fractionated sediments are probably a result of high Fe content and
lower carbons. The high surface areas of these sediments suggest that
surface adsorption would be of great importance in the Restronguet
Creek. However the chemical composition of the particles
and their porosities and the relative availability of the surface

areas within the pores are unique to each of the sediment fractions. This suggests that the overall sorptive behaviour of the sediments will be a sum of the individual fractions sorptive behaviour, and removal of a given fraction of sediment with a particular microstructural feature could alter the sorptive capacity of the sediment.

3.3.3 SURFACE AREAS OF SEDIMENTS FROM KEITHING BURN

Bottom sediments were collected from the iron contaminated Keithing Burn in Fife, Scotland by Philip Newton. The sediments from the stream bed have been identified as the iron mineral Akagenite (Hunter and Liss, 1979). Samples of uncontaminated sediment upstream from a mine adit discharge and from various points below the input were collected over a 3.5 km long transect of the stream bed. Further samples were also taken where the stream entered the Firth of Forth. A basic physical separation of material through a 45 μm sieve was carried out followed by surface area analysis. The results obtained are summarized in Table 3.11. The data shows that the surface area of sediments contaminated with fresh precipitates of Fe are very high, in the range 110-200 m^2/g (<45 μm) and 28-129 m^2/g (>45 μm) which is similar to values for other crystalline Fe oxide phases such as goethite and lepidocrocite. The uncontaminated sediment has a surface area that is lower by 2 orders of magnitude. Thus the potential adsorptive capacity of the Keithing Burn sediments is greatly increased.

| Location | BET surface area, m²/g | | Electrophoretic Mobility* (U_E) (10^{-8} m² s^{-1} V^{-1}) (Unsieved Seds.) |
	<45 μm	>45 μm	
Above iron input	14.2	3.2	-1.2
Below iron input	65-160	18-129	-0.4 to -0.8
Firth of Forth	13.9	6.3	-1.0

*Data from Newton and Liss (1987).
Table 3.11
Surface areas and electrophoretic mobilities of Keithing Burn sediment collected from above mine drainage, below mine drainage input to the stream and sediments associated with the Burn in the Firth of Forth.

The electrophoretic mobilities of the sediment were at their lowest in the section of the stream contaminated by Fe oxides, and hence they coincided with the highest surface areas. The low U_E values suggest that the particles surfaces are not coated with organic material which have low BET surface areas, and thus it appears that the dominating iron oxides are not associated with pore blocking organic materials. Pore size distributions of coarse fraction and fine fraction of the bed sediment from Keithing burn were obtained using the C&I method from adsorption isotherms. The pore size distributions are shown in Figure 3.15, and the results indicate that the solids from both the coarse and fine fraction are highly microporous. Best fit regression lines from this data are shown in Figure 3.16. The highly microporous nature of the solid surface coupled with the large surface area gives the sediments in Keithing Burn great potential for adsorption and permanent removal of dissolved trace constituents from the water column.
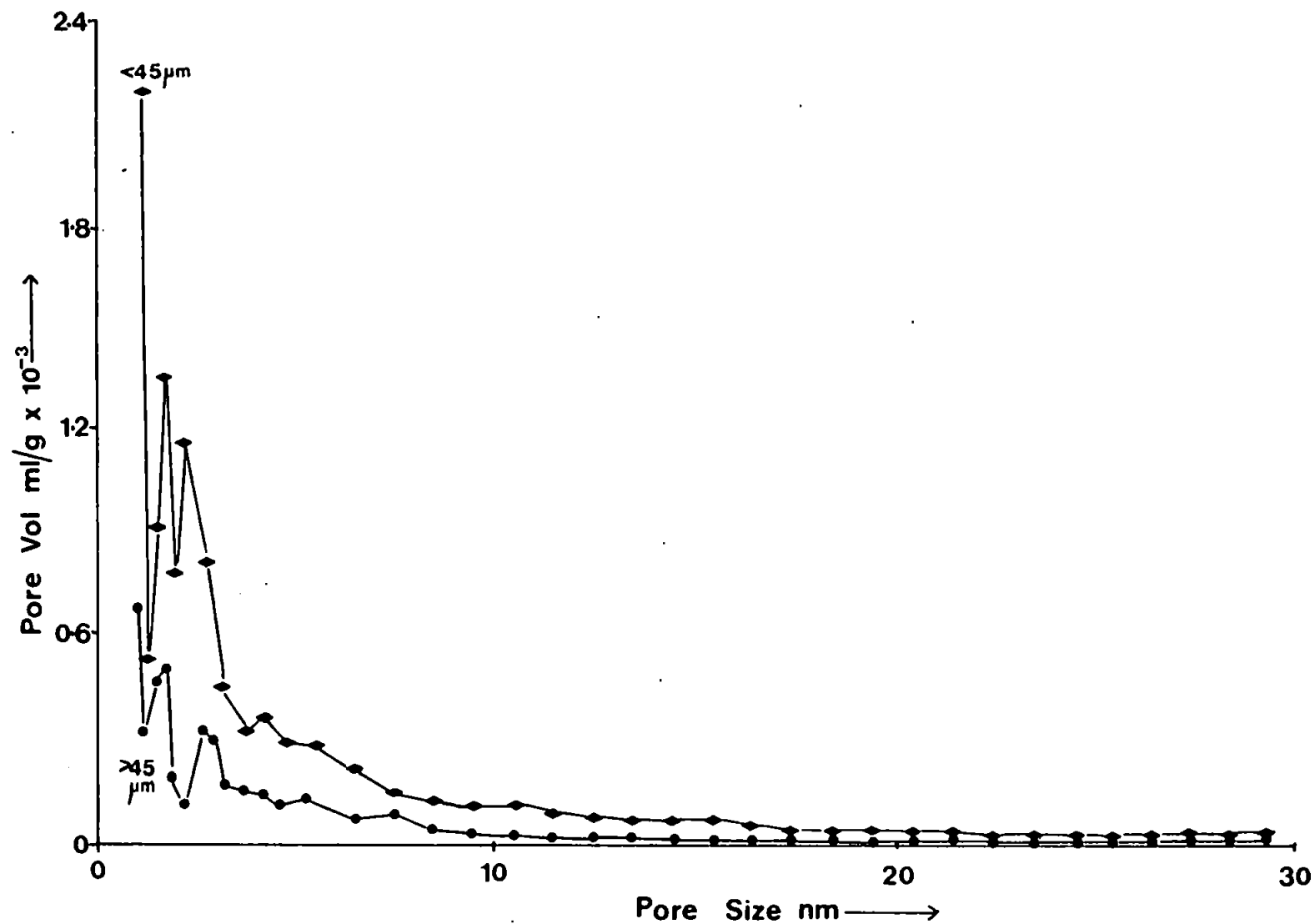
Figure 3.15. The C&I pore size distributions of sediments from Keithing Burn. The sediments had been separated across a 45 μm sieve.
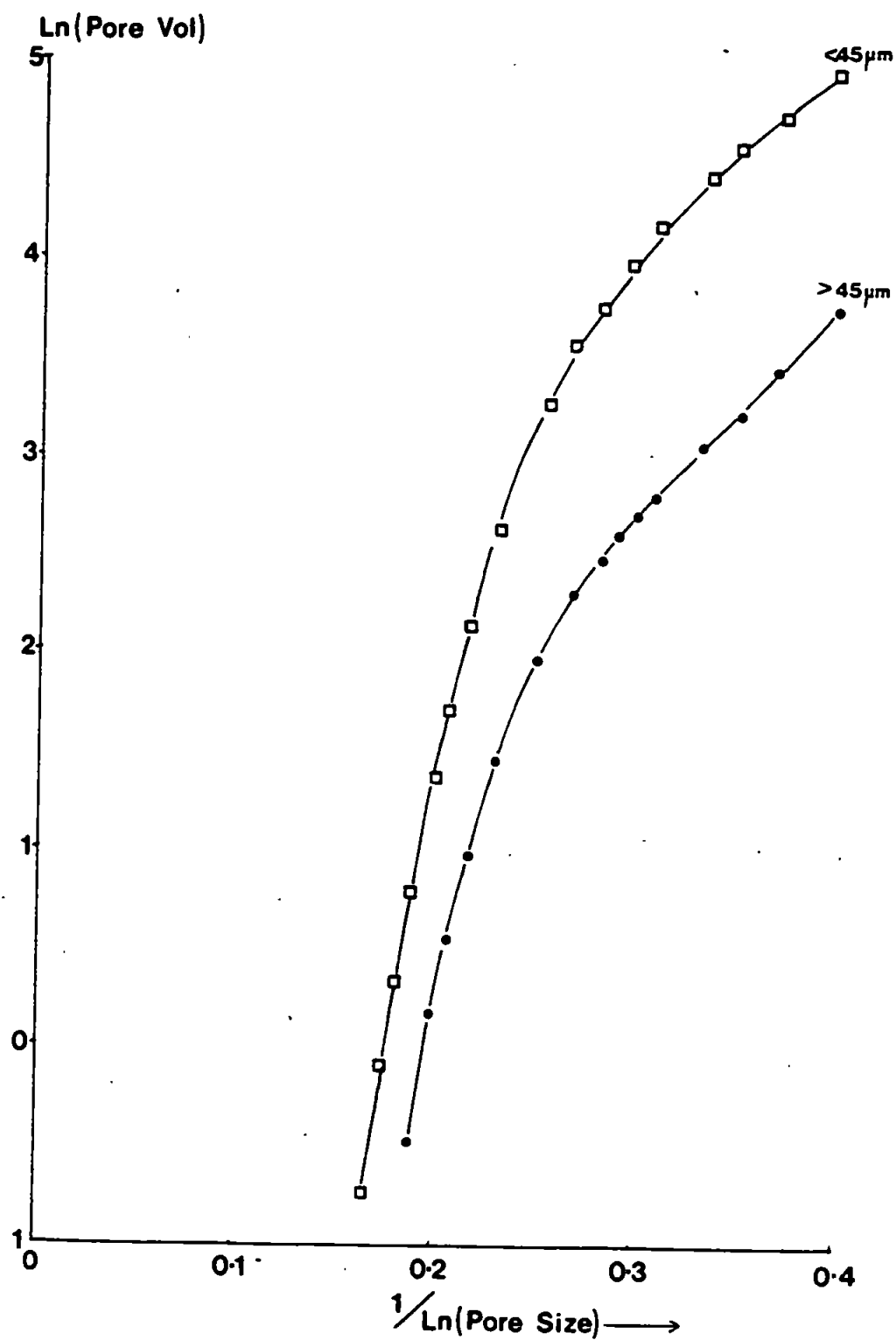
Figure 3.16. Regression lines fitted through the C&I pore size distributions shown in Figure 3.15. The sediments had been separated across a 45 μm sieve.

3.4 INTER ESTUARINE VARIABILITY OF THE MICROSTRUCTURES OF BED

SEDIMENTS

The variability of both surface areas and porosities of bed sediments
are strongly linked to the chemical coatings on the particle
surfaces. The role of Fe is thought to be especially important. A
plot of Fe content versus surface area is shown in Figure 3.17
(values from Restronguet Creek). A clear relationship between the
surface area and Fe content is apparent for these sediments.
However this system is heavily dominated by Fe and carbon content is
unusually low. Results from the Tamar do not correlate with Fe
content directly, this is probably due to the lower levels of Fe
present and also the masking effect of higher carbon content.
Combining carbon and Fe as a ratio provides a good indicator of
surface area (Table 3.12). The data shows that highest C:Fe ratios

Estuary	Sieve Fraction μm	Mean Surface Area m²/g	Mean Carbon %	Mean Fe mg/g	C:Fe
Tamar	<45	13.8	3.45	14.9	2.31
	>45	8.0	7.05	14.0	5.03
Restron-	<45	28.6	2.70	36.4	0.74
guet	>45	21.5	1.73	34.4	0.50

Table 3.12
Average surface areas and associated properties of bed sediments
from the Tamar Estuary and Restronguet Creek.

are associated with the lowest surface areas, and vice versa.
This parameter can be used to differentiate the surface properties
of bed sediments within the Tamar Estuary and also between the Tamar
and Restronguet Creek. However this parameter does not differentiate
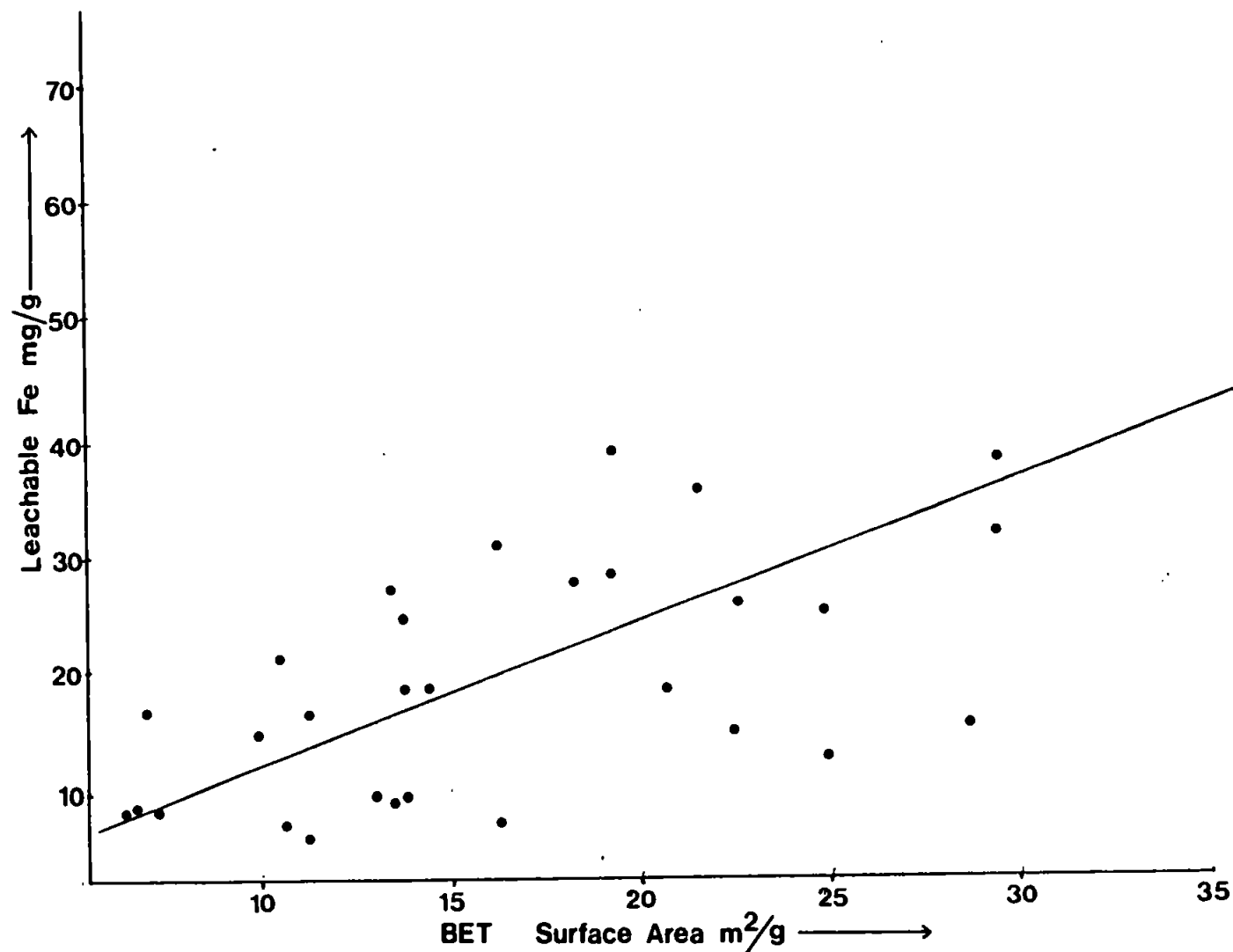
Figure 3.17. A plot of Fe content versus surface area for bed sediments from Restronguet Creek. The correlation co-efficient suggests that the relationship is significant at 99% confidence interval.

between the different grain fractions of sediments from Restronguet Creek.

In conclusion, this chapter has shown the high degree of variability of the surface areas and porosities of bed sediment that occurs within different estuarine environments. It has shown that the key factors controlling the surface characteristics of the sediments are coatings of Fe and carbon content which act in opposition to each other. The reduction in surface area of the coarse fractions of sediment with depth suggests that the adsorptive capacity of the particles will be reduced with increasing depth. This could lead to release of trace constituents into pore waters.

The internal pore structures of the sediments have significant potential for irreversible adsorption of trace species within the estuarine environment. The porosities of the surface sediments particularly in the coarser fractions had pore size distributions skewed in favour of the smallest micropores. However with depth this skewness in distribution had altered with loss of microporosity, presumably as a result of crystallization processes. Trace constituents in these pores when closure takes place would therefore be trapped permanently within the internal structures.

Bed sediments make a substantial contribution to the suspended solid particle population in macrotidal estuaries, due to tidal forces acting on the bed sediments. The microstructural properties of suspended solids and their potential importance in chemical behaviour within the estuarine environment will be discussed in Chapter 4.

167

CHAPTER FOUR

THE MICROSTRUCTURES OF SUSPENDED PARTICLES IN ESTUARIES

Preamble

In Chapter 2 it was shown that the N_2 gas sorption method can be used to assess the morphology of estuarine solids which have been removed from their natural environment. In Chapter 3 the method was applied in a systematic study of the bed sediments from the Tamar Estuary, and Restronguet Creek, S.W. England. The study showed inter and intra variations in the surface properties of the sediments, which were related to the composition of the particles.

This Chapter continues the analysis by considering the surface properties of suspended sediments from the Tamar Estuary, Restronguet Creek, and the Mersey Estuary.

4.1 SUSPENDED SOLIDS IN THE TAMAR ESTUARY

A series of surveys were undertaken to isolate suspended solids from
the Tamar Estuary for microstructural analysis. Five axial surveys
were carried out over the complete hydrodynamic range of the Tamar
to collect bulk water samples containing suspended solids from
throughout the salinity range of the estuary. One additional survey
was carried out in the low salinity region (at the fresh-water
brackish-water interface) to monitor changes in the particle
surfaces as the sediments were mobilized by the incoming tide.
The surveys were carried out between June 1985 and March 1987, and
data from two axial surveys carried out by Glegg, (1987) will be
included here for completeness and to allow a full intra-estuarine
comparisons to be undertaken.

4.1.1 SURFACE AREAS OF SUSPENDED PARTICLES

The principal aim of the surveys was to collect bulk water samples
containing suspended solids from throughout the salinity range of
the estuary. During the sampling runs estuarine master variables
were recorded, and these are summarised (together with river flow and
tidal data) in Table 4.1. Previous work showed that surface areas of
suspended particles within the Tamar Estuary are non-conservative
with respect to salinity (Titley, *et al.*, 1987), the largest surface
areas coinciding with the low salinity region of the estuary (Glegg,
1987; Titley *et al.*, 1987). Inclusion of all suspended solid data
from the Tamar reveals a similar trend (Figure 4.1), with the
largest surface areas encountered at salinities of 0.5-2.0°/oo. The
data from 29-01-87 is out of sequence with relatively low surface
areas and show a decrease in the low salinity region of the estuary,

169
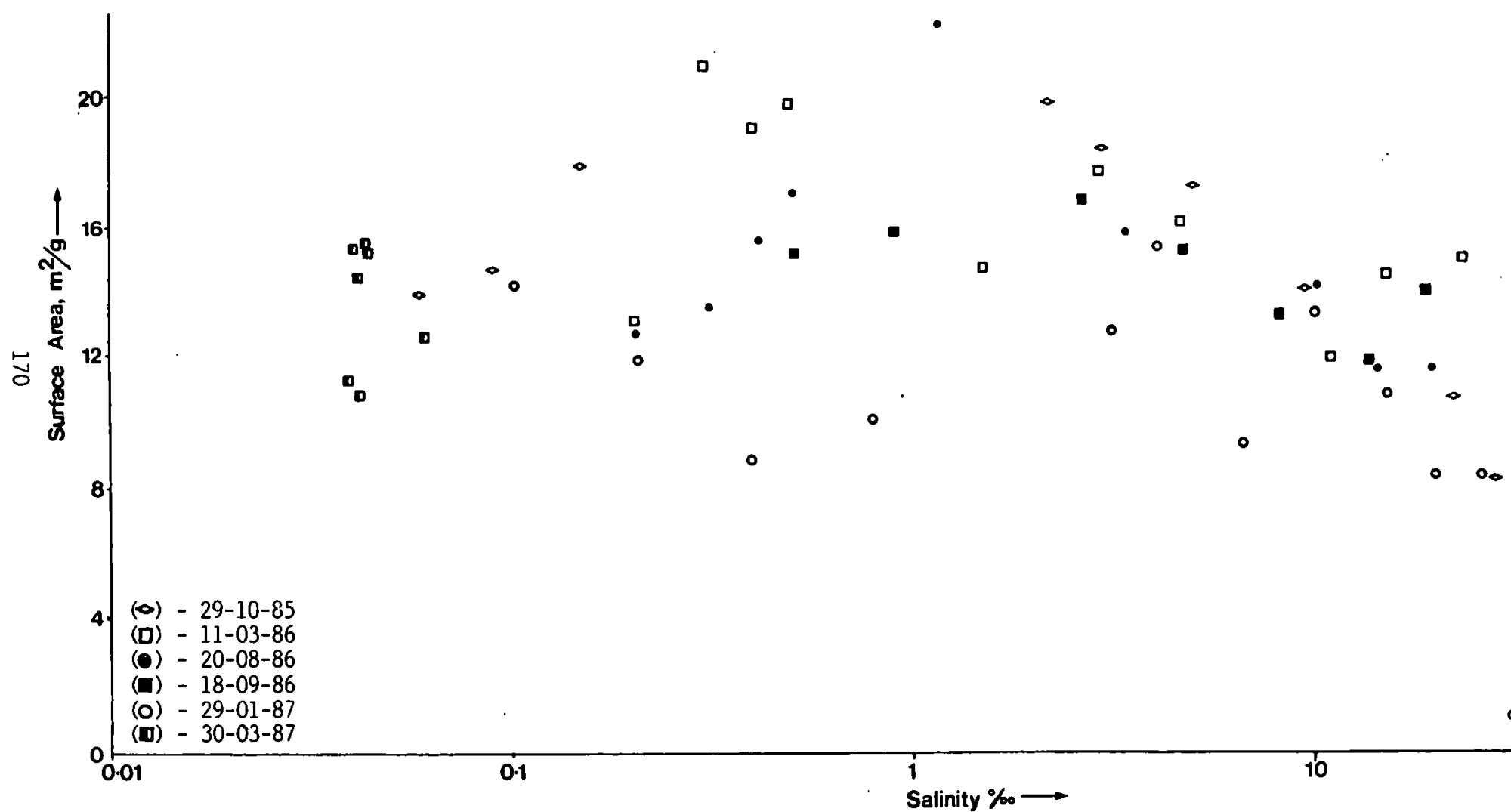
Figure 4.1. Surface areas of suspended sediments from the Tamar Estuary plotted as a function of salinity. The individual surveys are identified as inset to the diagram.

170

in contrast with the increase observed on other surveys. This may
result from higher carbon contents (see Figure 4.18) and will be
discussed later.

Survey Date	Salinity Range, %	Temperature Range, °C	Turbidity Range, mg/l	pH range	Rainfall Previous Week, mm	Tidal Range, m	River Flow, m³/s[#]
29-10-85[*]	0.06-28.5	8.0-10.7	80-530	7.7-7.9	0.1	4.4	5.7
11-03-86	0.03-23.6	6.4-7.2	25-540	7.1-8.2	25.9	4.9	6.7
20-08-86	<0.5-19.5	12.2-15.2	21-213	---	14.1	4.8	8.0
18-09-86[*]	<0.5-19.0	11.4-13.2	70-580	7.4-7.8	17.7	5.0	8.9
29-01-87	0.05-33.6	3.8-7.0	2-170	7.7-8.1	0.3	4.5	8.3
30-03-87	0.04-0.06	8.6-9.1	35-170	7.7-8.1	52.3	5.1	32.0

[*]From Glegg, (1987). [#]Data supplied by South West Water.

Table 4.1
Main hydrographic conditions of the six surveys undertaken in the
Tamar Estuary.

Surface areas, turbidities and salinities for the six surveys of the
Tamar Estuary are shown in Tables 4.2-4.4. The data in the tables
reveal the highly variable character of the suspended solids
surface. The general trend reported by Glegg, (1987) and Titley *et
al.*, (1987) shows a maximum surface area in the low salinity, high
turbidity region of the estuary. The surface area values themselves
show substantial variability, some surveys have peak surface area
values of 20-22 m²/g, for example 29-10-85, 11-03-86, and 20-08-86
surveys, whereas others show a maxima of 15-17 m²/g. A plot of
geometric and BET surface area versus turbidity (see Figure 4.2 a
and b) reveals that higher surface areas are associated with greater
suspended solid load (Titley *et al.*, 1987).

29-10-85* Survey			11-03-86 Survey		
Salinity °/oo	Turbidity mg/l	Surface Area m²/g	Salinity °/oo	Turbidity mg/l	Surface Area m²/g
28.5	60	8.4	23.6	32	15.0
22.5	190	10.7	15.3	52	14.5
9.7	115	14.0	11.1	323	12.0
5.0	130	17.2	4.6	129	16.2
3.1	470	18.0	2.9	238	17.8
2.2	480	19.8	1.5	351	14.7
0.15	530	17.8	0.5	240	19.6
0.09	140	14.6	<0.5	228	19.0
0.06	215	13.9	<0.5	540	20.7
--	-	--	<0.5	25	13.2

*From Glegg, (1987).

Table 4.2
Surface areas, salinity and turbidity values for the first two Tamar
Estuary surveys.

20-08-86 Survey (Ebb)			18-09-86* Survey		
Salinity °/oo	Turbidity mg/l	Surface Area m²/g	Salinity °/oo	Turbidity mg/l	Surface Area m²/g
19.7	99	11.6	19.0	70	14.2
14.4	213	11.8	13.5	210	12.0
10.1	168	14.2	8.2	150	13.3
3.3	108	15.7	4.7	235	15.1
1.1	162	22.1	2.6	500	16.7
0.5	202	16.8	0.9	580	15.8
<0.5	83	15.2	<0.5	410	15.2
<0.5	25	13.3	--	-	--
<0.5	21	12.7	--	-	--

*From Glegg, (1987).

Table 4.3
Surface areas, salinity and turbidity values for late summer and
early autumn surveys. Data for 20-08-86 is on the ebb tide.

Figure 4.2a and 4.2b. BET and geometric surface areas of suspended particles from the Tamar Estuary. Results are from all the surveys.
Key: (O) - 29-10-85   (■) - 11-03-86   (⊠) - 20-08-86
      (●) - 18-09-86   (★) - 29-01-87   (□) - 30-03-87
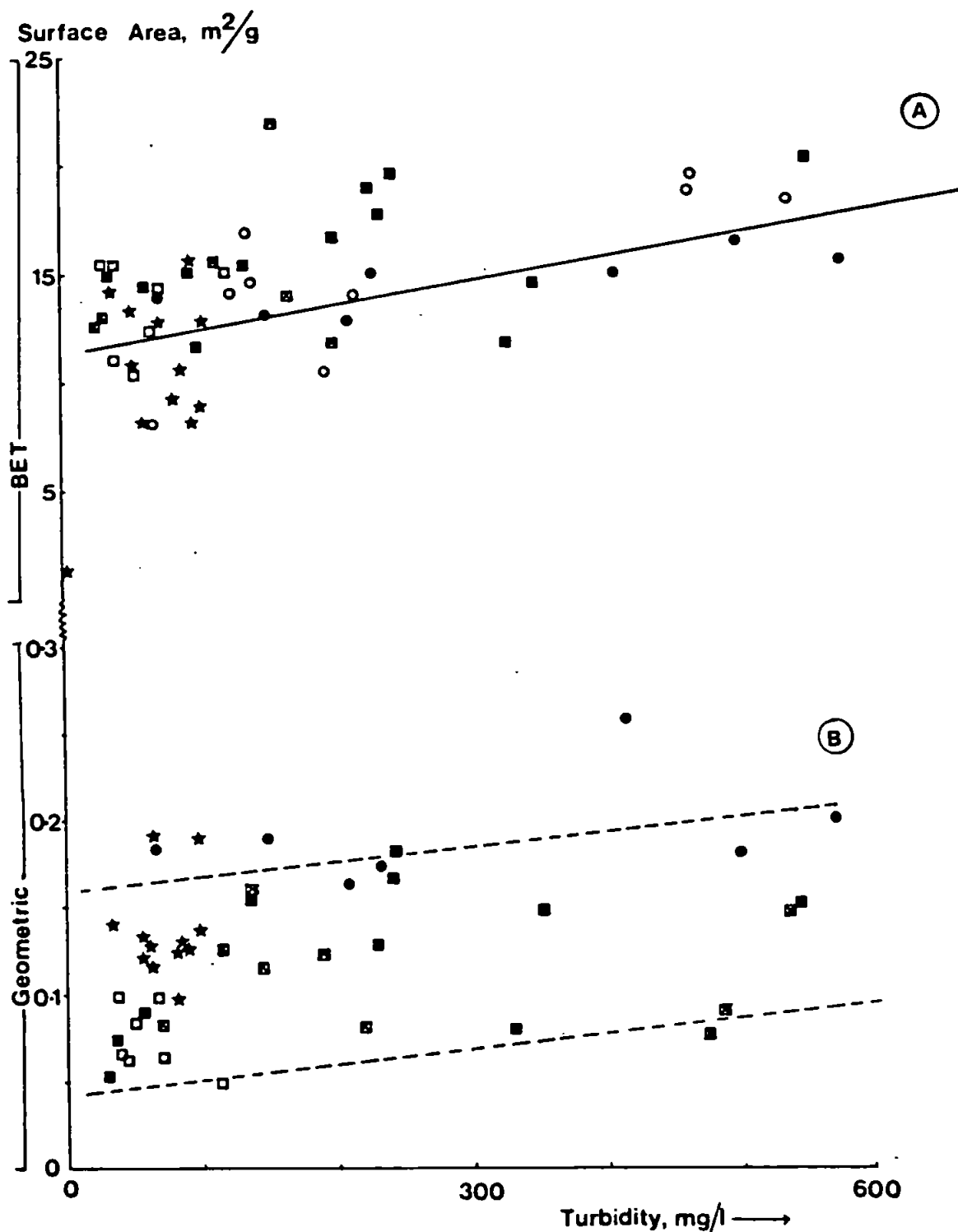
29-01-87 Survey			30-03-87 Survey[*]		
Salinity °/°°	Turbidity mg/l	Surface Area m²/g	Salinity °/°°	Turbidity mg/l	Surface Area m²/g
33.6	1	1.1	0.060	62	12.5
25.6	60	8.3	0.044	117	15.1
20.1	91	8.3	0.041	71	14.4
15.1	52	10.9	0.038	36	11.1
10.3	50	13.4	0.041	48	10.6
6.7	80	9.1	0.043	44	15.3
4.1	80	15.2	0.040	40	15.4
3.0	72	12.9	--	--	--
0.8	89	10.2	--	--	--
0.4	101	8.8	--	--	--
0.2	104	11.9	--	--	--
<0.1	36	14.2	--	--	--

[*]Stationary survey, monitoring the freshwater-brackishwater interface.

Table 4.4
Surface area, salinity and turbidity values recorded for suspended sediments in the Tamar Estuary early in 1987.

The data are fairly scattered, which is probably caused by localized resuspension of unconsolidated sediments or mudbanks by tidal currents, away from the normal location of the main turbidity maximum. These results may be generated due to the disaggregative effect of vigorous tidal currents in the upper reaches of the estuary encouraging the break-up of flocs, reduction in particle size and a resultant increase in the surface area of the particles (Bale, 1987). The geometric surface areas calculated from particle size are plotted against turbidity in Figure 4.2b. The data are fairly scattered but it is apparent from the plot that the geometric surface area of the suspended particles tends to increase (i.e. particle size decreases) as the water column becomes more turbid. The degree of scatter in the data is thought to arise from problems

associated with discrete sampling of the particles which can disrupt delicate aggregates. *In-situ* measurement of particle size is preferable to discrete sampling, but this approach was not extended to cover this work because for most of the study the method was still under development.

Figure 4.3 shows the results of the survey undertaken on 11-03-86. The hydrodynamic conditions within the estuary on this survey reveal an unevenly mixed salinity profile in the mid-estuarine section (7-15 km), and this produces several peaks in turbidity (>300 mg/l). The surface area values for the discrete samples collected at these points are also variable, but the highest surface areas generally correspond with the highest turbidities. The identification of high surface areas with the low salinity, high turbidity region has been shown by Titley *et al.*, (1987).

Particle size analyses of the suspended sediment collected on this survey were used to calculate geometric surface areas which were in the range 0.05-0.2 m²/g. These values, although smaller than the BET values by a factor of 100-150 appeared to co-vary with the latter throughout the profile (Figure 4.3). The larger surface areas of the BET method are generated by the penetration of the particle pore structure by the nitrogen molecules, this internal surface is ignored in the calculation of geometric surface area from particle size, therefore the agreement observed is surprising, but it suggests that particle size is implicated in the high BET surface areas. Thus it appears that tidal shear forces in the low salinity region of the estuary resuspend bed sediments which have lower surface areas than suspended solids. However, during the
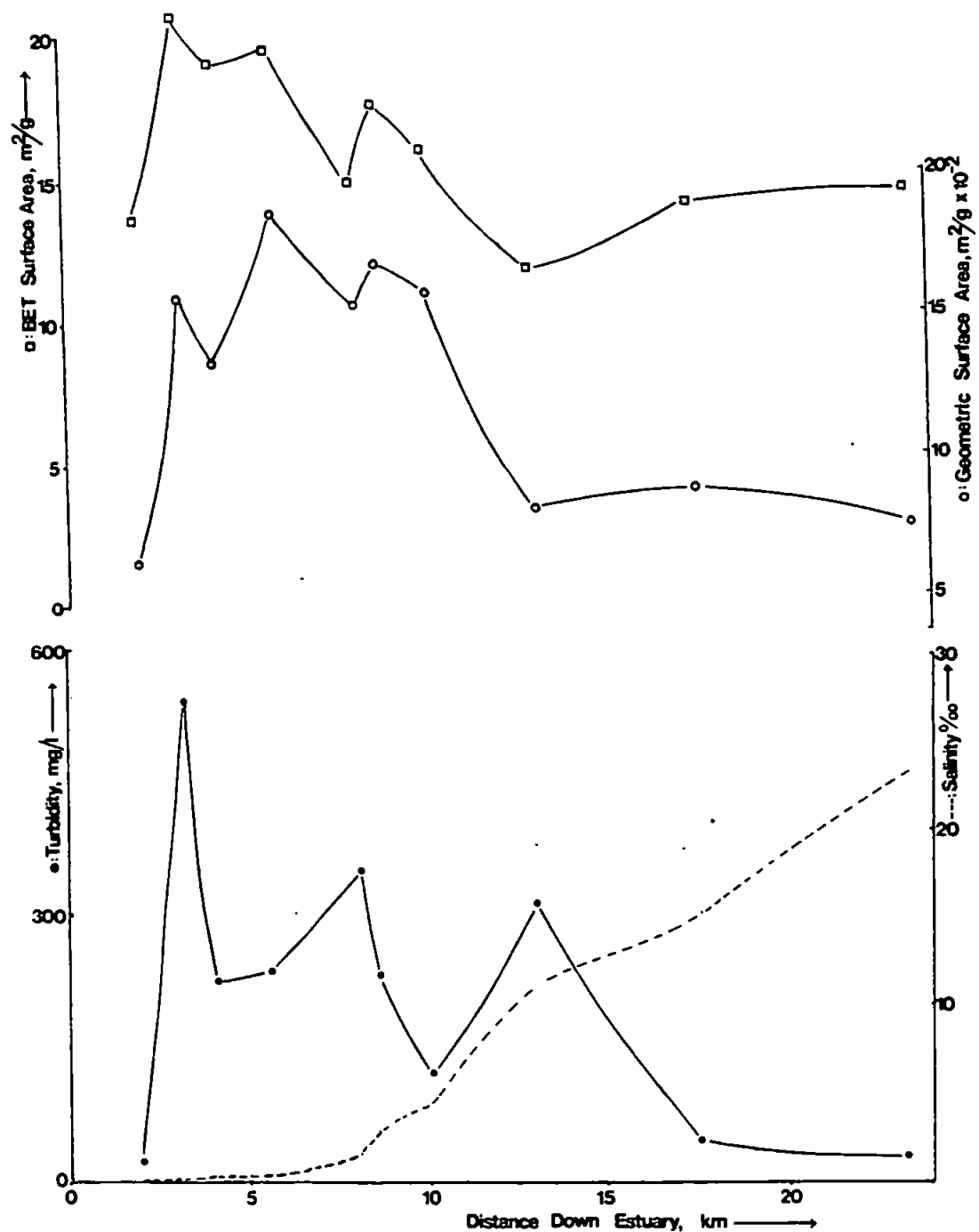
Figure 4.3.   BET and Geometric surface areas of suspended sediments from the Tamar Estuary (11-03-86 survey).

resuspension process the shear forces may also disaggregate the particles and produce an increase in surface area. The relationship between internal and external surface area is a key factor, and will be considered in Section 4.2.2.

Data from the axial surveys may also be presented as surface area per litre of water, thereby combining turbidity and surface area results (Martin *et al.*, 1986). This gives a measure of the potential total surface activity in the water column. Results of two surveys are shown in this way (Figure 4.4a and b) and a substantial difference in the results is apparent, the data in Figure 4.4a (from 29-01-87) range between 0.5 and 1.3 m^2/l, with maximum values in the low salinity region of the estuary. In contrast, the data in Figure 4.4b (from 29-10-85) range between 0.5 and 10 m^2/l, with the maximum values concentrated in the chemically reactive low salinity region of the estuary. The high potential activity in the water column observed in Figure 4.4b could give rise to enhanced removal of trace metals from the dissolved phase as observed in July 1984, under highly turbid conditions (i.e 50-400 mg/l); (Ackroyd *et al.*, 1986).

Conventional understanding of estuarine chemistry suggests that the main requirement for metal removal is sufficiently high turbidity. However the difference in turbidity between the two surveys in Figure 4.4 is a factor of 5 in the turbidity maximum, but the surface area per litre varies by a factor of 10. Thus the surface area makes a significant contribution to the overall activity in the water column and provides for the enhanced removal of trace metals as observed by Glegg, (1987) and Ackroyd *et al.*, (1986). The

177
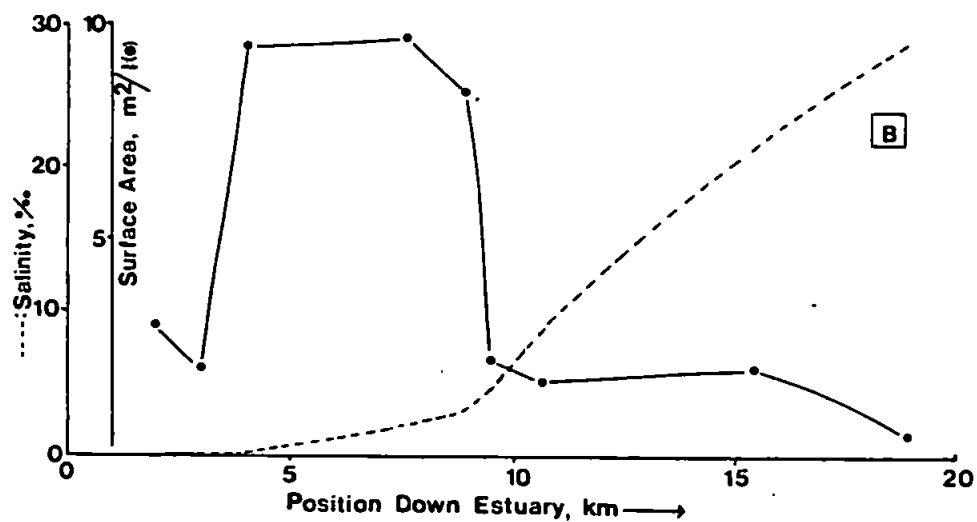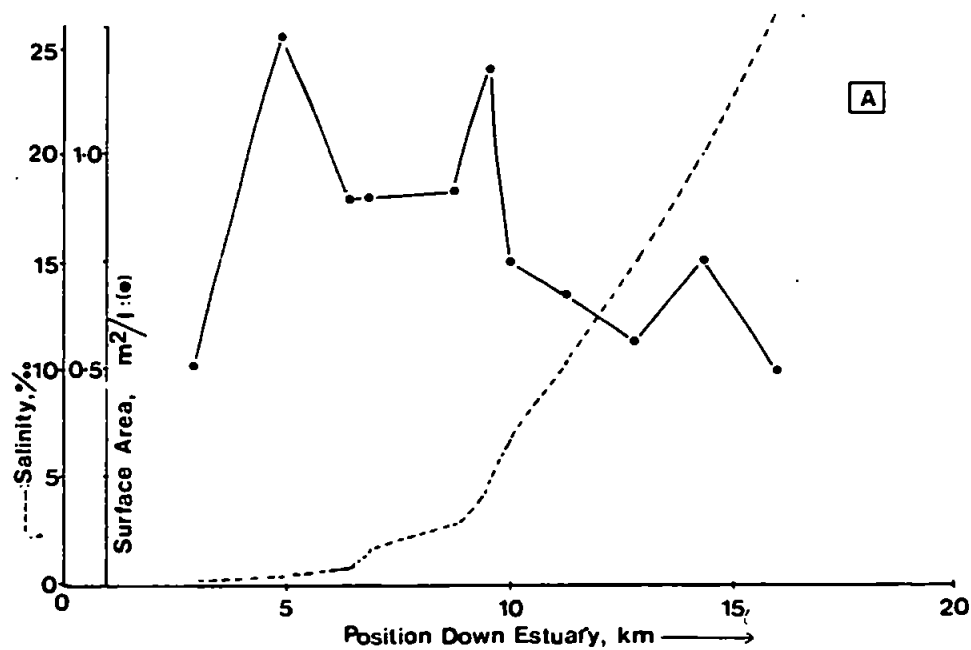
Figure 4.4 a&b Surface area per litre of suspended sediments from the Tamar Estuary, (29-01-87 and 29-10-85 surveys respectively).

implication here is that high turbidity has to be accompanied by a high surface area leading to high surface area per litre values. Thus for 29-01-87, relatively little removal of dissolved metal would be predicted, whereas on the 29-10-85, there is much greater potential for adsorption. Values of surface area per litre for the other surveys are listed in Table 4.5.

29-10-85 Survey		18-09-86 Survey		20-08-86 Survey		30-03-87 Survey		11-03-86 Survey	
Salin-ity $°/_{oo}$	BET Surface Area/l m^2/l	Salin-ity $°/_{oo}$	BET Surface Area/l m^2/l	Salin-ity $°/_{oo}$	BET Surface Area/l m^2/l	Salin-ity $°/_{oo}$	BET Surface Area/l m^2/l	Salin-ity $°/_{oo}$	BET Surface Area/l m^2/l
28.5	0.50	19.0	0.99	19.7	1.15	0.060	0.78	23.6	0.48
22.5	2.03	13.5	2.52	14.4	2.50	0.044	1.77	15.3	0.75
9.7	1.61	8.2	2.00	10.1	2.39	0.041	1.02	11.1	3.88
5.0	2.24	4.7	3.55	3.3	1.70	0.038	0.40	4.6	2.09
3.1	8.46	2.6	8.35	1.1	3.59	0.041	0.51	2.9	4.24
2.2	9.50	0.9	9.16	0.5	3.39	0.043	0.67	1.5	5.16
0.15	9.43	<0.5	6.23	<0.5	1.26	0.040	0.62	0.5	4.70
0.09	2.04	--	--	<0.5	0.34	---	--	<0.5	4.33
0.06	2.99	--	--	<0.5	0.27	---	--	<0.5	11.18
--	--	--	--	--	--	---	--	<0.5	0.33

Table 4.5
BET surface area values expressed as surface area per litre of water, calculated from turbidity values for five surveys in the Tamar Estuary.

The results in Table 4.5 show that the variability in activity in the water column could mean that removal is greatly favoured in some situations relative to others. For example the potential for trace metal removal would be much greater during 11-03-86 survey than during the 20-08-86 survey. The survey undertaken on the 30-03-87 centered on monitoring the surfaces of suspended particles at a fixed location in the low salinity region during the flood tide. On

the day river flow exceeded 31 m³/s, hence the salinities recorded did not exceed 0.1 °/oo. The surface area results from the survey are listed in Table 4.4. The surface areas per litre are low (<1 m²/l) compared with some surveys e.g. 11-03-86, where the activity of the water column reached 10 m²/l in this region of the estuary.

The results of the 30-03-87 survey are also presented in Figure 4.5. The survey started 2 hours after low water and continued until about 1 hour before high water. Due to the high river flow the overall surface flow of the water was down-estuary until about 3.5 hours after low water, and therefore the survey encompassed a delayed period of slack water. During the first two hours the rapid outflowing water had a consistent salinity of 0.04 °/oo and a turbidity of 40-50 mg/l. Following the change in current direction salinity increased to 0.07 °/oo and the turbidity reached 120 mg/l. Thus it appears that the location selected for the survey was slightly upstream of where the turbidity maximum might be expected to occur under these hydrodynamic conditions.

The BET surface areas of the particles collected at discrete intervals during the survey ranged between 11 and 15.5 m²/g which is lower than is normally encountered at the freshwater-brackishwater interface (Glegg, 1987; Titley et al., 1987). However the surface areas showed an increase as the turbidity rose ahead of the approaching saline wedge (see Figure 4.5). The salinity values although increasing slightly remained very low (<0.1°/oo) and it appears that the high river flow pushed the fresh-water brackish water interface further down estuary than usual, and therefore the conditions encountered are basically riverine. The BET surface

180
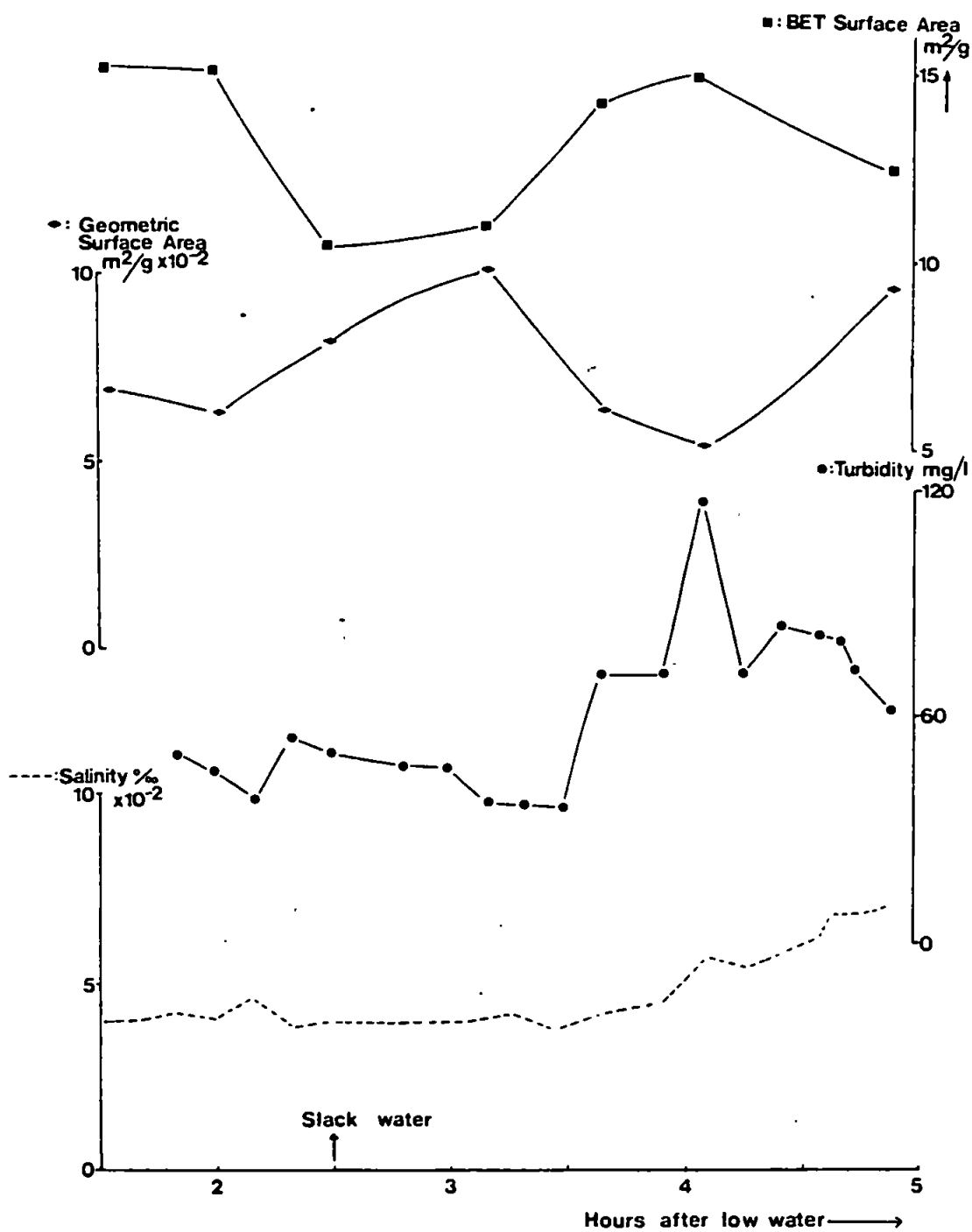
Figure 4.5. BET and Geometric surface areas of suspended sediments collected on 30-03-87 survey at one point in the Tamar Estuary on an incoming tide.

areas of these estuarine particles are similar to those of riverine particles, surface area 14.5 m²/g.

Geometric surface areas calculated from particle size data are in the range 0.05-0.1 m²/g which are smaller by a factor of 110-270 than the BET values. Riverborne particles are known to be larger than those found in the low salinity region of the estuary (Bale 1987) which accounts for the small geometric surface areas. The overall pattern shows an apparent inverse relationship between BET surface area and geometric surface areas calculated from particle size. This contrasts sharply with the results obtained during the 11-03-86 survey (see Figure 4.3), where the geometric and BET surface areas co-varied throughout the estuarine profile. *In-situ* measurements of particle size by Bale (1987) show a consistent decrease in particle size within the turbidity maximum zone. The particles analysed in this survey are however freshly carried from the river, and the surface areas are likely to be a reflection of the underlying lithogenous phase. Furthermore the particles would not yet have become involved in the complex processes within the turbidity maximum that lead to the observed decline in particle size and fresh coatings of Fe/Mn oxides and organic materials.

Any relationship between BET and geometric surface area such as in two surveys described above was not observed in any of the other surveys. This lack of correlation may be explained in terms of the highly variable nature of the estuarine environment, i.e. the surface area of particles may be controlled by a number of different variables such as Fe/Mn oxide coatings, particle size, carbon coatings or the presence of swelling clays such as montmorillonite

or chlorite within the particle population. The surface areas of the particles would therefore be a composite value with each component contributing to a greater or lesser degree. Under certain conditions the role played by one or two of these components may become dominant and therefore identifiable.

Alternatively Bale *et al.* (1984) showed that removal of particles from the estuary followed by size analysis in the laboratory can cause substantial changes to the particles, especially in terms of either disintegration of floccs or in some cases particle aggregation, thereby reducing the likelyhood of observing the particle sizes as they are in their natural environment. It is therefore possible that the variation in BET surface areas may be purely related to particle size, although this is unlikely because of the highly complex nature of the particle composition. *In-situ* deployment of the Malvern Instruments Laser Particle Sizer System as described by Bale *et al.*, (1984) in conjunction with use of the BET apparatus would therefore be a worthwhile development of this work.

4.1.2 POROSITIES OF SUSPENDED PARTICLES

The internal surfaces of estuarine particles, together with their pore spaces are of great importance for chemical behaviour in the estuarine environment, because the internal spaces have great potential for adsorbing dissolved species. The external surface areas of particles (calculated from particle size data) are 100-200 times lower than BET surface area measurements, and this extra surface area observed must be located within pores. The ratio of BET surface area to geometric (external) surface area therefore

183

gives a crude estimate of porosity and data from the Tamar Estuary has been examined in this way.

The BET/geometric surface area ratios for the surveys are shown in Figures 4.6 and 4.7. Data for the axial survey of the 11-03-86; where a relationship between BET and geometric surface areas was observed (Figure 4.6) shows distinct non-conservative behaviour, with a decrease in the internal/external surface area ratio (from 200 to 100) occurring in the low salinity region of the estuary, this being a result of the reduction in particle size due to disaggregation in the highly dynamic turbidity maximum (Bale, 1987).

Particles collected from the low salinity region of the estuary (Figure 4.7) showed no obvious pattern of this kind although the absolute value of the ratio varies by a factor of 2.5 over a time period of just 1h. Here, the water column was dominated by the high river flow (31 m³/s) and the environment was relatively undynamic, with low turbidity, and only a slight change in salinity. The surface area of the sediments is not controlled by particle size although an inverse relationship between the BET and geometric surface area is apparent from Figure 4.5. In Chapter 3, the surface properties of the sediments, especially Fe/Mn oxides and organic carbon coatings were found to be major controls on the morphology of of the sediments. The role of these coatings on suspended particles will be examined more fully in Section 4.2.

Data from other axial surveys had internal/external surface area ratios ranging between 45 and 200, but these do not show any decrease in the low salinity region of the estuary like that found for the 11-03-86 survey (Figure 4.6).

184
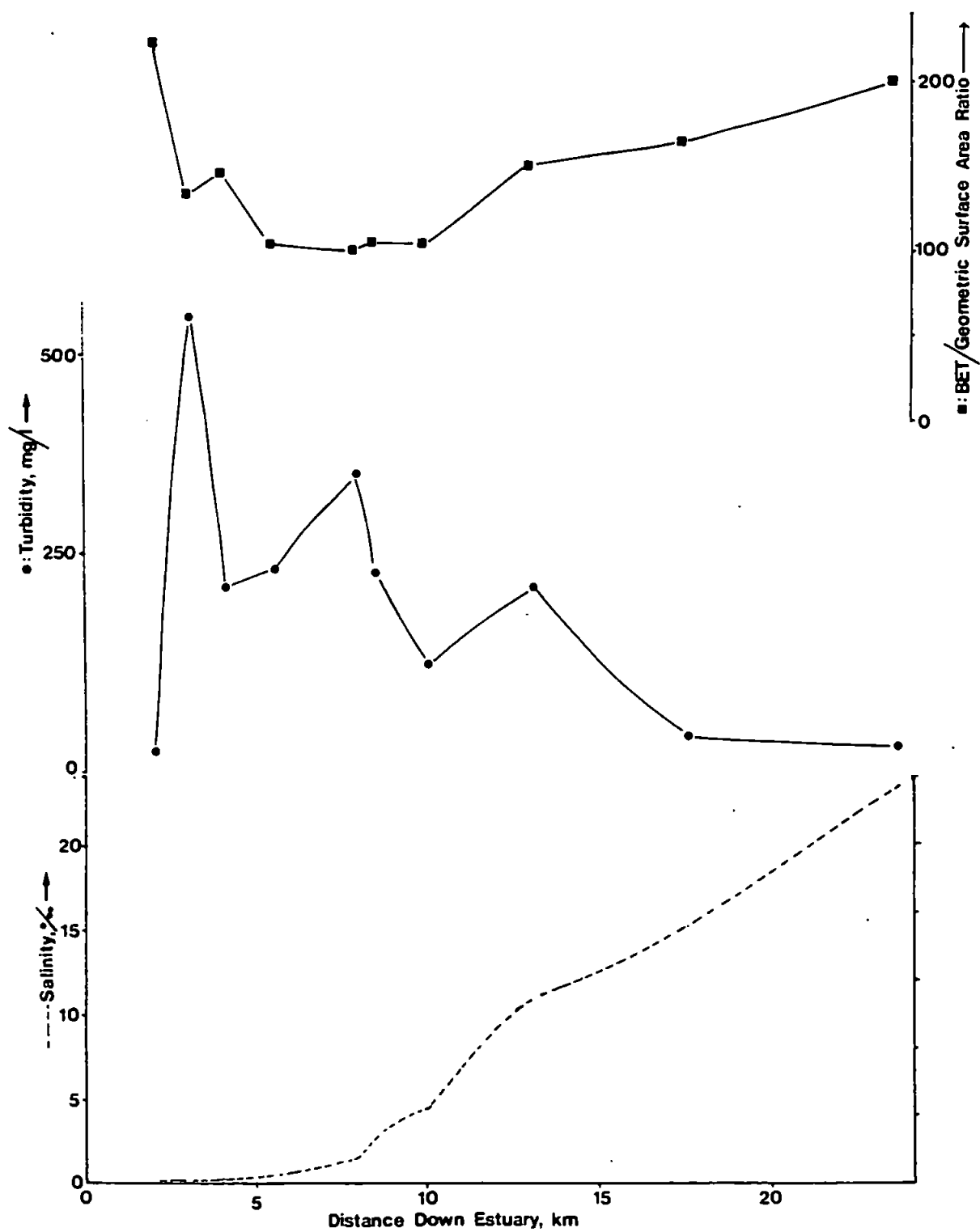
Figure 4.6. BET/Geometric surface area ratio of suspended sediments from the Tamar Estuary (11-03-86 survey).

185
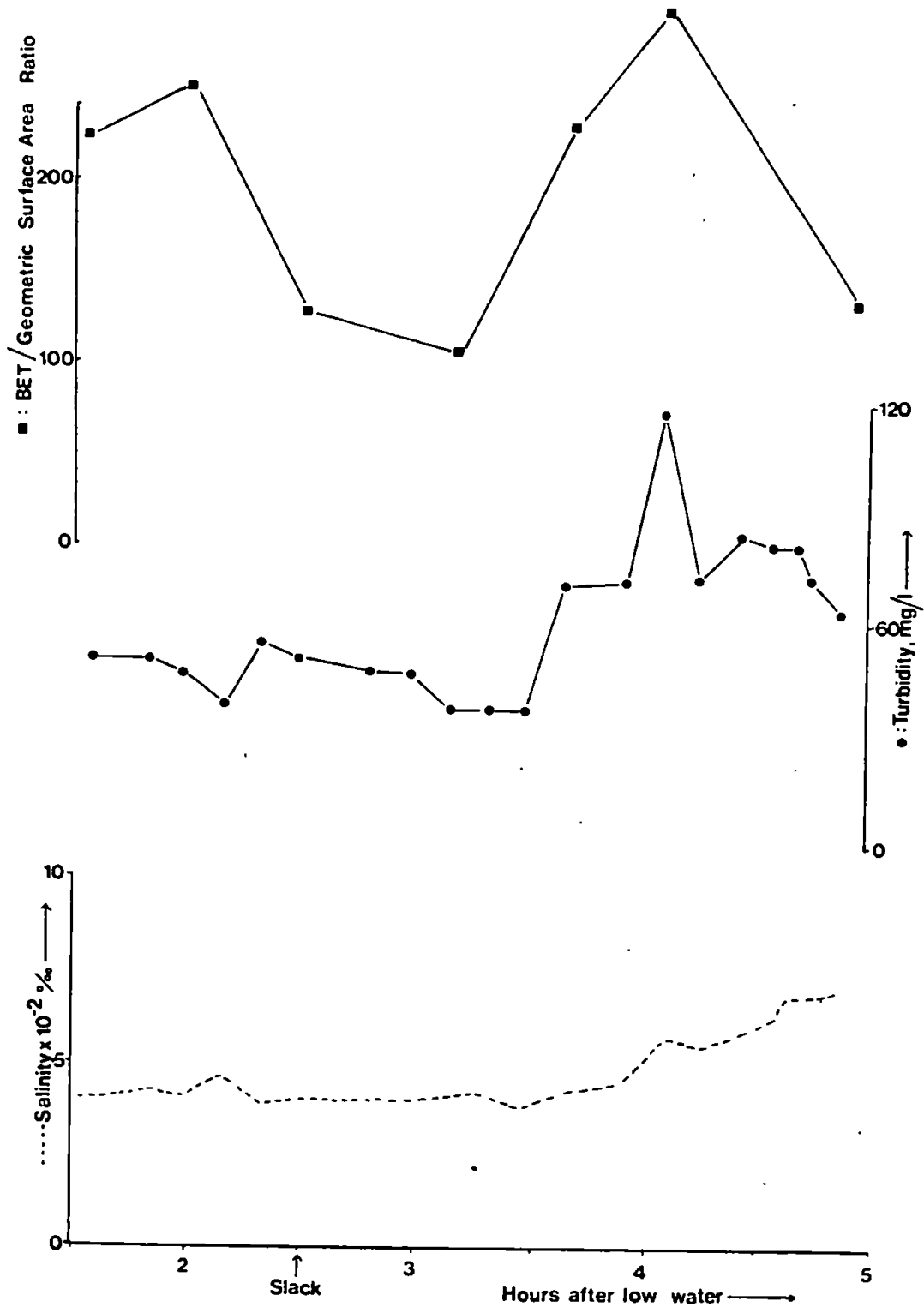
Figure 4.7. BET/Geometric surface area ratios for suspended sediments collected from the Tamar Estuary on 30-03-87.

The observed variation in internal/external surface area, especially the decrease in this value in the reactive low salinity region (Figure 4.6) is likely to be of great importance for estuarine chemical processes. There is a potential doubling in the the number of readily accessible surface sites, which are implicated in initial fast adsorption reactions observed by Li *et al.*, (1984).

A fuller investigation of the distribution of the internal surface area and the pore size distributions associated with the particle matrix was also undertaken, as this internal surface area has significant potential for adsorbing dissolved trace species.

The internal porosity of the particles was investigated by the N_2 gas sorption method coupled with the interpretative techniques of de Boer (1958) and Cranston and Inkley (1957). Pore shapes, size distributions and the location of surface area within the pore network were obtained on selected samples from the surveys using the methods described in Chapter 2.

Adsorption isotherms and their associated hysteresis loops for two suspended sediment samples collected on the 20-08-86 survey are shown in Figure 4.8. Hysteresis loop A was obtained from a suspended sediment sample from the low salinity region of the estuary (1.1°/oo; surface area 22.1 m²/g), whereas loop B was obtained on sediments from the fresh water end above the salt intrusion, and the particles have a lower surface area (12.7 m²/g). Loop A shows greater adsorption of nitrogen and more hysteresis than loop B, suggesting a more active surface and greater porosity. Both hysteresis loops are of type 'B' which suggests that the pores are

188
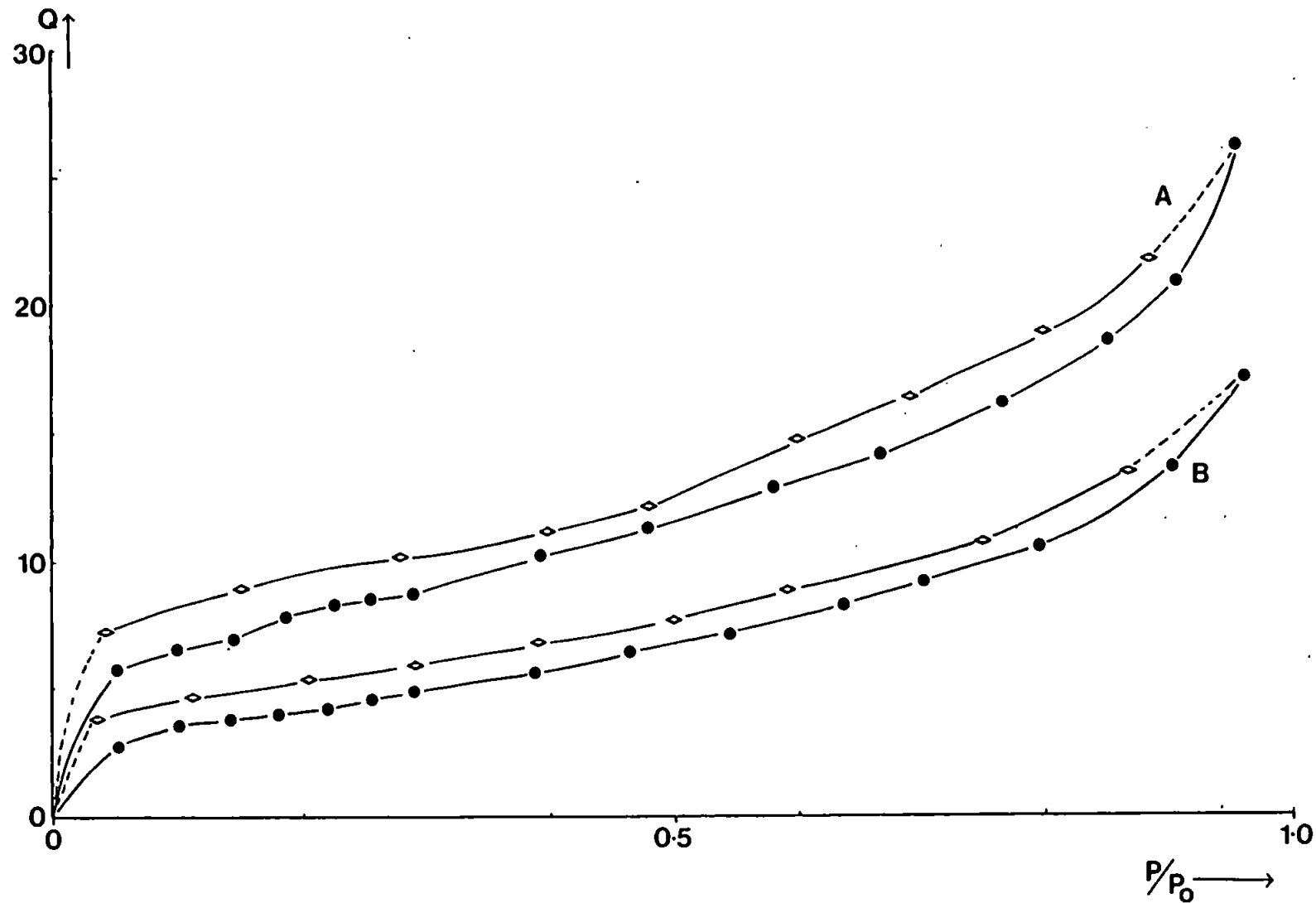
Figure 4.8. Hysteresis loops obtained on suspended sediments from the Tamar Estuary (20-08-86 survey). Loop A: Surface area 22.1 m²/g (salinity 1.1°/oo). Loop B: Surface area 12.7 m²/g (Fresh water).

slit shaped overall, which is typical of estuarine sediments (Glegg *et al.*, (1987). The C&I pore size distributions for these two samples are shown in Figure 4.9a and 4.9b corresponding to the hysteresis loops described. Distributions of pores for both samples appears to favour <10 nm size range. The data in Figure 4.9a show substantially more porosity (by a factor of 2) throughout the size range than for the sample shown in Figure 4.9b. This feature is especially pronounced for pores <10 nm diameter. The C&I pore size distributions for two more suspended sediment samples from the same survey are shown in Figure 4.10. Figure 4.10a is for particles collected at $10.1^{\circ}/_{\circ\circ}$ (surface area 14.2 m^2/g) and Figure 3.10b shows the distributions from $0.5^{\circ}/_{\circ\circ}$ (surface area 16.8 m^2/g).

Interpretation of these pore size distributions was undertaken by regression analysis of the log-normalized data. Data from the pore size distribution plots e.g. Figure 4.9a and 4.9b were log-normalized to reduce the scatter which is evident as the smaller pores in the size range are approached. The best-fit polynomial regression lines of the data obtained from samples collected at $10.1^{\circ}/_{\circ\circ}$ and at $1.1^{\circ}/_{\circ\circ}$ from 20-08-86 survey are shown in Figure 4.11. Differences between the samples are apparent, including the total porosity and the overall distributions. Statistical comparisons were undertaken as described in Chapter 2 and these revealed significant differences between the samples at >0.1% confidence level.

Samples collected during the 11-03-86 showed a clear relationship between the external (geometric) and internal (BET) surface areas. The co-variance of these two measurements is surprising, given the probable complexity of the internal porosity. It can be
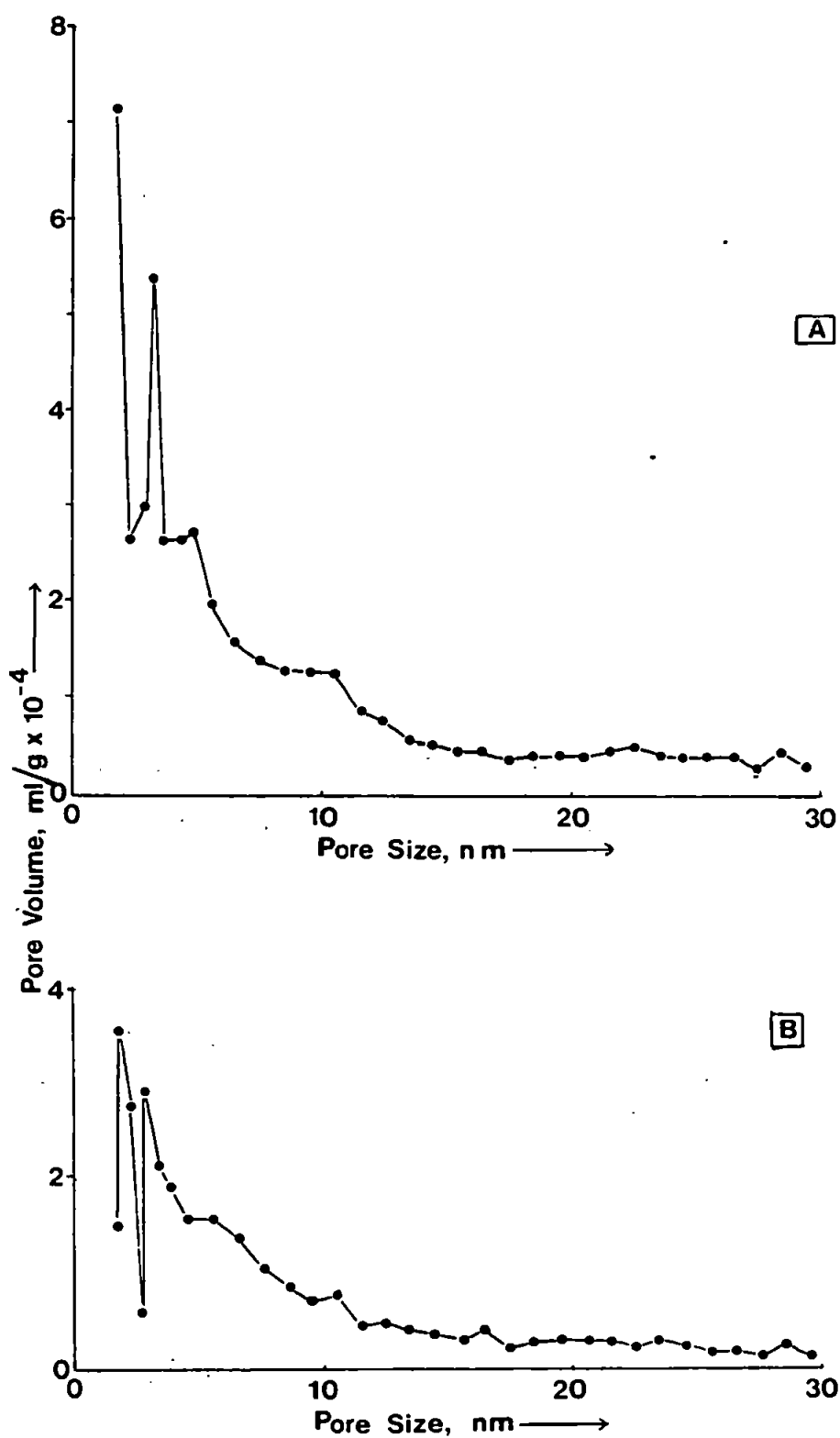
Figure 4.9. C&I pore size distributions of the sediments described by the hysteresis loops in Figure 4.8. Distribution A as loop A distribution B as loop B.

190
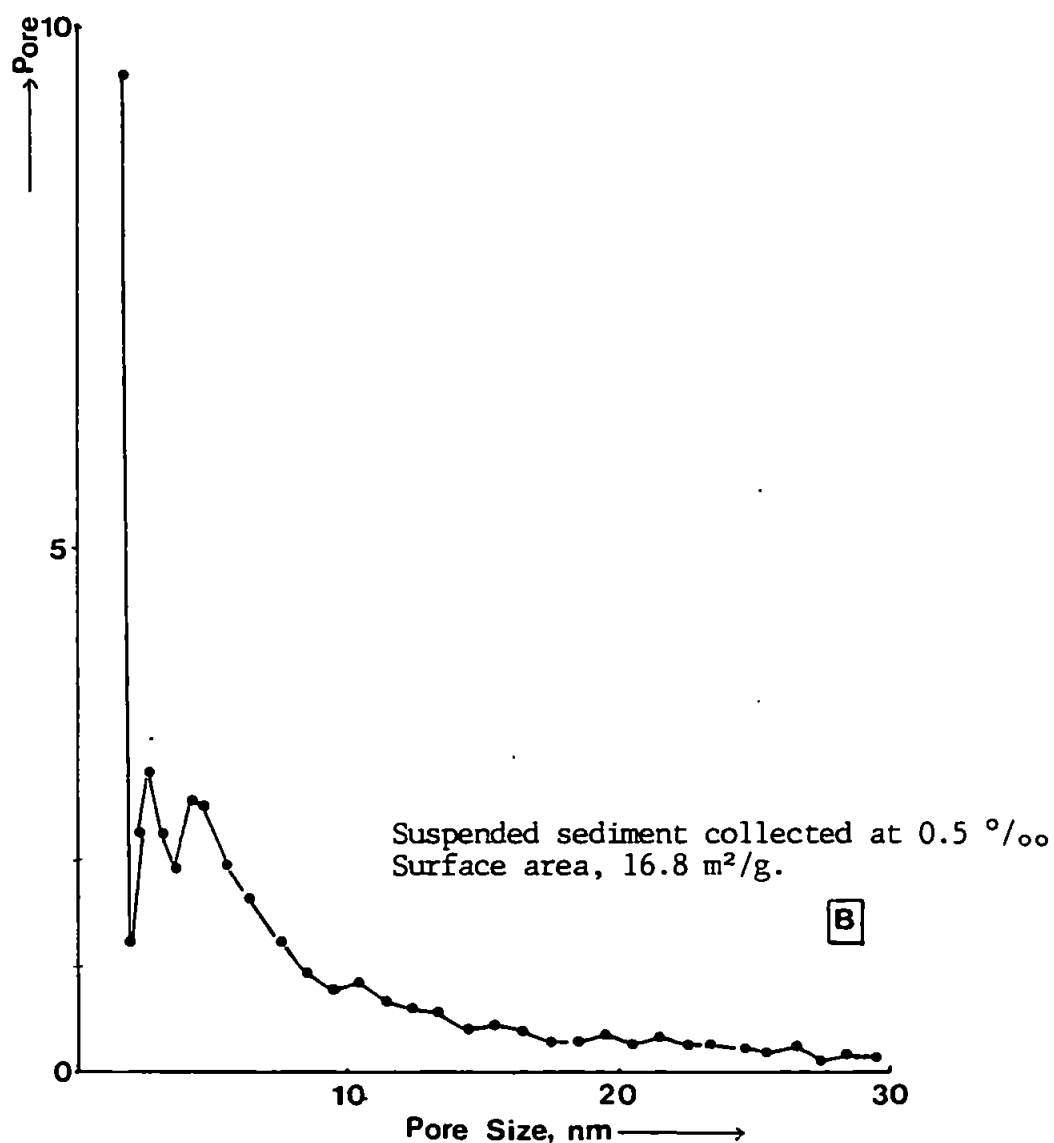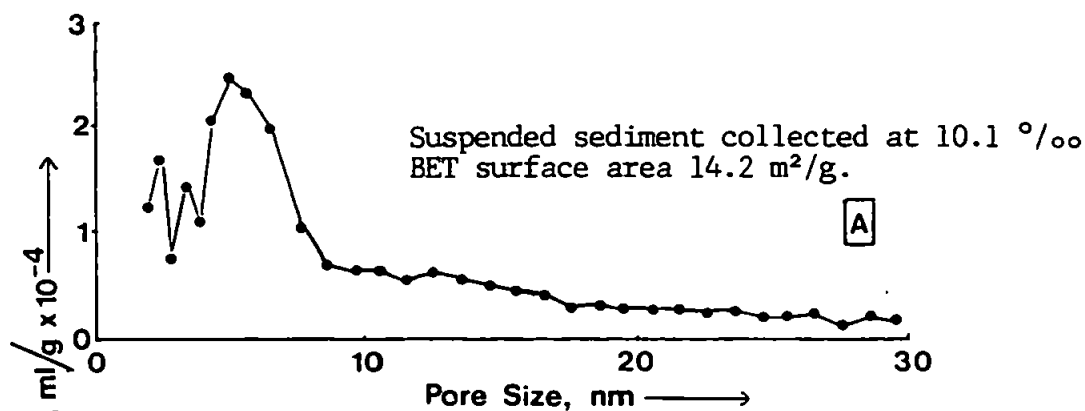
Figure 4.10. C&I pore size distributions obtained on suspended sediments from the Tamar Estuary (20-08-86).
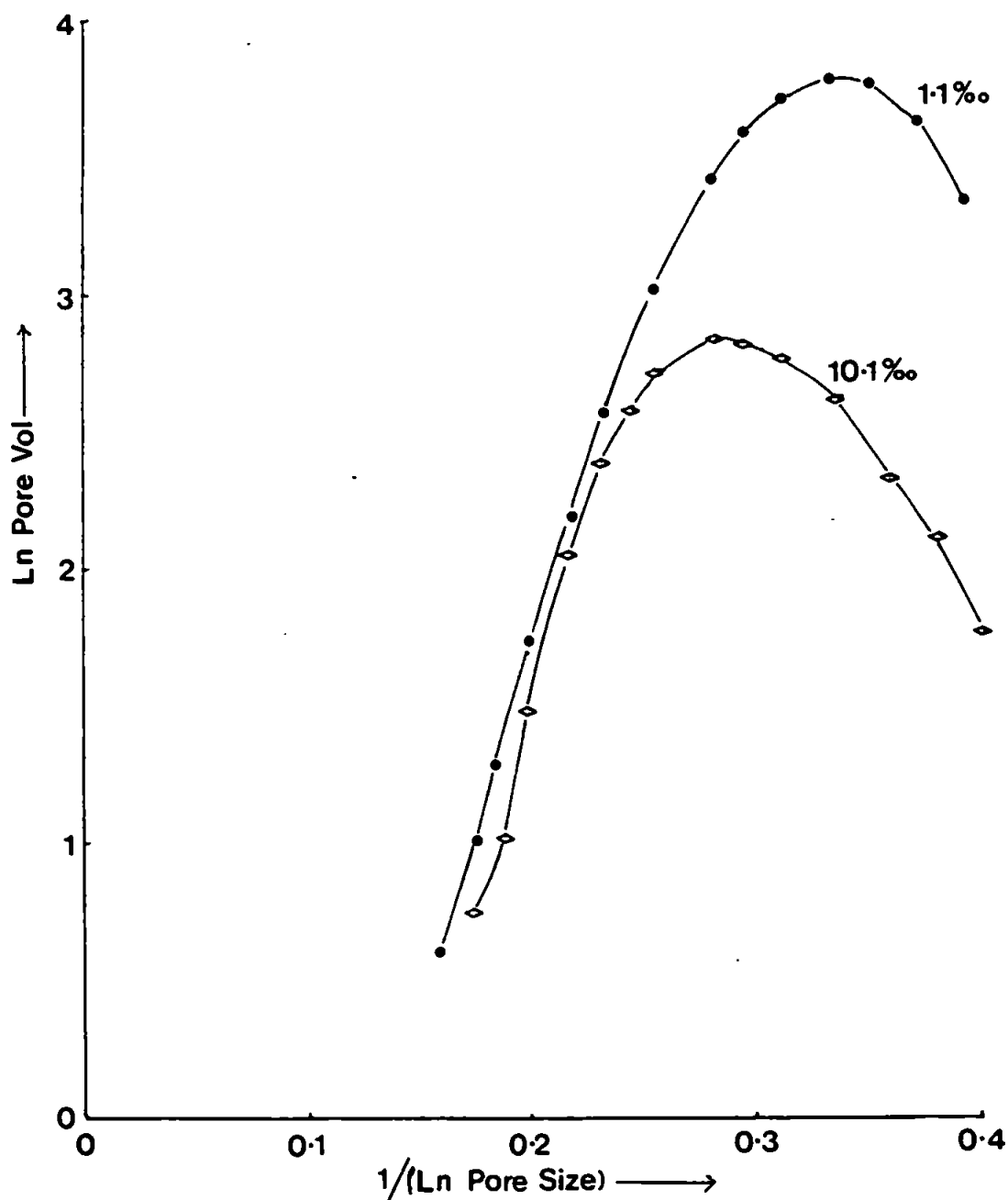
Figure 4.11. Regression lines fitted through the C&I pore size distributions shown in Figure 4.9a and 4.10a.

hypothesized that if a relationship exists between the internal and the external surface area for a set of samples then the porosities of these samples must have similar size distributions. Best fit regression lines for the samples are shown in Figures 4.12 and 4.13. The overall patterns are very similar although the samples collected in the low salinity region of the estuary ($\leq 0.5°/oo$) have different microporosities compared with the samples collected at higher salinities. The C&I pore size distributions for the more saline samples are shown in Figure 4.14. Statistical comparisons made between all of the samples show significant differences if the 5% confidence interval is chosen but not if the 1% is used. Use of the 1% confidence interval can be justified because the relationship observed between the internal and external surface area is unlikely to be simple. A plot of the two measures (11-03-86) showed a non-linear relationship (see Figure 4.6). Similarity between the sample porosities is apparent from the best fit lines in Figures 4.12 and 4.13. Consideration of sample porosity from other surveys, such as 20-08-86 (Figure 4.11) reveals very much greater variation in porosity than those observed on the 11-03-86. Given the complex nature of estuarine behaviour, and the heterogeneous nature of the particle composition, the similarities in the porosities between the samples is probably sufficient to explain the observed relationship.

Microstructural data on the samples collected in the low salinity region of the estuary (30-03-87) are presented as log-normalized plots in Figure 4.15. An inverse relationship between internal and external surface area was observed for these samples, which contrasts strongly with the samples collected on 11-03-86. The data
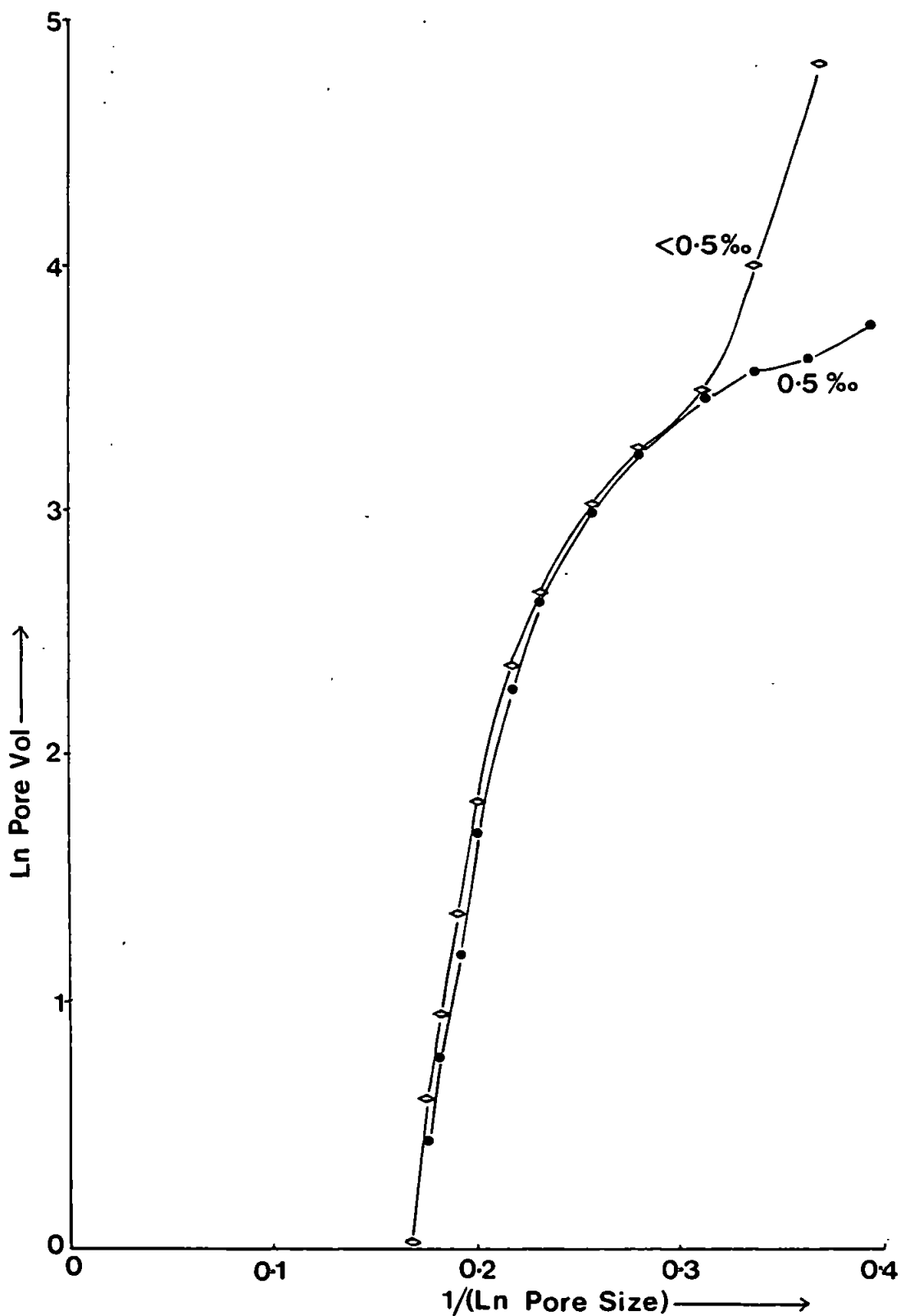
Figure 4.12 Regression lines fitted through C&I pore size distributions obtained from suspended sediments from the Tamar Estuary (11-03-86 survey) at salinities shown.
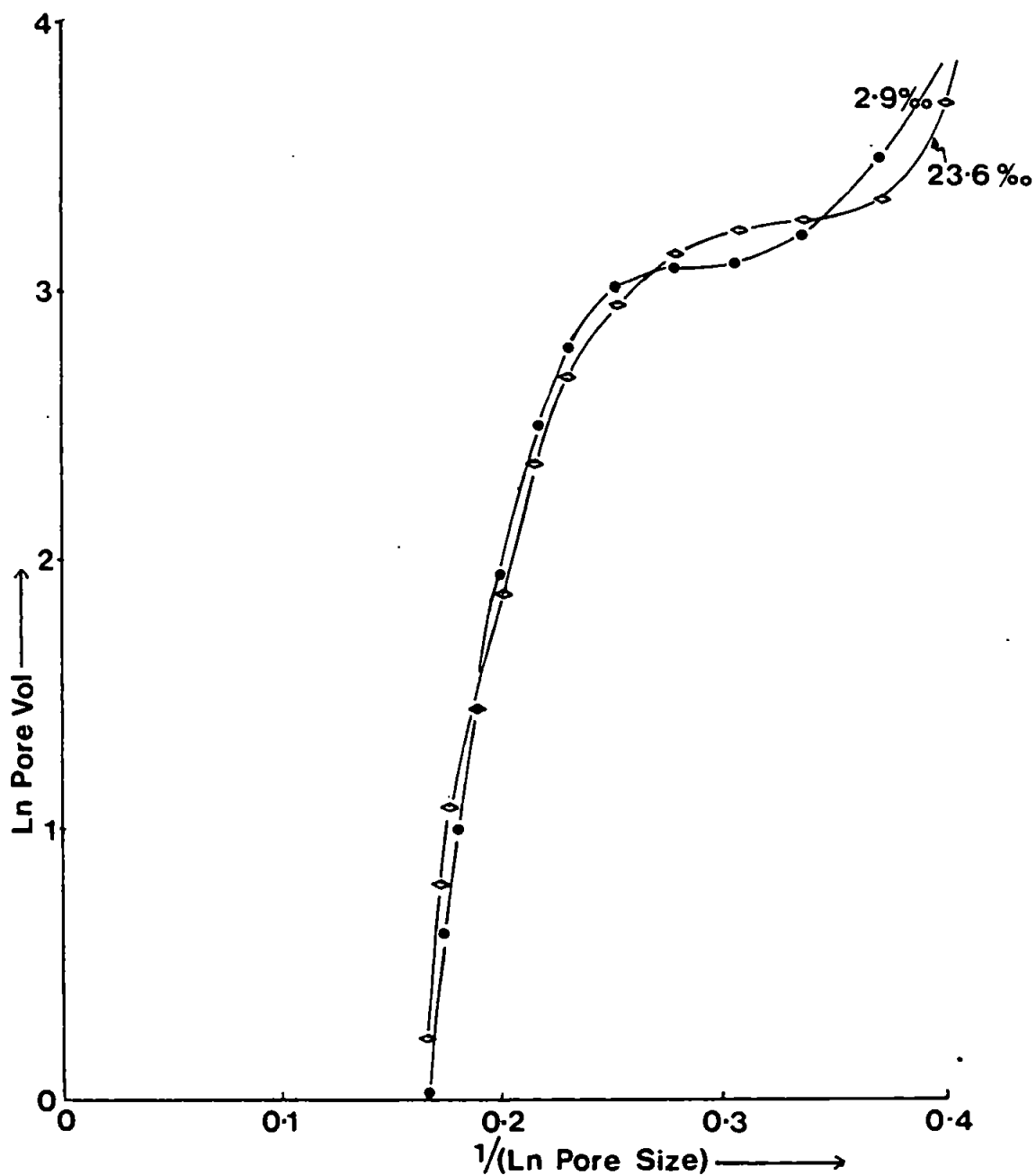
Figure 4.13. Regression lines fitted through C&I pore size distribution data obtained from suspended solids from the Tamar Estuary. (Survey 11-03-86) Two different salinities are shown.
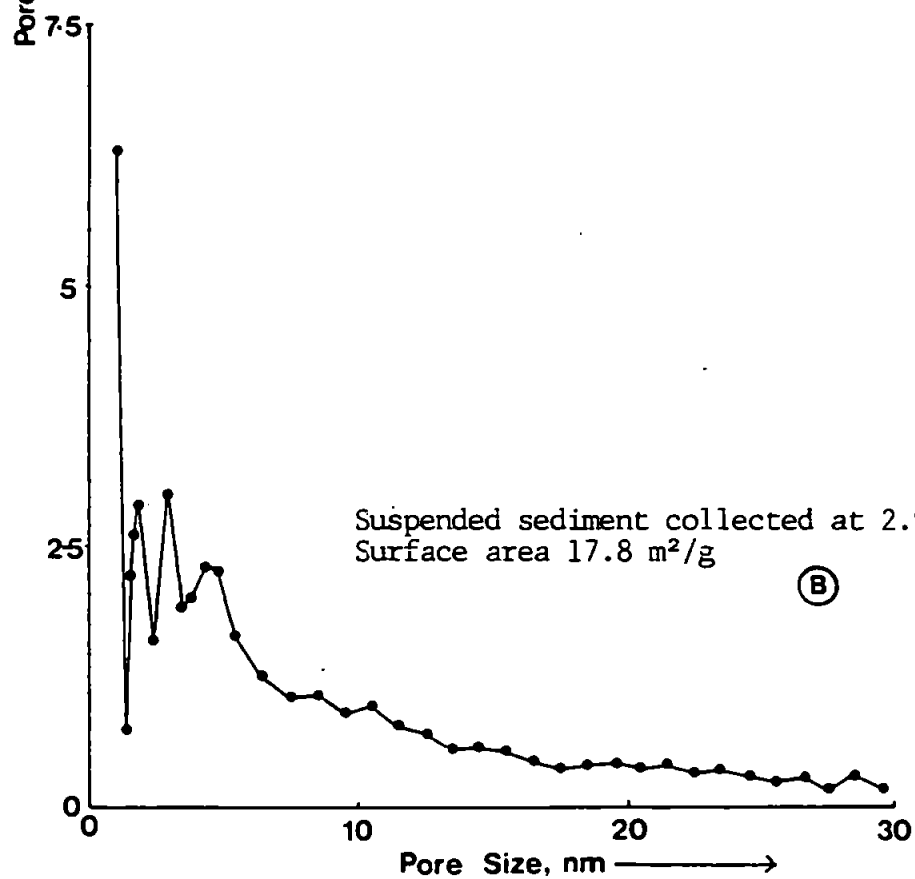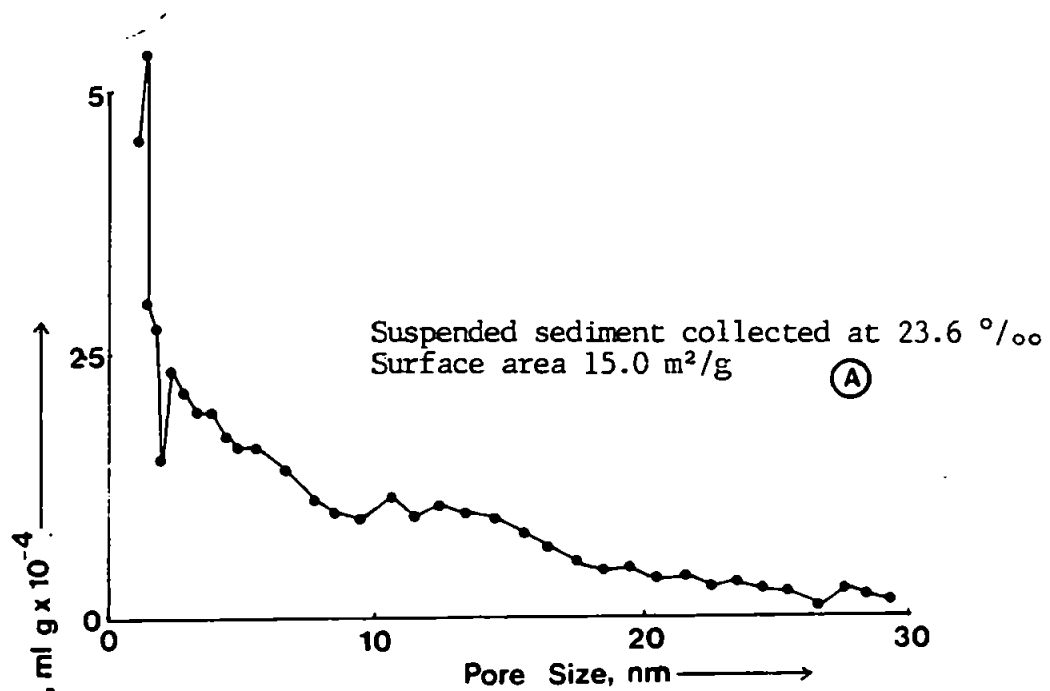
Figure 4.14. C&I pore size distributions obtained from suspended sediments in the Tamar Estuary and corresponding to Figure 4.13.
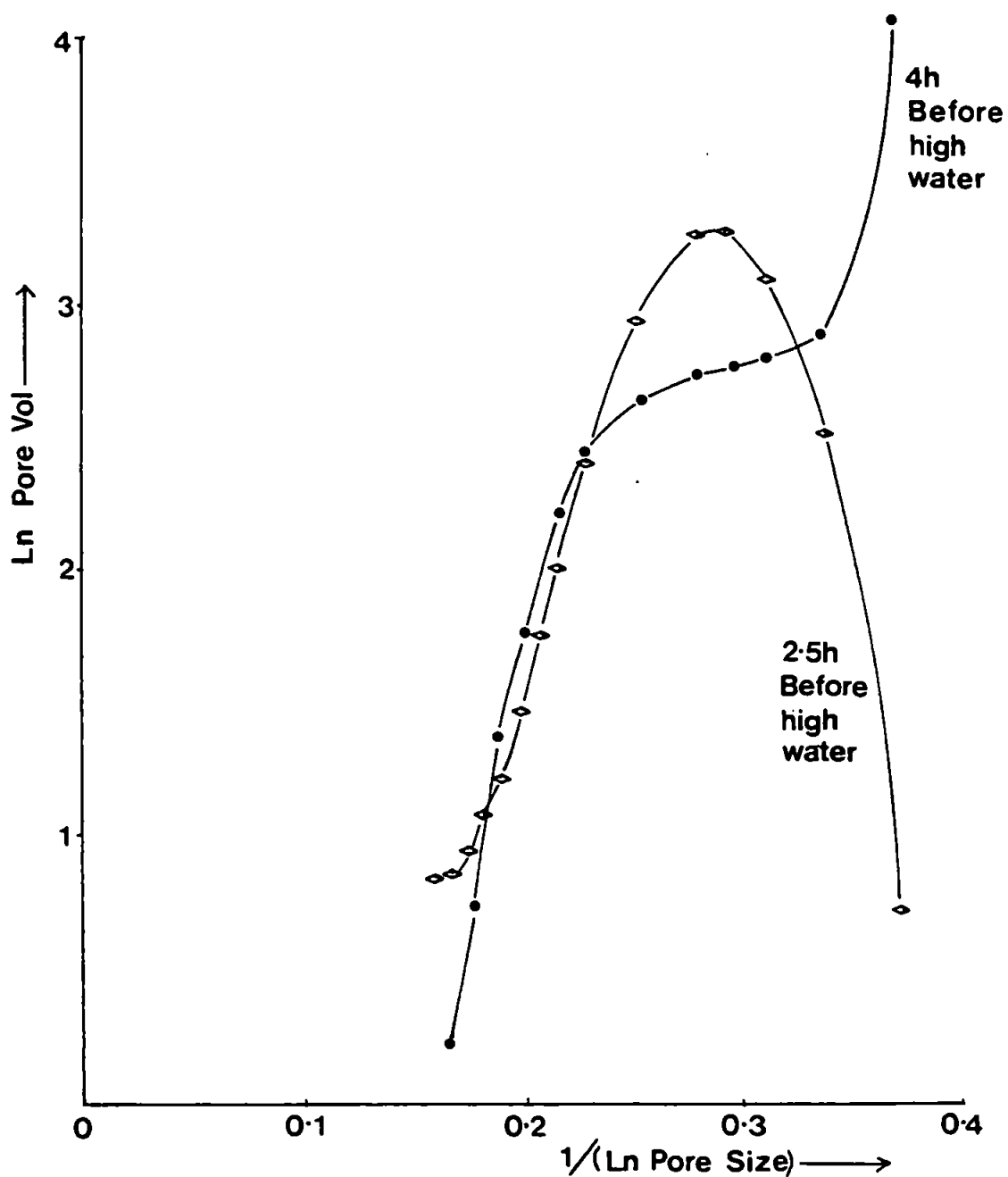
Figure 4.15. Regression lines fitted through C&I pore size distributions obtained on suspended sediment from the low salinity region of the Tamar Estuary (stationary survey; 30-03-87).

show different pore distributions, the sample collected 4 hours

before high tide shows increasing porosity in the micropore size

range (<2 nm) whereas the sample collected 2.5 h before high water

shows a peak in pore volume in the smaller mesopores (2-4 nm);

followed by a decline with decreasing pore size. Table 4.6

summarises the porosity data as discussed here.

Salinity $°/_{oo}$	BET Surface Area, m^2/g	Total Pore Vol, $ml/g*10^{-2}$	Mean Pore Size, nm
<0.5*	20.7	2.73	5.22
0.5*	19.6	2.44	5.80
2.9*	17.8	2.44	6.33
23.6*	15.0	2.59	6.20
<0.5[*]	12.7	1.88	7.17
0.5[*]	16.8	2.32	6.17
1.1[*]	22.1	2.75	7.08
10.1[*]	14.2	1.89	8.05
0.04[1]	15.3	2.38	7.84
0.04[2]	15.1	1.89	8.94
Kaolinite	13.1	1.87	4.94
Amorphous FeOOH	303.0	23.10	2.66

*11-03-86 Survey.
[*]20-08-86 Survey.
[1]4 hours before; [2]2.5 hours before; high water; 30-03-87 survey.

Table 4.6
Pore volumes and BET surface areas of estuarine suspended sediments,
kaolinite and an amorphous Fe oxide.

The pore volumes shown in the table are similar to those reported

by Glegg, (1987) who found values of 1-1.6 x 10^{-2} ml/g for Tamar

sediment and Crosby, (1982) who reported 1.9 x 10^{-1} ml/g for

amorphous iron oxide. The data in Table 4.6 also show no direct

relationship between surface area and total porosity. This

observation is intuitive, because surface area is more likely to be related to the actual pore size distributions, as the ratio between surface area and pore volume will vary with pore size. Therefore a sample that has pores skewed in favour of the smaller size range will have a greater surface area than a sample with larger pores but the same total pore volume.

Surface area distributions within pores can be calculated from pore size distributions, and examples are shown in Table 4.7 and 4.8. This is a key aspect of particle microstructure because of the availability of the surface area to an adsorbing species. A sample with a large surface area may not necessarily be reactive in the water column if part or all of the surface is located within pores that are too small to permit relatively easy access to an adsorbable species.

	11-03-86 Survey			20-08-86 Survey	
Salinity °/oo	Pore Size, nm	% of Total Surface Area	Salinity °/oo	Pore Size, nm	% of Total Surface Area
<0.5	<2	46.2	<0.5	<2	15.2
	2-5	34.7		2-5	50.8
	5-10	11.4		5-10	22.6
	10-20	6.3		10-20	8.6
	20-30	1.5		20-30	2.8
0.5	<2	34.1	0.5	<2	25.6
	2-5	38.7		2-5	44.8
	5-10	18.3		5-10	19.9
	10-20	7.2		10-20	7.7
	20-30	1.7		20-30	2.0
2.9	<2	32.6	1.1	<2	14.2
	2-5	37.5		2-5	54.6
	5-10	15.0		5-10	20.0
	10-20	7.5		10-20	8.2
	20-30	2.1		20-30	2.9
23.6	<2	42.8	10.1	<2	4.2
	2-5	30.9		2-5	50.4
	5-10	14.5		5-10	31.9
	10-20	10.0		10-20	10.7
	20-30	1.9		20-30	2.8

Table 4.7
Surface area distributions within the microstructures of various estuarine suspended solids.

4 hours before high water		2.5 hour before high water	
Pore Size nm	% of total Surface Area	Pore Size nm	% of total Surface Area
<2	20.0	<2	2.7
2-5	44.0	2-5	59.1
5-10	21.2	5-10	24.2
10-20	11.4	10-20	10.3
20-30	3.3	20-30	3.7

Table 4.8
Surface area distributions within the pore structure of particles collected on 30-03-87 survey.

The data in Tables 4.7 and 4.8 show that the surface area distributions fall into two broad categories; those where a substantial proportion of the surface area (>33%) is located in pore <2nm in diameter, and particles where the 45-60% of the surface area is found in pores in the size range 2-5 nm. The former category is associated with the type of log-normalized pore size distributions shown in Figures 4.12 and 4.13, which show a continuing increase with decreasing pore size. The latter type is associated with the pore size distributions of the type shown in Figure 4.11, where pore volumes increase with decreasing pore size down to a particular pore diameter, when the trend inverts and the pore volumes start to decrease through the micropore size range. These pore distribution types are not artefacts of the experimental procedure, but are real environmental features according to the reproducibility studies carried out on sediments (Chapter 2), and are in agreement with results obtained by Stul, (1985) on expanding clays.

However it must be noted that the results obtained in the micropore

size range show increasing scatter as the pore sizes decrease. Pores <2 nm in diameter are more difficult to assess reproducibly because of the increased local effects on the sorbing nitrogen molecules such as surface activation energies which will have more effect as pore wall separation decreases. This is confirmed by the observed lack of closure of hysteresis loops caused by retention of nitrogen molecules in micropores. However the good reproducibility of the technique on sediment samples even in the micropore size range shows that the trends observed here are real environmental features, although the precision of the analysis will be less in the micropore size range.

4.2 CHEMICAL COMPOSITION AND PARTICLE MICROSTRUCTURE OF SUSPENDED SOLIDS

Results from the previous section reveal that the surface areas of particles collected from the Tamar Estuary are controlled by a number of complex features in addition to a dependence on particle size. Both the underlying particle matrix and particle coatings are important in this respect (Glegg, 1987; Martin *et al.*, 1986), the latter being involved in other aspects of particle characteristics such as surface charge (Hunter and Liss, 1982; Loeb and Neihof, 1977). In this work particle composition was assessed by (i): X-ray diffraction to identify the principal crystalline components making up the underlying lithogenous phases; (ii): Combustimetric C/H/N analysis to determine carbon content; and (iii): Selective leaching methods to extract Fe/Mn hydrous oxide phases.

4.2.1 CRYSTALLINE COMPONENTS

X-ray diffraction analyses of suspended solids from the Tamar Estuary revealed 5 major components in the underlying lithogenous phase. A typical X-ray trace for an estuarine suspended solid is shown in Figure 4.16. The strongest signal was obtained from $\alpha-SiO_2$, which has a highly crystalline, regular structure and relative low surface area usually 2-5 m²/g. This material was ubiquitous and was even found in suspended solids from coastal waters. Most suspended solids from the Tamar Estuary also contained kaolinite, (surface area 10-75 m²/g)(This work, van Olphen, 1976; Dutta and Gupta, 1974), muscovite (surface area 10-46 m²/g; by water adsorption)
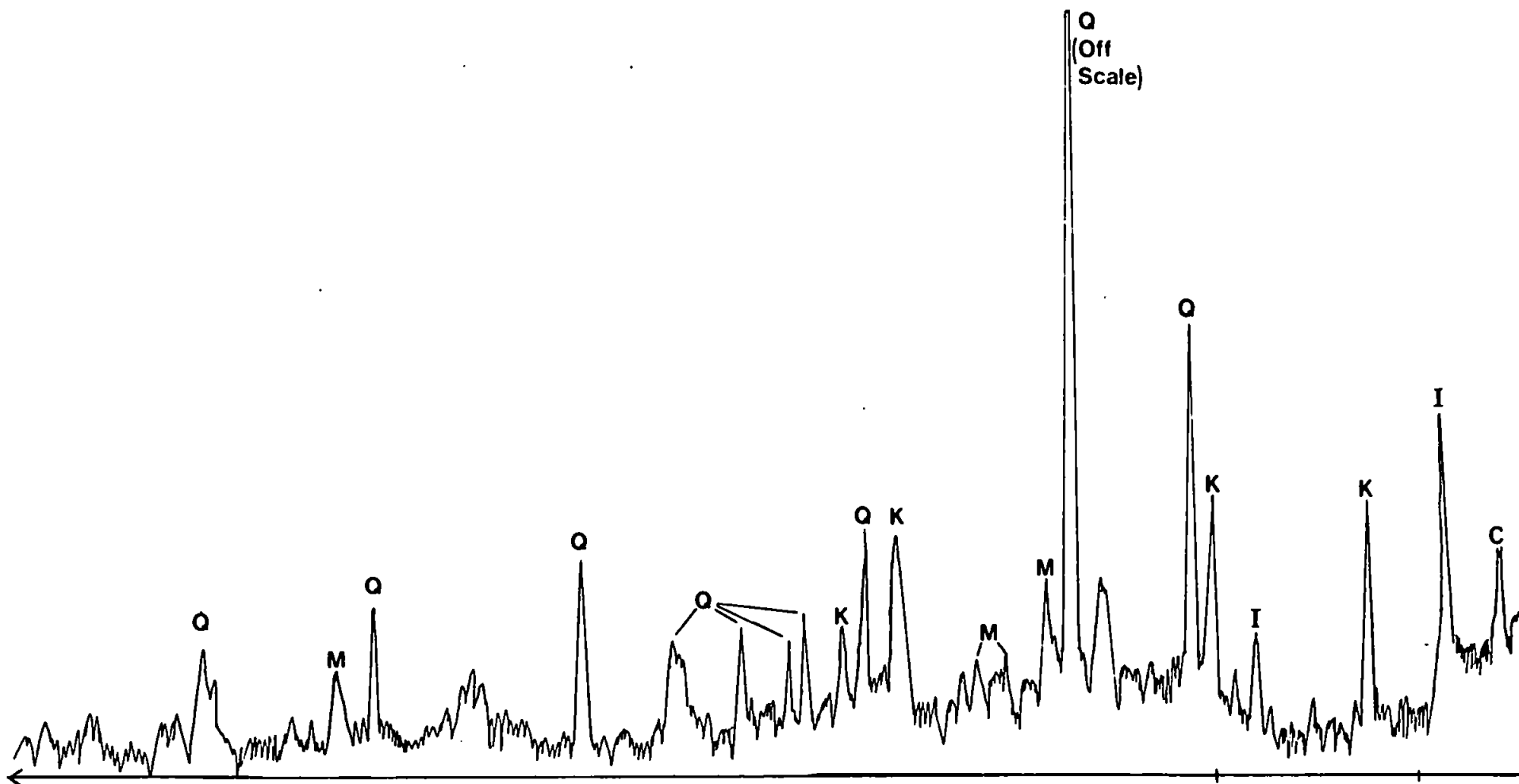
Figure 4.16. Example of an Xray trace obtained on a suspended solid from the Tamar Estuary.
Key: Q Quartz. M Muscovite. K Kaolinite. I Illite. C Chlorite.

(Mikhail *et al.*, 1979), illite (surface area 93-130 m²/g)(Martin *et al.*, 1986; Greenland and Quirk, 1962) and chlorite.

Small amounts of crystalline Fe phases were identifiable in most samples as lepidocrocite, magnetite or goethite. However the quantities present were small producing low peak heights that were difficult to discriminate from the background.

The presence of swelling clays within the suspended particle population may help to account for the porosity profiles obtained from the C&I analysis. Some samples had pore size distributions that showed a substantial increase in the micropore size range e.g. Figures 4.12 and 4.13 and these are in agreement with work by Stul, (1985). Clays such as chlorite can expand when wetted, the aluminosilicate sheets that make up the structure are separated by water molecules. Dissolved Fe can precipitate within this structure and permanently separate the clay layers allowing N_2 molecules to enter during surface area analysis. (Oades, 1984; van Olphen, 1976). This can explain the pore size distributions that show an extensive micropore network.

4.2.2 ORGANIC COATINGS

The role of organic materials as particle coatings and their impact on surface area was assessed in this study in two ways. Firstly, combustimetric C/H/N analysis of the particles collected during the axial surveys of the Tamar Estuary was undertaken to determine the carbon and nitrogen contents of the sediments. The results of these studies were then used to aid interpretation of the surface area data. Secondly the effect of organic carbon coatings on surface areas was assessed by removal of these coatings by H_2O_2 digestion

followed by surface area analysis. This second approach, although somewhat crude provides a valuable insight into the role of organic coatings which are known to control surface charge (Hunter and Liss, 1982; Hunter and Liss, 1979; Neihof and Loeb, 1972), and are believed to modify the adsorptive behaviour of the underlying lithogenous phase. This study concentrated on assessment of the carbon content rather than the removal of organic coatings.

Work already carried out in the Gironde, Loire and Tamar Estuaries has shown that the removal of these coatings with H_2O_2 increases the surface area of the sediment to a fairly uniform 23-27 m^2/g irrespective of the initial surface area (Glegg, 1987; Titley *et al.*, 1987; Donard and Bourg, 1986; Martin *et al.*, 1986). This higher surface area is thought to be a result of the removal of organic material that was functioning as a pore blocking agent. However treatment of natural samples with a vigorous oxidizing agent such as H_2O_2 may have several other effects which contribute to the increased surface area. Estuarine particles collected at the turbidity maximum are composed of aggregates that are held together in part by their organic coatings. Removal of these organics would therefore lead to break-up of flocculated materials into their component parts, of smaller particle size and therefore larger surface area. Experiments by Bale (Pers. Comm.) using natural samples showed that the disaggregative processes were taking place and resulting in smaller particle sizes after oxidation. However the decrease in particle size observed was not sufficient to account for the recorded increases in surface area. A further effect likely to be of importance and requiring consideration is the potential impact of a vigorous oxidation reaction on clay particle

microstructures. Opening up and re-ordering of domain structures may take place leading to greatly increased surface areas. In Chapter 2 it was observed that rewetting and freeze drying of a clay can have a substantial effect on the microporosity. Experiments were undertaken to assess the impact of this mechanism on surface area using a sample of china clay (initial surface area 11.2 m^2/g) of low carbon content (<0.02%). After oxidation the surface area was increased by 22%, presumably as a result of the impact of the reaction on the domain structure. This increase is small compared with the much greater increase in surface area observed when natural samples were digested in the same manner. It is therefore reasonable to surmise that the much of the increase in surface area is a result of the unblocking of micropores. Analysis of the pore structure of a natural suspended sediment sample was undertaken before and after oxidation with 6% H_2O_2 and also after an acetic acid leach designed to remove Fe/Mn oxide coatings. The pore size distribution plots obtained in these experiments are shown in Figure 4.17. Best fit regression lines of this data show that the pore size distributions favour sizes of 2.5-6 nm. The pore sizes at maximum pore volume for each of the samples (estimated from the point of inflection) are in the order:

oxidized sediment > leached sediment > natural sediment.

The results of the pore size analyses are shown in Table 4.9.

207
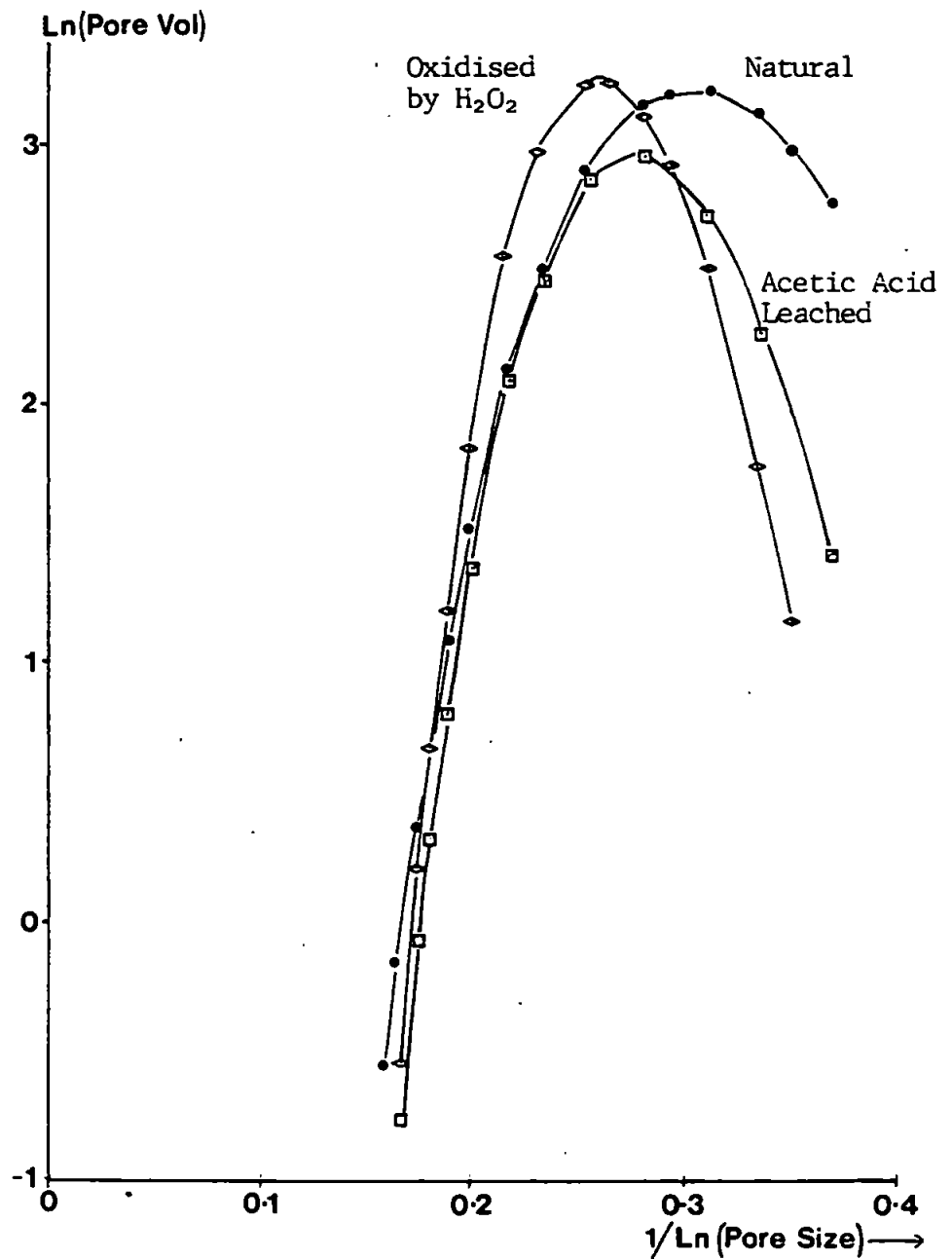
Figure 4.17. Regression lines fitted through C&I pore size distributions obtained from suspended solids in the Tamar Estuary, before and after chemical treatment.

Sample	Total Pore Vol, ml/gx10^{-2}	Mean Pore Size, nm	Pore Size at Max. Pore Vol, nm
Natural	1.87	8.15	2.8
Leached	1.85	6.91	3.7
Oxidized	2.70	8.29	4.6

Table 4.9.
Porosity data for a suspended sediment sample leached and oxidized to remove surface coatings.

The oxidized sample has greater total pore volume (by 30%) than the leached and natural samples. The average pore size of the oxidized sample is also larger, which confirms the hypothesis that destruction of organic carbon coatings unblocks pores in the underlying sample and thereby increases surface area and pore volume. Relative to the volume of a trace metal ion like Zn (Pauling radius 0.2 nm, Zn ion volume = 3 x 10^{-29}m^3) the pore volumes of the samples studied here are very large and could potentially accommodate $\approx$ 10^{21} ions per gramme (or 0.05-0.1 g of Zn ions) within the particle matrix.

Combustiometric analysis of organic carbon coatings on the sediments was undertaken for all samples collected in the Tamar Estuary to build up an overall picture of spatial and temporal trends which may be important in controlling particle surface activity. Carbon contents of the suspended sediments were found to be quite variable, ranging between 20% in coastal waters, 10-15% in river inputs and 4.5-7% in the estuary itself. Seasonality is apparent, the highest carbon values being in the summer survey (20-08-86). A plot of carbon versus turbidity (mg/l) is shown in Figure 4.18. The overall trend in the data is very similar to that observed by Morris *et al.*,
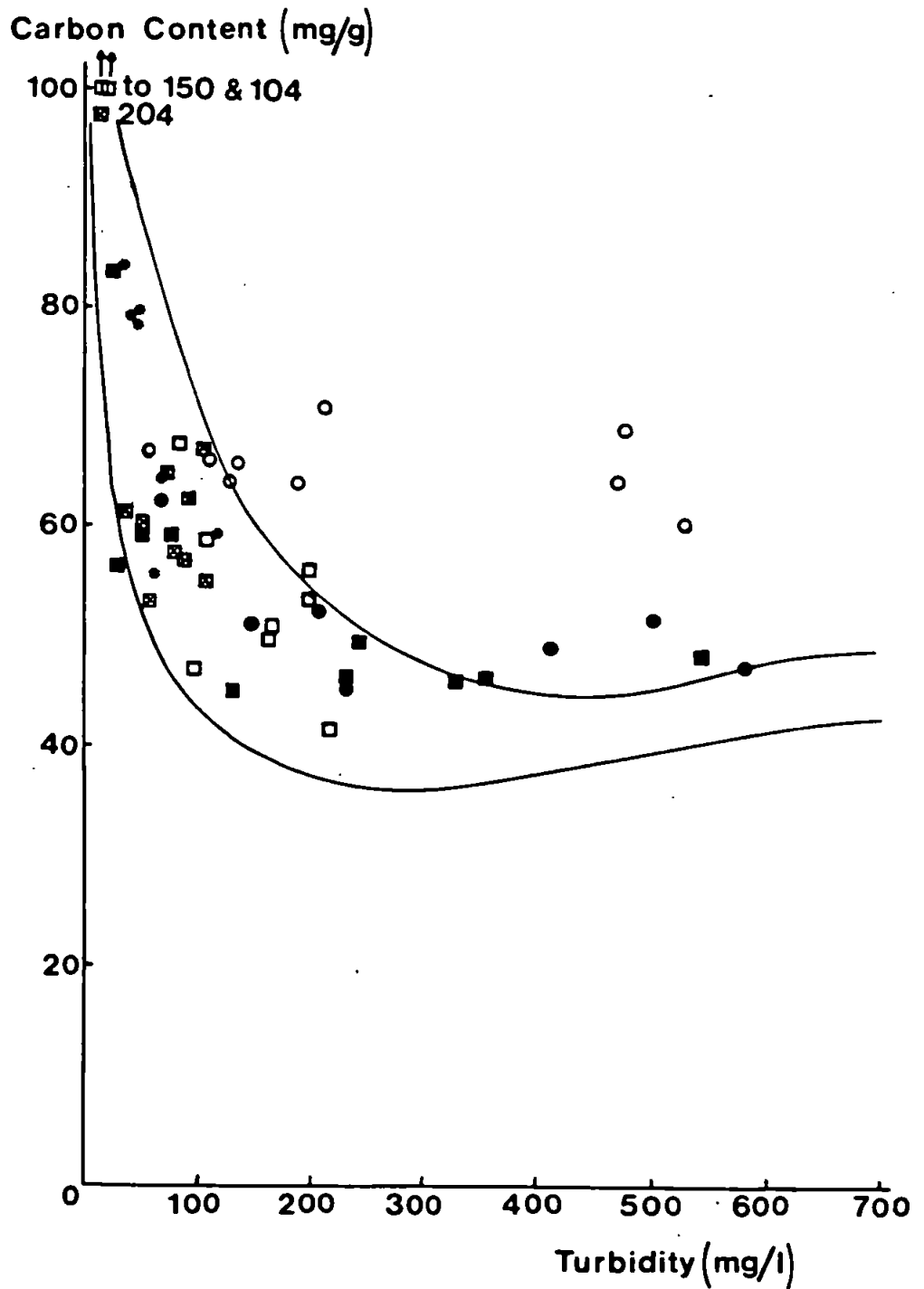
Figure 4.18. A plot of carbon content versus turbidity for suspended
sediments from the Tamar Estuary. Included in the data is
an outline of the results obtained by Morris et al., (1982).
Key: (o) - 29-10-85   (■) - 11-03-86
     (□) - 20-08-86   (●) - 18-09-86
     (▨) - 29-01-87   (◆) - 30-03-87

(1982) and Bale, (1987). The overall pattern shows a decline in carbon with increasing turbidity followed by a slight rise as the turbidity exceeds about 400 mg/l. The relationship between carbon and turbidity corresponds with the relationship between surface area and turbidity observed in Figure 4.2 (a and b) which showed a decrease in particle size with increasing turbidity. This occurs as a result of the reduced carbon content which leads to the break-up of flocs. Additionally, carbon is implicated in reducing the surface areas of particles by covering active sites and blocking pores on the particle surfaces.

Morris *et al.*, (1982) differentiated the data into organic and inorganic carbon, the results indicating that the turbidity maximum region is a zone of limited primary production, the overall process being respiration. This is confirmed by Morris *et al.*, (1982a) who showed a reduction of dissolved oxygen in the turbidity maximum. Organic carbon coatings are thought responsible for stabilizing sediment flocs (Shanks and Trent, 1979) thus the reduced carbon content in the turbidity maximum may be responsible for the smaller particle sizes observed in this study and by Bale, (1987).

An inverse relationship between surface area and carbon content of the sediment is implied by these results, as surface area tends to increase as the turbidity rises. However there was no discernible relationship between carbon content and surface area despite the results which show an increase in surface area when the organic carbon coatings are destroyed. The results for the surveys are shown in Tables 4.10 and 4.11. Carbon : nitrogen ratios vary between 4.8 and 33 with a general dependence on season.

29-10-85 Survey*			11-03-86 Survey			20-08-86 Survey		
Turbidity mg/l	Carbon %	C:N Ratio	Turbidity mg/l	Carbon %	C:N Ratio	Turbidity mg/l	Carbon %	C:N Ratio
60	6.65	12.1	33	5.63	7.0	99	4.64	11.3
190	6.34	13.2	52	5.62	7.1	213	4.16	12.6
115	6.64	12.3	323	4.63	8.4	168	5.08	12.4
130	6.38	13.3	130	4.49	8.0	108	5.87	17.8
470	6.40	12.3	238	4.98	8.3	162	5.05	13.3
480	6.94	13.1	351	4.66	8.3	202	5.68	11.6
530	5.95	11.9	240	4.55	7.7	83	6.84	11.6
140	6.59	12.2	228	4.65	8.0	25	10.51	11.2
215	7.14	12.1	540	4.81	7.9	21	15.03	11.3
-	--	--	25	8.28	7.8	--	--	--

*From Glegg, (1987)

Table 4.10
Carbon content and turbidity data for suspended samples collected in the Tamar Estuary.

18-09-86 Survey*			29-01-87 Survey			30-03-87 Survey		
Turbidity mg/l	Carbon %	C:N Ratio	Turbidity mg/l	Carbon %	C:N Ratio	Turbidity mg/l	Carbon %	C:N Ratio
70	6.19	4.8	1	20.60	33.0	62	5.50	10.0
210	5.17	6.8	60	5.30	15.1	117	5.90	10.0
150	5.10	5.6	91	6.20	15.0	71	6.40	10.0
235	4.53	6.2	52	5.80	13.8	36	8.40	9.2
500	5.21	6.2	50	6.00	13.7	48	7.90	9.6
580	4.71	6.2	80	--	--	44	7.80	9.3
410	4.88	6.6	80	5.70	13.7	40	7.90	9.9
-	--	-	72	6.50	14.3	-	--	--
-	--	-	89	5.70	14.3	-	--	--
-	--	-	101	6.70	15.9	-	--	--
-	--	-	104	5.50	13.7	-	--	--
-	--	-	36	6.10	13.0	-	--	--

*From Glegg, (1987).

Table 4.11
Turbidities and organic carbon content of suspended sediments from the Tamar Estuary.

Aquatic algae would be expected to have a C:N ratio of 6.6:1 (Stumm and Morgan, 1981) whereas organic material with a greater carbohydrate component (e.g. decaying vegetation) would have a higher C:N ratio, as would contributions to plankton from calcareous shell producing organisms (McClusky, 1981). Variations in C:N ratio with season should reflect the relative contribution played by *in situ* primary production, inputs of organic detritus from terrestrial and marine sources and the level of decompositional activity within the water column and bed sediments. A plot of nitrogen content (%) in the suspended sediment versus turbidity is shown in Figure 4.19a. The data (from all 6 surveys) reveals a similar pattern to the carbon plot of Figure 4.18. The results are more consistent than the carbon data although the results from 18-09-86 survey are notably higher than the other data.

A plot of C:N ratio versus turbidity is shown in Figure 4.19b, and the results are less consistent than the nitrogen data, but within each survey the C:N ratios are very self consistent. The C:N ratios form a pattern with surveys taken in autumn and winter months having C:N ratios of between 12 and 15, which suggests that in the winter months river run-off may be bringing terrestrial organic detritus with a high carbohydrate content into the estuary. Data from surveys undertaken in spring and summer show evidence of *in-situ* biological production, with lower C:N ratios. These are nearer the expected values for algal biomass (Stumm and Morgan, 1981). Data from 20-08-86 are however out of sequence with these surveys. The sediment inputs into the estuary from the river had very high carbon contents (about 3x the average) which suggests that an abnormally high discharge of carbon rich material had entered the river,

213
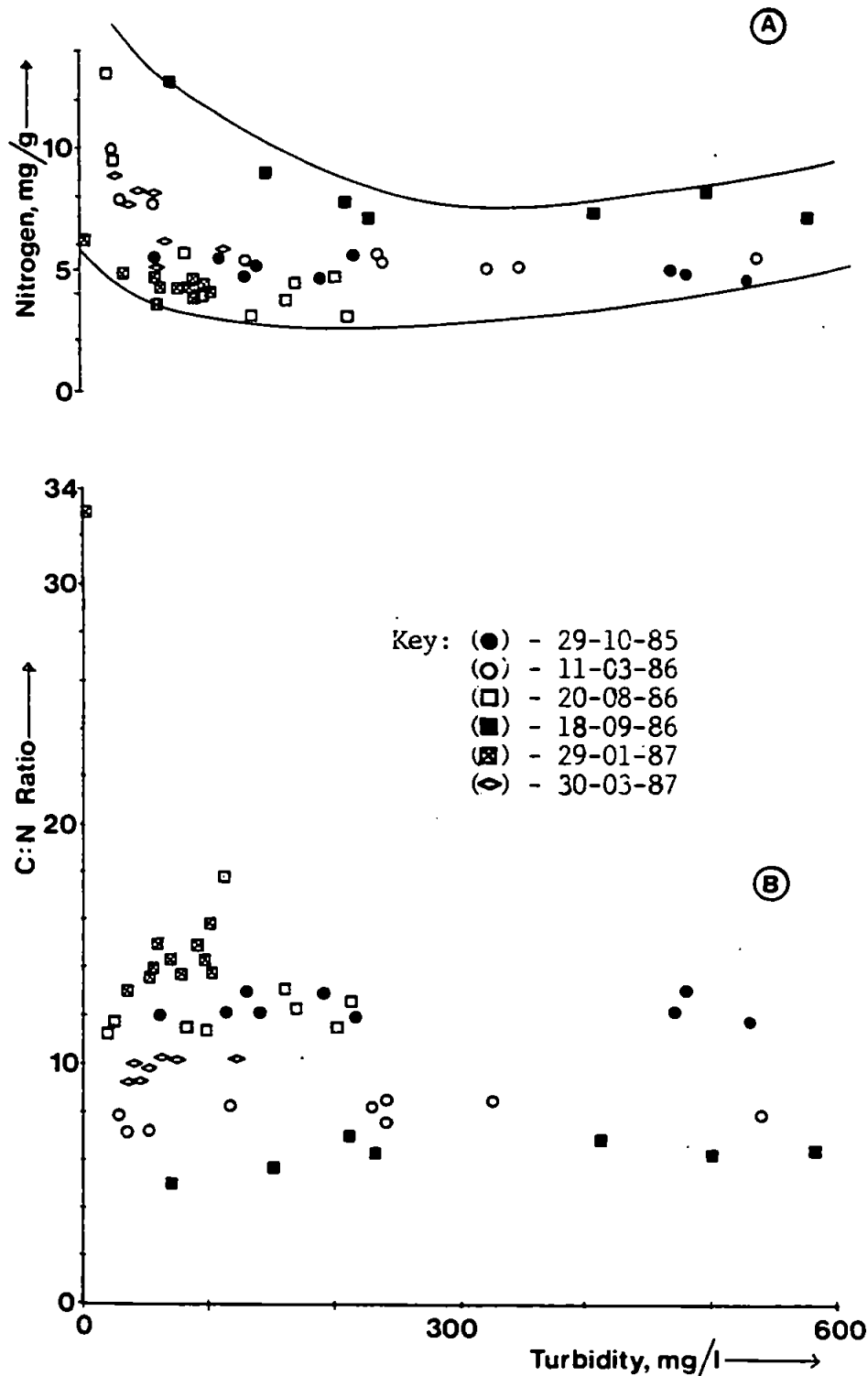
Figure 4.19a Plot of Nitrogen content versus turbidity for suspended
sediments from the Tamar Estuary.

Figure 4.19b Plot of C:N ratio versus turbidity for suspended
sediments from the Tamar Estuary.

214

possibly from a silage input from farmland. This would account for the anomalously high C:N ratios observed in this survey. The survey undertaken on 18-09-86 has the lowest C:N ratios of all the surveys with a mean of 6.06 which is less than the value for algal biomass (McClusky, 1981; Stumm and Morgan, 1981). This implies that the particles from this survey may be coated with nitrogen rich organic material, such as protein rich cell contents or fecal material with high ammonia content suggesting high bacterial activity. High degradational activity may be a result of the high carbon input into the system observed on 20-08-86. The particles from the 18-09-86 survey are probably either coated with bacterial secretions or have attachments of bacterial colonies (Plummer et al., 1987). The surface areas of the particles collected on this survey range between 12 and 16.7 m^2/g, which is the smallest range found during all the axial surveys undertaken. Furthermore, the two other surveys carried out in late summer have peak surface area values of 20-22 m^2/g. Therefore it appears that the particles from this particular survey are coated with organic secretions that reduce both the range and absolute value of the surface detectable by the N_2 gas sorption method. This phenomena may be a relatively short-lived bacterial induced response to the high carbon input observed in the survey carried out in the previous month.

4.2.3 HYDROUS OXIDE COATINGS

The non-conservative behaviour (removal) of riverborne dissolved and colloidal Fe in the low salinity region of the estuarine mixing zone has been reported by a number of workers (Morris et al., 1987; Li et al., 1984; Mayer, 1982; Boyle et al., 1977). Flocculation of the

colloidal Fe oxides in the reactive low salinity region of an estuary results in fresh amorphous coatings on the natural particles (Anderson *et al.*, 1985; Eastman and Church, 1984; Aston and Chester, 1973).

Amorphous iron oxides have large surface areas often in the range 100-300 m^2/g (Marsh *et al.*, 1984; Crosby *et al.*, 1983) but the impact that these naturally occurring coatings have on the surface areas of the sediments has only recently been examined (Titley *et al.*, 1987; Martin *et al.*, 1986). Initial results have shown that the removal of Fe/Mn oxides from the surfaces of the particles results in a reduction of the surface area to a fairly uniform 10 m^2/g (Gironde Estuary) and 16.3 m^2/g (Tamar Estuary) (Martin *et al.*, 1986; Titley *et al.*, 1987). The surface area results obtained after leaching are lower than the surfaces exposed after oxidization to remove organics ($\approx$ 26 m^2/g).

This suggests that the surface exposed by Fe oxide removal was that of the underlying crystalline lithogenous phase e.g. kaolinite and quartz (surface area 10-19 and 2-5 m^2/g respectively) (Titley *et al.*, 1987). However the amounts of Fe or of Mn leached from the particles and the surface areas of the sediment before or after leaching did not show any inter correlations.

This study aimed to investigate further the effect of Fe/Mn oxide coatings on the surface areas and porosities of sediments by selective leaching of Fe and Mn oxyhydroxides using chemical extracting procedures described in the literature (Aggett and Roberts, 1986; Borggaard, 1982; 1979; Tessier *et al.*, 1980). The surface areas and porosities of the sediment were assessed both

216

before and after leaching (Titley *et al.*, 1987). The non-detrital Fe and Mn contents of the sediment are shown in Figure 4.20(a and b) and Tables 4.12 and 4.13. The Fe values (Figure 4.20a) are in agreement with those reported in Morris *et al.*, (1987), ranging between 0.3 and 18 mg/g of sediment. However the distribution with respect to salinity tends to favour the riverine end members and the sea-ward section of the estuary which is different to the results

29-10-85 Survey[1]			11-03-86 Survey				20-08-86 Survey				
Turb-idity mg/l	Fe mg/g	Mn mg/g	Turb-idity mg/l	Fe mg/g	Mn mg/g	Al mg/g	Turb-idity mg/l	Fe mg/g	Mn mg/g	Fe* mg/g	Mn* mg/g
60	9.92	0.62	33	13.79	0.25	1.35	99	9.10	0.96	10.10	0.99
190	7.09	0.49	52	6.67	0.39	1.60	213	6.00	0.67	8.24	0.52
115	7.98	0.54	323	5.88	0.54	1.25	168	2.70	0.33	11.70	0.58
130	7.00	0.48	130	5.21	0.56	1.50	108	13.95	0.52	11.30	0.51
470	6.52	0.50	238	5.59	0.58	1.50	162	7.70	0.42	11.60	0.45
480	6.55	0.52	351	6.65	0.33	1.73	202	8.40	0.70	11.60	0.65
530	7.47	0.44	240	3.66	0.36	2.40	83	10.00	1.39	13.50	1.50
140	7.11	0.55	228	5.23	0.42	1.70	25	---	--	18.60	2.70
215	7.25	0.74	540	4.87	0.61	1.80	21	17.90	1.53	27.50	3.80
-	--	--	25	1.88	1.54	2.27	-	---	--	--	--

*EDTA Leached, by the method of Borggaard (1979). [1]Data from Glegg (1987).

Table 4.12
Non detrital (acetic acid leachable) Fe and Mn contents of suspended sediment from the first 3 surveys.
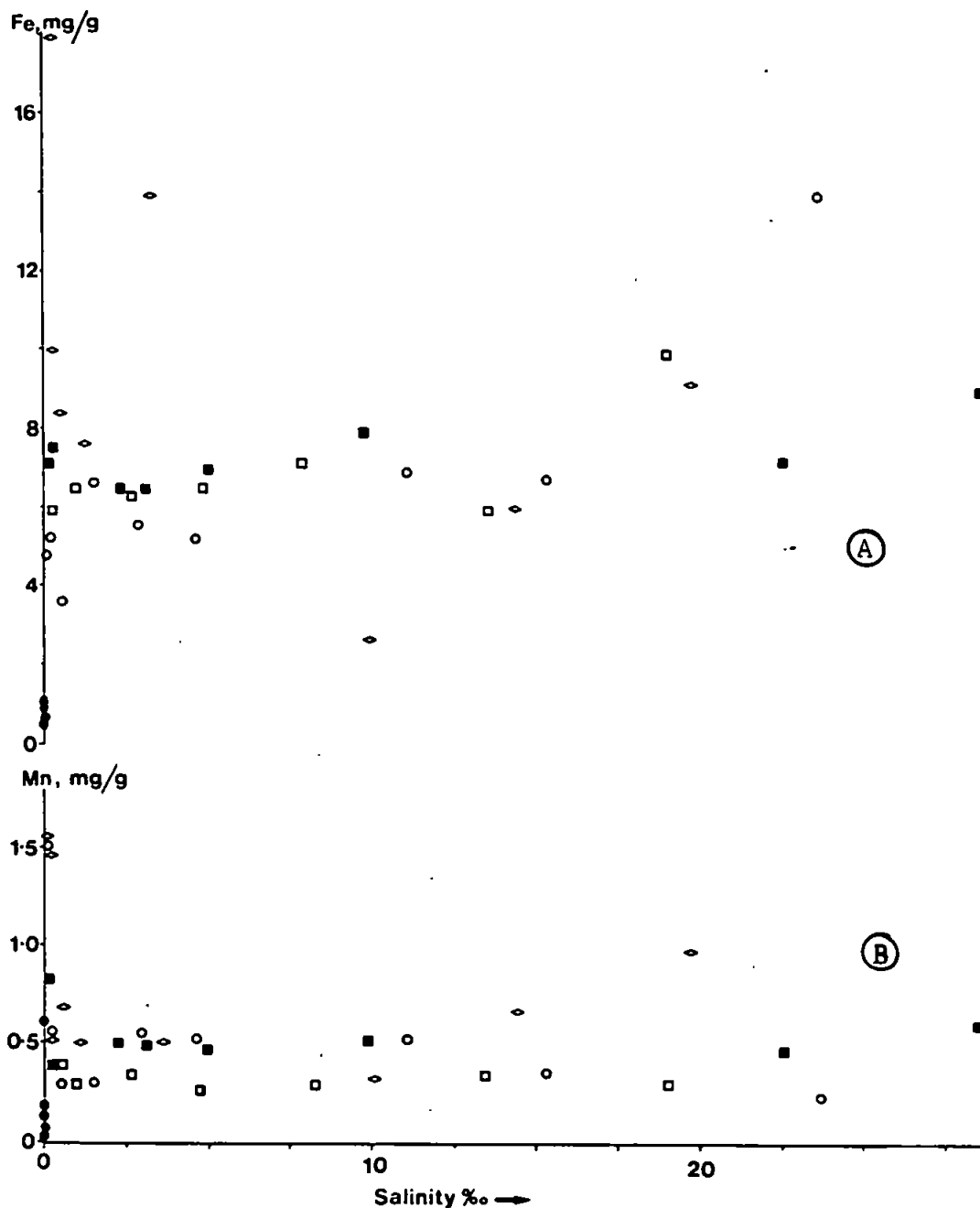
Figure 4.20a Plot of Fe content and salinity for suspended particles from the Tamar Estuary.

Figure 4.20b Plot of Mn content and salinity for suspended particles from the Tamar Estuary.

Key: (■) - 29-10-85 (o) - 11-03-86 (◇) - 20-08-86
     (□) - 18-09-86 (●) - 30-03-87

18-09-86 Survey			29-01-87 Survey			30-03-87 Survey		
Turbidity mg/l	Fe* mg/g	Mn* mg/g	Turbidity mg/l	Fe* mg/g	Mn* mg/g	Turbidity mg/l	Fe mg/g	Mn mg/g
70	9.85	0.31	1	19.22	0.35	62	0.50	0.16
210	5.96	0.37	60	4.04	0.34	117	1.14	0.20
150	7.16	0.32	91	10.33	0.29	71	0.74	0.15
235	6.42	0.29	52	12.09	0.34	36	0.80	0.63
500	6.35	0.37	50	12.09	0.34	48	0.66	0.08
580	6.45	0.33	80	14.76	0.47	44	0.58	0.07
410	6.01	0.41	80	13.10	0.46	40	0.81	0.06
-	--	--	72	19.34	0.47	--	--	--
-	--	--	89	11.42	0.38	Riverine	1.00	0.42
-	--	--	101	13.27	0.31	--	--	--
-	--	--	104	15.70	0.38	--	--	--
-	--	--	36	---	--	--	--	--

*EDTA leach by the method of Aggett and Roberts (1986) (Data from Glegg, 1987). *EDTA leach by the method of Borggaard (1979).

Table 4.13
Fe and Mn content of suspended sediment determined by acetic acid leach and two EDTA leaching methods from the literature.

reported by Morris et al., (1987) who found highest Fe values in the mid-estuarine region of the estuary. Mn results (Figure 4.20b) ranged between 0.2 and 1.5 mg/g of sediment which is in excellent agreement with those reported by Morris et al., (1986). The distribution of Mn generally favoured the fresh-water suspended sediments and then show a marked decline in the reactive low salinity region of the estuary, before becoming fairly constant throughout the rest of the profile; this distribution also being reported by Morris et al., (1986). However, the low salinity survey (30-03-87) shows a highly variable Mn content which varied by an order of magnitude.

Fe results from this survey are an order of magnitude lower than other surveys and are close to that of the riverborne solids. This

is probably because much Fe is transported in the colloidal state and therefore passes through the 0.45 μm filters. The Fe content of the sediment shows a distinct increase with rising turbidity (Table 4.13). This is probably due to the increase in salinity, sea water electrolytes are thought to destabilize riverine Fe colloids and cause flocculation and aggregation of Fe colloids (Cameron and Liss, 1984).

Selective removal of freshly adsorbed amorphous Fe oxides was undertaken by leaching sediments with EDTA at pH >7.5 over time periods >85 days. Studies have shown that other leaching methods, such as acetic acid attack crystalline phases such as lepidocrocite and haematite in addition to the amorphous Fe oxides (Borggaard, 1976; 1979). Samples from the survey carried out on 20-08-86 were subdivided and one portion leached by acetic acid and the other by the EDTA leaching method of Borggaard (1979). The EDTA leach removed greater quantities of both Fe and Mn (see Table 4.12) than the acetic acid method, as summarised in Table 4.14.

Surface Area, m^2/g Natural	Acetic Acid Leach			EDTA Leach			
	Fe, mg/g	Mn, mg/g	Fe:Mn	Fe, mg/g	Mn, mg/g	Fe:Mn	Surface Area m^2/g
14.8 ±3.3	9.5 ±4.7	0.8 ±0.4	12.2 ±7.0	13.8 ±5.9	1.3 ±1.2	8.2 ±8.6	12.1 ±2.5

Table 4.14
Fe, Mn, and Fe:Mn ratios obtained from two different leaching methods. Surface areas before and after leaching are shown.

No correlation was found between the amount of Fe and Mn removed using

the two different methods. This suggests that the EDTA method is selectively removing different Fe phases to those leached by acetic acid. The results from this survey are therefore considered in greater detail. The results in the Table 4.14 also show that removal of Fe/Mn oxides by EDTA leaves a smaller surface area (12.1 ±2.5 m²/g) than leaching by acetic acid (16.3 ±1.4 m²/g) (Titley et al., 1987). Glegg, (1987) leached suspended sediment using EDTA (Aggett and Roberts, 1986) and found that the removal of the Fe/Mn oxide phases exposed the same mean surface area of 12.1 ±2.5 m²/g.

The Fe results obtained by the EDTA leaching method in this study are generally more consistent than the acetic acid leach results on the same samples (see Table 4.12). Despite the apparent greater efficiency of the leaching method no correlation was found between the Fe oxide phases removed and the original surface area. However a plot of Fe:Mn ratio and surface area (Figure 4.21 and Table 4.15) shows a strong co-variation of BET surface area and the Fe:Mn ratio of the suspended sediment. The 43% reduction in specific surface area from 22.1 m²/g to 12.7 m²/g (at salinities of 1.1°/oo and fresh-water respectively) corresponds to a decline in total pore volume of 32%. The decline in surface area therefore represents losses of both external and internal surfaces. This suggests that Mn could be acting as a pore blocking on Fe oxide active sites, or functioning to join particles together to form aggregates impermeable to N_2 gas penetration (Glegg et al., in press). Cuttler et al., (1984) showed that during the formation of green rust from Fe(II) and Fe(III) mixtures the surface area of freshly precipitated Fe(III) can be significantly reduced by the addition of small amounts of Fe(II). From the data in Table 4.15
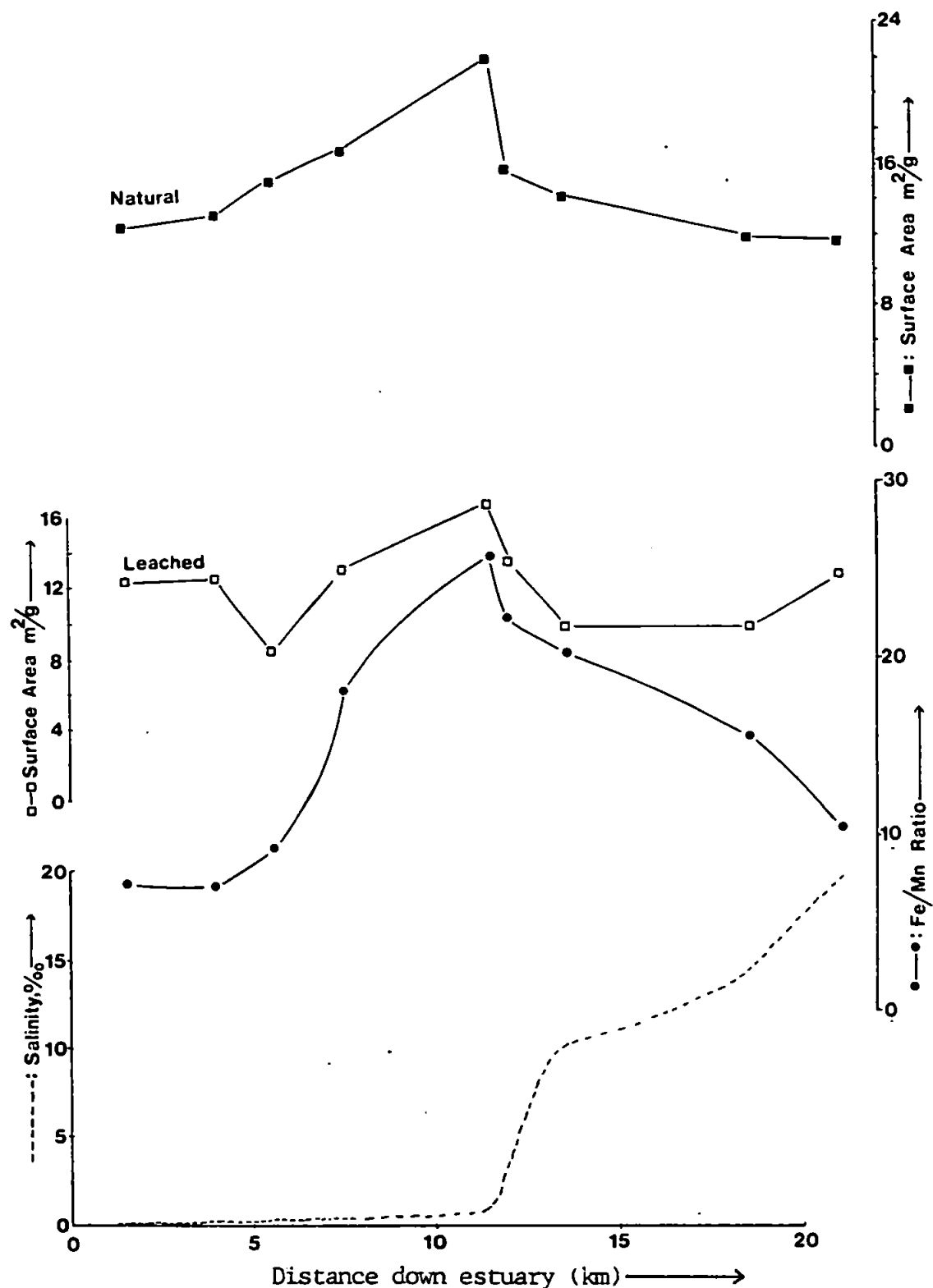
Figure 4.21. Surface areas of suspended particles from the Tamar Estuary
(20-08-86 survey). Fe:Mn ratios obtained from EDTA leach
and surfaces areas of the particles following leach are
shown. All data plotted as function of position in Estuary.
(See Table 4.15).

Salinity $°/_{oo}$	Turbidity mg/l	Surface Area m^2/g	Pore Vol $ml/gx10^{-3}$	Fe:Mn*	Fe:Mn•
19.7	99	11.6	--	10.2	9.5
14.4	213	11.8	--	15.7	8.9
10.1	168	14.2	18.9	20.2	8.0
3.3	108	15.7	--	22.3	26.8
1.1	162	22.1	27.5	25.9	18.3
0.5	202	16.8	23.2	18.0	12.0
<0.5	83	15.2	--	9.2	7.2
<0.5	25	13.3	--	7.0	-
<0.5	21	12.7	18.8	7.2	6.5

*EDTA Leached; as Borggaard, (1982)
•Acetic Acid leached; as Tessier et al., (1980)

Table 4.15
Surface areas and Fe:Mn ratios in the sediment obtained by 2
leaching methods.

it appears that the presence of small amounts of dissolved Mn (II)
during the precipitation of fresh Fe(III) oxide produces a similar
reduction in surface area.

A series of experiments was carried out to investigate the
relationship between Fe:Mn ratio and surface area. Precipitation
experiments to create pure amorphous Fe oxides, mixtures of Fe and
Mn oxides in various ratios, and pure phases of MnOOH were carried
out. The surface areas of these solids are shown in Table 4.16. The
experiment was difficult to complete because of the gelatinous
nature of the Fe/Mn oxide precipitates which were difficult to
dry. The data show that pure amorphous oxides have the largest
surface areas, and increasing the Mn content of the precipitate
leads to a reduction in the surface areas, possibly because of the
loss of internal space in the Fe oxide surface. This is a similar
process to that observed by Anderson et al., (1985), who reported

that phosphate caused the aggregation of goethite phases and a
reduction in surface area.

Precipitate	Surface Area, m^2/g
Amorphous FeOOH	303
Fe:Mn; 20:1	251
Fe:Mn; 5:1	270
MnOOH*	400

*Data from Glegg, (1987).
Table 4.16
Surface areas of some co-precipitates of
Fe and Mn oxyhydroxides.

The Fe and Mn content of the sediments as obtained by acetic acid
leach do not show any relatationship with surface area for any of
the surveys (see Table 4.15). This is in contrast to the results
obtained with the EDTA leaching method of Borggaard, (1979; 1976),
and suggests that the acetic acid leach does not selectively extract
the most active amorphous Fe and Mn oxides.

Borggaard (1979; 1976) showed that most acid leaching methods such
as acetic acid, partially extract all phases of Fe and Mn oxides
present on the surface. However the ability of EDTA to selectively
extract the most active phases was not completely proved, as leaches
of sediment from the 29-01-87 survey showed no relationship between
Fe/Mn oxide phases and surface area. This aspect of the study
requires further investigation.

Particles free of organic coatings have surface areas
of $\approx$ 26 m^2/g, and once stripped of Fe/Mn oxides this falls to 12-16
m^2/g (Titley et al., 1987). Fe/Mn oxide coatings therefore
contribute 10-14 m^2/g. The average concentration of Fe and Mn

oxides in the sediments is 13.8 mg/g and 0.5 mg/g respectively. This is not enough to account for all of the surface area change observed. A contribution of about 5 m^2/g to the organic free surface area of the sediment comes from other sources, such as swelling clays. The intercalate spacings of freeze-dried swelling clays are usually inaccessible to adsorbing N_2 molecules. However they may be held open by precipitated Fe or Al oxides allowing N_2 gas to penetrate during surface area analysis (Oades, 1984; van Olphen, 1976). Removal of these precipitated Fe/Al "props" during a leaching experiment could enable the interlayer spacings to close up. Swelling clays that have iron flocs between the aluminosilicate sheets (e.g. montmorillonite) can have surface areas in excess of 700 m^2/g (Oades, 1984; van Olphen, 1976). A relatively small amount of a clay of this type could therefore have a substantial effect on the surface area and pore size distribution of the sediments. Traces of chlorite and trioctahedral illite were detected in the sediments by x-ray diffraction, and therefore the process described could account for the changes in surface area described.

Pore size distributions of suspended sediment described earlier (see Figures 4.13 and 4.14) were skewed towards the micropore size range which implies that the intercalate spacings of clays present in the sediment were being detected. The porosity of samples collected on an axial survey of the Tamar Estuary were assessed before and after removal of Fe/Mn oxides by glacial acetic acid leaches. Figure 4.22 shows the hysteresis loop and associated C&I pore size distribution obtained from an amorphous Fe oxide (surface area 303 m^2/g). This reveals the highly microporous nature of the
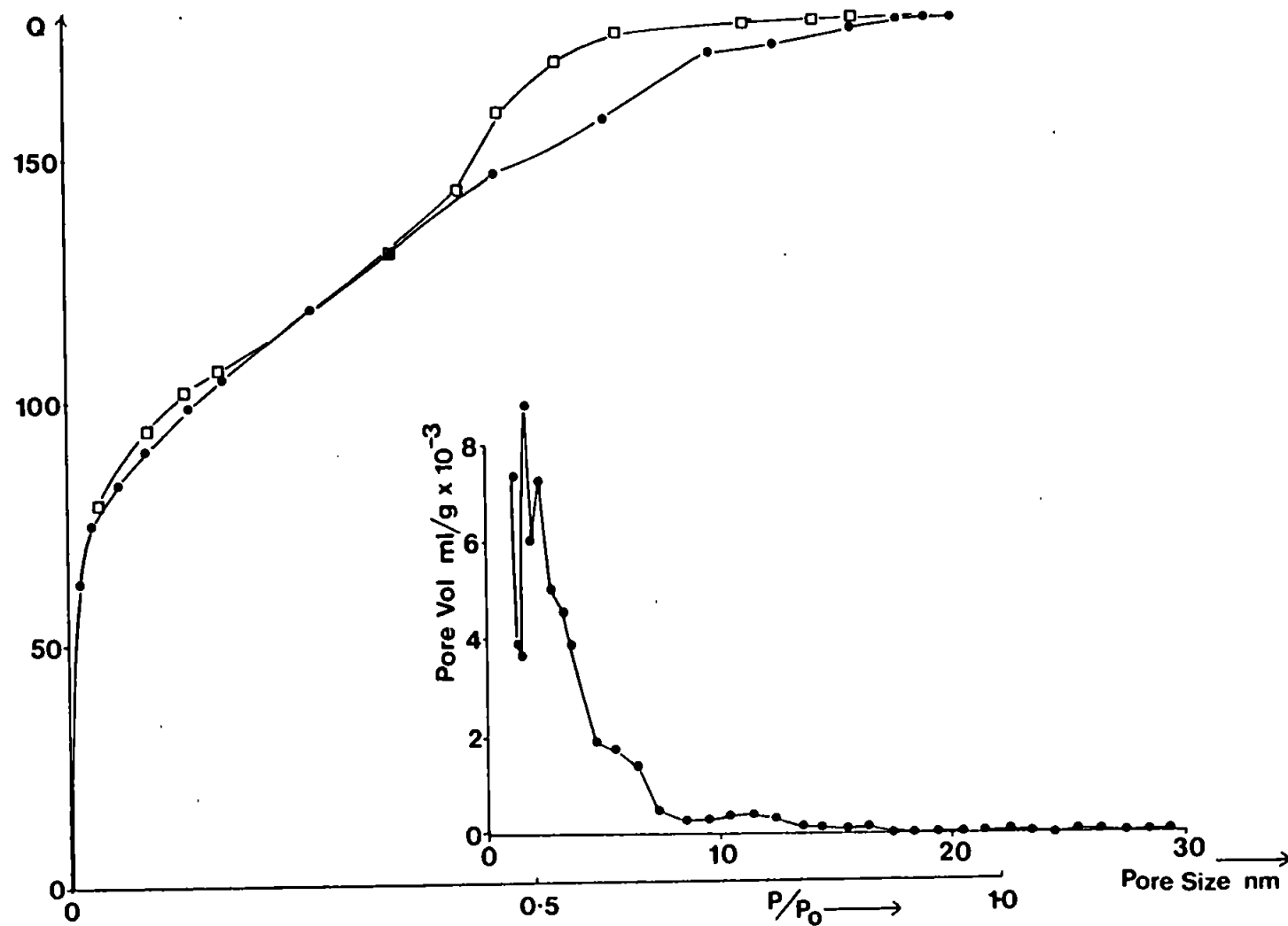
Figure 4.22. Hysteresis loop obtained on an amorphous Fe oxide (surface area 303 m²/g). Inset is the Cranston and Inkley pore size distribution for the sample.

solid which shows a profound distribution in favour of pores <5 nm in diameter. The best fit regression lines obtained from the log-normalized plots of this data together with that of kaolinite (surface area 13 m²/g) are shown in Figure 4.23. Both samples have an extensive pore volume in the size range <5 nm and the amorphous Fe oxide shows a relatively even distribution in this micropore size range. Pores in the kaolinite sample show a decline in volume in pores of <2 nm, therefore they are not responsible for the microporosity observed in some samples. Figure 4.24 shows the pore size distributions of sediments from the fresh water end of the estuary. The best fit regression data for the untreated sample is similar to the kaolinite sample especially in the 1.5-5 nm size range, although the kaolinite sample has more total volume in the larger pores. The porosity appears to be a composite of amorphous Fe oxide and kaolinite. The surface area distributions within the pores of the sediments before and after leaching are shown in Table 4.17.
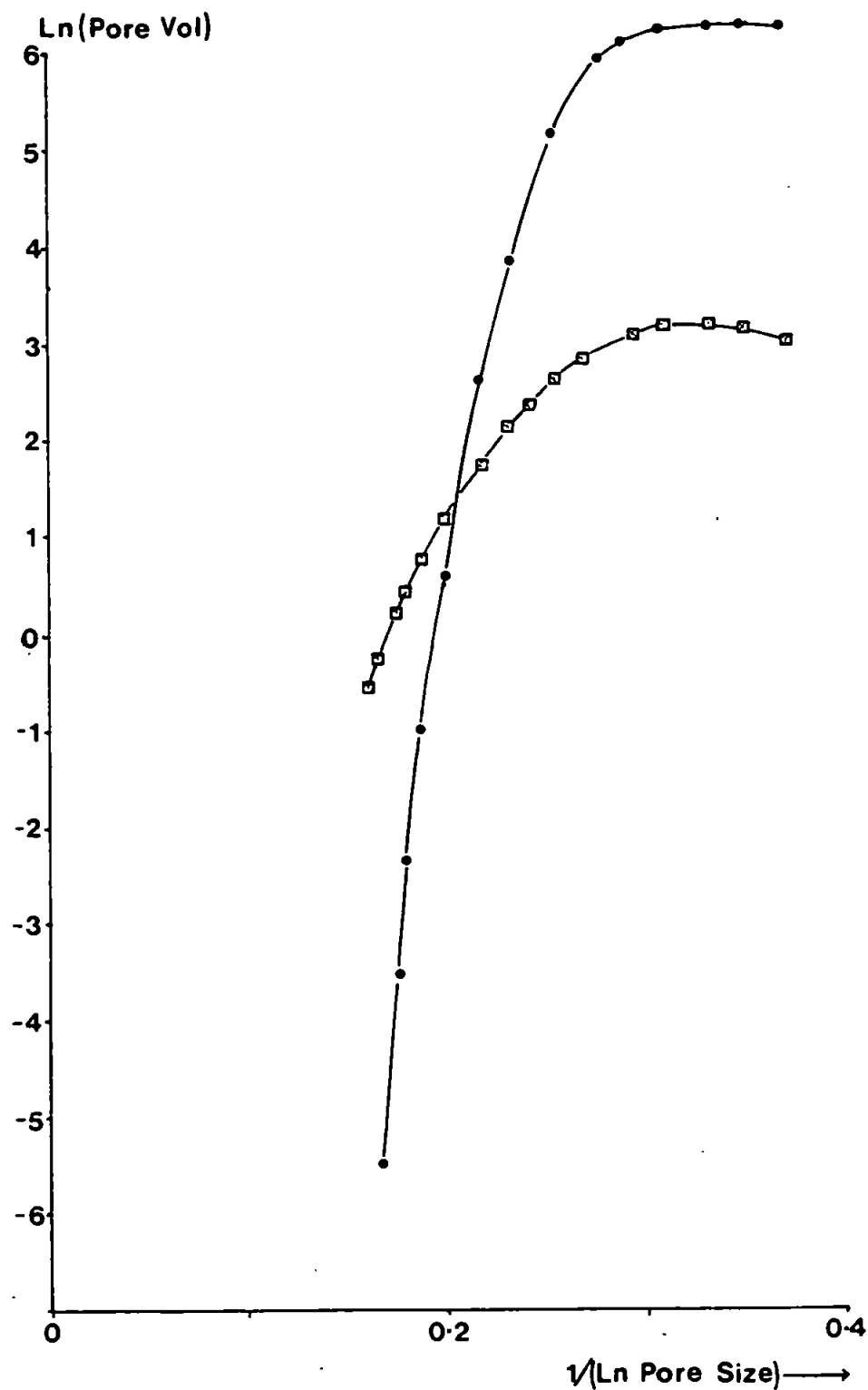
Figure 4.24. Regression lines fitted through C&I pore size distributions
(●) - Amorphous FeOOH. (□) - Kaolinite
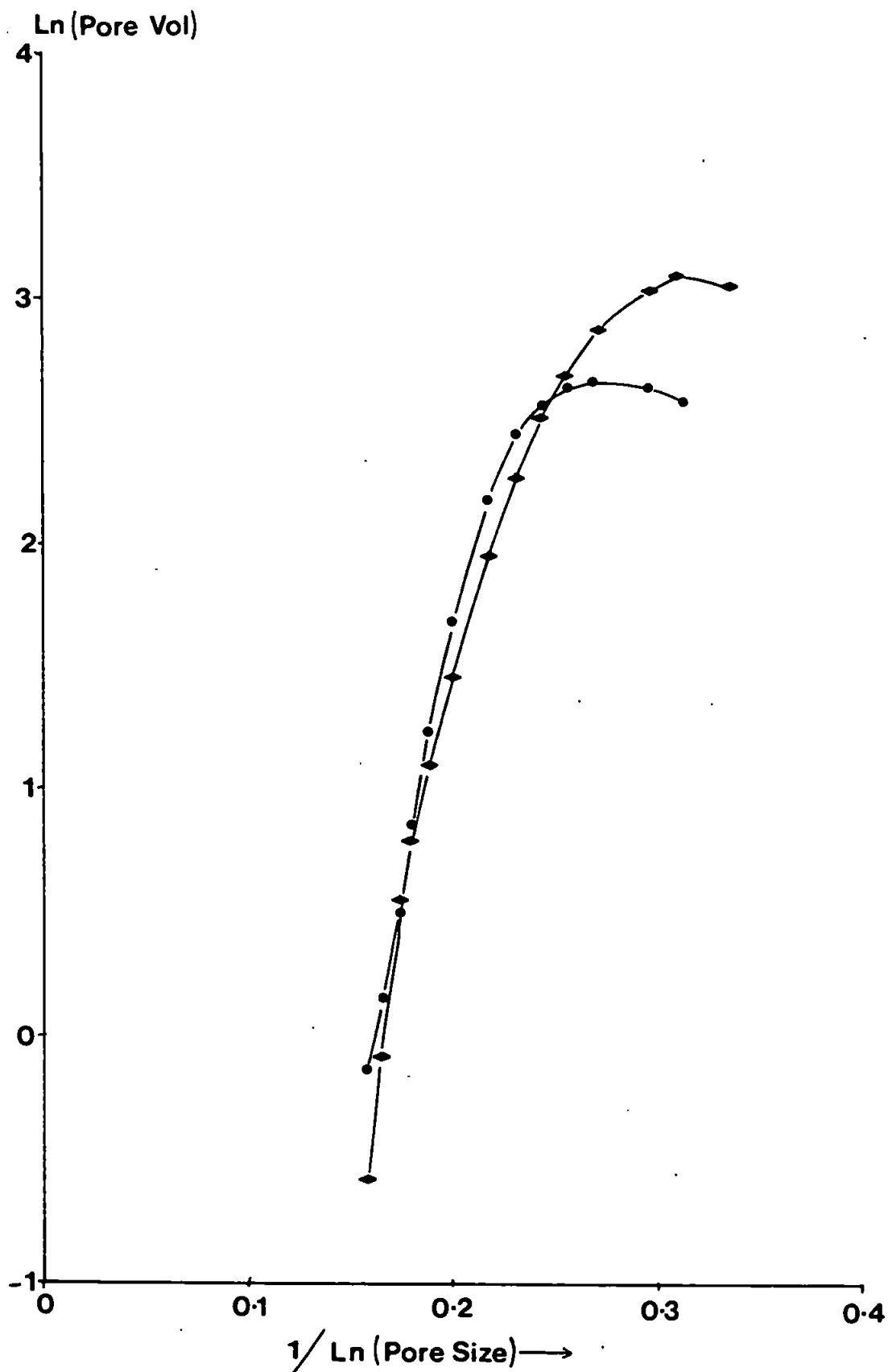
Figure 4.24 Regression lines fitted through C&I pore size distributions
obtained from suspended sediment in the fresh water end
member of the Tamar Estuary.
(●) - Unleached particles. (◆) - Leached particles.

20-08-86 Survey					Natural	Leached*
Salinity	% Carbon	Fe:Mn	Pore Size nm	% of Surface Area	% of Surface Area
<0.5	15.0	7.2	<2	15.2	22.0
			2-5	50.8	40.0
			5-10	22.6	20.1
			10-20	8.6	15.4
			20-30	2.8	2.5
0.5	5.6	18.0	<2	25.6	9.4
			2-5	44.8	46.9
			5-10	19.9	28.5
			10-20	7.7	12.7
			20-30	2.0	2.5
1.1	5.1	25.9	<2	14.2	31.4
			2-5	54.6	38.6
			5-10	20.0	18.1
			10-20	8.2	9.2
			20-30	2.9	2.7
10.1	5.1	20.2	<2	4.2	0.0
			2-5	50.4	48.9
			5-10	31.9	34.6
			10-20	10.7	12.3
			20-30	2.8	4.3

*Leached by EDTA (Borggaard, 1982).

Table 4.17.
Distribution of surface area within the pores of suspended sediments from the Tamar Estuary from various salinities before and after leaching with EDTA.

After leaching the pore size distribution of the sediment shifted to favour larger pores, as did the surface area distribution (see Table 4.17). The total pore volume increased by 25% from 18.8×10^{-3} to 24.5×10^{-3} ml/g but the total surface area was largely unchanged (12.7 m²/g before leach, 12.3 m²/g after). Figure 4.25 is a best fit pore distribution plot for a suspended sediment sample collected
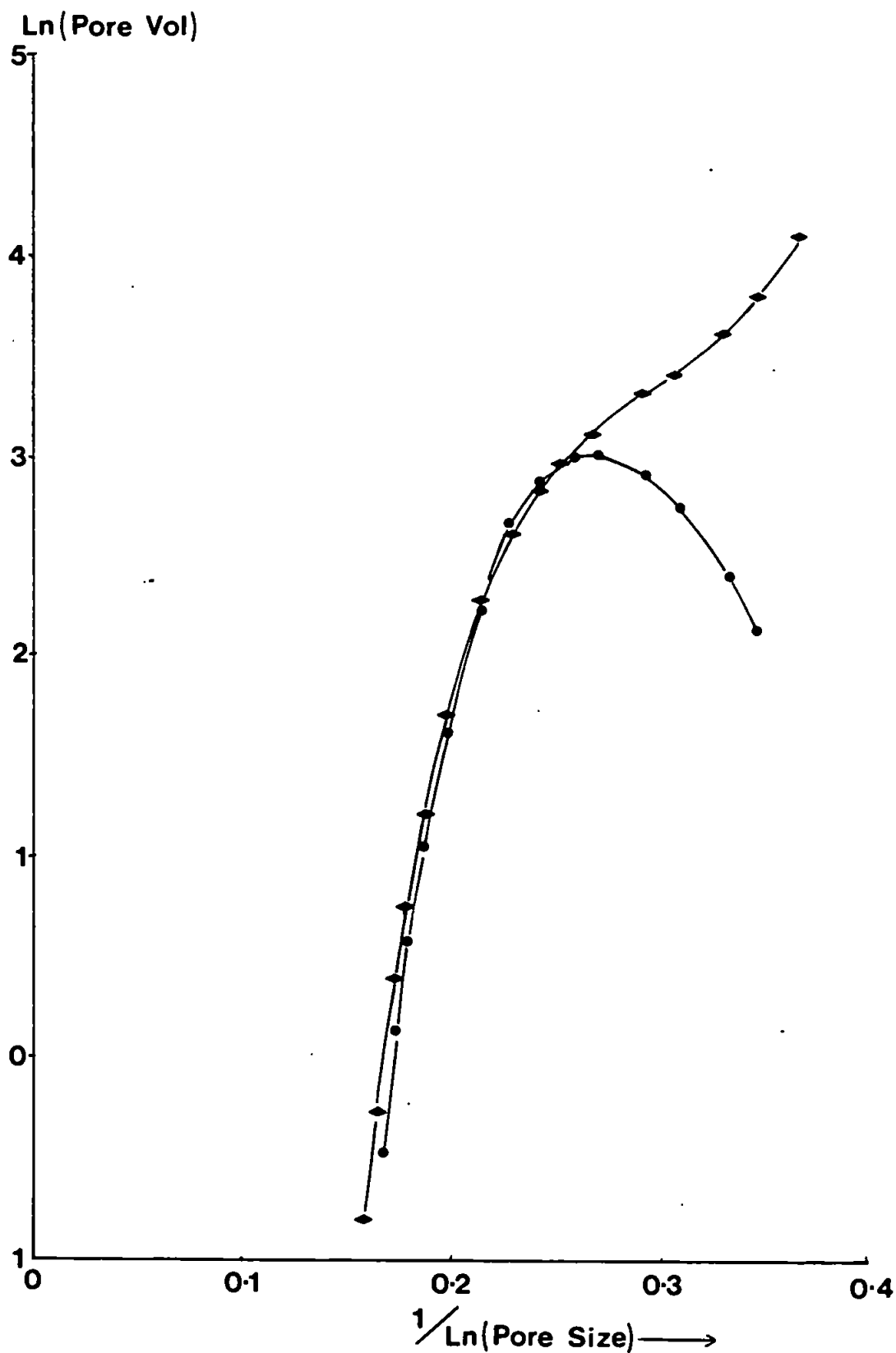
Figure 4.25. Regression lines fitted through pore size distributions obtained by the C&I method on suspended sediments from the low salinity region of the Tamar Estuary.
(◆) - Unleached (●) - Leached

231

from the low salinity region of the estuary ($0.5°/oo$) and has a larger surface area (see Table 4.15). The untreated sample has a distribution that favours micropores very markedly, which suggests that the intercalate spacings of swelling clays are being detected by the adsorbing N_2 molecules. Following EDTA leach to remove amorphous Fe/Mn oxides, the microporosity is lost and the pore volume declines as the pore diameter decreases, suggesting that the Fe/Al "props" in the intercalate structure were removed following the leaching, allowing the clay structure to close and preventing penetration by the N_2 molecules. This shows that the underlying matrix of the particle can have a significant effect on the surface properties of the particles, especially where surface coatings become incorporated into the particle matrix. Diffusion processes into the clay structure can be an important process in aquatic chemistry as trace metals may become substituted within the structure and permanently removed from solution.

4.3 SUSPENDED SOLIDS IN THE MERSEY ESTUARY

Inter-estuarine comparisons were made between the Tamar Estuary and the Mersey Estuary (Liverpool). Survey work in the Mersey was undertaken in collaboration with Dr. G. Glegg and the North West Water Authority on 5-11-87. Suspended solids were collected on an axial survey and the surface areas of the particles were determined following freeze drying. Surface area studies were complimented by chemical analyses on the particles, including C/H/N analyses, and acetic acid leaching of Fe/Mn oxides. The results are shown in Table 4.18.

Salinity °/oo	Turbidity mg/l	Surface Area m²/g	Carbon %	C:N	Fe* mg/g	Mn* mg/g	Fe:Mn
31.9	155	8.2	4.7	10.0	3.5	1.3	2.7
30.1	60	14.9	5.1	9.4	4.4	1.6	2.7
27.8	105	10.9	5.2	10.6	4.1	1.6	2.6
28.2	105	10.2	5.3	10.4	-	1.5	-
21.7	50	9.2	5.5	9.2	4.8	1.4	3.4
16.3	50	8.5	6.1	9.2	5.4	1.3	4.1
15.1	100	6.0	6.9	10.8	4.8	1.3	3.7
9.1	50	11.6	8.4	9.1	6.5	0.9	7.2
3.5	65	8.8	9.1	10.1	4.3	0.8	5.3
0.4	115	8.9	7.8	9.3	5.2	0.7	7.4

*Acetic Acid leach.

Table 4.18
Surface areas and chemical data for suspended solids collected from the Mersey Estuary.

Surface area results obtained from particles in the Mersey Estuary are lower than those obtained in the Tamar. Little trend is apparent, the surface areas of the sediments ranged between 6 and 15 m²/g which are about 5 m²/g less than those found in the Tamar Estuary. No low salinity maximum is apparent within the estuary and overall the turbidities observed were low, ranging between 50 and

155 mg/l. The flushing time of the Mersey is 1 month which is 4-5 times longer than the Tamar Estuary, and there is less channelling of tidal energy. The comparatively low suspended solid concentrations and surface areas suggest that the activity in the water column would be less and there would be reduced uptake of trace metals and other dissolved species onto the solid phase.

A full adsorption-desorption isotherm from a suspended solid isolated from the estuary is shown in Figure 4.26 together with the C&I pore size distribution plot. This shows that the freeze dried sediment has a fairly extensive micropore network, although the total pore volume is smaller than that of most sediments isolated from the Tamar Estuary.

The chemical composition of the particles from the Mersey shows similarities with the Tamar, for example the carbon content ranges between 4.7% in the marine end of the estuary and 9.5% in the fresh-water end. C:N ratios in the sediment are also similar to those observed in the Tamar Estuary. Values of 9-10 are intermediate between summer (6-8) and winter (12-15) values. This is consistent with the time of year when the survey was undertaken i.e. November. Ferromanganese oxides present in the particles were determined by acetic acid leach to allow a comparison with those obtained in the Tamar. The Fe content of the sediment is lower, ranging between 3.5 and 6.5 mg/g, whereas the Mn content is double the average Tamar value (1.2 mg/g). The overall Fe:Mn ratio is therefore lower than the Tamar Estuary by a factor of three, which may explain the lower surface areas recorded.

Surface area values for the survey are presented as surface area per
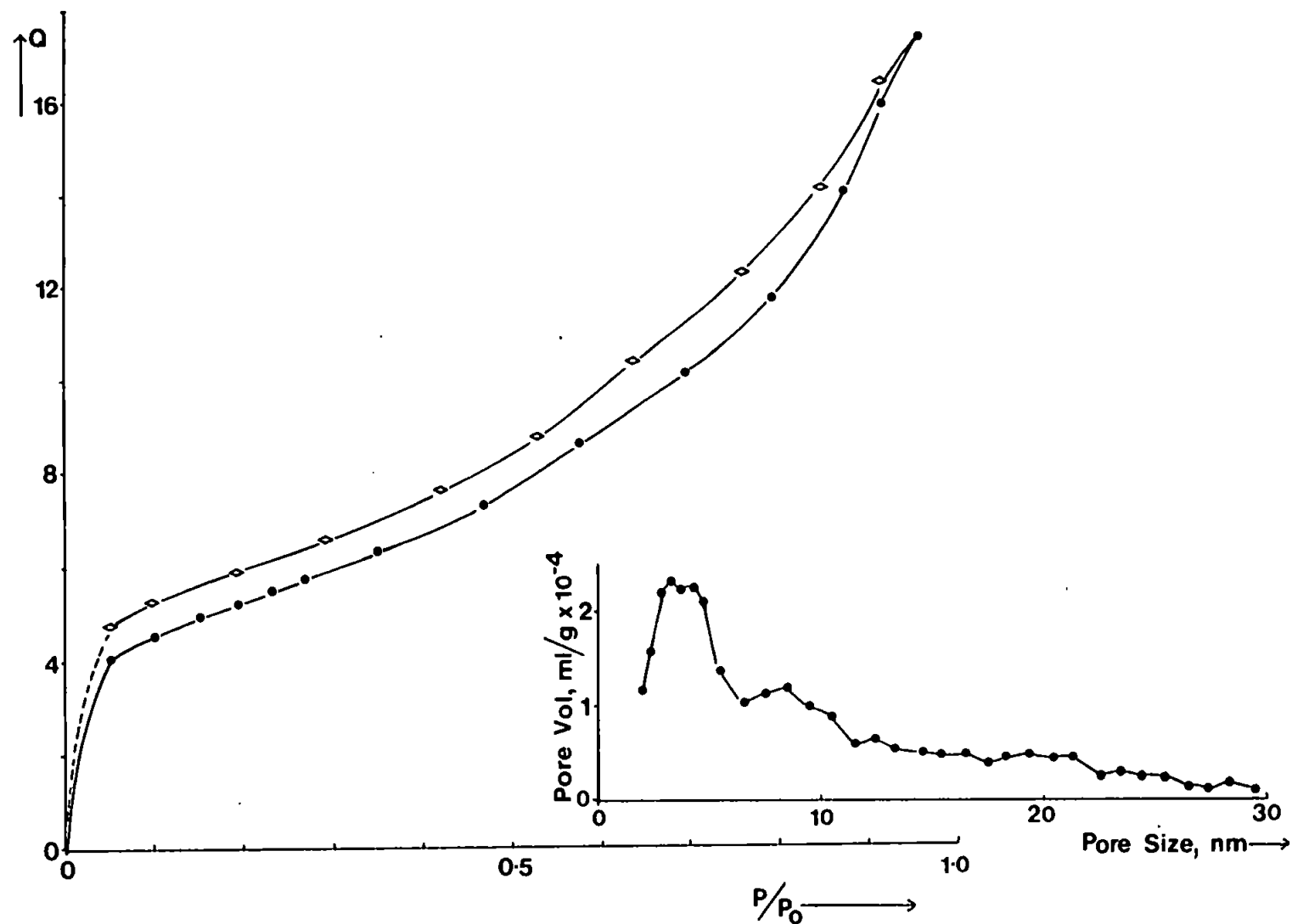
Figure 4.26. Hysteresis loop obtained on a sample of suspended sediment from the Mersey Estuary.
Inset is the C&I pore size distribution for the sample.

litre of water (Table 4.19) to give a measure of the total potential
adsorptive capability within the water column.

Mersey Survey		Tamar Estuary
Salinity °/oo	Surface area per litre m²/l	Surface area per litre m²/l (typical range)
31.9	1.27	0.5-11.5
30.1	0.89	
28.2	1.07	
27.8	1.15	
21.7	0.46	
16.3	0.43	
15.1	0.60	
9.1	0.58	
3.5	0.57	
0.4	1.03	

Table 4.19
Surface area data from the Mersey Estuary expressed as surface area
per litre. Values from the Tamar Estuary for comparison are included.

Data in the Table shows the low level of particle reactivity in the
water column as compared with the Tamar Estuary, where surface area
per litre values are up to 10 times larger. Data from the Tamar also
showed a substantial increase in surface area per litre in the low
salinity region near the limit of the salt intrusion. However the
data from the Mersey shows a gradual decrease as this region is
approached, and the highest values are encountered in the marine end
of the estuary. Thus it appears that suspended sediments in the
Mersey Estuary have less potential for adsorption of trace metals
although Airey and Jones (1982) have shown that Hg tends to adsorb
onto particulate matter in the fresh water especially during low
river flows.

4.4 SUSPENDED SOLIDS IN RESTRONGUET CREEK

In contrast to the Mersey, suspended sediments collected from
Restronguet Creek had very much higher surface areas, (21-32 m^2/g)
which is thought to be due to coatings of Fe/Mn oxides and lower
carbon content. Due to the low turbidities encountered in the
estuary during the survey suspended solids from the low salinity
region ($< 10^o/oo$) only, were collected for surface area analysis
(see Table 4.20).

Salinity Range, $^o/oo$	Surface Area, m^2/g	Carbon %	C:N	Fe mg/g	Mn mg/g	Fe:Mn
3.6-9.0	28.1	3.2	6.1	30.0	0.16	190

Table 4.20
Surface areas and chemical data for sediments collected from
Restronguet Creek.

Restronguet Creek is iron rich (Boyden *et al.*, 1979); thus
sediments from this system should have relatively high surface areas
due to the contribution from Fe/Mn oxides (surface area 200-400 m^2/g)
(Crosby *et al.*, 1983; Marsh *et al.*, 1984). Surface areas and
chemical data of suspended particles collected from Restronguet
Creek are shown in Table 4.20. The particles had surface areas in
the range 21-32 m^2/g which are similar to those observed in the
Gironde Estuary. The carbon content of the sediments is relatively
low (3.2%) compared with the Tamar and Mersey Estuaries, while
leachable Fe content is three times higher than those from the Tamar
and four times greater than suspended sediments from the Mersey
Estuary. The sediments are low in Mn giving high Fe:Mn values
($\approx$ 190). Thus there is a clear relationship between the the large

237

surface areas of the particles and the high Fe oxide content and low
carbon values of the particles.

4.5 INTER AND INTRA-ESTUARINE VARIABILITY OF THE MICROSTRUCTURES OF SUSPENDED SOLIDS.

Natural particles from the Tamar Estuary comprise a complex mixture of quartz, kaolinite, illite and chlorite which are coated with organic material of varying composition and Fe and Mn oxides. These particles have surface areas ranging between 8 and 22 m^2/g, the highest values being associated with the chemically active low salinity, high turbidity region of the Estuary. The surface areas varied slightly between surveys, with maxima ranging between 15 and 22 m^2/g. Mean surface area values for each of the six surveys ranged between 10.3 ±3.8 m^2/g and 16.3 ±2.9 m^2/g, the former being from a mid winter survey and the latter from early spring. Other surveys undertaken in summer and autumn were more consistent with average results of about 14.8 m^2/g.

Combinations of turbidity and surface area results produced a measure of surface area per litre of water, and these values ranged between 0.2 and 11 m^2/g. These values showed considerably greater variation between surveys, with some estuarine profiles showing low activity (maximum 1.5 m^2/l) while in other surveys the active surfaces in the water column reached 10 m^2/l in the low salinity region. These highly variable results observed within the estuary suggest that chemical activity at the particle water interface could vary by an order of magnitude and this therefore has implications for the distribution and transport of pollutants within the estuarine environment.

An examination of the particle size of samples showed that mean particle size was not directly related to BET surface area. The

geometric surface areas calculated from particle size were smaller than the BET surface areas by a factor of 40-250. This difference is due to the internal surface structure and porosity. Despite the complexity of the pore structure of the particles some surveys showed an apparent co-variation of geometric surface area (calculated from particle size) and BET surface area but overall the results were inconclusive. However both BET and geometric surface area showed a reasonable relationship with turbidity, with increasing surface area at higher turbidities. This may be due to the disaggregation of particles by strong tidal currents, or because of fresh precipitation of dissolved Fe as amorphous coatings.

Scanning electron micrographs of the sediments showed that the surface of the particles was highly disordered. Adsorption and desorption experiments using nitrogen gas quantified the pores on the particle surface and indicated the presense of micro and meso pores. The pore size distributions obtained using Cranston and Inkley's method (1957) showed that much of the pore volume was located in pores of 1-10 nm diameter. Some sediments had pore size distributions that favoured the micropore size range (<2 nm), with the suggestion that the modal size range may occur below the resolveable size for the method (<1 nm). Such pore size distributions are thought to be associated with the presense of expanding clays such as illite, which had been opened by Fe/Mn oxides that had precipitated within the intercalate structure of the clays. Other samples had pore size distributions with maximum pore volume in the 2-4 nm size range. The pores present were thought to be predominantly slit shaped from the clay structure or ink-bottle

shaped. Most of the particles from the Tamar Estuary contained 5-7 % carbon. Organic carbon coatings are important in aggregative processes as they can function to hold aggregates together. A strong relationship was observed between the carbon content of the sediment and turbidity, with the lowest carbon values occuring in the higher turbidity region. This was in good agreement with other work, e.g. Bale, (1987) and Morris et al., (1982).

Removal of carbon from the particles by H_2O_2 oxidation increased the surface area of the particles. This was due to a combination of factors, including particle disaggregation, alteration of the clay domain structure by the oxidation reaction, and exposure of Fe/Mn oxides with a more active surface that had previously been masked by the organic coatings. Pore size analysis of sediments before and after oxidation showed an increase in pore size and total pore volume, which confirmed the masking of pores by organic matter of low surface area.

Fe/Mn oxides coatings on the particle surface were removed by leaching. The samples had average Fe contents that ranged between 5.5 and 14 mg/g of sediment, and these were in reasonable agreement with other work. Highest Fe contents were found in the riverine and marine ends of the estuary. Mn results agreed very well with other work e.g. Morris et al., (1986). However no consistent correlation between Fe/Mn oxide content of the sediment and surface area was found, although for one survey a strong co-variation of Fe:Mn content (EDTA leach) and surface area was found. After removal of Fe/Mn oxides the particles had lower surface areas, which varied from survey to survey. Pore size distributions of the samples

before and after leaching showed an increase in mean size and a change in the size distribution towards larger pores. This is probably due to the loss of Fe oxide which has an abundance of micropores, and also to leaching and removal of Fe/Al precipitates from within the intercalate spacings of the expanding clays, allowing them to close and prevent the penetration of nitrogen gas molecules.

Thus it appears that the microstructures of sediments collected in the Tamar Estuary are controlled by three parameters. These are (i) organic material, which covers more active surfaces, blocks pores and reduces the surface areas of the particles; (ii) hydrous oxides of Fe/Mn which are dispersed over the particle surfaces and within the clay structure and confer a larger surface area on the particle matrix; and (iii) the underlying matrix, especially expanding clays which may interact with the surface coatings and contribute to the pore size distributions penetrable by the N_2 gas.

A complex interplay between the carbon content of the sediment and fresh Fe/Mn oxide precipitates is probably taking place to control the surface areas of the particles and a further interaction with the underlying crystalline matrix also occurring.

Comparisons of these results with other macrotidal estuaries demonstrates the unique characteristics of individual estuaries. Table 4.21 compares the surface areas and controlling chemical variables of suspended sediments (in summarised form) for the Gironde and Loire Estuaries (Martin et al., 1986), the Tamar, Mersey, and Humber Estuaries, and Restronguet Creek. The comparison reveals the importance of both Fe and carbon content in controlling

Estuary	Average BET Surface Area, m^2/g	Average Fe mg/g	Average Mn mg/g	Average Carbon %	Average C:N	Average C:Fe	Reference
Rest-ronguet	28.1	30.0	0.2	3.2	6.1	1.1	This Work
Humber	25.6	9.8	1.0	5.4	9.7	5.5	Turner*
Gironde	21.0[1]	12.0•	-	2.2	--	5.5	Martin et al., 1986
Tamar: 10/85	14.9	7.4	0.5	6.6	12.5	8.9	Titley et al., 1987
03/86	16.3	5.9	0.6	5.3	7.9	8.9	This Work
08/86	14.8	9.5	0.8	7.0	12.6	7.4	This Work
Mersey	9.7	4.8	1.2	6.4	9.8	13.3	This Work

*Recently available unpublished data. •Leached with NaOH and Na-Dithionite. [1]Determined using Argon.

Table 4.21
Summary of microstructural and chemical information from 5 estuaries.

surface area. The results are ranked with lowest carbon : iron ratio (in the suspended solids) first and highest last. When ranked in this way the surface areas of the suspended sediments also fall into order with the highest first (Restronguet Creek) and the lowest last (Mersey). Results from the literature, i.e. Martin et al., (1986) fit into this regime despite the slightly different surface area measurement conditions and chemical analysis.

Thus it appears that the inter-estuarine variability of surface area of suspended solids depends on the complex interplay between carbon content and coatings of Fe oxides.

In conclusion, this chapter has shown that estuarine suspended solids have highly complex surface properties that are related to particle size, carbon content, hydrous oxide coatings and the nature of the underlying particle structure. No single chemical parameter controls the particle surface, although there is strong evidence that inter-estuarine variability of the surface areas depends on the presence of Fe oxides. Intra-estuarine variability probably depends on all the mentioned chemical features functioning together, although under certain conditions one feature may become domiminant for a time.

The microstructural features of the particles observed in this study are of potential importance in adsorption kinetics. Li *et al.*, (1984) implicated diffusional processes as an important sorption step, with dissolved species penetrating the particle matrix during adsorption. The particle matrix may then become the ultimate location of an adsorbing species (Bolan *et al.*, 1985; Theis and Kaul, 1985; Nyffeler *et al.*, 1984; Barrow, 1983). The adsorption of phosphate has been the most widely examined, and it has been shown that the sorption process is two stage, fast uptake followed by slower diffusion, the rate of the latter being dependent on the crystallinity of the surface and the shapes and pore size distribution of the surface porosity (Bolan *et al.*, 1985; Madrid and De Arambarri, 1985; Crosby *et al.*, 1984). At present there is only limited information on the sorptive behaviour of phosphate onto natural particles and in natural solutions. In Chapter 5, the sorption behaviour of dissolved phosphate onto the surface and within the pore structures of the natural estuarine particles will be examined.

CHAPTER FIVE.

THE SORPTION BEHAVIOUR OF DISSOLVED PHOSPHATE IN ESTUARINE MEDIA.

5.1. RATIONALE.

The characteristation studies performed on particles in Chapters 3 and 4 show that sediments from the low salinity region of the Tamar Estuary have the greatest potential for adsorption of dissolved species as compared with other sections of the estuary.
Particles from the low salinity, high turbidity region of the Tamar Estuary have the largest surface areas. The combination of large surface area and high turbidity produce a total potential adsorptive capacity in the water column up to 10 times that found in the more saline sections of the estuary.

In addition to surface area an extensive network of micropores within the particle surface structure was identified. These physical features are also implicated in the sorptive behaviour of dissolved species as the micropores contain a substantial proportion of the available surface area of the particles. Diffusion of adsorbing species into the pore network followed by adsorption onto active sites is an important physico-chemical process in the environment.

The main objectives of the sorption studies carried out in this work were to examine the relationship between the particle microstructure and the sorptive behaviour of dissolved phosphate and to obtain quantitative information on reaction rates which could be related to the hydrodynamic timescales in estuaries.

Kinetic data so far published concerning chemical reactions with

natural sediments in estuarine environments is limited. Sorption studies have however been undertaken using single mineral phases as the adsorbate, especially iron oxides (for example Crosby, 1982; Millward, 1980). These simple systems provide qualitative and quantitative information on the probable behaviour of natural systems, but due to the complexity of natural media and the highly complex surface characteristics of sediments the results obtained can only provide a limited amount of applicable information.

Field measurements of the distribution of dissolved phosphate in the Tamar Estuary have been undertaken by Morris *et al.* (1981) and laboratory studies of the adsorptive behaviour of phosphate have been undertaken by Bale and Morris (1981) although the time dependent nature of the uptake process was not examined in the latter work. In addition, the behaviour of dissolved phosphate in the Amazon Estuary, the Mississippi River Estuary, and the Potomac River Estuary has been studied by Fox *et al.*, (1986; 1985); Callender and Hammond (1982) and Chase and Sayles (1980). However, most work in this area has been carried out in fresh waters using natural sediments for example: Twinch and Peters (1984); Boström and Pettersson (1982); Logan (1982), or with single solid phases such as Fe oxides and oxhydroxides (Anderson *et al.*, 1985; Crosby, *et al.*, 1984; 1981; Crosby, 1982; Barrow, *et al.*, 1981). A substantial quantity of work has also been carried out over the last thirty years with soils for example; Barrow and Ellis (1986); Bolan *et al.*, (1986); Barrow (1983; 1983a); Obihara and Russell (1972).

The sorption behaviour of phosphate onto Fe oxides is controlled

246

by the pH and ionic strength of solution (Crosby, 1982), with increased uptake of phosphate occurring at lower pH and at higher salinities. In addition, the distribution and shape of the internal structures of the solids are thought important in the overall adsorption process, especially Fe oxides surfaces (Crosby et al., 1984), and on soil particles (Madrid and De Arrambarri, 1985). Other work has shown the importance of phosphate in aggregation processes especially with respect to goethite phases where the phosphate ion may become part of the internal structure of the solid (Anderson, et al., 1985).

Studies of the distribution of dissolved phosphate in estuaries shows complex behaviour. In the Tamar and Amazon River Estuaries complex non-conservative behaviour of dissolved reactive phosphate was observed, with removal processes in the low salinity region and addition in the more saline regions (Fox et al., 1986; Morris et al., 1981). Sediments from the Amazon River Estuary were found to release substantial quantities of soluble phosphate over a period of days. This behaviour contrasts with the Humber Estuary however, where removal of dissolved phosphate from solution along an estuarine transect was observed (Turner, Pers. Comm.). In view of the inter-estuarine variability in the behaviour of dissolved phosphate and the lack of information on the sorptive behaviour of dissolved phosphate with natural sediments in the estuarine environment, there is a need for further work to be undertaken. Of especial interest is the sorptive behaviour of dissolved phosphate onto natural particles under natural conditions of pH, ionic strength and temperature. The information should be applicable to the timescales encountered in the estuarine mixing zone i.e. 1 hour

to 5 days, which are equivalent to the flushing times in the low salinity regions of most U.K. estuaries. This data can then be used to refine understanding of the transport and availability of this important nutrient in the biologically productive estuarine environment.

In this study, experiments were carried out using populations of well characterised particles from the low salinity region of the Tamar Estuary which were used to study the sorption behaviour of dissolved phosphate in a number of media. The samples used included fresh water from the River Plym, water from the low salinity region of the Plym Estuary (the latter containing high concentrations of phosphate from a treated sewage outfall), and sea water from Plymouth Sound spiked with reactive phosphate. Use of solutions containing high concentrations of reactive phosphate allows a simplifying assumption to be made: i.e. that the quantity of phosphate present on the particle surfaces is small compared with dissolved phosphate in the media.

All of the water samples were collected 24-48h prior to the start of adsorption experiments in order to keep conditions as near to the natural environment as possible and to prevent undesirable chemical changes from taking place. Additionally a number of experiments were undertaken in buffered distilled water with dissolved phosphate added. The chemical conditions for all of the experiments were maintained near to the natural environmental conditions (pH, 6-8; turbidity, 150-850 mg/l. The experiments were carried out at room temperature, usually 19-25°C and the individual experiments were found to vary ±1°C during a run.

5.2. MIXING EXPERIMENTS USING NATURAL PARTICLES

5.2.1. MICROSTRUCTURAL CHARACTERISTICS OF THE NATURAL PARTICLES

All the mixing experiments were undertaken using particles from the
turbidity maximum region of the Tamar Estuary. The samples were
collected as described in Chapter 2, and then filtered through a
0.45 μm membrane. The solid isolated from the solution was
resuspended in 800 ml of distilled water and stirred for several
hours to provide an homogenous suspension. Subaliquots of this were
extracted and stored frozen prior to use in the mixing experiments.
This technique provided subaliquots of particles with essentially
the same surface properties and the same turbidities. Two particle
populations were sampled, collection taking place in March and June
1987. The principle characteristics of the particles are shown in
Table 5.1. The results show that the particles are typical of

Date of Collect- ion	Salinity At Which Collected	Surface Area, m²/g	Fe mg/g	Mn mg/g	Fe:Mn	C, %	N, %	C:N	C:Fe
25-03-87	0.3 °/oo	16.1	5.06	0.26	19.5	5.34	0.65	8.19	10.27
24-06-87	0.5 °/oo	16.9	5.20	0.50	10.4	5.43	0.61	8.85	10.73

Table 5.1
Principle chemical and physical characteristics of the two particle
populations used in the sorption experiments.

those found in the Tamar Estuary. The Fe and Mn results are in good
agreement with those from the axial surveys as are the C and N
contents.

The central aspect of this study is the importance of the

249

microstructural features of the particles on the sorptive behaviour of dissolved species, in this case phosphate. Microstructural examination of the particles was undertaken, and the results from adsorption-desorption isotherms analysed using the Cranston and Inkley (1957) method as described in Chapter 2. The surface area distributions within the pores of the particles are shown in Table 5.2 and the pore size distributions themselves are shown in Figure 5.1.

Sample	Pore Size (nm)	% of Total Surface Area	Sample	Pore Size (nm)	% of Total Surface Area
25-03-87	<2	30.47	24-06-87	<2	35.13
	2-5	37.87		2-5	39.51
	5-10	19.19		5-10	15.56
	10-20	9.55		10-20	7.78
	20-30	2.92		20-30	2.01

Table 5.2.
Surface area distributions within the pores of the particles used in the sorption experiments.

The porosity data show that both particle populations are largely microporous, although pores in the particle population from the 24-06-87 are skewed towards the smallest micropores. In both cases a significant proportion of the surface area (35 %) is located in pores of <2 nm diameter which will be relatively inaccessible to adsorbing phosphate species (ionic diameter ≈ 0.3 nm) with slow diffusion taking place. Additionally the internal pore stuctures probably contain substantial quantities of adsorbed phosphate which may be permanently sorbed within the matrix of the particle.
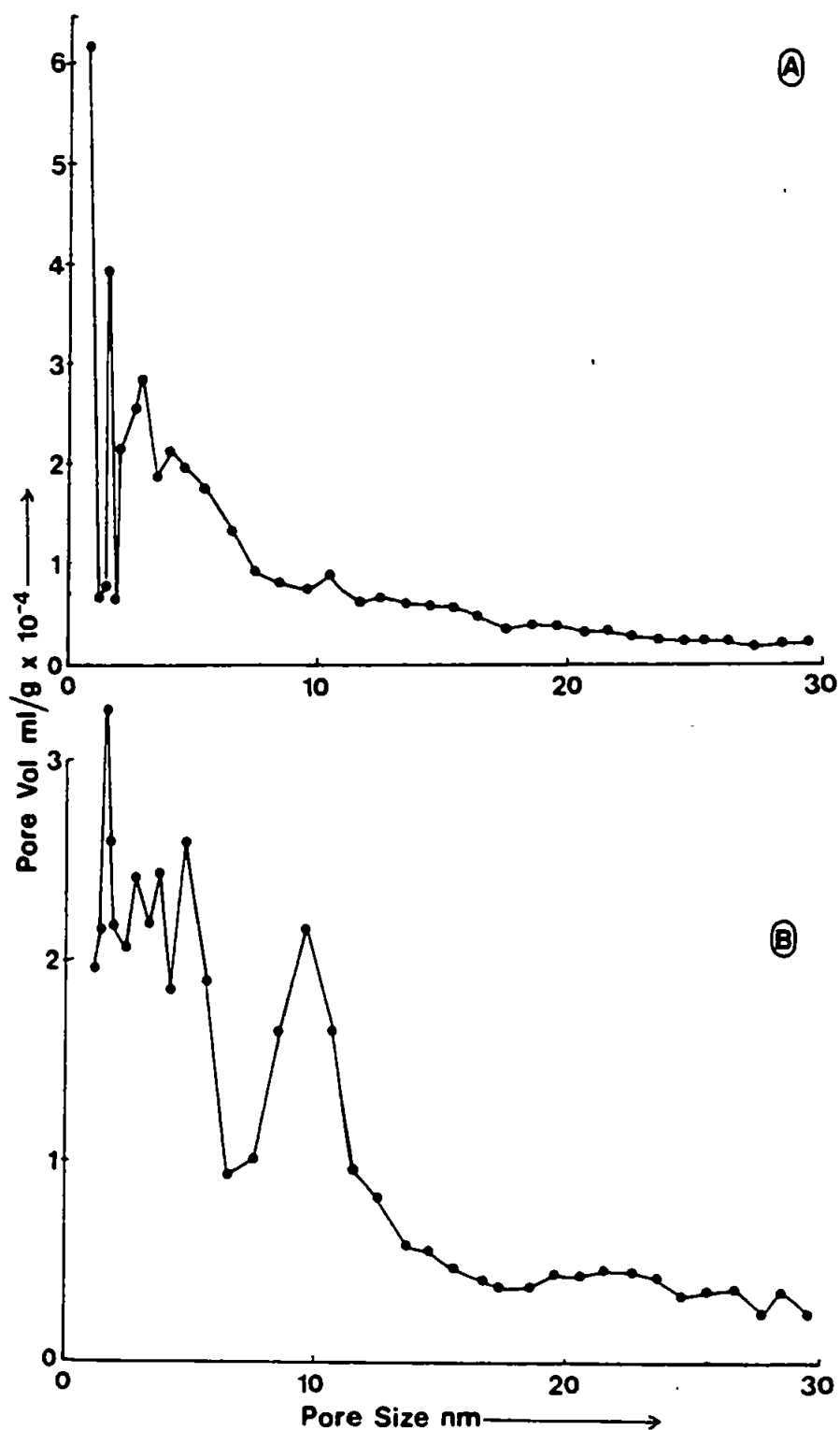
Figure 5.1. Cranston and Inkley pore size distributions of sediments used in phosphate mixing experiments.
A: Tamar Suspended Solids from 24-06-87
B: Tamar Suspended Solids from 25-03-87

5.2.2. ADSORPTION EXPERIMENTS USING NATURAL WATERS

The majority of the adsorption experiments were carried out in
filtered waters from the low salinity region of the Plym Estuary
which is an environment contaminated with high concentrations of
phosphate from a nearby sewage works.

An initial experiment was undertaken using fresh water from the Plym
River itself. Of all the experiments this sample contained the
highest concentration of dissolved phosphate (concentration 3.28
mg/l of PO_4^{3-}) as it was collected from downstream of the outfall at
low tide. The experiment was undertaken as outlined in Chapter 2.
The filtered water sample was introduced into the reactor vessel,
and stirred continually for several hours to establish equilibrium
with the container walls before the particles were introduced. The
adsorption profile obtained following the introduction of particles
is shown in Figure 5.2.

The experiment was carried out at a particle concentration of 200
mg/l (using particles from 25-03-87) which is within the range of
particle concentrations encountered in the low salinity region of
the Tamar Estuary. The phosphate concentration was 2 orders of
magnitude higher than values recorded in the low salinity region of
the Tamar Estuary by Morris *et al.*, (1981). However, these
concentrations are typical of those encountered in the low salinity
region of the Plym Estuary, but are lower than the values used in
adsorption experiments by soil scientists. For example Madrid and De
Arrambarri (1985) worked with iron oxide phases in dissolved
phosphate concentrations of 50-100 mg/l. The results they obtained
showed rapid removal of dissolved phosphate, usually within the

Figure 5.2. Adsorption of dissolved phosphate onto estuarine sediment with time. Tamar particles from 25-03-87. Plym River water; Salinity 0 °/oo; pH 8.3; Turbidity 200 mg/l; Temp 21°C.

253

first 60 seconds followed by a long slow uptake. The adsorption
profile shown in Figure 5.2 is similar to this, with rapid removal
of dissolved phosphate occuring over the first 30 seconds after the
addition of particles at time t_0. This was followed by apparent
equilibrium over the next 6h, with no evidence of continuing uptake.
The initial rapid uptake phase removed 18% of the dissolved
phosphate present and suggests that there are a relatively large
number of adsorption sites on the external surface of the particles
capable of taking up phosphate. The quantity taken up by the
particles in this experiment was 2.64 mg of phosphate/g of sediment
which was the greatest uptake onto the particles of any of the
experiments.

A series of experiments were then undertaken to observe the sorptive
behaviour of dissolved phosphate in brackish waters. Adsorption
experiments were undertaken using Plym Estuary samples collected at
mid-tide. These were contaminated with phosphate but at lower
concentrations (2.4-2.6 mg/l) due to the diluting effect of the
tide. The results of two adsorption experiments which used the same
bulk water sample are shown in Figures 5.3 and 5.4. The pH of one of
the two experiments was lowered to 6.5 and maintained at this value
for the duration of the experiment because lower pH values are
thought to encourage adsorption of phosphate. The pH of other
experiment was left at the natural value at which it was collected
(8.2). The experimental conditions are similar in all other aspects,
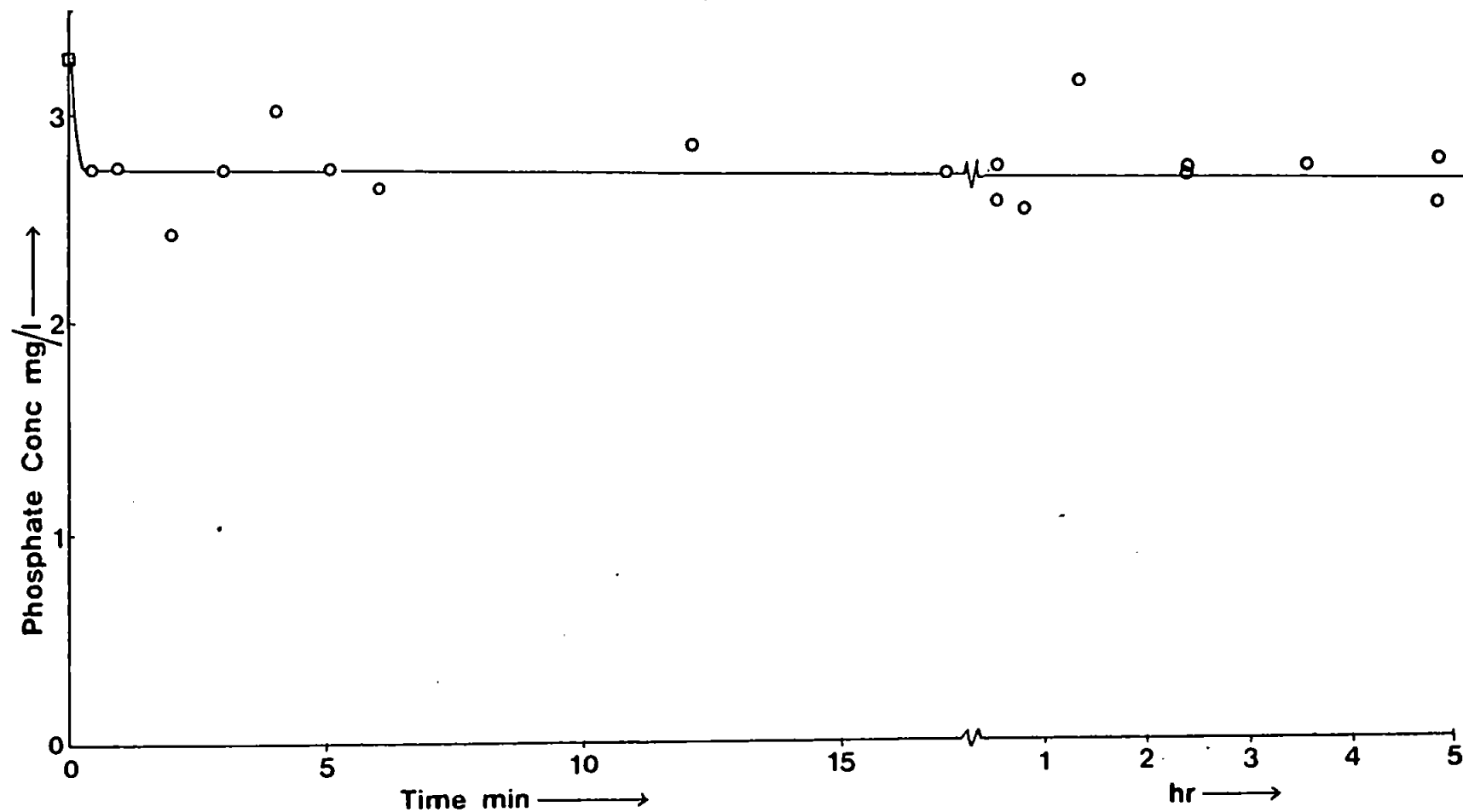and the results are summarised in Table 5.3.
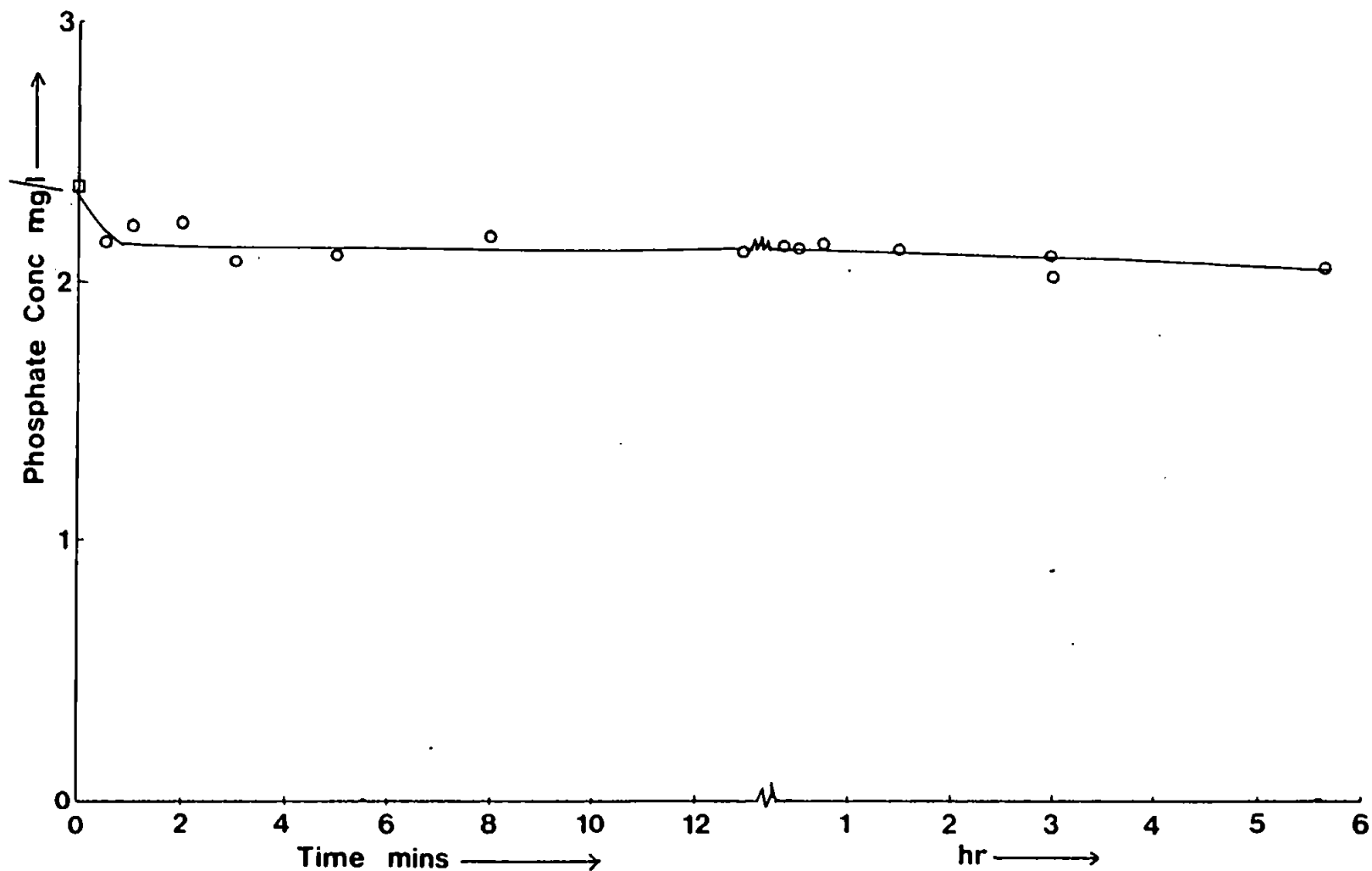
Figure 5.3. Adsorption of dissolved phosphate onto estuarine sediment with time. Tamar particles from 25-03-87. Plym estuary water; Salinity 0.9°/oo; pH 6.5; Turbidity 330 mg/l; Temp 23°C.

Figure 5.4. Adsorption of dissolved phosphate onto Tamar Estuary sediments (25-03-87). Plym estuary water. Salinity 0.9 °/oo; pH 8.2; Turbidity 330 mg/l; Temp 21°C.

256
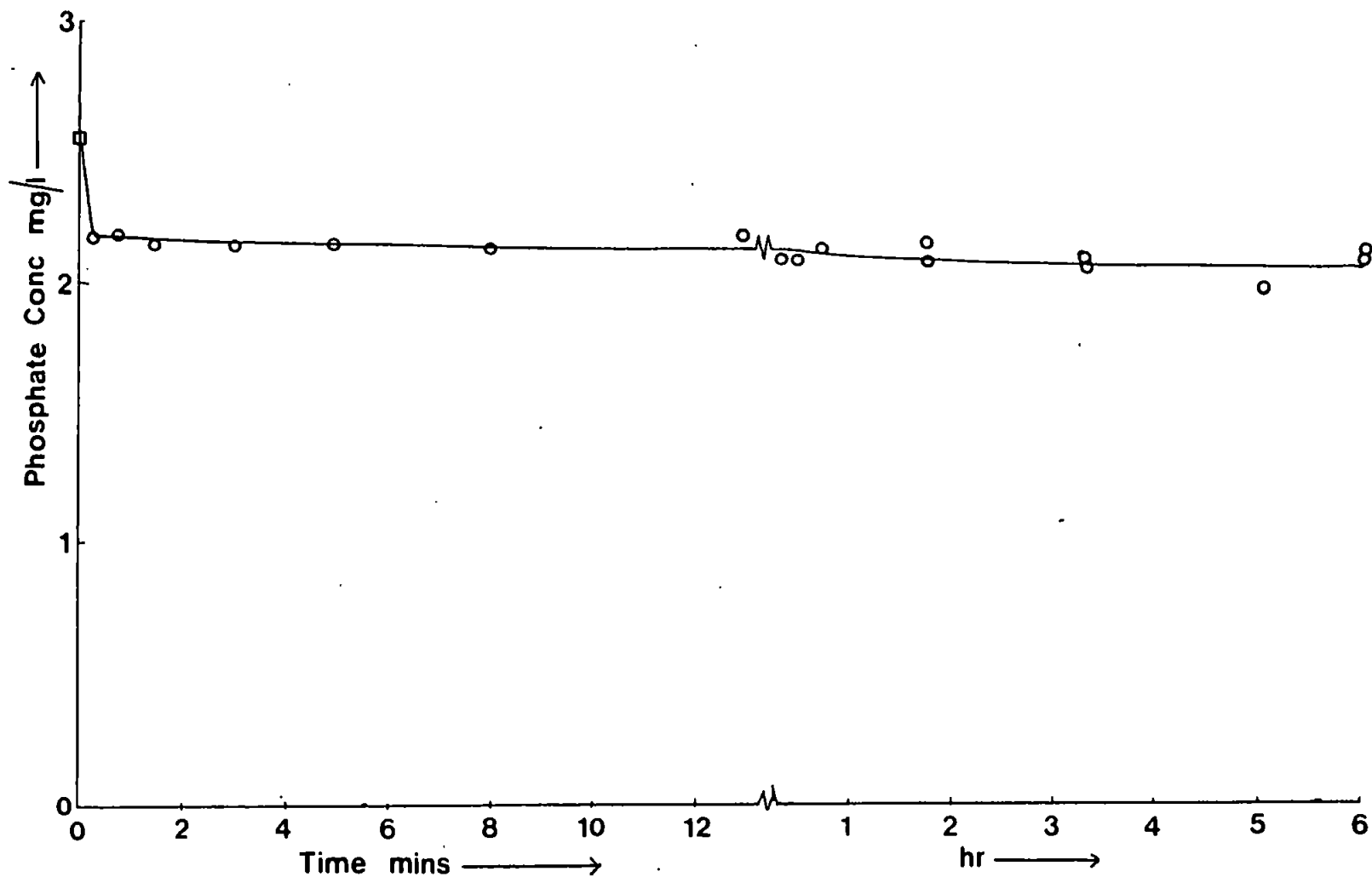
Particle Batch	Starting Conc. mg/l	Turbidity mg/l	pH	Temp. °C	Salinity °/oo	Uptake % of Starting
25-03-87	2.57	330	8.2	20-22	0.9	18.8
25-03-87	2.39	330	6.5	21-24	0.9	11.8

Table 5.3
Principle physico-chemical characteristics of mixing experiment
shown in Figures 5.3 and 5.4.

The data shows that the uptake behaviour of phosphate is dependent
on pH, but that adsorption is greater at higher pH. This
contradicts the predicted adsorptive behaviour of orthophosphate
ions onto surfaces covered in ionizable functional groups (Crosby,
1982; Balistrieri and Murray, 1979), but is in agreement with
results obtained by Gunatilaka (1982) using lake sediments.

At a pH lower than 7.1 and in organic free media the surfaces of
FeOOH carry a net positive charge (Balistrieri and Murray, 1979) and
therefore the uptake of negatively charged orthophosphate ion
species should be enhanced. However at low pH the orthophosphate ion
occurs as H_3PO_4, and therefore is adsorbed less readily from
solution. At pH 7 in distilled water both $H_2PO_4^-$ and HPO_4^{2-} species
are present in about equal concentrations, whereas at about pH 8 in
seawater, HPO_4^{2-} is the dominant form. Therefore, at some optimal
pH, where the surface charge and the phosphate species present may
result in maximum uptake of phosphate ions.

Both Crosby (1982) and Lijklema (1980) showed that adsorption of
dissolved phosphate onto pure Fe and Al oxide phases in fresh waters
is enhanced at lower pH. Lijklema (1980) also showed that particle
surfaces respond only slowly to changes in pH with gradual

rearrangement of adsorbed phophate ions on the particle surfaces

taking place until optimal coverage is achieved under the prevailing

conditions of pH and ionic strength. Edzwald *et al.*, (1976) showed

that some clays adsorb phosphate more readily in the pH range 7-8

than at lower pH. This is thought to be related to the presence of

calcium within the clay lattice which can react with phosphorus to

form an insoluble calcium phosphate phase and this may explain the

behaviour observed. This process also explains the adsorptive

behaviour of lake sediments observed by Gunatilaka (1982). In

addition to these processes adsorption of Ca^{2+} and Mg^{2+} ions onto

the particle surfaces at higher pH may provide additional sites for

phosphate adsorption (Balistrieri and Murray, 1979).

Examination of the adsorption profiles shown in Figures 5.3 and 5.4

show that an initial adsorption reaction takes place in the

first 30 seconds after the addition of particles, and this appears

to account for the majority of the adsorption. However over longer

timescales (4h) there is evidence of continuing uptake at both

natural and lower pH. This latter feature has often been observed in

adsorption experiments with soil and with clays; for example Madrid

and De Arrambarri (1985); Edzwald *et al.* (1976), and the process is

thought to be associated with diffusion of ions into the pore

structures. This is possible as the particles used in these

experiments have a substantial internal pore structure, with a large

proportion of surface area ($\approx$ 30%) located in pores of <2nm

diameter and although the accessibility of these pores to phosphate

ions with diameters of the order 0.3-0.5 nm is likely to be reduced

compared with larger pores, some diffusion into these spaces is

likely to occur.

Further adsorption experiments at natural pH and low salinity were undertaken using lower concentrations of dissolved phosphate to determine if the uptake processes were concentration dependent. Natural waters from the Plym Estuary were again used, and the natural variations in concentration caused by changes in run-off and tidal state enabled the collection of samples with the same salinities but differing phosphate loads. The water samples collected had dissolved phosphate concentrations of 1.68 and 1.98 mg/l which are 30-40% lower than the previously described experiment. Additionally, the added suspended solid concentration was lower at 180 and 290 mg/l; respectively, although the particles were from the same batch. Under these conditions and at natural pH, uptake was extremely low at about 2% of the original concentration. This suggests that high concentrations of suspended particles and dissolved phosphate are required to induce uptake. Natural particle surfaces may be already coated with phosphate from rapid adsorption reactions in the low salinity region of the Tamar Estuary. Additionally the matrix of the particles may contain adsorbed phosphate from processes occurring when the particles were part of the soil horizon. Phosphate ions may become incorporated in the particle matrix through the aggregation of goethite mineral phases (Anderson *et al.*, 1985) or by diffusion of dissolved phosphate into particle pores (Madrid and De Arrambarri, 1985). Thus phosphate may be transported into the estuarine environment in this form and natural particles may not have much sorptive capacity for phosphate unless the concentrations in the water column are high.

259

Experiments were undertaken to determine if the observed

concentration dependency of the uptake was influenced by pH. The

uptake profile of two experiments are shown in Figure 5.5. The

initial concentrations of phosphate in solution for the two

experiments was 1.70 mg/l (30% lower than previously) and the pH was

maintained at 7 and 8.2. Under these conditions uptake of 9% was

observed at pH 7 and <2% at natural pH. The low pH uptake is similar

to the result obtained at reduced pH but higher intial phosphate

concentration. This suggests that in brackish-waters and natural pH

≈ 8 adsorption of dissolved phosphate is concentration dependent,

However, when the pH was reduced to 6.5-7 the concentration

dependency of the adsorption was reduced.

The apparent K_d values for these experiments were calculated from

the equilibrium values and are shown in Table 5.4.

Initial Conc. mg/l	Equil- Conc. mg/l	% Adsor- bed	Salinity °/oo	Temp. °C	pH	Turb- idity mg/l	Uptake on Particles mg/g	Apparent K_d ml/g
3.28	2.74	16	0	21	8.3	200	2.64	960
2.57	2.09	19	0.9	21	8.2	330	1.45	690
1.73	1.64	5	0.9	22	7.0	230	0.40	250
2.39	2.11	12	0.9	23	6.5	330	0.40	190
1.99	1.96	2	0.9	22	7.9	180	0.14	70
1.68	1.66	1	0.9	21	8.2	290	0.07	40

Table 5.4
Summary of adsorption experiment results undertaken in brackish
waters.

The values of K_d are ranked in order and from this it is apparent

that the main controlling factor is the initial phosphate

concentration. Adsorption onto the particle surfaces appears to be

independent of turbidity.
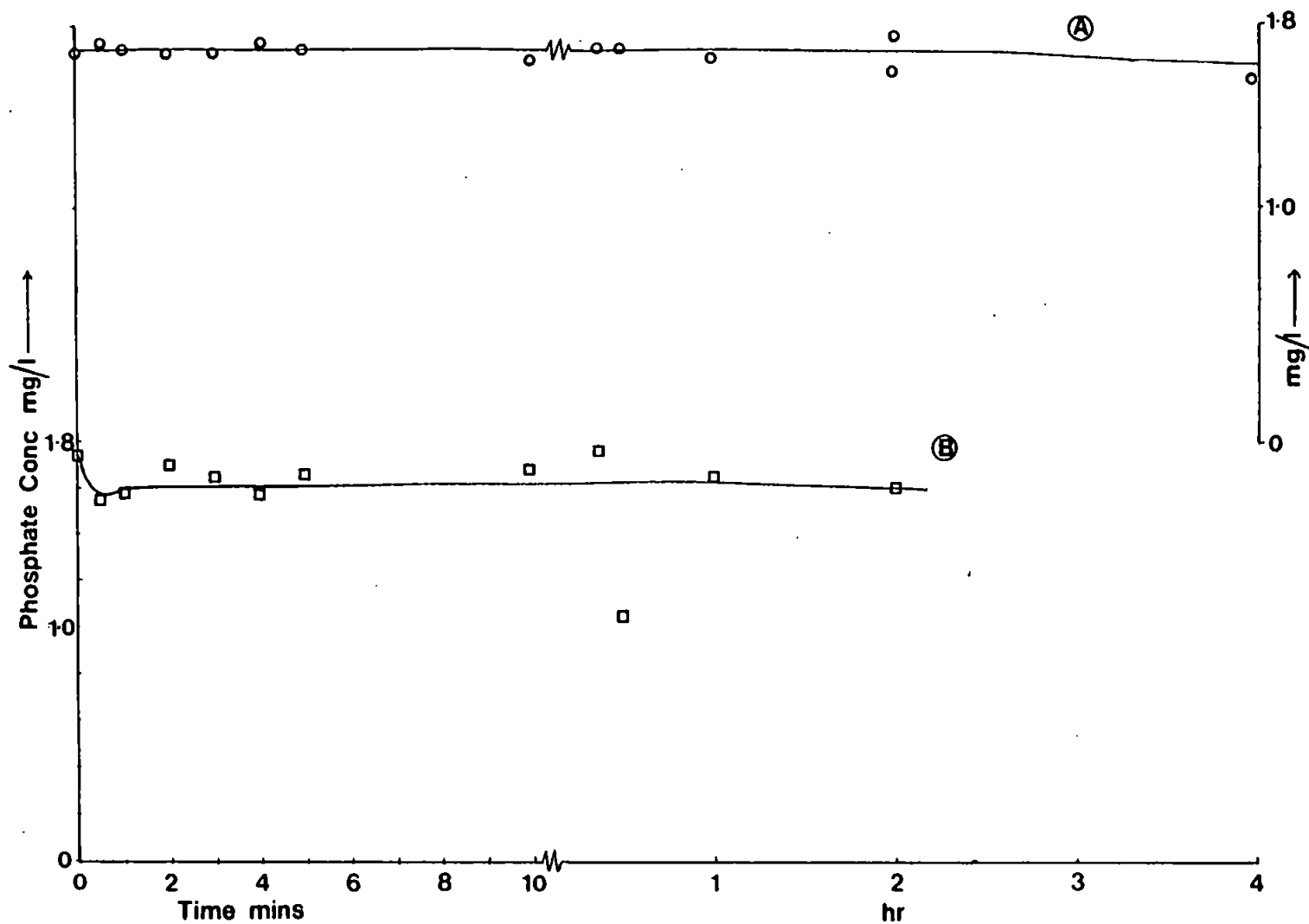
Figure 5.5. Adsorption of dissolved phosphate onto sediments from the Tamar Estuary (25-03-87).
Plym Estuary water. Salinity 0.9°/oo; Temp 22°C; Turbidity A: 230 mg/l; B: 290 mg/l
pH A: 8.2; B: 7.0.

Additional experiments were undertaken using more saline waters from the mid estuarine section of the Plym and from Plymouth Sound. Adsorption experiments using water from the estuary (salinity 5.8 ^{0}/oo, initial phosphate concentration 0.20-0.26 mg/l; pH 6.4 and 7.7) showed restricted uptake of 3% at pH 7.7 and 8% at pH 6.4. There was evidence that the experiment undertaken at natural pH did not reach equilibrium but showed an apparent process of release and uptake that was ongoing throughout the experiment. The pH of the experiment also varied through the experiment, starting at 7.6 and reaching 8.1 and the phosphate showed some desorption as the pH increased. The experiment undertaken at lower pH is shown in Figure 5.6, and the profile shows rapid removal of phosphate from solution in the first 3 minutes, followed by more gradual uptake over the next 6 hours.

Adsorption experiments were also undertaken at higher salinities, using water samples collected from Plymouth Sound (salinity 33 ^{0}/oo). Phosphate was added to the solutions to raise the initial concentrations to 150-370 µg/l, and the particle concentrations were in the range 250-500 mg/l using particles from 25-03-87. The phosphate concentrations are 5-10 times the normal concentrations found in sea water but are near the values found in the mid-estuarine sections of the Plym.

All these adsorption profiles exhibited slow uptake with no initial fast reaction, which is in agreement with the results obtained by Crosby (1982) with synthetic Fe oxides. The uptake continued over long timescales (20h) but the overall uptake did not exceed 10%. Two profiles are shown in Figure 5.7, both of which were undertaken
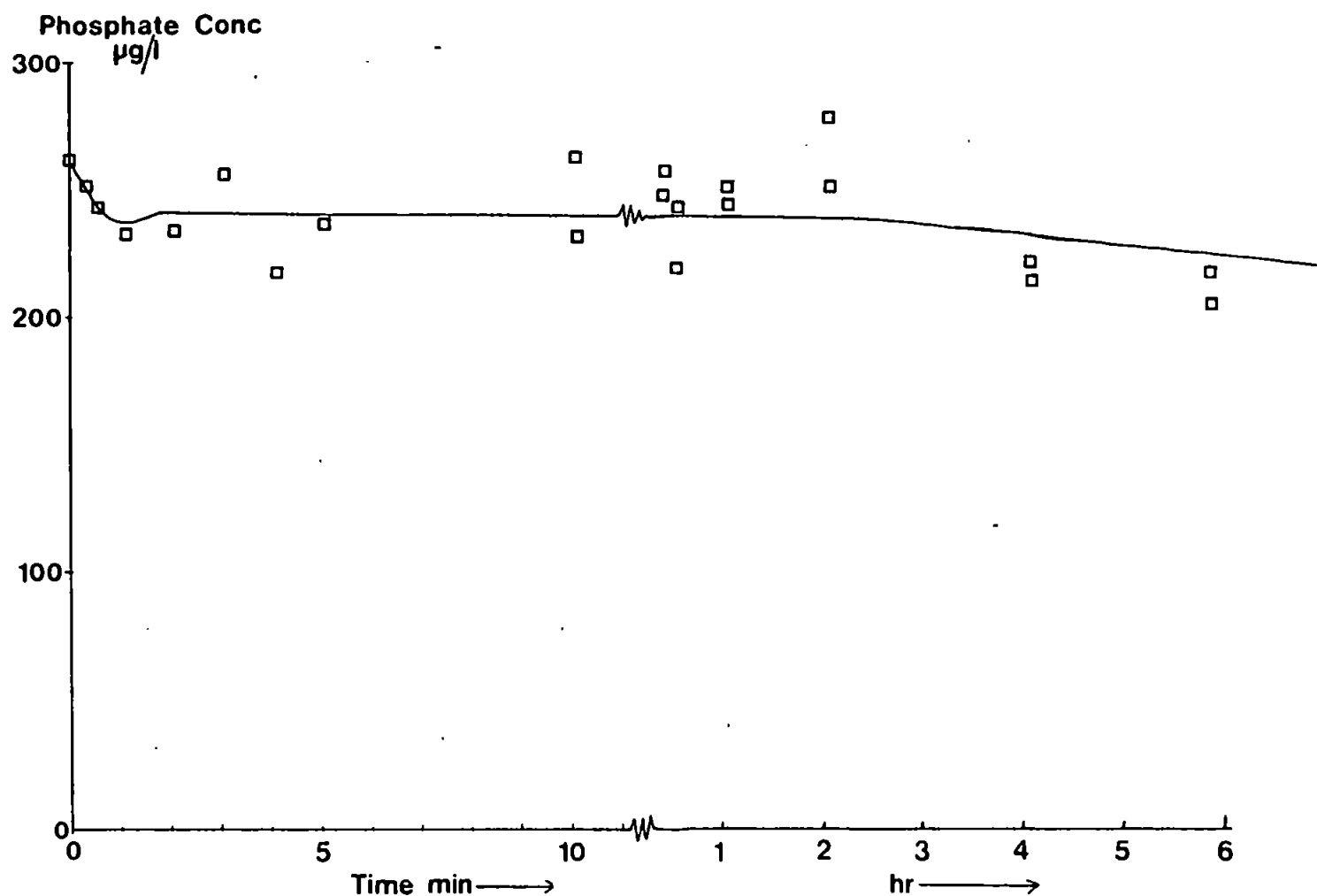
Figure 5.6. Adsorption of dissolved phosphate with time onto Tamar Estuary sediment. Plym Estuary Water Salinity 5.8 °/oo; Temp 21°C; pH 6.4; Turbidity 390 mg/l.
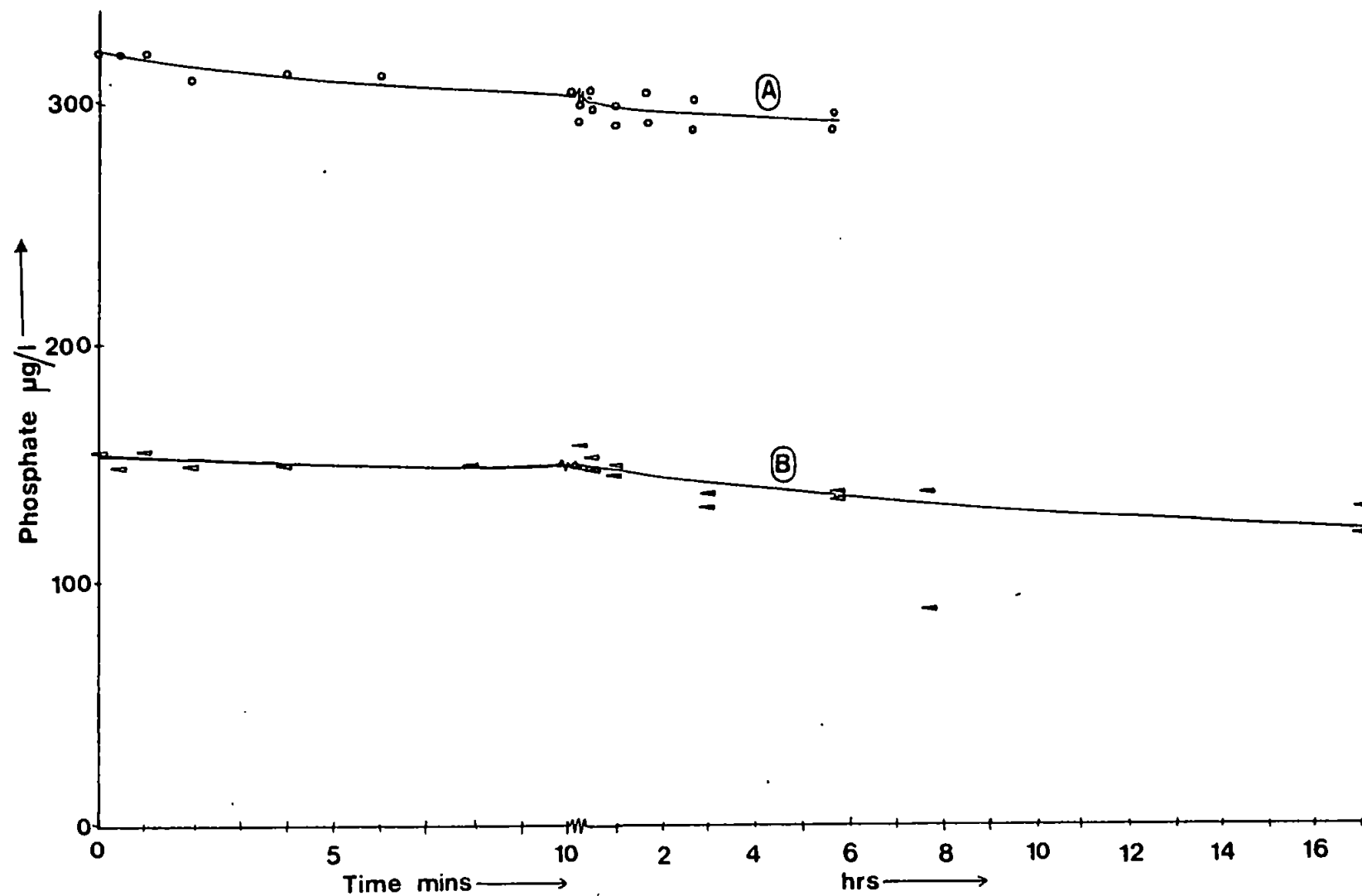
Figure 5.7. Adsorption of dissolved phosphate onto Tamar Estuary particles with time. A: Salinity 33.3°/oo Turbidity 480 mg/l; Temp 23°C; pH 5.9. B: Salinity 33.4 °/oo; Turbidity 300 mg/l; Temp 21°C; pH 6.5.

at   reduced pH's of 6.0 to 6.5. In general the profiles obtained were all much smoother than the experiments undertaken in brackish waters and the data were less scattered. Crosby (1982) showed that the uptake mechanism of dissolved phosphate onto synthetic Fe oxides in sea water was a physisorption process with the total amount adsorbed at equilibrium enhanced relative to distilled water.

The minimum distribution coefficients, (K_d) for each of the reactions are shown in Table 5.5.

Initial Conc. $\mu g/l$	Equil- Conc. $\mu g/l$	% Adsor- bed	Salinity $^o/oo$	Temp. ^oC	pH	Turb- idity mg/l	Uptake on Particles $\mu g/g$	Apparent K_d ml/g
253	212	16	33.3	20	6.5	330	126	590
155	138	11	33.4	21	6.5	300	55	400
373	337	10	32.9	20	7.9	270	132	390
264	241	9	5.8	21	6.4	390	59	245
322	297	8	33.3	23	5.9	480	52	180
213	206	3	5.8	21	7.6	460	13	65

Table 5.5.
Summary of results from adsorption experiments undertaken in more saline waters.

The results are ranked with the highest K_d at the top. This reveals that the more saline samples adsorb phosphate more readily than the less saline estuarine waters. Reducing the pH with acid to 6 did not enhance uptake. However, Crosby (1982) and Balistrieri and Murray (1979) observed enhanced uptake of dissolved ions onto amorphous Fe oxides in sea water at natural pH. This was thought to be due to the surface charge of the Fe oxide which varies with pH. At pH 7.0 in sea water, 40% of the surface sites are thought to be neutrally charged, 27% positively charged mainly from Mg^{2+} and Ca^{2+} adsorption

and 33% negatively charged from adsorption of SO_4^{2-} and Cl^- ions.

Z.P.C. calculations predict that the surface of Fe oxides will

become predominantly negatively charged at higher pH's

thereby reducing adsorption of negatively charged HPO_4^{2-} ions.

However, the increased negative charge of the surface may also cause

the adsorption of Mg^{2+} and Ca^{2+} producing more sites for phosphate

adsorption. The phosphate ions may also complex with Ca^{2+} and Mg^{2+}

ions and adsorb onto the particles as cation-phosphate complexes.

The complexity of the particle surfaces, which are composed of

adsorbed organic complexes clay minerals and amorphous Fe oxide

phases (Titley *et al.*, 1987), may result in an adsorption profile

relating to the individual components of the particles surface.

Amorphous Fe oxide coatings make an important contribution to the

surface area of the solids but organic materials occlude much of the

surface area and provide a wide range of potential adsorption sites.

The data in Table 5.5 suggests that overall pH is not important for

controlling the adsorption of dissolved phosphorus. A negative

relationship between particle concentration and uptake is apparent,

the experiments undertaken with the largest suspended particle

concentrations have the smallest K_d values. This suggests that the

sorption processes are basically reversible, and the particles may

already be loaded with phosphate. Thus when they are introduced

into a solution containing dissolved phosphate both uptake and

desorption from the particle surfaces takes place. At high phosphate

and low particle concentrations the reaction is dominated by uptake,

but when phosphate concentrations are lower and particle

concentrations are enhanced desorption from the surface becomes more

important and the K_d values are reduced. This is especially true in

266

brackish waters where many of the profiles suggest that there is an
on-going process of adsorption and desorption throughout the mixing
experiment. The desorptive capabilities of the sediments were
therefore examined by resuspending the sediments in buffered
distilled water.

5.2.3. MIXING EXPERIMENTS USING DISTILLED WATER.

A series of experiments were carried out in distilled water buffered
with $NaHCO_3$ in a similar manner to those of Crosby (1982) except for
the use of natural particles. Initially the water samples were
spiked with phosphate to increase the concentrations to 600 µg/l and
the pH manipulated so that individual experiments were undertaken at
pH's ranging between 6.5 and 8.2. This was to attempt to observe
phosphate uptake in a simplified media free of major cations, anions
and ligands. Using particles from 25-03-87 (see Table 5.1) in each
experiment and at particle concentrations of 350-430 mg/l; small
amounts of desorption were observed at all the pH values under
investigation. This confirms the conclusion from the natural water
experiments, namely that the processes occurring at the particle
surfaces are reversible, and in the simplified media of distilled
water release of previously adsorbed phosphate into the water can
occur even when concentrations in solution are 600 µg/l. There
appeared to be no pH dependence in the reactions (i.e. enhanced
uptake at lower pH) which is contrary to the observations of Crosby
(1982) who found enhanced uptake of phosphate onto Fe oxides at low
pH.

Further experiments were carried out using the batch of particles

collected on (24-06-87) as characterised in Tables 5.1 and 5.2. The phosphate concentration in the distilled water was lower than previously at 80 µg/l, the pH maintained at 6.5 and the particle concentration from the new batch was 834 mg/l. Under these conditions neither uptake nor desorption was observed. This suggests that the presense of dissolved species in natural waters encourages uptake of phosphate onto natural particles. As adsorption of phosphate onto natural particles did not occur in distilled water even after manipulation of pH, experiments were undertaken to see if release of phosphate from the particle surfaces occured. The experiments were undertaken at particle concentrations of 600-800 mg/l in distilled water containing 20 µg/l of phosphate (pH 8-8.5). Over long timescales (>10h) substantial quantities of phosphate were released into solution producing upwards of a 5 fold increase in solution concentration. During these experiments the particles disaggregated which may have contributed to the release of phosphate. The results of two desorption experiments are shown in Figure 5.8. One of the experiments was allowed to continue for 120h and from the results it is apparent that release of phosphate into solution was approaching a plateau. The results from these experiments are in good agreement with the the results from laboratory mixing experiments using sediments from the Amazon Estuary and various clays (Fox et al., 1986; Edzwald et al., 1976). Sediments collected from under the Amazon plume and resuspended in sea water showed persistent desorption of phosphate which continued for >4 days. Offshore sediments however showed rapid desorption over the first ten hours followed by readsorption of the phosphate over the next 14 hours. The adsorption profile produced in the
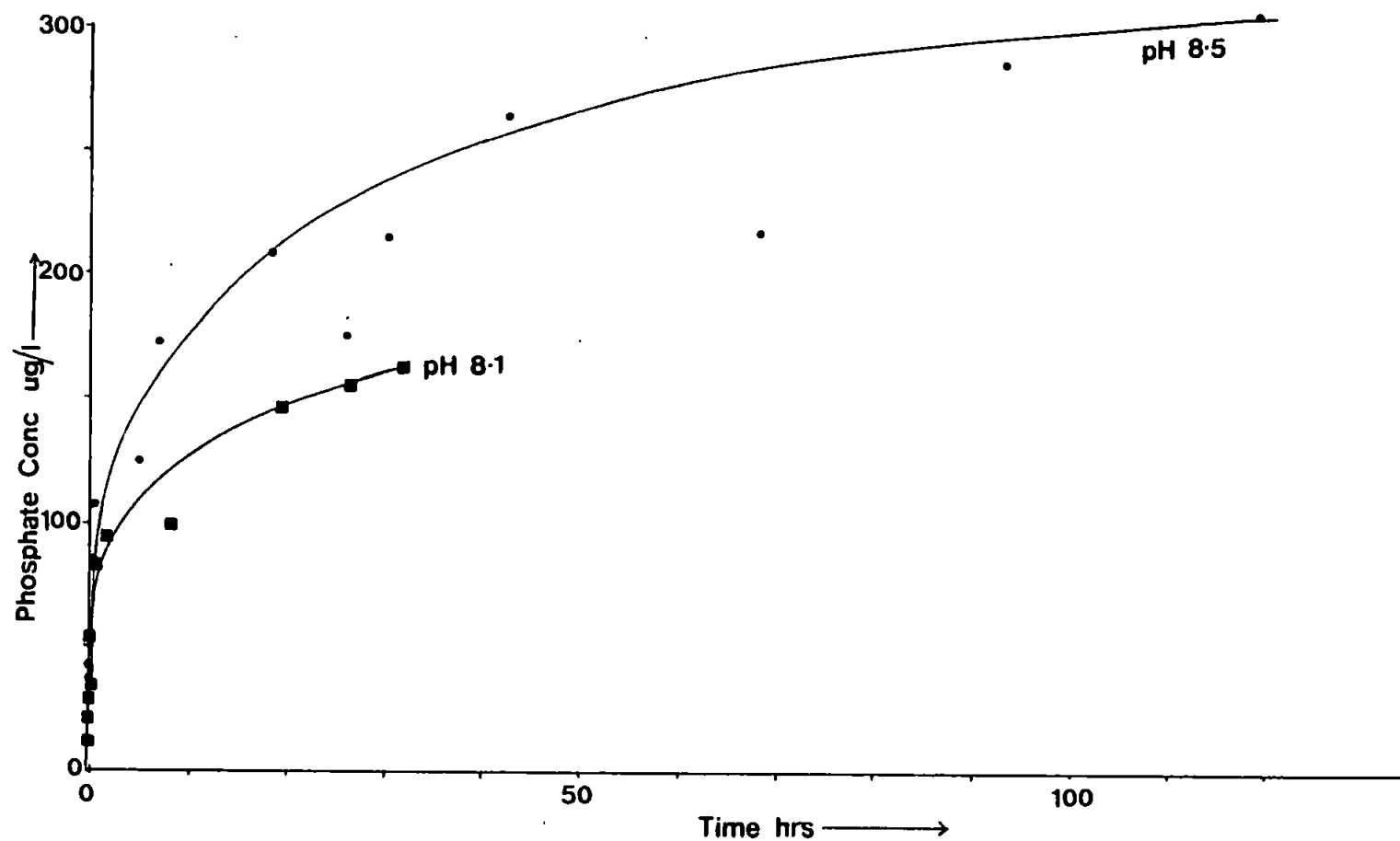
Figure 5.8. Desorption of phosphate into solution with time from Tamar Estuary particles (24-06-87) into distilled water. Turbidity 700 mg/l; Temp 22°C; (■) pH 8.1; (●) pH 8.5.

latter experiment is similar to desorption profiles obtained for Zn, Cu and Th with natural sediments.(Glegg *et al.*, in press; Moore and Millward, 1988).

Kinetic analysis of the desorption profiles was undertaken using a reversible first reaction of the type:

$$M + S \underset{k_{-1}}{\overset{k_1}{\rightleftharpoons}} MS \qquad \text{Equation 5.1}$$

where M is dissolved phosphate, S represents an active site on the particle, MS is the surface adsorbed or labile phosphate ion and k_1 and k_{-1} are the rate constants for the adsorption and desorption reactions respectively.

An integrated form of the rate equation used to obtain the desorption rate constant k_{-1} is shown below:

$$k_{-1}t = \frac{[M]_E}{[MS]_0} \ln\{[M]_E/([M]_E-[M]_t)\} \qquad \text{Equation 5.2}$$

where $[M]_E$ is the concentration of phosphate at equilibrium, $[M]_t$ is the concentration at time t and $[MS]_0$ is the initial concentration of labile phosphate. Plotting the right hand side of the equation against time allows the rate constant for the desorption reaction to be calculated from the slope of the line. A reasonable value for $[MS]_0$ is difficult to obtain, but Chase and Sayles (1980) suggest 500-900 μg/g are likely concentrations. Assuming that the desorption process shown in Figure 5.8 has reached equilibrium a value for $[M]_E$ of 300 μg/l was chosen. At a turbidity of 700 mg/l and for particle phosphate concentrations of 500-900 μg/g, rate constants for the reaction are in the range 4.3×10^{-2} - 7.8×10^{-2} h^{-1}, giving half lives for the desorption process of 9-16 h.

The reaction profile examined here assumes that the desorption process is only related to a reaction at the surface of the particles. Release of large quantities of phosphate over long timescales is explicable in terms of the distribution of phosphate within the pore structure of the sediment. Release of surface bound phosphate takes place rapidly; over the first few hours, and is followed by release of phosphate from the larger pores and then the more gradual diffusion of phosphate ions from the smaller pores. The longer term desorption ($>$4 days) is maintained by the very much slower release of phosphate from within the smallest of the micropores. Thus the desorption mechanism may be simplified into a three stage release process as shown in Figure 5.9. The gradual release of strongly bound phosphate from micropores within the particle matrix (shown as M^2X in Figure 5.9) would also be enhanced by the break-up of the particles during the experiment. These results contrast with those of Glegg et $al.$, (in press) and also from experiments using offshore sediments (Fox et $al.$, 1986). In these latter experiments, the initial release of surface bound material was followed by readsorption. The mechanism for this experiment is also shown in Figure 5.9.

5.2.4. CONCLUSION FROM PHOSPHATE SORPTION STUDIES.

This chapter has shown that the adsorptive behaviour of phosphate onto estuarine particles in natural solutions at low salinity is complex and depends in part on the initial concentration of the dissolved phosphate. The adsorption process was thought to comprise of a reversible process at the surface of the particles with the

271.

$$M^2X \rightleftharpoons M^1X \rightleftharpoons MX \rightleftharpoons M+X$$

'Tightly' matrix   matrix   surface   solution
      bound   bound   adsorbed   phosphate

$$M^1X \rightleftharpoons MX \rightleftharpoons M+X$$

matrix   surface   solution
bound   adsorbed
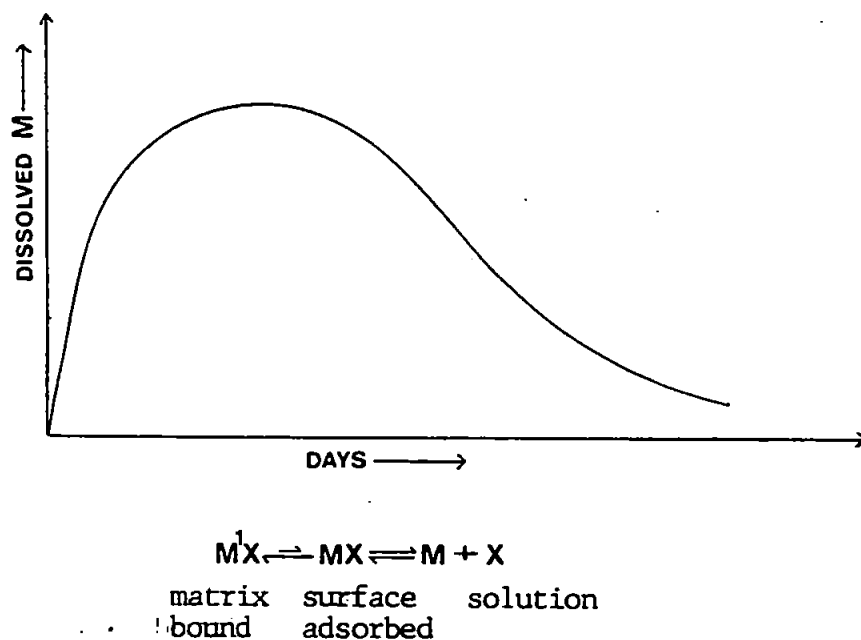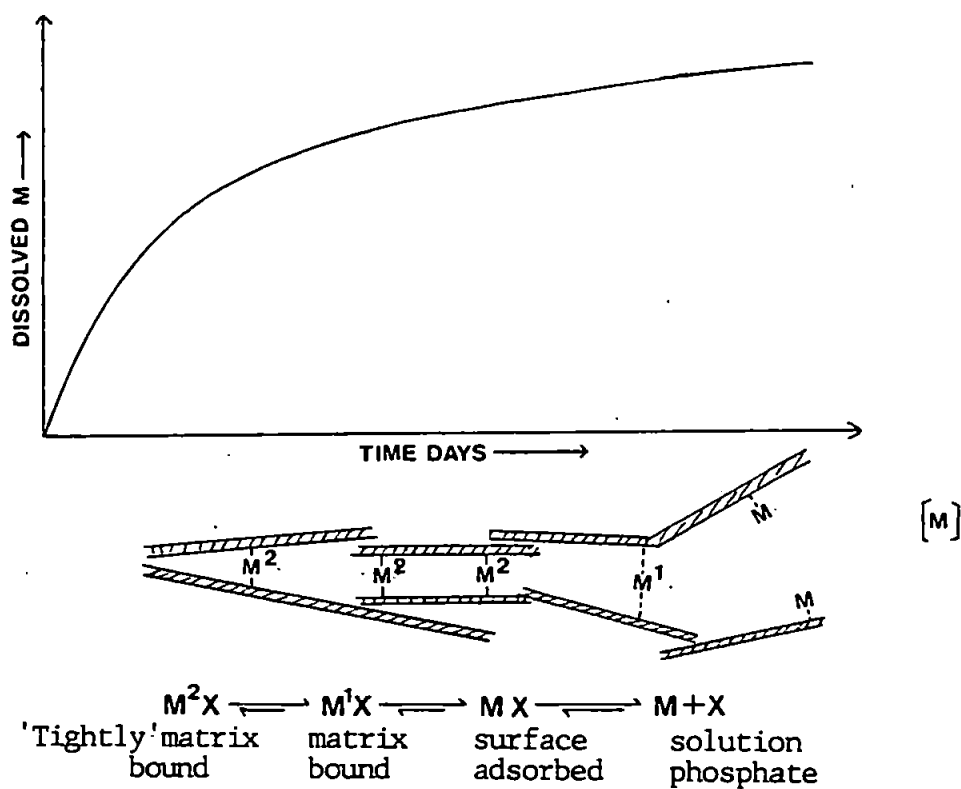
Figure 5.9. Top: Showing possible adsorbed phases of phosphate; including
2 matrix bound phases. Desorption profile obtained is shown.
Bottom: Single matrix bound phase and desorption profile obtained
(Glegg et al., in press).

distribution of phosphate between the solid phase and solution being controlled by the concentration in solution and by the amount of phosphate desorbing from the particle surface. Overall the results were inconclusive with little evidence of diffusion of dissolved phosphate into the particle matrix as observed by Madrid and De Arrambarri (1985) and Crosby (1982) on soils and Fe oxides respectively.

In sea water at salinities of 33 ^{o}/oo the uptake of phosphate was slow, with a steady adsorption continuing over a number of hours. This was in good agreement with the work of Crosby (1982) who showed that the uptake occurred through a physical adsorption process. In the simplified media of distilled water particles showed a tendency to desorb phosphate into solution which is thought to be amplified by the break-up of the particles during the mixing experiment and the resultant emptying of pores. The adsorption process therefore appears to be reversible with uptake onto the particles dominating at higher phosphate concentrations and lower suspended particle load. At lower phosphate concentrations and higher particle loads the release of phosphate from the surface is greater with a shift in the distribution between the dissolved and solid phase, and lower apparent K_d values.

Thus it is possible to suggest a mechanism to explain the transport of phosphate between terrestrial environment and estuarine systems. Relatively large amounts of phosphate are adsorbed onto soil particles from the soil waters with phosphate concentrations several orders of magnitude higher than those found in even the most contaminated aquatic systems. In the soil environment phosphate

273

becomes incorporated into the particle matrix through aggregation processes. Following wash out into rivers the particles are introduced into the estuarine environment where in the low salinity region of the estuary further adsorption may take place. Under high river flow conditions the particles may be carried a long way down estuary or even out to sea (Bale *et al.*, 1985), where adsorption of phosphate occurs more slowly. Under certain conditions when particle break-up occurs the phosphate associated with the internal structure can be released in a process that occurs over 4 days or more. This mechanism may explain the dissolved phosphate profiles observed by Morris *et al.*, (1981) in the Tamar Estuary; where limited removal of dissolved phosphate from the water column occurred in the low salinity region and addition occurred at higher salinities.

CHAPTER SIX.

CONCLUDING DISCUSSION.

6.1. THE ASSESSMENT OF PARTICLE MICROSTRUCTURES.

6.1.1. INVESTIGATION OF METHODS.

A systematic description of the surfaces of natural sediments in water bodies such as rivers, lakes, and estuaries has been lacking from studies concerned with the transfer of dissolved species onto the surfaces of particles. Most published work makes indirect assessment of the surface characteristics of particles either by selective chemical leaching methods or by assumptions made from particle size data. This study is one of the few to attempt to analyse the surface characteristics of natural particles related to chemical sorption processes (i.e. surface area and porosity) by direct measurement.

In order to accomplish this a number of problems associated with the approach had to be overcome. These were:

1) To assess the precision of surface area measurements made.
2) Difficulties associated with removal of particles from their natural environment and sample preparation prior to analysis.
3) The reproducibilty of the techniques employed on natural particles.

The first of these was addressed by calibration of the equipment using standard solids of known surface area, and the application of different mathematical approaches to the determination of surface area. Agreement between the standard surface area values of the

solids and those obtained using the technique was good (within 10%). This was expected because the method chosen is well proven industrially.

Additionally, a series of interlaboratory comparisons were undertaken between the gravimetric apparatus used in the study and volumetric techniques used in other laboratories. A range of highly microporous samples were used in the interlaboratory studies, and these highlighted the need for consistent sample preparation techniques, but showed also that when the drying methods were consistent, agreement between the laboratories was usually ±10%. The second problem was approached by maintaining both a consistent sampling technique and drying method. Investigations into the different drying methods available were undertaken and these showed the need to select a method where surface tension effects generated by the evaporation of water were minimized. These forces cause collapse of particle porosity from the micro to macro sizes which produces shrinkage and compaction of the particles.

Drying methods that avoid the passage of the gas-liquid interface through the particle structure were assessed and it was found that freeze drying was the most suitable as it produced a finely divided solid with pore structures intact. However the experiments also showed that the surface areas and porosities results are dependent on the sample preparation method. Therefore the data obtained is a relative description of the porosity and surface area of the particles rather than an absolute measure.

The main requirement in the study was that the results be used for

276

inter and intra estuarine comparisons.

To enable inter and intra estuarine comparisons to be made with
confidence, the reproducibilty of the technique on estuarine solids
was assessed by replicate analyses on aliquots of estuarine
particles. The surface area results had a co-efficient of
variation of ± 5-10%. The reproducibilty of the porosity analyses on
similar aliquots showed that no significant differences occurred
within individual particle populations.

These preliminary studies showed that the method can be applied to
estuarine solids for comparisons and to provide a description of the
surfaces of estuarine particles.

6.1.2. THE SURFACE AREA OF SYNTHETIC MATERIALS

6.1.2.1. Hydrous Oxides.

Oxides of Fe and Mn prepared in the laboratories had surfaces areas
in the range 200-400 m^2/g arising from the highly microporous nature
of the surface. These values were in good agreement with other work
e.g. Crosby (1982) and provide an explanation for the high sorptive
capacity of Fe oxides for trace metals and phosphate in the water
column. Additionally it was shown that co-precipitation of Fe and Mn
oxides under laboratory conditions reduced the surface areas by
aggregation and pore blocking effects.

6.1.2.2. Humic Materials

Low surface area values (<0.5 m^2/g) were obtained on soil humic
acids and organic materials isolated from the Tamar Estuary using
the technique. Work by Glegg (1987) and Martin *et al.*, (1986) showed

that removal of organics from estuarine particles exposed more active surfaces which suggests that organic materials such as humic acids function to mask the surfaces of particles and reduce the potential of the particle for adsorption. This is a surprising finding given the high affinity of trace metals such as Cu and Pb for organic coatings on natural particles. Additionally dye adsorption studies on soils using organic molecular dyes (which can adsorb onto the organic materials) suggest that humics have large surface areas, in the range 100-200 m²/g (Burford et al., 1964). This may be explained in terms of the nature of the surface of the dehydrated humic materials used in surface area measurements. In the dried state humic materials do not have a large physical surface area which can be detected by the BET method.

The high adsorptive capacity of humic materials for trace metals complexed with organics in solution e.g. Cu probably arises from a predominantly chemical binding to the abundant functional groups. The large number of adsorption sites will give rise to a large chemical surface area, resulting in extensive species specific binding processes, especially trace metals that are complexed with organics in solution, e.g. Cu.

Many trace metals have been shown to adsorb preferentially onto other phases such as Fe oxide surfaces or onto clay surfaces, which have highly porous surfaces resulting in large surface areas. Organic materials are present mostly as thin films of low density, which are not porous and therefore have BET surface areas that are equivalent to their geometric dimensions.

Although the BET method cannot assess the high chemical adsorptive capability of organic films, it does provide an assessment of the ability of organics to coat particle surfaces and to alter the surface activity of Fe and Mn oxides and clay surfaces.

6.1.3. PARTICLE CHARACTERISATION STUDY

Analyses of particles from the Tamar Estuary showed that they are composed of a mixture of quartz, kaolinite, illite, muscovite and chlorite, with surface coatings of organic matter and hydrous ferric oxides. The surface areas of suspended particles from the Tamar Estuary were in the range 8-22 m^2/g, and particles with the highest surface areas occurred in the low salinity, turbidity maximum region of estuary. A relationship between turbidity and surface area was found which suggested that disaggregation of the particles in the low salinity region resulted in the particles with larger surface areas. However, no simple relationship between particle size and surface area was observed for the particle populations in total although some of the individual surveys did show some relationships. Assessment of the relationship between the surface areas of suspended particles and coatings of Fe and Mn oxides (range 1-15 mg Fe/g; 0.1-1.0 mg Mn/g of particles) except in one of the particle populations where a strong co-variation of surface area and Fe/Mn ratio (EDTA leach) was found. In addition, no simple relationship was observed between the carbon content of the sediments (range 4-8%) and surface areas obtained.

Removal of Fe and Mn oxides coatings by chemical leaching methods exposed a less active surface thought to be associated with the underlying lithogenous material, especially the clays, quartz phases

and the organic material. The surface areas of the particles exposed by the leaching methods tended to converge on a constant low level for the axial surveys of the estuary. These values varied between 6 and 16 m^2/g, and the result depended on the leaching method employed and the amount of Fe and Mn removed. These results are in agreement with those obtained by Martin et al., (1986) in the Loire and Gironde Estuaries. Suspended particles collected from the Mersey Estuary had lower surface areas than those from the Tamar and Humber Estuaries. The surface areas of the particles from the Mersey did not appear to be related to turbidity, organic carbon or Fe content.

Suspended solids from Restronguet Creek had the highest surface areas of the estuaries studied, values in the range 22-35 m^2/g which were associated with carbon contents of 1-3% and leachable Fe contents of 20-80 mg/g. The surface areas of suspended sediments in Restronguet Creek were similar to those found in the Gironde and Humber Estuaries. Agreement between organic carbon and Fe content of the particles from the latter three estuaries was good.

In addition to suspended particles, the surface areas of bed sediments in the Tamar Estuary and Restronguet Creek were examined. The surface areas of Tamar sediments were lower than those of the suspended solids (in the range 6-14 m^2/g), which is probably due to compaction and the increased crystallinity of the particles in the sediment. The highest surface areas of the sediments were found in the low salinity region of the estuary in the mud shoals associated with the turbidity maximum. Additionally, surface areas of the bed sediments varied with depth and showed a tendency to decrease with

increasing depth, especially in the >45 μm fractions of the
sediment. The largest surface areas were consistently associated
with the <45 μm fraction throughout the core length. This fine
fraction would therefore provide most of the available surface area
for diagenetic processes within the sediments.

Sieve fractionations of the sediments showed that the largest surface
areas were associated with larger grain sizes which also had
the highest Fe content. Comparisons of these results with those
obtained from Restronguet Creek showed similar patterns although the
surface areas of the sediments were higher, in the range 13-40 m^2/g.
These higher values were associated with Fe contents in the
sediments of 20-80 mg/g (acetic acid leach) and low carbon content
(1-3%). The coarse fractions of the sediments (>45 μm) had lower
surface areas than the finer materials and generally had lower Fe
contents. The surface areas of the sediments correlated strongly
with acetic acid leachable Fe content.

The inter-relationship between organic carbon and Fe content of the
sediments from the different estuaries was investigated by comparing
the ratio of C:Fe with the surface areas of suspended and bed
sediments from the estuaries. The result of this is shown in Figure
6.1. The plot shows that the highest surface areas are associated
pure Fe and Mn oxide phases (200-300 m^2/g). The suspended solids
from the different estuaries have highest surface areas where the Fe
content relative to carbon is greatest. The surface areas of the
sediments decline as the C/Fe ratio increases. The lowest surface
areas are associated with humic acids with C/Fe ratios much greater
than 100:1. Bed sediments follow a similar pattern although it is

281
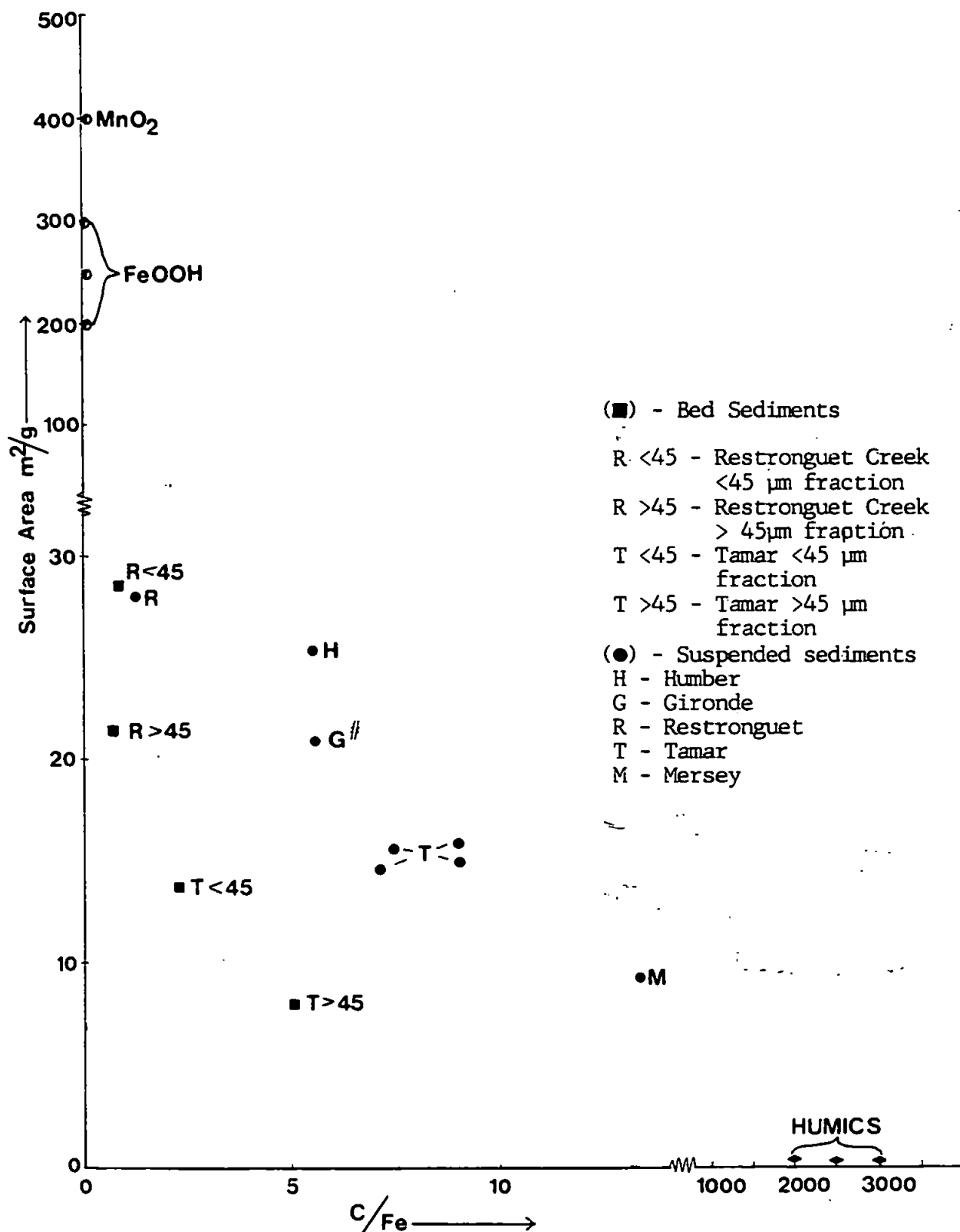
Figure 6.1. Plot of surface areas of sediments from 5 temperate
macrotidal estuaries as a function of carbon to iron ratios.
Results shown are averages from seperate surveys.
Fe content determined by acetic acid leach
// - results from Martin et al., 1986.

apparent from the plot that bed sediments have a different composition to suspended sediments and that their surface areas are also different. The plot suggests that suspended solids from Restronguet Creek are essentially resuspended fine bed sediment material (<45 μm). However the suspended solids from the Tamar Estuary are essentially different in character from the bed sediments.

The results obtained allow predictions to be made concerning the inter-estuarine variability.in the adsorptive capacity of natural particles. Thus the ability to predict some aspects of the physico-chemical behaviour of dissolved species within different estuaries can be made on the basis of turbidity, surface area and C:Fe ratio. For example in the Tamar Estuary removal of trace metals such as Zn and Cu was observed by Ackroyd et $al.$ (1986) when turbidities were greater than about 300 mg/l. The surface areas of particles would be expected to be 15-22 m²/g, giving water column activity of at these turbidities of 5-10 m²/l. In the Humber Estuary, where particle surface areas exceeded 25 m²/g, turbidity values would need to be 200 mg/l to provide the same surface activity. Hence the potential for removal of trace metals from the water column in the Humber Estuary would be greater assuming other factors such as the solution chemistry are equal.

6.1.4. POROSITIES OF PARTICLES

The gas adsorption experiments also provided a method of assessing the porosities of natural particles from the estuaries studied. Bed sediments and suspended particles had pores in the size range

1-50 nm, with a total pore volumes of 1-3 x 10^{-2} ml/g. Pore size distributions of the sediments showed that much of this volume was located in pores <10 nm in diameter, which are in agreement with the results of Stul (1985) and Quirk (1978) for soils and clays. The pore size distributions are too small to be resolved by electron microscopy. The pore size distributions detected in the natural sediments were of two types; those where the peak in pore volume occurred in pore sizes of 2-3 nm; and those where the pore volumes increased into the smallest size range <1 nm. These latter features are thought to be associated with the interlamellar spacings of clay structures as found by Stul (1985). The distributions of surface areas within the pore structures showed that up to 45% of of the total surface area could be located within pores <2 nm diameter.

6.1.5. EFFECT ON ADSORPTION MECHANISMS AND KINETICS.

From the particle characterisation study it is possible to determine models to describe the adsorption mechanisms that can take place at the particle-water interface.

The gross morphological structure of the particles (μm scale) is probably similar to the cardhouse/pincushion flocs created during the flocculation of clays. These structures are fragile and organic carbon coatings are implicated in the stabilisation of these flocs. In the low salinity region of estuaries where turbidity is high and orgnic carbon content low, the tidal shear forces lead to the break-up of the floccs, a decrease in particle size and an increase in surface area. On a smaller scale, the domain structures of clays are the dominant features that control the pore sizes and surface areas. The domains are blocks of aluminosilicate sheets that are disordered

284

and produce pores in the 3-50 nm size range (Quirk, 1978). The C&I pore size analysis of these structures show that 30-50% of the surface area of particles is associated with these structures. To an adsorbing ion (Pauling radius $\approx$ 0.2 nm) much of the surface area in the domains should be readily accessible. C&I pore size analysis from the sediments also shows the presence of micropores (<2 nm diameter). These features are probably associated with spacing between aluminosilicate sheets. For example the interlamellar spacings in montmorillonite clays is 1.2-1.9 nm. In the wetted state some metal ions such as K^+ and organic molecules such as RNH_3 can diffuse into these spacings in a process that takes several days.

Given the large hydration spheres of metal ions such as Na^+, the availability of this internal pore space to adsorbing species is not easy to define. However, if the internal space is accessible, then the available surface area is substantial ($\approx$ 800 m^2/g). C&I pore size analysis of sediments show that up to 50% of the total surface area of the particles may be located within these spacings. However, N_2 molecules may not be able to penetrate the spacings between aluminosilicate sheets of <1 nm, and thus potentially large surface areas are not detected. The availability of the surface area depends in part on the ability of water to seperate the sheets and to wet the surfaces. Water cannot penetrate the interlamellar structures of of some kaolinites, but is able to seperate and expand some swelling clays. In natural waters, the presence of colloidal Fe and organics may modify the behaviour of pure clays, for example Fe oxides can coat the clays or may precipitate as minute accretions within the clay structure. Organic molecules may diffuse into the clay layer

285

spaces and block the pores.

The particle surface therefore provides a highly variable physical surface, much of this being located in pores of <10 nm diameter. In the wetted state adsorption of ions takes place through chemical adsorption processes onto the compositionally inhomogenous surface through ion exchange and specific adsorption mechanisms. Initially adsorption will occur onto the most accessible surfaces, in larger pores and onto the surficial morphological features of the sediments.

Diffusion of ions in solution (radii <1 nm) or ions in association with macromolecular humic materials (radii 1-4 nm) (Sheppard *et al.*, 1980) into pores of diameter <10 nm would take place over longer timescales (hours) and more persistent adsorption would occur as ions diffused into pores of smaller diameter ($\approx$ 3 nm). Below this size range it might be expected that the outer diffuse Gouy layer in the electrical double layer on opposing faces of pores would start to overlap and the progress of the ion would be slowed still further. Some ions have larger diameters due to associated hydration spheres, complexing ligands or macromolecular humics and these may prevent the penetration of the ions into the smallest pores. The penetration of ions between the interlamellar spacing of clays (size range 1-2 nm) is therefore likely to be mediated by surface charge effects and physical dimensions of the adsorbing species and will be a key aspect in the desorption processes from particle surfaces in the natural environment. Evidence is available in the literature to show that adsorption into these spaces can take place and therefore this aspect of adsorption must be an important process in the environment. This is especially true for the transport, long term

fate of adsorbed species and for their bioavailability.

This work has shown some important aspects of the physical surface
of particles. In particular it has provided a direct measure of the
surface area of particles and also the microporosity of the surface
which may control long term transport, cycling and bioavailability
of adsorbed trace metals and nutrients. The observed inter and intra
estuarine variability in physical characteristics of the particles
provides new insight into the unique geochemical behaviour of
individual estuaries. Additionally the work has shown a need to
link the physical properties of particles with chemical aspects,
especially the compositional and surficial features.

6.3. RECOMMENDATIONS FOR FUTURE WORK

The results obtained in this study suggest that future work on the microstructures of estuarine particles should be directed as follows:

1) Investigations into the surface areas of suspended particles in estuaries should be linked to *in situ* measurements of particle size as developed by Bale *et al.*, (1984). This would be a partial step toward the actual assessment of surface areas *in situ* which is highly desirable in order to bridge the gap between physical surface data and the chemical behaviour of particles.

2) Investigations of the surface area of particles by the BET method should be augmented by "wet" determinations using negative adsorption or dye adsorption methods. This should provide a second link between the BET method and the true state of the particle surfaces. This will also provide additional information on the surface area of organic materials and would provide a link between porosity measurements (which can only be made on dry surfaces at present) with the wet surface of estuarine particles.

3) BET surface area studies should be carried out in conjunction with studies of the chemical nature of the particle surface. This could include acid-base titrations and cation exchange capacity. This would also help to link physical and chemical properties of particle surfaces.

4) Further work should also be undertaken to understand the complex behaviour of clay surfaces and Fe and Mn oxides which appear to dominate the surface areas and porosities of natural particles.

The value of these suggestions is that the sorption behaviour
of trace constituents could be better related to the most important
aspects of the surface characteristics of natural particles. The
adsorption mechanisms by which dissolved constituents are adsorbed
could be better understood.

REFERENCES.

Ackroyd, D.R;
The removal and remobilization of heavy metals during estuarine
mixing.
Ph.D. thesis, Plymouth Polytechnic. 222pp. (1983).

Ackroyd, D.R., Bale, A.J., Howland, R.J.M., Knox, S., Millward, G.E.
and Morris, A.W.;
Distributions and behaviour of dissolved Cu, Zn and Mn in the Tamar
Estuary.
Estuar. Cstl. Shelf Sci., 23, p.621, (1986).

Adamson, A.W.;
Physical Chemistry of surfaces. 4th Edition.
John Wiley, New York. 664pp. (1982).

Adamson, A.W.;
Physical chemistry of surfaces. 3rd Edition.
Wiley-Interscience, 698pp. (1976).

Aggett, J. and Roberts, L.S.;
Insight into the mechanismsof accumulation of arsenic and phosphate
in hydro-lake sedimentsby measuring the rate of dissolution with
ethylenediaminetetraacetic acid.
Environ. Sci. Technol., 20, p.183. (1986).

Airey, A. and Jones, P.D.;
Mercury in the River Mersey, its estuary and tributaries during 1973
and 1974.
Water Res., 16, p.565. (1982).

Allen, G.P., Castaing, P. and Klingebiel, A.;
Suspended sediment transport and deposition in the Gironde Estuary
and adjacent shelf.
Mem. Inst. Géol. Bassin Aquitane, 7, p.27. (1974).

Allen, G.P., Salomon, G.P., Bassoullet, P., DuPenhoat, Y. and De
Grandpré, C.;
Effects of tides on mixing on suspended sediment transport in
macrotidal estuaries.
Sediment. Geol., 26, p.69. (1980).

Anderson, M.A., Tejedor-Tejedor, M.I. and Stanforth, R.R.;
Influence of aggregation on the uptake kinetics of phosphate by
goethite.
Environ. Sci. Technol., 19, p.632. (1985).

D' Anglejan, B.F. and Smith, E.C.;
Distribution, transport and composition of suspended matter in the
St. Lawrence Estuary.
Can. J. Earth Sci., 10, p.1380. (1973).

290

Aston, S.R. and Chester, R.;
Influence of suspended particles on precipitation of Fe in natural waters.
Estuar. Cstl. Mar. Sci., 1, p.225. (1973)

Atkinson, R.J., Posner, A.M. and Quirk, J.P.;
Adsorption of potential determining ions at the ferric-oxide-aqueous electrolyte interface.
J. Phys. Chem., 71, p.550. (1967).

Aylmore, L.A.G.;
Microporosity in montmorillonite from nitrogen and carbon dioxide sorption.
Clays Clay Miner., 25, p.148. (1977).

Bale, A.J.;
The characteristics, behaviour and heterogeneous chemical reactivity of estuarine suspended particles.
Ph.D thesis, Plymouth Polytechnic. 216 pp. (1987).

Bale, A.J. and Morris, A.W.;
Laboratory simulation of chemical processes induced by estuarine mixing: the behaviour of iron and phosphate in estuaries.
Estuar. Cstl. Shelf Sci., 13, p.1. (1981).

Bale, A.J., Morris, A.W. and Howland, R.J.M.;
Seasonal sediment movement in the Tamar Estuary.
Oceanol. Acta, 8, p.1. (1985).

Bale, A.J., Morris, A.W. and Howland, R.J.M.;
Size distribution of suspended material in the surface waters of an estuary as measured by Laser Fraunhofer Diffraction.
In: "Transfer Processes in Cohesive Sediment Systems". (Eds. Parker, W.R. and Kinsman, D.J.J.) p.75
Plenum Publishing Corp., New York. (1984)

Balistrieri, L.S. and Murray, J.W.;
Chemistry of goethite (α-FeOOH) in seawater.
In: "Chemical Modelling in Aqueous Systems - Speciation, Sorption, Solubility and Kinetics". (Ed. Jenne, E.A.).
A.C.S. Symp. Ser. 93, p.275. (1979).

Barrer, R.M., Mackenzie, N. and Reay, J.S.S.;
Capillary condensation in single pores.
J. Colloid Sci., 11, p.479. (1956).

Barrow, N.J.;
A mechanistic model for describing the sorption of phosphate by soil.
J. Soil Sci., 34, p.733. (1983).

Barrow, N.J.;
On the reversibility of phosphate sorption by soils.
J. Soil Sci. 34, p.751. (1983a).

Barrow, N.J. and Ellis, A.S.;
Testing a mechanistic model. V. The points of zero salt effect for
phosphate retention, for zinc retention and for acid/alkali
titration of a soil.
J. Soil Sci., 37, p.303. (1986).

Barrow, N.J., Madrid, L. and Posner, A.M.;
A partial model for the rate of adsorption and desorption of
phosphate by goethite.
J. Soil Sci., 32, p.399. (1981).

Benjamin, M.M. and Leckie, J.O.;
Multiple site adsorption of Cd, Cu, Zn and Pb on amorphous iron
oxyhydroxide.
J. Colloid Interf. Sci., 79, p.209. (1981).

Berger, P., Etcheber, H., Ewald, M., Lavaux, G. and Belin, C.;
Variation of organic matter extracted from particles along the
Gironde Estuary (France).
Chem. Geol., 45, p.1. (1984).

Bland, S., Ackroyd, D.R., Marsh, J.G. and Millward, G.E.;
Heavy metal content of oysters from the Lynher Estuary, U.K.;
Sci. Total Environ., 22, p.235. (1982).

Bolan, N.S., Barrow, N.J. and Posner, A.M.;
Describing the effect of time on the sorption of phosphate by iron
and aluminium hydroxides.
·J. Soil Sci., 36, p.187, (1985).

Bolan, N.J., Syers, J.K. and Tillman, R.W.:
Ionic strength effects on surface charge and adsorption of
phosphate and sulphate by soils.
J. Soil Sci., 37, p.379. (1986).

Borggaard, O.K.;
Effect of surface area and mineralogy of iron Oxides on their
surface charge and anion adsorption properties.
Clay. Clay Miner. 31, p.230. (1983).

Borggaard, O.K.;
The influence of iron oxides on the surface area of soil.
J. Soil Sci., 33, p.443. (1982).

Borggaard, O.K.;
Selective extraction of amorphous iron oxides by EDTA from a Danish
Sandy Loam.
J. Soil Sci., 30, p.727. (1979).

Borggaard, O.K.;
Selective extraction of amorphous iron oxide by EDTA from a mixture
of amorphous iron oxide, goethite and hematite.
J. Soil Sci., 27, p:478. (1976).

Boström, B. and Pettersson, K.;
Different patterns of phosphorus release from lake sediments in
laboratory experiments.
Hydrobiologia, 92, p.415. (1982).

Bourg, A.C.M.;
Trace metal adsorption modelling and particle-water interactions in
estuarine environments.
Cont. Shelf Res., 7, p.1319. (1987).

Bourg, A.C.M.;
Role of fresh water/sea water mixing.
In: "Trace Metals in Sea Water." (Eds. Wong, C.S., Boyle, E.A.,
Bruland, K.W., Burton, J.D. and Goldberg, E.D.)
NATO Conf. Series IV-9, Plenum Press, New York, p.195. (1983).

Boyde, A. and Jones, S.J.;
Bone and other hard tissues.
In: "Principles and Techniques of Scanning Electron Microscopy".
(Ed. Hayat, M.A.) Vol. 2.
Van Nostrand Reinhold Co., p.123. (1974).

Boyden, C.R., Chester, S.R. and Thornton, I.;
Tidal and seasonal variations of trace elements in two Cornish
Estuaries.
Estuar. Cstl. Mar. Sci., 9, p.303. (1979).

Boyle, E.A., Huested, S.S. and Grant, B.;
The chemical mass balance of the Amazon plume - II, copper, nickel,
and cadmium.
Deep Sea Res., 29, p.1355. (1982).

Boyle, E.A., Edmond, J.M. and Sholkovitz, E.R.;
The mechanism of iron removal in estuaries.
Geochim. Cosmochim. Acta, 41, p.1313. (1977).

Boyle, E.A., Schlater, F. and Edmund, J.;
The distribution of dissolved copper in the Pacific.
Earth Planet. Sci. Lett., p.47. (1977a).

Brunauer, S., Deming, L.S., Deming, W.S., and Teller, E.;
J. Amer. Chem. Soc., 62, p.1723. (1940).

Brunauer, S., Emmett, P.H. and Teller, E.;
Adsorption of gases in multimolecular layers.
J. Amer. Chem. Soc., 60, p.309. (1938).

Burford, J.R., Deshpande, T.L., Greenland, D.J. and Quirk, J.P.;
Influence of organic materials on the determination of the specific
surface areas of soils.
J. Soil Sci., 15, p.192. (1964).

Burton, J.D.;
Basic properties and processes in estuarine chemistry. In:
"Estuarine Chemistry" (Eds. Burton, J.D. and Liss, P.S.).
Academic Press, London. p.1. (1976).

Burton, J.D. and Liss, P.S. (Eds.);
Estuarine Chemistry.
Academic Press, London. 229pp. (1976).

Cabrera, F., De Arrambarri, P., Madrid, L. and Toca, C.G.;
Desorption of phosphates from iron oxides in relation to equlibrium
pH and porosity.
Geoderma, 26, p.203. (1981).

Callender, E. and Hammond, D.E.;
Nutrient exchange across the sediment-water interface in the Potomac
River Estuary.
Est. Cstl. Shelf Sci., 15, p.395. (1980).

Cameron, A.J. and Liss, P.S.;
The stabilization of "dissolved" iron in freshwaters.
Water Res., 18, p.179. (1984).

Carter, M.A.;
Carbon and coke reactivity in zinc-lead blast furnace practice.
Ph.D. thesis, Plymouth Polytechnic. 365pp. (1983).

Chase, E.M. and Sayles, F.L.;
Phosphorus in suspended sediments of the Amazon River.
Est. Cstl. Shelf Sci., 11, p.383. (1980).

Chester, R. and Hughes, M.J.;
A chemical technique for the separation of ferro-manganese minerals,
carbonate minerals and adsorbed trace elements from Pelagic
sediments.
Chem. Geol., 2, p.249. (1967).

Cohen, A.L.;
Critical point drying.
In: "Principles and Techniques of Scanning Electron Microscopy".
(Ed. Hayat, M.A.) Vol. 1.
Van Nostrand Reinhold Co., p.44. (1974).

Cornell, R.M. and Schindler, P.W.;
Photochemical dissolution of goethite in acid/oxalate solution.
Clay. Clay Miner. 35, p.347, (1987).

Craig, P.J. (Ed.);
Organometallic compounds in the environment: Principles and
reactions.
Longman Group, Harlow;. 368pp. (1986).

Craig, P.J. and Rapsomanikis, S.;
Methylation of tin and lead in the environment: Oxidative methyl
transfer as a model for environmental reactions.
Environ. Sci. Technol., 19, p.726. (1985).

Cranston, R.W. and Inkley, F.A.;
Determination of pore structures from nitrogen adsorption isotherms.
Adv. Cat., 9, p.143. (1957).

Crosby, S.A.;
The interaction of phosphate with iron oxyhydroxides in simulated estuarine conditions.
Ph.D. thesis, Plymouth Polytechnic. 281pp. (1982).

Crosby, S.A., Butler, E.I., Turner, D.R., Whitfield, M., Glasson, D.R. and Millward, G.E.;
Phosphate adsorption onto iron oxyhydroxides at natural concentrations.
Environ. Technol. Letts., 2, p.371. (1981).

Crosby, S.A., Glasson, D.R., Cuttler, A.H., Butler, I., Turner, D.R., Whitfield, M. and Millward, G.E.M.;
Surface areas and porosities of Fe (III) and Fe (II) derived oxyhydroxides.
Environ. Sci. Technol., 17, p.709. (1983).

Crosby, S.A., Millward, G.E., Butler, E.I., Turner, D.R. and Whitfield, M.;
Kinetics of phosphate adsorption by iron oxyhydroxides in aqueous systems.
Estuar. Cstl. Shelf Sci., 19, p.257. (1984).

Curtis, G.P. and Roberts, P.V.;
Sorption of halogenated solutes by aquifer materials: comparison between batch equilibrium measurements and field observations.
Technical Report No.285.
Dept. of Civil Engineering, Stanford University, California.

Cuttler, A.H., Glasson, D.R. and Mann, V.;
Vacuum balance and related studies of green and red rusts.
Thermochim. Acta, 82, p.231. (1984).

Davis, J.A. and Leckie, J.O.;
Effect of adsorbed complexing ligands on trace metal uptake by hydrous oxides.
Environ. Sci. Technol., 12, p.1309. (1978)..

DeBoer, J.H.;
The shapes of capillaries.
In: " The Structure and Properties of Porous Materials". (Eds. Everett, D.H. and Stone, F.).
Butterworth, London. p.68. (1958).

Donard, O. and Bourg, A.C.M.;
A biogeochemical model for toxic trace metal fluxes in the macrotidal Gironde Estuary.
Rapp. P.-v. Réun. Cons. int. Explor. Mer., 186, p.263. (1986).

Draper, N.R. and Smith, H.;
Applied regression analysis. 2nd Edition.
John Wiley and Sons. 709pp. (1976).

Duinker, J.C.;
Suspended matter in estuaries. In: "Chemistry and Biogeochemistry of
Estuaries." (Eds. Olausson, E. and Cato, I.), p.71.
John Wiley, Chichester. (1980).

Duinker, J.C., Hildebrand, M.T.J., Nolting, R.F., Wellershaus, S.
and Jacobson, N.K.;
The River Varde A: Processes affecting the behaviour of metalts and
organochlorines during estuarine mixing.
Neth. J. Sea Res. 14, p.237. (1980).

Duinker, J.C. and Nolting, R.F.;
Mixing, removal and remobilization of trace metals in the Rhine
Estuary.
Neth. J. Sea Res., 12, p.205. (1978).

Duinker, J.C., Van Eck, G.T.M. and Nolting, R.F.;
On the behaviour of copper, zinc, iron and manganese, and evidence
of mobilization processes in the Dutch Wadden Sea.
Neth. J. Sea Res., 8, p.214. (1974).

Dutta, R. and Gupta, V.K.;
Surface area of Indian clay minerals.
J. Indian Chem. Soc., L1. (1974).

Eastman, K.W. and Church, T.M.;
Behaviour of iron, manganese, phosphate and humic acid during mixing
in a Delaware salt marsh.
Estuar. Cstl. Shelf Sci., 18, p.447. (1984).

Eckert, J.M. and Sholkovitz, E.R.;
The flocculation of iron, luminium and humates from river water by
electrolytes.
Geochim. Cosmochim. Acta, 40, p.847. (1976).

Edzwald, J.K., Toensing, D.C. and Leung, M.C.Y.;
Phosphate adsorption reactions with clay minerals.
Environ. Sci. Technol., 10, p.485. (1976).

Edzwald, J.K., Upchurch, J.B. and O'Melia, C.R.;
Coagulation in estuaries.
Environ. Sci. Technol., 8, p.58. (1974).

Egashira, K. and Aomine, S.;
Effects of drying and heating on the surface area of Allophane and
Imogolite.
Clay Sci., 4, p.231. (1974).

Eisma, D., van der Gaast, S.J., Martin, J.M. and Thomas, A.J.;
Suspended matter and bottom deposits of the Orinoco Delta:
turbidity, mineralogy and elemental composition.
Neth. J. Sea Res., 12, p.224. (1978).

296

Elbaz-Poulichet, F., Holliger, P., Huang, W.W. and Martin, J.M.;
Lead cycling in estuaries; illustrated by the Gironde Estuary,
France.
Nature 308, p.409. (1984).

Elderfield, H., Hepworth, A., Edwards, P.N. and Holliday, L.M.;
Zn in the Conway River and Estuary.
Estuar. Cstl. Shelf Sci., 9, p.403. (1979).

Florence, T.M.;
Trace metal species in fresh waters.
Water Res., 11, p.681. (1977).

Folk, R.L.;
A review of grainsize parameters.
Sedimentology, 6, p.73. (1966).

Fox, L.E., Sager, S.L. and Wofsy, S.C.;
The chemical control of soluble phosphorus in the Amazon Estuary.
Geochim. Cosmochim. Acta, 50, p.783. (1986).

Fox, L.E., Sager, S.L. and Wofsy, S.C.;
Factors controlling the concentrations of soluble phosphorus in the
Mississippi Estuary.
Limnol. Oceanogr., 30, p.826. (1985).

Fox, L.E. and Wofsy, S.C.;
Kinetics of removal of iron colloids from estuaries.
Geochim. Cosmochim. Acta, 47, p.211. (1983).

Gallenne, B.;
Study of fine material in suspension in the estuary of the Loire and
its fine grading.
Estuar. Cstl. Mar. Sci., 2, p.261. (1974).

Gearing, P.J., Gearing, J.N., Pruell, R.J., Wade, T.S. and Quinn,
J.G.;
Partition of No.2 fuel oil in controlled estuarine ecosystems.
Sediments and suspended matter.
Environ. Sci. Technol., 14, p.1129. (1980).

George, K.J.;
The tides and tidal streams of the Tamar Estuary.
PhD. thesis, University of London. 555pp. (1975).

Gerlach, S.A;
Marine pollution.
Springer-Verlag, Berlin. 218pp. (1981).

Gibbs, R.J.;
Transport phases of transition metals in the Amazon and Yukon
Rivers.
Geol. Soc. Am. Bull., 88, p.829. (1977).

297

Glasson, D.R. and Linstead-Smith, D.E.B.;
Vacuum microbalance studies of the formation and reactivity of some
synthetic and natural phosphates.
In: Progress in Vacuum Microbalance Techniques, Vol.2. (Eds. Bevan,
S.C., Gregg, S.J. and Parkyns, N.D.).
Heyden, London. p.209. (1973).

Glegg, G.A.;
Estuarine chemical reactivity at the particle-water interface.
Ph.D. thesis, Plymouth Polytechnic. 264 pp. (1987).

Glegg, G.A., Titley, J.G., Glasson, D.R., Millward, G.E. and Morris,
A.W.;
The microstructures of estuarine particles.
In: "Particle Size Analysis 1985". (Ed. Lloyd, P.J.).
John Wiley, Chichester. p.591. (1987).

Greene-Kelly, R.;
The preparation of clay soils for determination of structure.
J. Soil Sci., 24, p.277. (1973).

Greenland, D.J. and Quirk, J.P.;
Surface area of soil colloids.
Trans. Comm. IV and V Int. Soc. Soil. Sci., p.79. New Zealand.
(1962).

Gregg, S.J. and Sing, K.S.W.;
Adsorption, surface area and porosity. 2nd Edition.
Academic Press, London. 303pp. (1982).

Gregg, S.J. and Sing, K.S.W.;
Adsorption, surface area and porosity.
Academic Press, London. 303pp. (1967).

Gunatilaka, A.;
Phosphate adsorption kinetics of resuspended sediments in a shallow
lake, Neusiedlersee, Austria.
Hydrobiologia, 91, p.293. (1982).

Hamilton-Taylor, J. and Price, N.B.;
Geochemistry of iron and manganese in the waters and sediments of
Bolstadfjord, S.W. Norway.
Estuar. Cstl. Shelf Sci., 17, p.1. (1983).

Hart, B.T.;
Uptake of trace metals by sediment and suspended particles: a
review.
Hydrobiologia, 91, p.299. (1982).

Hingston, F.J., Posner, A.M. and Quirk, J.P.;
Anion adsorption by goethite and gibbsite 1.
The role of the proton in determining adsorption envelopes.
J. Soil Sci., 23, p.177. (1972).

Holliday, L.M. and Liss, P.S.;
Behaviour of dissolved iron, manganese and zinc in the Beaulieu
Estuary, S. England.
Estuar. Cstl. Mar. Sci., 4, p.349. (1976).

Howard, A.G., Arbab-Zavar, M.H. and Apte, S.;
The behaviour of dissolved arsenic in the Estuary of the River
Beaulieu.
Estuar. Cstl. Shelf Sci., 19, p.493. (1984).

van den Hul, H.J. and Lyklema, J.;
Determination of specific surface areas of dispersed materials.
Comparison of the negative adsorption method with some other
methods.
J. Amer. Chem. Soc., 90, p.3010. (1968).

Hunter, K.A. and Liss, P.S.;
Organic matter and the surface charge of suspended particles in
estuarine waters.
Limnol. Oceanogr., 27, p.322. (1982).

Hunter, K.A. and Liss, P.S.;
The surface charge of suspended particles in estuarine and coastal
waters.
Nature, 282, p.823. (1979).

Johnson, C.A.;
The regulation of trace element concentrations in river and
estuarine waters contaminated with mine drainage: The adsorption of
Cu and Zn on amorphous Fe oxyhydroxides.
Geochim. Cosmochim. Acta, 50, p.2433. (1986).

Keng, J.C.W., Morita, H. and Ramia, N.T.;
Cryoprotective effect of Dimethyl Sulfoxide (DMSO) on soil structure
during freeze drying.
Soil Sci. Soc. Am. J., 49, p.289. (1985).

Langston, W.J.;
The behaviour of arsenic in selected United Kingdom Estuaries.
Can. J. Fish. Aquat. Sci., 40, (Suppl. 2). p.143. (1983).

Li, Y.H., Burkhardt, L., Buchholtz, M., O'Hara, P. and Santschi,
P.H.;
Partition of radiotracers between suspended particles and seawater.
Geochim. Cosmochim. Acta, 48, p.2011. (1984).

Li, Y.H., Burkhardt, L. and Teraoka, H.;
Desorption and coagulation of trace elements during estuarine
mixing.
Geochim. Cosmochim. Act., 48, p.1879. (1984a).

Lippens, B.C., Linsen, B.G. and De Boer, J.H.;
Studies on pore systems in catalysis 1. The adsorption of nitrogen,
apparatus and calculation.
J. Catalysis, 3, p.32. (1964).

Lockwood, S.J.;
Fisheries interests in relation to the management of estuaries.
Presented to the European Intensive Course: "Evaluation of the
criteria for the management of estuarine systems", Southampton
University. (1986).

Loeb, G.I. and Neihof, R.A.;
Adsorption of an organic film at the platinum- seawater interface.
J. Mar. Res., 35, p.283. (1977).

Logan, T.J.;
Mechanisms for the release of sediment bound phosphate to water and
the effects of agricultural land management on fluvial transport of
particulate and dissolved phosphate.
Hydrobiologia, 92, p.519. (1982).

Loring, D.H.;
Geochemical factors controlling the accumulation and dispersal of
heavy metals in the Bay of Fundy sediments.
Can. J. Earth Sci., 19, p.930. (1982).

Loring, D.H., Rantala, R.T.T., Morris, A.W., Bale, A.J. and Howland,
R.J.M.;
Chemical composition of particles in a turbidity maximum zone.
Can. J. Fish. Aquat. Sci. 40, (Suppl. No. 1), p.201. (1983).

Luoma, S.M. and Brian, G.W.;
A statistical assessment of the form of trace metals in oxidizing
estuarine sedments employing chemical extractants.
Sci. Total Environ. 17, p.165. (1981).

McCave, I.N., Bryant, R.J., Cook, H.F. and Coughanowr, C.A.;
Evaluation of a laser-diffraction size analyzer for use with natural
sediments.
J. Sediment. Petrology, 56, p.561. (1986).

McClusky, D.S.;
An introduction to the estuarine ecosystem.
Blackie, London, 150. pp. (1981).

Madrid, L. and De Arambarri, P.;
Adsorption of phosphate by 2 iron oxides in relation to their
porosity.
J. Soil Sci., 36, p.523. (1985).

Marsh, J.G.;
The removal of arsenic from aquatic systems by iron oxyhydroxides.
Ph.D. thesis, Plymouth Polytechnic, 258pp. (1983).

Marsh, J.G., Crosby, S.A., Glasson, D.R. and Millward, G.E.;
BET nitrogen adsorption studies of iron oxides from natural and
synthetic sources.
Thermochimica Acta, 82, p.221. (1984).

Martin, J.M. and Maybeck, M.;
Elemental mass-balance of material carried by major world rivers.
Marine Chem., 7, p.173. (1979).

Martin, J.M., Mouchel, J.M. and Nirel, P.;
Some recent developments in the characterisation of estuarine particulates.
Water Sci. Technol., 18, p.83. (1986).

Matsunaga, K., Igarashi, K., Fukase, S. and Tsubota, H.;
Behaviour of organically bound iron in seawaters of estuaries.
Estuar. Cstl. Shelf Sci., 18, p.615. (1984).

Mayer, L.M.;
Aggregation of colloidal Fe during estuarine mixing. Kinetics; mechanisms; seasonality.
Geochim. Cosmochim. Acta, 46, p.2527. (1982).

Mayer, L.M.;
Retention of riverine iron in estuaries.
Geochim. Cosmochim. Acta, 46, p.1003. (1982a).

Mikhail, R.S., Guindy, N.M. and Hanafis, S.;
Vapour adsorption on expanding and non-expanding clay minerals.
J. Colloid Interf. Sci., 70, p.282. (1979).

Mikhail, R.S. and Robens, E.;
Microstructure and thermal analysis of solid surfaces.
John Wiley. 496pp. (1983).

Millward, G.E.;
The adsorption of cadmium by iron III precipitates in model estuarine solutions.
Environ. Technol. Lett., 1, p.394. (1980).

Millward, G.E.M. and Marsh, J.G.;
Dissolved arsenic behaviour in estuaries receiving acid mine wastes.
In: "Chemicals in the Environment" (Eds: Lester, J.N., Perry, R. and Sterritt, J.M.).
Selper, London. p.470. (1986).

Millward, G.E. and Moore, R.M.;
The adsorption of Cu, Mn and Zn by Fe oxyhydroxides in model estuarine solutions.
Water Res. 16, p.981. (1982).

Millward, G.E. and Titley, J.G.;
The microstructures of estuarine particles and their relationship to heteorogeneous chemical reactivity.
Report to N.E.R.C. 27pp. (1986).

Moore, R.M., Burton, J.D., Williams, P.J. Le B. and Young, M.L.;
The behaviour of dissolved organic material, iron and manganese in estuarine mixing.
Geochim. Cosmochim. Acta, 43, p.919. (1979).

Moore, R.M. and Millward, G.E.;
The kinetics of reversible Th reactions with marine particles.
Geochim. Cosmochim. Acta, 52, p.113. (1988).

Morris, A.W.;
Removal of trace metals in the very low salinity regions of the
Tamar Estuary, S.W. England.
Sci. Total Environ., 49, p.297. (1986).

Morris, A.W.;
Chemical processes in estuaries: the importance of pH and its
variability. In: "Environmental Biogeochemistry and
Geomicrobiology." Vol. 1 (Ed. Krumbein, W.E.).
Ann Arbor Sci., Michigan, p.179. (1978).

Morris, A.W. and Bale, A.J.;
Effect of rapid precipitation of dissolved Mn in river water on
estuarine distributions.
Nature, 279, p.318. (1979).

Morris, A.W., Bale, A.J. and Howland, R.J.M.;
Chemical variability in the Tamar Estuary, S.W. England.
Estuar. Cstl. Shelf Sci., 14, p.649. (1982a).

Morris, A.W., Bale, A.J. and Howland, R.J.M;
The dynamics of estuarine manganese cycling.
Estuar. Cstl. Shelf Sci. 14, p.175. (1982b).

Morris, A.W., Bale, A.J. and Howland, R.J.M.;
Nutrient distributions in an estuary: evidence of chemical
precipitation of dissolved silicate and phosphorus.
Estuar. Cstl. Shelf Sci., 12, p.205. (1981).

Morris, A.W., Loring, D.H., Bale, A.J., Howland, R.J.M., Mantoura,
R.F.C. and Woodward, E.M.S.;
Particle dynamics, particulate carbon and the O_2 minimum in an
estuary.
Oceanol. Acta, 5, p.349. (1982).

Morris, A.W., Bale, A.J., Howland, R.J.M., Loring, D.H. and Rantala,
R.T.T.;
Controls of the chemical composition of particle populations in a
macrotidal estuary (Tamar Estuary, U.K.).
Cont. Shelf Res., 7, p.1351. (1987).

Morris, A.W., Bale, A.J., Howland, R.J.M., Millward, G.E., Ackroyd,
D.R., Loring, D.H. and Rantala, R.T.T.;
Sediment mobility and its contribution to trace metal cycling and
retention in a macrotidal estuary.
Water Sci. Technol., 18, p.111. (1986).

Mouvet, C. and Bourg, A.C.M.;
Speciation (including adsorbed species) of copper, lead, nickel and
zinc in the Meuse River.
Water Res., 17, p.641. (1983).

Murgatroyd, A.L;
Fluvial transport in the Narrator Brook, Devon. A summary of
sources, dynamics and controls.
Ph.D. thesis, Plymouth Polytechnic. 286pp. (1980).

Natural Environmental Research Council;
Research on Estuarine Processes.
Report of a multidisciplinary workshop at the University of East
Anglia on 14-17 September, 1982.
N.E.R.C., 32pp. (1983).

Neihof, R.A. and Loeb, G.I.;
Dissolved organic matter in sea water and the electric charge of
immersed surfaces.
J. Mar. Res., 32, p.5. (1974).

Neihof, R.A. and Loeb, G.I.;
The surface charge of particulate matter in seawater.
Limnol. Oceanogr., 17, p.7. (1972).

Newton, P.P. and Liss, P.S.;
Positively charged suspended particles: Studies in an iron rich
river and its estuary.
Limnol. Oceanogr. 32, p.1267. (1987).

Nyffeler, U.P., Li, Y.H. and Santschi, P.H.;
A kinetic approach to describe trace element distributions between
particles and solution in natural aquatic systems.
Geochim. Cosmochim. Acta, 48, p.1513. (1984).

Oades, J.M.;
Interactions of polycations of aluminium and iron with clays.
Clay. Clay Miner. 32, p.49. (1984).

Obihara, C.H. and Russell, E.W.;
Specific adsorption of silicate and phosphate by soils.
J. Soil Sci., 23, p.105. (1972).

Olausson, E. and Cato, I. (Eds.);
The chemistry and biogeochemistry of estuaries.
John Wiley, Chichester. 452pp. (1980).

van Olphen, H.;
Clays.
In: "Characterisation of powder surfaces". (Eds. Parfitt, G.D. and
Sing, K.S.W.).
Academic Press, London. p.428. (1976).

van Olphen, H.;
An introduction to clay colloid chemistry.
Wiley and Sons, New York. 301pp. (1965).

Olsen, C.R., Cutshall, N.H. and Larsen, I.L.;
Pollutant-particle associations and dynamics in coastal marine
environments: a review.
Mar. Chem., 11, p.501. (1982).

Plummer, D.H., Owens, N.J.P. and Herbert, R.A.;
Bacteria-particle interactions in turbid estuarine environments.
Cont. Shelf Res. 7, p.1429. (1987).

Postma, H.;
Sediment transport and sedimentation.
In: "Chemistry and Biogeochemistry of Estuaries" (Eds. Olausson, E
and Cato, I.).
John Wiley and Sons, Chichester, p.153. (1980).

Pritchard, D.W.;
What is an estuary, a physical viewpoint. In: "Estuaries." (Ed
Lauff, G.H.).
Amer. Assoc. Adv. Sc., Washington. p.3. (1967).

Quirk, J.P.;
Some physico-chemical aspects of soil structure - A review. In:
"Modification of Soil Structure." (Eds. Emerson, W.W., Bond, R.D.
and Dexter, A.R.).
John Wiley, Chichester. p.3. (1978).

Rasmuson, A.;
Modelling of solute transport in aggregated/fractured media
including diffusion into the bulk matrix.
Geoderma, 38, p.41. (1986).

Readman, J.W., Mantoura, R.F.C. and Rhead, M.M.;
The physico-chemical speciation of polycyclic aromatic hydrocarbons
(PAH) in aquatic systems.
Fresenius Z. Anal. Chem., 319, p.126. (1984).

Rowell, D.L. and Dillon, P.J.;
Migration and aggregation of Na and Ca clays by the freezing of
dispersed and flocculated suspensions.
J. Soil Sci., 23, p.442. (1972).

Salomons, W.;
Adsorption processes and hydrodynamic conditions in estuaries.
Environ. Technol. Lett., 1, p.356. (1980).

Shanks, A.L. and Trent, J.D.;
Marine snow: microscale nutrient patches.
Limnol. Oceanogr. 13, p.72. (1979).

Sheppard, J.C., Campbell, M.J., Cheng, T. and Kittrick, J.A.;
Retention of radionuclides by mobile humic compounds and soil
particles.
Environ. Sci. Technol., 14, p.1349. (1980).

Sholkovitz, E.R.;
Flocculation of dissolved organic and inorganic matter during the
mixing of river and sea water.
Geochim. Cosmochim. Acta, 40, p.831. (1976).

Sigleo, A.C. and Helz, G.R.;
Composition of estuarine colloidal material: major and trace
elements.
Geochim. Cosmochim. Acta, 45, p.2501. (1981).

Smart, P.;
Particle arrangements in kaolin.
Proc. 15th. Nat. Conf. Clay. Clay Miner., 154, p.241. (1966).

So, C.L.;
Environmental pollution of estuaries – a problem of hazards.
Environ. Conserv. 5, p.205. (1978).

Sposito, G.;
The surface chemistry of soils.
Oxford University Press. 234 pp. (1984).

Strickland, J.D.H. and Parsons, T.R.;
A practical handbook of seawater analysis. 2nd Edition.
Ottawa Fisheries Research Board of Canada. 301pp. (1972).

Stul, M.S.;
The porosity of deferrated montmorillonites: ethanol and
methylbromide sorption.
Clay Miner., 20, p.301. (1985).

Stul, M.S. and Bock, J.D.;
Adsorption of n-aliphatic alcohols from dilute aqueous solutions on
RNH₃ montmorillonites.
(iii) Interlamellar aggregation of the adsorbate.
Clay. Clay Miner., 33, p.350. (1985).

Stumm, W. and Morgan, J.J.;
The solid solution interface.
In: "Aquatic chemistry; an introduction emphasizing chemical
equilibria in natural waters." (2nd Ed.)
Wiley, Chichester. p.599. (1981).

Sundby, B., Silverberg, N. and Cheeselet, R.;
Pathways of manganese in an open estuarine system.
Geochim. Cosmochim. Acta, 45, p.293. (1981).

Swallow, K.C., Hume, D.N. and Morel, F.M.M.;
Sorption of copper and lead by hydrous ferric oxide.
Environ. Sci. Technol., 14, p.1326. (1980).

Swift, D.J.P. and Pirie, R.G.;
Fine-sediment dispersal in the Gulf of San Miguel, Western Gulf of
Panama: a reconnaissance.
J. Mar. Res., 28, p.69. (1970).

Tessier, A., Campbell, P.G.C. and Bisson, M.;
Trace metal speciation in Yamaska and St. Francois Rivers (Quebec).
Can. J. Earth Sci., 17, p.90. (1980).

Tessier, A., Campbell, P.G.C. and Bisson, M.;
Sequential extraction procedurs for the speciation of particulate trace metals.
Anal. Chem., 51, p.844. (1979).

Theis, T.L. and Kaul, L.W.;
Rates of sorption at the goethite-water interface.
American Chemical Society Symposium Series, Division of Environmental Chemistry, 25, p.418. (1985).

Tipping, E.;
The adsorption of aquatic humic substances by iron oxides.
Geochim. Cosmochim. Acta, 45, p.191. (1981).

Tippkötter, R.;
The use of critical point drying for light and electron microscopy of soils.
Z. Pflanzenernaehr. Bodenk., 148, p.92. (1985).

Titley, J.G., Glegg, G.A., Glasson, D.R. and Millward, G.E.;
Surface areas and porosities of particulate matter in turbid estuaries.
Cont. Shelf Res. 7, p.1363. (1987).

Torres-Sanchez, R.M., Palm-Gennan, M.H., Stone, W.E.E., Herbillon, A.J. and Rouxhet, P.G.;
Retention of iron (III) by kaolinite and silica: adsorption and induced precipitation.
American Chemical Society Symposium Series, Division of Environmental Chemistry, 25, p.326. (1985).

Turner, A.;
Non-conservative behaviour of phophate in the Humber Estuary.
Microstructures of particles in the Humber Estuary.
Personal Communication of unpublished data.

Twinch, A.J. and Peters, R.H.;
Phosphate exchange between the littoral sediments and overlying water in an oligotrophic North-Temperate Lake.
Can. J. Fish. Aquat. Sci., 41, p.1609. (1984).

Uncles, R.J., Bale, A.J., Howland, R.J.M., Morris, A.W. and Elliott, R.C.A.;
Salinity in a partially mixed estuary, and its dispersion at low run-off.
Oceanol. Acta, 6, p.289. (1983).

Uncles, R.J., Elliott, R.C.A. and Weston, S.A.;
Observed fluxes of water, salt and suspended sediment in a partially mixed estuary.
Estuar. Cstl. Shelf Sci., 20, p.147. (1985).

Vazquez-Lopez, F., Pire, S.I. and Armijo Castro, F.;
Oil foreign particles in freeze dried injectible powders.
J. Parenter Sci., 36, p.259. (1982).

Waslenchuk, D.G. and Windom, H.L.;
Factors controlling the estuarine chemistry of arsenic.
Estuar. Cstl. Shelf Sci., 7, p.455. (1978).

Weaver, C.E. and Pollard L.D.;
Developments in sedimentology 15:
The chemistry of clay minerals.
Elsevier, Amsterdam. 213 pp. (1973).

Williams, D.J.A. and James, A.E.;
Rheology of suspensions.
N.E.R.C. Grant F60/b4/02, Report 5. University of Swansea. (1978).

APPENDIX 1.

Published Work.

Glegg, G.A., Titley, J.G., Glasson, D.R., Millward, G.E. and Morris, A.W.;
The microstructures of estuarine particles.
In: "Particle Size Analysis 1985". (Ed. P.J. Lloyd).
John Wiley, Chichester. p.591. (1987).

Titley, J.G., Glegg, G.A., Glasson, D.R., Millward, G.E.;
Surface areas and porosities of particulate matter in turbid
estuaries.
Continental Shelf Research, 7, p.1363. (1987).

Glegg, G.A., Titley, J.G., Millward G.E., Glasson, D.R. and Morris, A.W.;
Sorption behaviour of waste generated trace metals in estuarine
waters.
Water Science and Technology, (In press).

THE MICROSTRUCTURES OF ESTUARINE PARTICLES

G.A. Glegg, J.G. Titley, D.R. Glasson, G.E. Millward*
and A.W. Morris†

Departments of Marine and Environmental Science,
Plymouth Polytechnic, Plymouth. PL4 8AA, U.K.

†Institute for Marine Environmental Research,
Prospect Place, the Hoe, Plymouth. PL1 3DH, U.K.

ABSTRACT

Samples of bed sediment have been collected from the Tamar Estuary
and the surface areas and porosities of the dried materials were
determined using a vacuum microbalance technique. The surface
areas, calculated from the BET plots, were in the range 4 - 19 m^2/g
and the hysteresis loops showed that the particles had slit-shaped
mesopores. The organic carbon contents of the particles varied
between 1 and 10%. Careful removal of the surface organic coating
lead to a systematic increase in the surface areas, suggesting that
adsorbed organic matter affects the porosity of lithogenic
particles. These results are of relevance to the sorption
behaviour of natural particles in estuarine systems.

INTRODUCTION

The surface characteristics of estuarine particles are important
in the partitioning of trace constituents between the dissolved and
solid phases (Stumm and Morgan, 1981; Li et al., 1984). Estuarine
bed sediments, which can be resuspended by tidal stirring (Bale
et al. 1985) are a complex mixture of quartz grains, aluminosili-
cates, Fe/Mn oxyhydroxides, organic detritus and biogenic materials
all of which are implicated in scavenging processes. However, the
amount of systematic information on natural particle microstructures
is limited to some surface area studies, especially on iron oxides
(Davis and Leckie (1978); Crosby et al., 1983; Marsh, et al., 1984).

It is surprising that this lack of knowledge in estuarine chemistry
exists given the existing quantitative basis for evaluating
particle microstructure (e.g. Greg and Sing, 1982) and it is a fact
that little of this theory has been applied to natural particles.
The reason is probably because ideally surface characterisation
studies should be carried out in situ, with the surface area being
determined by the uptake of some dissolved constituent. This
presents a problem because one has to assume a non-porous surface,
as is the case with negative adsorption (Hul and Lyklema, 1968).
The major advantages of the BET gas adsorption method using the
dried solid are that estimates of porosity and assessments of the
control of particle morphology by surface coatings can be made.
Comparable experiments are very difficult to perform in situ. Thus,

591

the objectives of this work were to determine the surface areas and porosities of bed sediments and to evaluate the role of adsorbed organic materials in the modification of particle microstructure.

METHODS

Sample Collection. The samples were collected from the Tamar Estuary, which is located in South West England. The samples were retrieved from the low salinity regions of the estuary. The bed sediments were obtained either by a surface scrape of mobile material (0 - 2 cm) or by a gravity cover from a survey vessel. In the laboratory the samples were washed in distilled water and filtered. This was followed by freeze drying using a vacuum freeze drier (Edwards High Vacuum Ltd.).

Experimental Techniques. A gravimetric BET nitrogen adsorption technique (Crosby et al., 1983) was used to determine the surface areas and porosities of the samples. Approximately 0.2 g portions of the dried samples were used which usually resulted in the adsorption of 1 mg of nitrogen or more. The microbalance was evacuated and the sample retained under vacuum at 77 K using liquid nitrogen. The sample was dosed repeatedly with nitrogen gas and up to 0.5 h was allowed for equilibration during the adsorption stage and up to 2 h in the desorption stage. In some cases the particles were gently heated with 6% v/v hydrogen peroxide, prior to microstructural analysis, in an attempt to assess the effect of organic coatings. Particle size analyses were carried out using a Malvern Instruments 2200 particle sizes system (Bale et al., 1984). Small aliquots of the samples were kept in suspension in a sample cell by stirring. Each sample was scanned 100 times using a lens of focal length 100 mm and the output from the detectors was transferred to a microcomputer which calculated particle diameters in the range 1.9 - 188 um. Standard beads of 5 µm diameter were used to calibrate the instrument. The organic carbon analyses were carried out using a combustimetric technique (Carlo Erba Elemental Analyser).

RESULTS AND DISCUSSION

Two difficulties arise when carrying out microstructural studies on natural particles. Firstly it is essential to use a consistent preparative method since one is interested in relative surface areas (Greg and Sing, 1982). In this work freeze drying was preferred over air drying since the former has been used effectively for iron oxides (Davis and Leckie, 1978) and structural changes have been observed in the air drying method (Egashira and Aomine, 1974). Linked to this is the problem of the variability in the composition of portions of material taken for analysis from the bulk sample. To establish the variability in the samples and the drying method, the surface areas of ten portions of a Tamar sediment sample were obtained. These analysis gave a surface area of 12.66 ± 1.19 m^2/g (coefficient of variation 9.4%) and a similar number of organic carbon analyses on the same sample gave 4.53 ± 0.12% organic carbon (coefficient of variation 3%). These results suggest that the

samples were reasonably homogeneous and that realistic comparisons between samples could be made. The second problem concerns the ageing of the material by water vapour uptake after drying (Egashira and Aomine, 1974). This phenomena was observed in this study and dried materials left open to the atmosphere lost 30% of their original surface area after 30 days. Thus, samples were analysed as soon as possible after collection and were stored in a dessicator under vacuum.

Laser particle size analyses were carried on the sediment samples and a typical analysis is shown in Fig. 1. The particle diameters fall in the range 1 to 100 um with a mean grain size of 13.6 um.
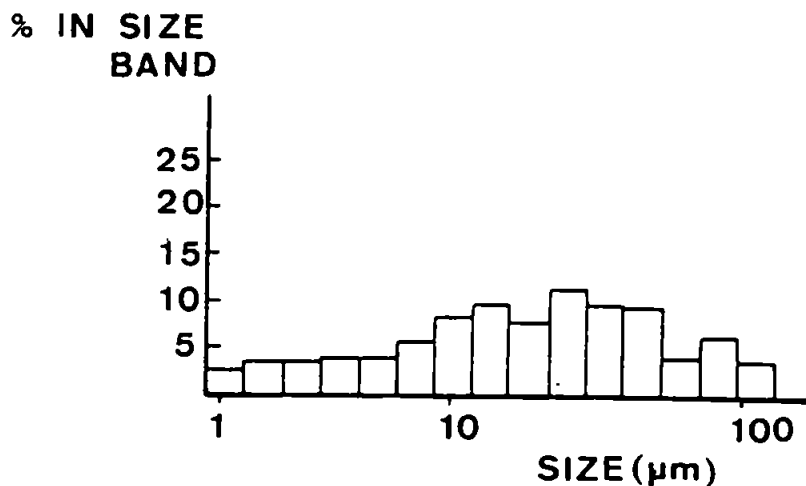

Fig. 1. Laser particle size analysis for a surface sediment from the Tamar Estuary.

In all the cases studied the range for the mean grain size was 8 - 15 um. These particle diameters give a specific surface area of the order 0.2 m^2/g (assuming a sediment density of 3000 kg/m^3). This surface area is two orders of magnitude less than the BET nitrogen adsorption value of 12.66 m^2/g which demonstrates the considerable quantity of internal surface in natural particles, which is available to adsorbates in the water column. Additional samples, including a sediment core, were taken in the Tamar Estuary. A surface sediment sample was particle fractionated using a 45 µm sieve and a complete isotherm was obtained for each fraction. Fig. 2 shows the hysteresis loop for the coarse fractions (> 45 µm) which had a surface area of 19.0 m^2/g. The fine fraction (< 45 um) had a surface area of 14.1 m^2/g and showed a similar hysteresis loop. The classification of the hysteresis loops suggests that
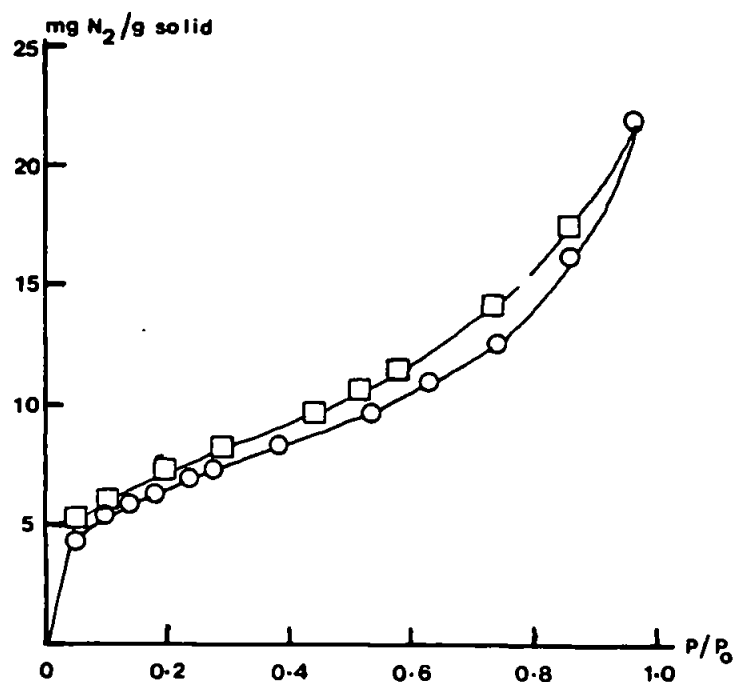
Fig. 2. The adsorption isotherm and hysteresis loop
for a surface sediment sample. ○- Adsorption;
□ - Desorption.

the particles have slit-shaped pores with pore radii in the range
2 - 20 nm and pore volumes of the order 20×10^{-9} m^3/g. The
results of the analysis of sections of the core (which had been
separated by a 45 μm sieve) are shown in Table 1. In general

TABLE 1. Surface areas and organic carbon contents of
a sediment core from the Tamar Estuary.

Depth in core, cm	Grain size % < 45 μm	Fraction > 45 μm		Fraction < 45 μm	
		Surface Area,m^2/g	% Carbon	Surface Area,m^2g	% Carbon.
0-2	76	10.74	5.40	10.34	3.20
6-8	77	9.50	9.70	10.48	3.16
11-13	76	8.40	5.70	10.20	2.45
17-19	84	6.12	10.0	10.31	2.65

the fine fraction had a constant surface area through the column.
These surface areas compare reasonably well with a pure kaolinite
sample (laser particle diameter 5 um) which gave a value of
12.9 m^2/g. They are, however, consistently lower than an amorphous
manganese dioxide, 470 m^2/g and amorphous iron oxides, 160 - 230
m^2/g (Crosby et.al., 1983). Thus, it appears unlikely that
ferromanganese coatings play a significant role in determining the
surface areas of these particles since one might have anticipated
higher values for the surface areas. Alternatively, organic carbon
may be involved in the surface coating. In the fine fraction the
organic carbon decreased by about 15% between the top and bottom
of the column suggesting that some carbon could have been
mineralised in the deeper anoxic zone (i.e. below about 4 cm).
Although the loss of this amount of carbon from the particle
appeared to have little effect on the surface area. In contrast
the coarse fraction (> 45 um) showed a consistent decrease in
surface area but this was not always accompanied by a systematic
change in the organic carbon content. However, closer inspection
of the material at the bottom of the core showed evidence of
remanant organic detritus, such as small pieces of terrestrial
vegetation, which may have contributed to the low surface area.
To investigate the role of the surface bound carbon a series of
experiments were carried out in which a sediment sample was
digested with 6% H$_2$O$_2$ for various times, see Table 2. These results

TABLE 2.   The surface areas and organic carbon contents
           of a sediment digested with H$_2$O$_2$ for different
           times.

Digestion Time, h	Surface[a] Area, m^2/g	% Carbon[a]
Untreated	12.66[b]	4.53[b]
0.5	11.22	4.00
2.5	15.14	2.46
4.5	17.57	1.21
24	22.99	0.71

[a] The average of 4 determinations.

[b] The average of 10 determinations.

show that the selective removal of surficial organic carbon leads
to an increase in surface area. This suggests that the loss is in
internal surface because the organic material adsorbed from the
water column occupies a significant portion of the pore space in
lithogenic materials.

In conclusion, this work is one of the first attempts to provide
urgently needed microstructural information on estuarine particles.

It has demonstrated that the wide variety of the solid phases in a sample can contribute to differences in surface areas. In particular, the incorporation of significant quantities of organic detritus can lead to a lowering of the surface area. Furthermore, in the case of lithogenic particles the adsorption of organic molecules leads to an occupation of pore space and a consequent loss of surface area. However, more work needs to be done on assessing the microstructural changes induced by the adsorption of organic and ferromanganese coatings onto natural particles. It is only with this kind of information that interfacial sorption phenomena involving natural particles will be fully understood.

ACKNOWLEDGMENTS

REFERENCES

Bale, A.J., Morris, A.W. and Howland, R.J.M. (1984). Size distributions of suspended material in the surface waters of an estuary as measured by laser Fraunhofer diffraction, in Transfer Processes in Cohesive Sediment Systems. (Eds. Parker and Kinsman), pp 75-85. Plenum Publishing Corp., New York.

Bale, A.J., Morris, A.W. and Howland, R.J.M. (1985). Seasonal sediment movement in the Tamar Estuary. Oceanologica Acta, 8, 1-6.

Crosby, S.A., Glasson, D.R., Cuttler, A.H., Butler, I., Turner, D.R., Whitfield, M. and Millward, G.E. (1983). Surface areas and porosities of Fe (III) - and Fe (II) - derived oxyhydroxides. Environmental Science and Technology, 17, 709-713.

Davis, J.A. and Leckie, J.O. (1978). Surface ionisation and complexation at the oxide/water interface. Journal of Colloid and Interface Science, 67, 90-107.

Egashira, K. and Aomine, S. (1974). Effects of drying and heating on the surface area of allophane and imogolite. Clay Science, 4, 231-242.

Greg, S.J. and Sing, K.S.W. (1982). Adsorption, Surface Area and Porosity. 303 pp. Academic Press, London.

Hul vanden, H.J. and Lyklema, J. (1968). Determination of specific surface areas of dispersed materials. Comparison of the negative adsorption method with some other methods. Journal of the American Chemical Society, 90, 3010-3015.

Li, Y-H., Burkhardt, L. and Teraoka, H. (1984). Desorption and coagulation of trace elements during estuarine mixing. Geochimica et Cosmochimica Acta, 48, 1879-1884.

Marsh, J.G., Crosby, S.A., Glasson, D.R. and Millward, G.E. (1984). BET nitrogen adsorption studies of iron oxides from natural and synthetic sources. Thermochimica Acta, 82, 221-229.

Stumm, W. and Morgan, J.J. (1981). Aquatic Chemistry: An Introduction Emphasising Chemical Equilibria in Natural Waters. 780 pp. Wiley Interscience, New York.

DISCUSSION

Dr.Wanogho, University of Strathclyde, asked: 1. Could you explain why you used two different percentages of hydrogen peroxide? Could the different times and percentages give different results?

Mr. Titley replied: The experiments carried out with the 6% hydrogen peroxide solution were designed to remove the surface carbon gradually over a period of several hours. We wished to demonstrate that carbonaceous coatings on particles tend to reduce the surface area. Having shown this we then used the 30% solution of hydrogen peroxide to effect the oxidation in a shorter time, even so the oxidation of all forms of organic matter was not complete. In almost all cases there was a resistant fraction which was not oxidised. Some of this may be organic detritus, such as fragments of vegetation, but we need to carry out further work on the contribution this makes to the overall surface area of the sample.

Mr. Kiff, Hydraulics Research Limited, asked: You quote an organic carbon figure of about 4% for one of you sediments. This corresponds to a volume percentage of organic matter of about 20%. Did you do any size gradings of sediment before and after the destruction of the organic matter to see if the organics are attached to the surface of the particle or entirely or partially absorbed with the particles.

Mr. Titley replied: The grading of sediment before and after an experiment has not yet been carried out. As we have already point out a natural sediment sample contains organic matter in three forms 1) as organic molecules adsorbed to particle surfaces; 2) as organic detritus, mainly land-derived and 3) as biogenic materials. It is not yet possible to assess the contribution made by each of these forms to the overall surface area of the particles. We are currently working on this problem, in the first instance looking at the contribution made by biogenic materials. It is through further experimentation of this kind that we intend to unravel the role that the organic mentioned has in determining the overall surface area.

Surface areas and porosities of particulate matter in turbid estuaries

J. G. TITLEY,* G. A. GLEGG,* D. R. GLASSON† and G. E. MILLWARD*

Abstract—A vacuum microbalance technique has been used to determine the specific surface areas and porosities of suspended solids and sediments from two turbid estuaries. In the Tamar Estuary, the suspended solids had specific surface areas in the range 8–20 m^2 g^{-1} whereas the sediments were in the range 5–15 m^2 g^{-1}. Sediments from the iron-rich system of Restronguet Creek were in the range 5–26 m^2 g^{-1}. The specific surface areas and porosities of the particles were influenced by the carbon and non-detrital iron contents. The results are relevant to sorption behaviour of dissolved trace constituents in the presence of natural particles.

INTRODUCTION

THE surface characteristics of estuarine particles are important to the partitioning of trace constituents between the dissolved and solid phases (CROSBY et al., 1984; LI et al., 1984; MORRIS, 1986). Estuarine bed sediments which are resuspended by tidal action (BALE et al., 1985) are a complex mixture of quartz grains, aluminosilicates, Fe and Mn oxides, organic detritus and biogenic materials. All of these solid phases could be implicated in sorption processes. Evidence is now emerging that the uptake and release of adsorbates is a two-stage process (NYFFELER et al., 1984). The two possible stages are (i) surface adsorption and (ii) migration of species from the external surface of the particles into the internal cavities and pores. Despite the fact that estuarine particles appear to exhibit this kind of reactivity (LI et al., 1984) there is only a limited amount of systematic information on their particle microstructure (CROSBY et al., 1983; MARSH et al., 1984; MARTIN et al., 1986; GLEGG et al., 1987). It is essential, therefore, that an improved understanding of the surface areas and porosities of estuarine particles is acquired to aid the interpretation of the kinetics of sorption reactions in estuarine systems.

EXPERIMENTAL

Sediment samples were obtained from the Tamar Estuary and Restronguet Creek, Southwest England by taking a surface scrape (0–2 cm) at low water or by using a gravity corer from a vessel. Suspended solids were isolated by filtration (passing 0.45 µm Millipore filters) of 10 l water samples collected from the low salinity, turbidity maximum zone of the Tamar Estuary. All the samples were washed with distilled water and freeze-dried immediately before analysis. The specific surface areas of the dried solids were

* Institute of Marine Studies. Plymouth Polytechnic. Plymouth PL4 8AA. U.K.
† Department of Environmental Sciences. Plymouth Polytechnic. Plymouth PL4 8AA. U.K.

determined using a gravimetric B.E.T. nitrogen gas adsorption technique on a C.I. Mark 2B vacuum microbalance. Nitrogen desorption experiments were also carried out and estimates of pore shape and size were obtained from the hysteresis loops (CROSBY et al., 1983; MARSH et al., 1984). The carbon contents of the particles were determined by a combustiometric technique (Carlo Erba Elemental Analyser). The non-detrital iron and manganese contents of the solids were determined by atomic absorption spectroscopy, following extraction by 0.05 mol l^{-1} hydroxylamine hydrochloride in 25% (volume by volume) glacial acetic acid (TESSIER et al., 1979).

RESULTS AND DISCUSSION

The specific surface areas of suspended solids in the turbidity maximum zone of the Tamar Estuary are in the range 8.4–19.8 $m^2 g^{-1}$, as shown in Table 1. The highest specific surface areas are found in the brackish water above the salt wedge, where the maximum suspended load is also located. The variation in the specific surface areas could be due to changes in either the particle size distribution or surface chemical composition. The particle size distribution in the turbidity maximum shows no consistent trend (see Table 1) but in any case the geometric surface areas are only of the order 0.02 $m^2 g^{-1}$. Examination of the role of surface coatings was achieved by the use of chemical extraction techniques on separate aliquots of the same sample. Removal of the ferro-manganese layer reveals the underlying lithogenous matrix which has a relatively low specific surface area of about 16 $m^2 g^{-1}$. However, if only the organic coatings are removed by digestion with hydrogen peroxide, the specific surface area increases by an average of 60% with little difference between the samples (see Table 1).

Similar trends have been observed by MARTIN et al. (1986) in suspended solids from the Gironde and Loire estuaries. The main reason for the increase in specific surface area is due to the exposure of new adsorption sites, rather than particle disaggregation during digestion which contributes <2 $m^2 g^{-1}$. The new sites are probably associated with surface coatings of iron and manganese oxides which are known to have high specific surface areas (CROSBY et al., 1983). Thus, the results in Table 1 which show a higher specific surface area in the low salinity region of the Tamar Estuary could be explained in

Table 1. Specific surface areas and associated properties of suspended particles from the turbidity maximum zone of the Tamar Estuary

Salinity (‰)	Turbidity (mg l^{-1})	Mean particle size (μm)	Particulate concentrations			Specific surface areas ($m^2 g^{-1}$)		
			Carbon (%)	Iron† (mg g^{-1})	Manganese† (mg g^{-1})	Natural	Oxidized*	Leached†
0.06	70	24	7.1	7.3	0.74	13.9	–	15.0
0.09	235	16	6.6	7.1	0.55	14.6	24.8	16.9
0.15	590	14	6.0	7.5	0.44	17.8	27.3	18.7
2.2	420	20	6.9	6.6	0.52	19.8	25.0	16.8
3.1	410	26	6.4	6.5	0.50	18.0	26.6	16.3
5.0	130	12	6.5	7.0	0.48	17.2	25.8	17.3
9.7	100	15	6.6	7.9	0.54	14.1	28.5	16.2
22.5	75	17	6.4	7.1	0.49	10.7	24.8	15.0
28.5	25	27	6.7	9.9	0.62	8.4	24.1	14.2

* Oxidized means digestion of original freeze-dried samples with 30% H_2O_2.
† Leached means digestion of original freeze-dried samples with 0.05 mol l^{-1} hydroxylamine hydrochloride in 25% (volume by volume) glacial acetic acid.

Table 2. *Specific surface areas and associated properties of the coarse and fine fractions of an oxic sediment core from the Tamar Estuary*

Core depth (cm)	<45 μm fraction				>45 μm fraction			
	Specific surface area ($m^2 g^{-1}$)	Carbon (%)	Fe ($mg\ g^{-1}$)	Mn ($mg\ g^{-1}$)	Specific surface area ($m^2 g^{-1}$)	Carbon (%)	Fe ($mg\ g^{-1}$)	Mn ($mg\ g^{-1}$)
Mobile	14.1	3.9	11.5	0.44	20.0	8.9	15.7	0.86
0–2	14.3	3.5	18.9	0.67	10.4	7.4	21.2	0.94
7–10	13.2	2.6	–	–	7.8	3.1	–	–
10–12	13.2	3.4	–	–	6.2	6.0	–	–
16–18	13.5	3.8	9.6	0.58	6.3	8.6	8.6	0.78
22–24	13.7	3.2	11.9	0.62	6.6	6.8	9.9	0.74
28–30	13.7	3.3	19.3	0.78	6.9	6.8	15.2	0.86

terms of flocculation of dissolved Fe and Mn (injected from pore waters) to form fresh oxide surfaces on suspended particles. Suspended material collected either side of this region will have oxide coatings which are aged and. as a consequence. have lower specific surface areas (CROSBY *et al.*, 1983). This variation in specific surface area across the freshwater–brackish water interface must influence the degree of the heterogeneous chemical reactivity in this zone (ACKROYD *et al.*, 1986: MORRIS, 1986).

Table 2 shows the results from the analysis of an oxic sediment core taken in the low salinity region of the Tamar Estuary. The seven core sections were sieved to provide fine (<45 μm) and coarse (>45 μm) fractions. In the former case the specific surface areas were uniform throughout the core and these were associated with a constant carbon content of about 3%. The coarse fraction generally had lower specific surface areas, particularly at depth. which were correlated with a significantly higher carbon content. In addition. the samples with the higher specific surface areas had greater Fe concentrations. whch supports the suggestion that oxide coatings contribute to surface properties. Similar trends were observed in a sediment core from Restronguet Creek. with the difference that the fine fraction had specific surface areas of about 25 m^2 g^{-1}. particulate carbon contents <2% and particulate iron concentrations of 26 mg g^{-1}.

The porosity analyses showed that the hysteresis loops of both suspended material and sediments were characteristic of solids with parallel plates or slits. The pore sizes were in the range 2–20 nm (mesopores) and the pore volumes were between 25 and 7 × 10^{-9} m^3 g^{-1}. The removal of the organic surface layer resulted in a doubling of the pore volume for a gain of 60% in the specific surface area.

In conclusion. the specific surface areas of estuarine particles are significantly controlled by organic and ferromanganese coatings. The natural organic compounds act as pore blocking agents which tend to reduce the specific surface areas of the particles. whereas the presence of Fe and Mn oxides leads to an increase. These solids have plate-like pores with dimensions in the nanometer size range. The pores are large enough to accommodate adsorbates in the solid matrix. as part of the second phase of heterogeneous chemical reactions in the water column (or sediment pore waters). The specific surface areas of suspended particles were highest in the brackish water above the salt wedge. where they contribute to the active removal of trace constituents from the dissolved phase.

REFERENCES

ACKROYD D. R., A. J. BALE, R. J. M. HOWLAND, S. KNOX, G. E. MILLWARD and A. W. MORRIS (1986) Distributions and behaviour of dissolved Cu, Zn and Mn in the Tamar Estuary. *Estuarine Coastal and Shelf Science*, 23, 621–640.

BALE A. J., A. W. MORRIS and R. J. M. HOWLAND (1985) Seasonal sediment movement in the Tamar Estuary. *Oceanologica Acta*, 8, 1–6.

CROSBY S. A., D. R. GLASSON, A. H. CUTTLER, E. I. BUTLER, D. R. TURNER, M. WHITFIELD and G. E. MILLWARD (1983) Surface areas and porosities of Fe(III)- and Fe(II)-derived oxyhydroxides. *Environmental Science and Technology*, 17, 709–713.

CROSBY S. A., G. E. MILLWARD, E. I. BUTLER, D. R. TURNER and M. WHITFIELD (1984) Kinetics of phosphate adsorption by iron oxyhydroxides in aquatic systems. *Estuarine Coastal and Shelf Science*, 19, 257–270.

GLEGG G. A., J. G. TITLEY, D. R. GLASSON, G. E. MILLWARD and A. W. MORRIS (1987) The microstructures of estuarine particles. *Proceedings of the Fifth Particle Size Analysis Conference*, Royal Society of Chemistry. P. J. LLOYD, editor. Wiley–Interscience, London, pp. 591–597.

LI Y.-H., L. BURKHARDT and H. TERAOKA (1984) Desorption and coagulation of trace elements during estuarine mixing. *Geochimica et Cosmochimica Acta*, 48, 1879–1884.

MARSH J. G., S. A. CROSBY, D. R. GLASSON and G. E. MILLWARD (1984) BET nitrogen adsorption studies of iron oxides from natural and synthetic sources. *Thermochimica Acta*, 82, 221–229.

MARTIN J.-M., J. M. MOUCHEL and P. NIREL (1986) Some recent developments in the characterisation of estuarine particles. *Water Science and Technology*, 18, 83–92.

MORRIS A. W. (1986) Removal of trace metals in the very low salinity region of the Tamar Estuary, England. *Science of the Total Environment*, 49, 297–304.

NYFFELER U. P., Y.-H. LI and P. H. SANTSCHI (1984) A kinetic approach to describe trace-element distribution between particles and solution in natural aquatic systems. *Geochimica et Cosmochimica Acta*, 48, 1513–1522.

TESSIER A., P. G. C. CAMPBELL and M. BISSON (1979) Sequential extraction procedure for the speciation of particulate trace metals. *Analytical Chemistry*, 51, 844–851.

SORPTION BEHAVIOUR OF WASTE-GENERATED TRACE
METALS IN ESTUARINE WATERS

G. A. Glegg*, J. G. Titley*, G. E. Millward*,
D. R. Glasson* and A. W. Morris**

*Institute of Marine Studies, Plymouth Polytechnic,
Plymouth, Devon PL4 8AA, England

**The Plymouth Marine Laboratory, Prospect Place,
The Hoe, Plymouth, Devon PL1 3DH, England

ABSTRACT

Samples of suspended particles have been collected from the turbidity maximum
region of the Tamar Estuary, S.W. England.   Specific surface areas and
porosities of the particles were determined by a BET nitrogen adsorption
technique. The role of surface coatings of organic matter and Fe and Mn oxides
was examined.   The data shows that the specific surface area was highest at
the turbidity maximum and was associated with high Fe/Mn ratios.   The
characterised particles were then used in time-dependent adsorption-desorption
experiments, with waters from the metal-rich Carnon River, S.W. England.
The rates and extents of the sorption processes were interpreted in terms of
a two-stage reaction which was related to the microstructures of the particles.
Kinetic analyses of the desorption profiles gave rate constants which are of
significance in the prediction of the fate of toxic metal wastes discharged
into estuaries.

KEYWORDS

Estuaries, trace metals, particle microstructures, adsorption, desorption,
rate constants.

INTRODUCTION

The estuarine turbidity maximum zone (Allen et al., 1980; Morris et al., 1982)
is known to contain large concentrations of highly active suspended particles.
The specific surface areas of particles in this region appear to be higher
than those either up- or down-estuary (Martin et al., 1986; Titley et al.,
1987).   This variation in particle activity is a major control on sorption
processes which give rise to the non-conservative behaviour of trace metals
(such as Zn and Cu) in estuarine systems (Morris, 1986).   For example,
Ackroyd et al. (1986) have shown that both Zn and Cu adsorb onto particles in
the freshwater of the turbidity maximum in the Tamar Estuary.   Down-estuary
of the high turbidity zone dissolved metal maxima for Zn and Cu are persistent
features, which appear to be generated, in part, by desorption from seaward
fluxing particles.   Field observations by Evans and Cutshall (1973) also
showed Zn desorption from suspended solids in the Columbia River.   In
addition laboratory mixing experiments have confirmed that both Zn and Cu
desorb from particles when riverwater and seawater are mixed (Van der Weijden
et al., 1977; Li et al., 1984; Campbell et al., 1985).   It is clear from
both types of experiment that for many estuaries dissolved trace metals are
not in equilibrium with the particulate phase throughout the mixing region.

This emphasises the need for studies of the rates and extents of heterogeneous chemical reactions which are essential to the development of quantitative models which can predict the fate of waste-generated toxic metals. The work reported here examines the rates of sorption reactions and attempts to relate the dissolved metal behaviour to particle reactivity.

METHODS

Sample Collection. Suspended solids were collected during an axial transect of the Tamar Estuary (S.W. England) in August 1986. The samples for microstructural analysis were filtered, washed in distilled water and freeze dried. Larger particulate samples were also collected for the mixing experiments and water samples for these studies were obtained from the River Carnon (S.W. England), which receives substantial inputs of acid mine waste (Johnson, 1986). This water was filtered (passing 0.45μm membrane filter) prior to use.

Analytical Methods. A gravimetric BET nitrogen adsorption technique was used for the determination of specific surface area and porosity of the particles (Crosby et al., 1983; Marsh et al., 1984; Glegg et al., 1987). The surface concentration of Fe and Mn on the particles was determined by an E.D.T.A. extraction for 85 days at pH 9 (Borggaard, 1982). The extracted metals were quantified by flame atomic absorption spectrophotometry (A.A.S.), using acidified standards for calibration. The carbon content of the particles was determined using a calibrated combustiometric technique (Carlo Erba Elemental Analyser).

Mixing Experiments. Ten litre samples of filtered River Carnon water were held at pH 7 and 10°C in a constant temperature room. The A.A.S. analysis showed the initial Zn concentration to be 16 mg/l and the initial Cu concentration to be 38ug/l. Samples of the suspended solids were added to the stabilised water to give a final particle concentration of 1500 mg/l. The uptake of trace metal was followed as a function of time by retrieving, at selected intervals, 200 ml samples of suspension for analysis. These aliquots were filtered using 0.45um membrane filters and preconcentrated using a Chelex-100 resin system (Ackroyd et al., 1986). The eluates from the Chelex-100 extraction were then analysed using A.A.S. Also after varying periods during the course of an adsorption run (i.e. after 1 h and 24 h) doped particles were retrieved and resuspended in metal-free distilled water (at pH 7 and 10°C) to examine their desorption behaviour. The appearance of Zn and Cu in solution was followed over time in the same way as the adsorption experiments described above.

RESULTS

Microstructures of Suspended Solids. Table 1 shows the data for the axial variation of specific surface area of suspended solids in the Tamar Estuary as a function of controlling variables. The specific surface area has its highest value in the turbidity maximum as has been found on previous surveys (Titley et al., 1987). However, in this case there appears to be little correlation between the specific surface area and the carbon content of the particles. The particulate Fe contents show a similar distribution to that of carbon with the highest values in the freshwater then decreasing down-estuary. On the other hand if the particulate Mn concentrations are also considered, then the maximum Fe/Mn ratios are apparently associated with the highest specific surface areas, and vice versa. The 43% reduction in specific surface area from 22.1 m³/g to 12.7 m³/g represents losses of external and internal surfaces. This suggests that Mn could be acting either as a pore blocking agent on active Fe sites or as a bridge between particles to form aggregates which have pore spaces that are impervious to the nitrogen gas used in the BET analysis. The latter possibility is preferred since it has been suggested that similar surface area reduction occurs during phosphate adsorption onto goethite (Anderson et al., 1985).
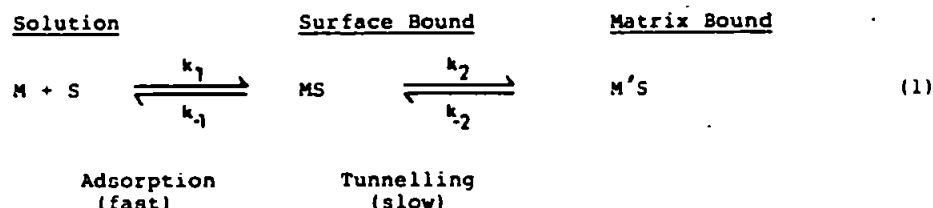
144

A13

TABLE 1 Specific surface areas and surface
chemical composition of suspended particles
taken during an ebb-tide axial transect
of the Tamar Estuary, August 1986

Salinity, $^o/oo$	Turbidity, mg/l	Specific Surface Area, m^3/g	Pore Volume,* ml/g	Carbon, %	Fe, mg/g	Fe/Mn
<0.5	20	12.7	18.8×10^{-3}	15.0	27.5	7.2
<0.5	25	13.3	-	10.0	18.6	7.0
<0.5	80	15.2	-	6.8	13.5	9.2
0.5	205	16.8	30.3×10^{-3}	5.6	11.6	18.0
1.1	160	22.1	27.5×10^{-3}	5.1	11.6	25.9
3.3	110	15.7	-	5.9	11.3	22.3
10.1	170	14.2	18.9×10^{-3}	5.1	11.7	20.2
14.4	210	11.8	-	4.1	8.2	15.7
19.7	100	11.6	-	4.6	10.1	10.2

*Estimated according to the method of Cranston
and Inkley (1957)

A full hysteresis loop is shown in Figure 1 for particles at 1.1‰ salinity
from the turbidity maximum. Microstructural analysis of this data shows
that the pore shape of the particles is either parallel plates or slits
between plates. The pore size distribution (Cranston and Inkley, 1957) for
the sample is illustrated in Figure 1b, with the percentage of pore radii in
size bands as follows: 3% in the size range 20-30 nm, 8% 10-20 nm, 20% 5-10
nm, 55% 2-5 nm and 14% <2nm. The maximum of the pore size distribution is in
the range which would allow surface adsorbed ions (like Zn and Cu) to penetrate
the matrix of the particles. There, the proximity of the parallel plates
could offer multiple bonding possibilities (i.e. across the plates or between
slits) such that once in the particle interior the Zn and Cu are adsorbed
irreversibly and the probability of desorption is less likely.

Adsorption-Desorption Experiments. The adsorption profiles for Zn and Cu are
shown in Figure 2. Zinc removal amounts to approximately 22% of the original
dissolved metal while about 80% of original dissolved Cu is removed.
However, there is considerably more Zn than Cu in the original solutions and
it is possible that the particles become rapidly saturated with Zn. The
other interesting feature of these profiles is that there are apparently two
phases during the period of the experiment. There is an initial rapid
adsorption phase for the first two hours which is then followed by a slower
approach to final equilibrium over a period of several days. This two-stage
process has been observed during phosphate adsorption onto soils (Barrow,1983;
Madrid and De Arambarri, 1985) and trace element uptake onto marine particles
in seawater (Nyffeler et al., 1984). It has been described mechanistically
as a consecutive reversible reaction; the first stage of which is surface
adsorption of the metal (M) which is then followed by migration from the
surface (S) to sites in the particle matrix (i.e. tunnelling):-

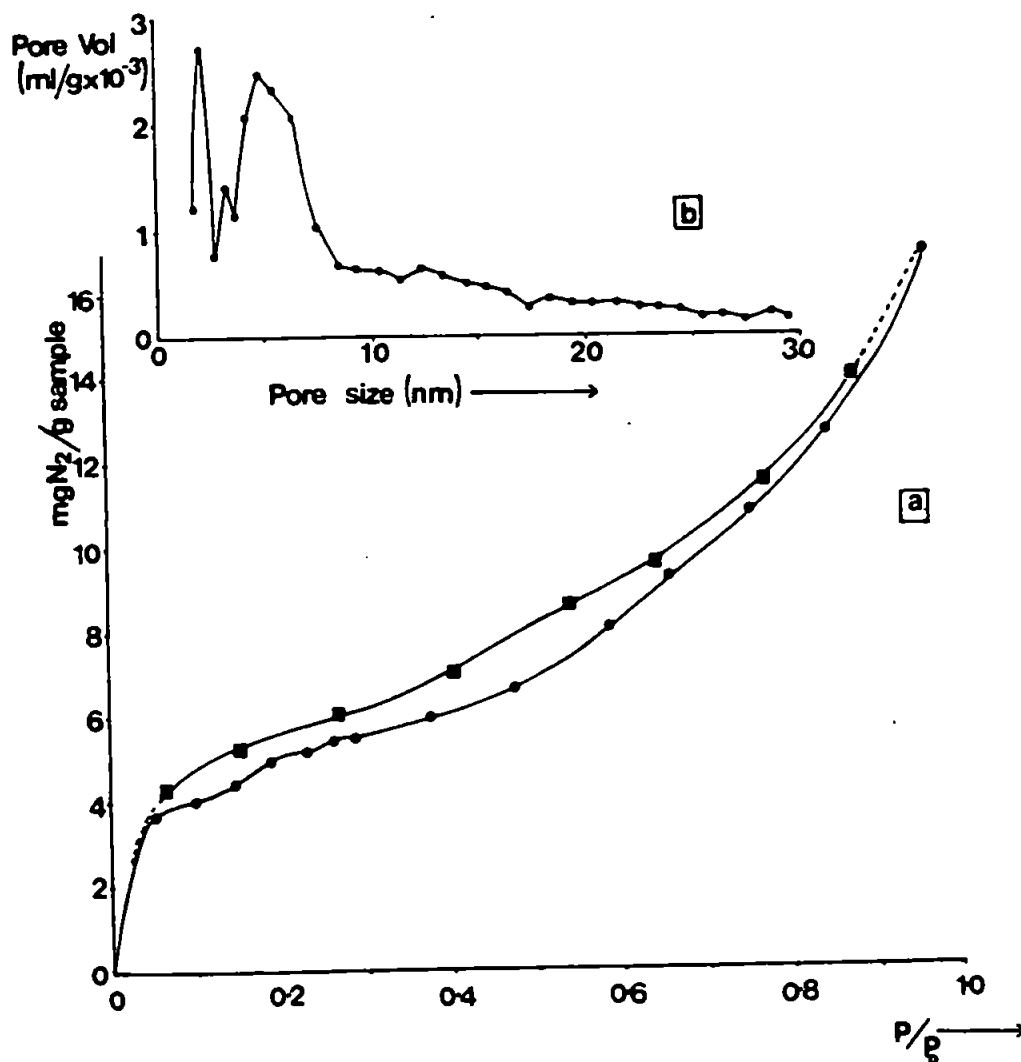| Solution	Surface Bound	Matrix Bound	
$M + S \underset{k_{-1}}{\overset{k_1}{\rightleftarrows}}$	$MS \underset{k_{-2}}{\overset{k_2}{\rightleftarrows}}$	$M'S$	(1)
Adsorption (fast)	Tunnelling (slow)		

145

A14

Fig. 1. (a) Adsorption isotherm and hysteresis loop for a suspended
solid sample taken from the turbidity maximum of the Tamar
Estuary. The abscissa is the relative pressure of
nitrogen gas, P/P_0, and the ordinate the weight of
nitrogen gas adsorbed on the sample. ● Adsorption;
■ Desorption. (b) The pore size distribution
for the same sample using the method of
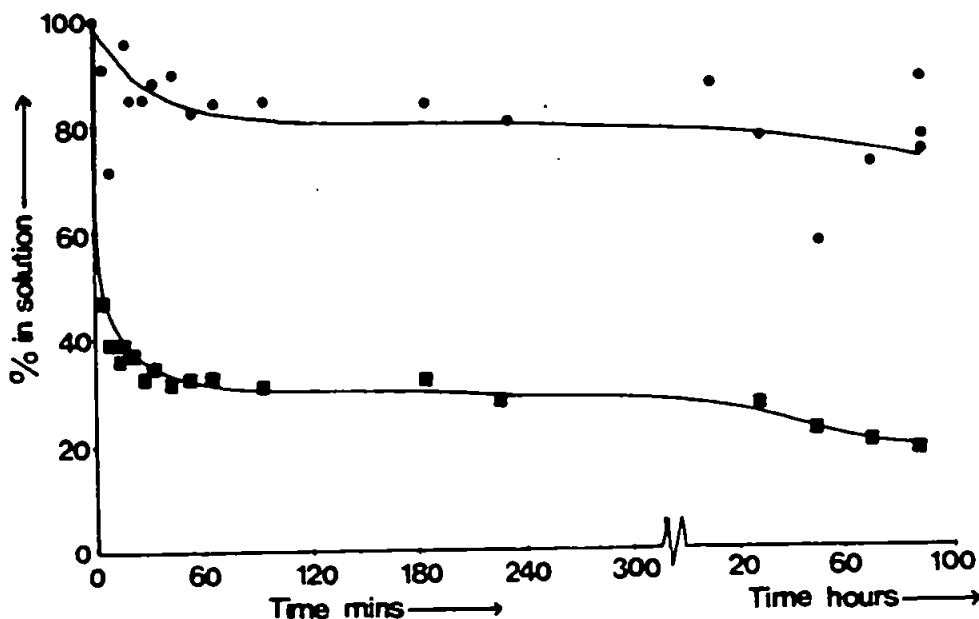Cranston and Inkley (1957).

Fig. 2. Adsorption profiles for the uptake of trace metals
from River Carnon water onto Tamar Estuary particles
at pH7 and 10°C. Particle concentration 1500 mg/l,
specific surface area 14 m²/g.

●- Zn, (Zn)₀ = 16 mg/l; ■- Cu, (Cu)₀ = 38μg/l

The results of the desorption of Zn from doped particles are illustrated in
Figure 3. In one experiment the particles had been in contact with the Zn-
rich solution for 1 h and in the other for 24 h. When the particles were
introduced into metal-free distilled water they showed a rapid desorption of
about 20% of the particulate metal, followed by a slow uptake over a period of
several days. There appeared to be little difference between the two runs
possibly because of the high concentrations of surface bound metal. The
picture is similar for Cu (see Figure 4) except that 4% of particulate Cu is
desorbed for particles in contact with River Carnon water for 1 h but only 1%
for those in contact for 24 h. The Cu results strongly support the proposed
two-stage mechanism because more of the metal would be incorporated into the
matrix after 24 h, and there would be less surface bound metal available for
desorption into solution. Furthermore, the results for both metals exhibit
a maximum followed by uptake which strongly suggests that the equilibration of
dissolved and surface bound metal is accompanied by another reaction. The
most likely possibility (since <10% of the metals was lost to the reactor
walls) is the solid state diffusion of metals attached to the particle surface
(Nyffeler et al., 1984). Estuarine particles have internal pore spaces which
can accommodate the metal ions and can offer multiple surface binding sites.
Under these conditions the metals could be irreversibly adsorbed leaving this
fraction of bound metal inaccessible to remobilisation either chemically or
biologically.

Fig. 3. Desorption profiles for Zn from suspended particles taken
1 h (●) and 24 h (◆) after contact with metal-rich River Carnon
water. The experiment was at 10°C, pH7 and a
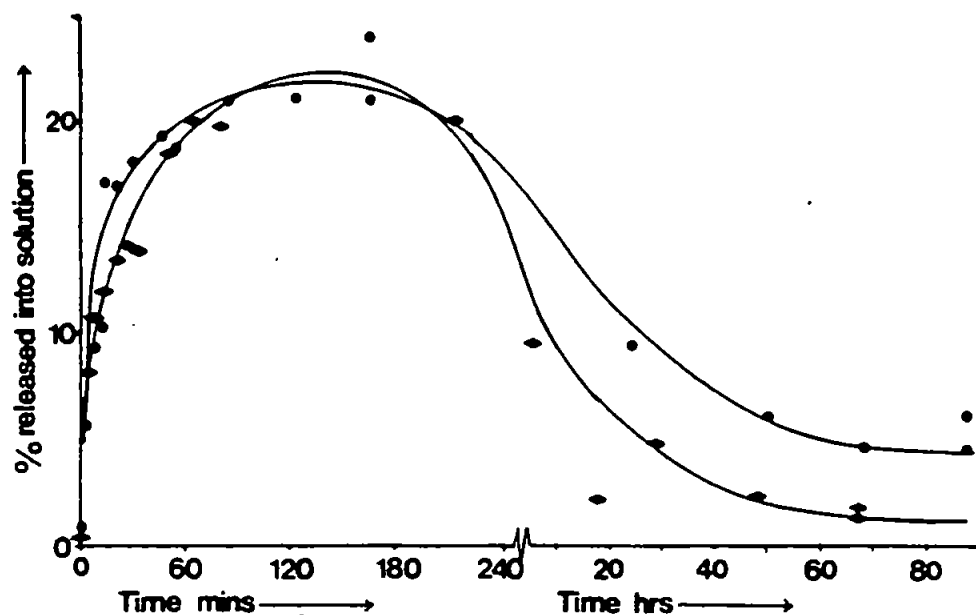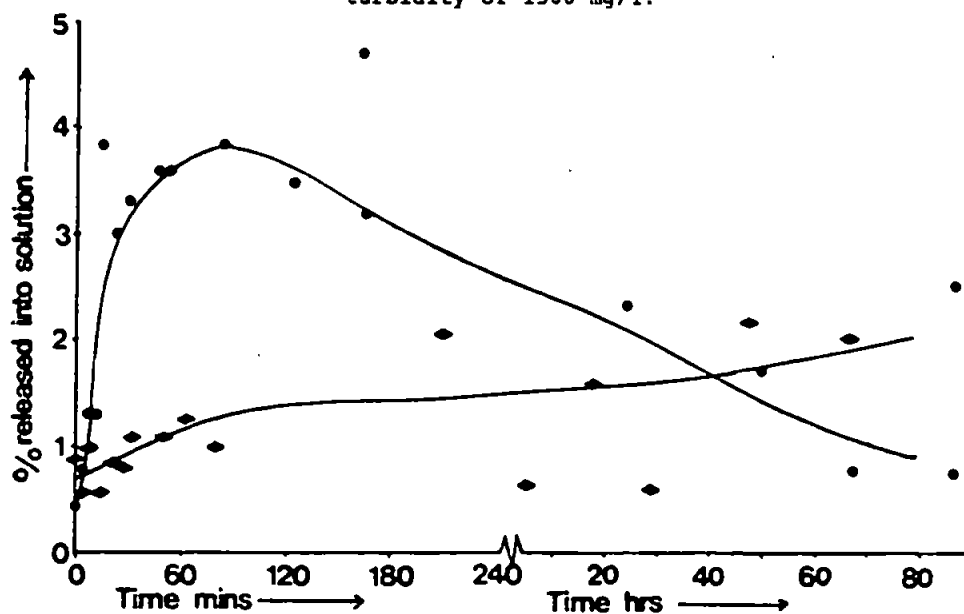turbidity of 1500 mg/l.

Fig. 4. Desorption profiles for Cu from suspended particles taken
1 h (●) and 24 h (◆) after contact with metal-rich River Carnon
water. The experiment was at 10°C, pH7 and a
turbidity of 1500 mg/l.

148

A17

Kinetic Analysis of Desorption Profiles. The mechanism represented by Equation 1 can be simplified by assuming that the reaction κ_{-2} (i.e. migration out of pore spaces) is very slow. Using this assumption, [2]Rodiguin and Rodiguina (1964) have shown that for a desorption experiment the appearance of metal in solution with time is given by :-

$$[M] = A \left[e^{-R_1t} - e^{-R_2t}\right] \tag{2}$$

where :
$$A = \frac{\kappa_{-1}[MS]_0}{R_2 - R_1} \tag{3}$$

$$R_{1,2} = \frac{-b \pm \sqrt{b^2-4g}}{2}$$

$$b = \kappa_1 + \kappa_{-1} + \kappa_2$$

$$g = \kappa_1\kappa_2$$

$[MS]_0$ = Concentration of weakly bound metal at time zero.

The numerical values of R_1R_2 and A were derived by a maximum likelihood curve fitting routine for Equation 2 (Ross, 1980) using the data where the particles were in contact with the solution for 1 h. This, together with the use of the first 3 h of the desorption data meant that the effect of the tunnelling reaction, κ_2, was small. The approach taken here allowed evaluation of both κ_1 and κ_{-1}; the results are given in Table 2 (note κ_1 is turbidity dependent so that it is quoted as $\kappa^*_1 = \kappa_1/p$, where p is the particle concentration in kg/l).

TABLE 2. Comparison of rate constants from this work and elsewhere

Particle Type	Adsorption Rate Constant κ^*_1, l/d/kg		Desorption Rate Constant κ_{-1}, d^{-1}		Ref.
	Zinc	Copper	Zinc	Copper	
Tamar Estuary	6.4×10^4	6.1×10^4	3.1×10^{-2}	5.3×10^{-2}	This work
Narragansett Bay	3.9×10^2	–	3.2×10^{-1}	–	Nyffeler et al. (1984)
San Clemente Basin	6.6×10^2	–	6.0×10^{-1}	–	"
MANOP Site H	1.0×10^4	–	7.0×10^{-2}	–	"
Settling Particles	7.3×10^3	–	2.0	–	"
Fecal Pellets	9.4×10^3	–	1.0	–	"

The data suggests the sorption rate constants are specific to the particle type (both surface chemical properties and microstructure) and the timescales over which the experiments were carried out. In this work emphasis has been placed on short-term adsorption reactions covering periods of hours, comparable to the flushing times of estuaries. Nyffeler et al. (1984) carried out

149

A18

experiments over periods of up to 50 days and so may have missed the short-term effects observed here. Nevertheless, the results from the two laboratories are reasonably comparable and demonstrate the value of carrying out time-dependent chemical kinetic studies.

CONCLUSIONS

The results of this study strongly suggest that a proportion of trace metals adsorbed onto estuarine particles is incorporated into the particle matrix. This fraction of particulate metal will desorb into solution extremely slowly and it is unlikely to be available for removal from particles by biota.

The kinetic analysis of the desorption profiles gave rate constants which compare favourably with data from other heterogeneous systems. The adsorption of dissolved metals from contaminated mine waters was turbidity dependent and had a half life of about 10 minutes for a particle concentration of 1500 mg/l. In contrast the desorption half life was 22 days for Zn and 130 days for Cu. Chemical timescales of this kind are of value when comparing to physical timescales of mixing and advection and ought to form the basis of future estuarine chemical research.

REFERENCES

Ackroyd, D. R., Bale, A. J., Howland, R. J. M., Knox, S., Millward, G. E. and Morris, A. W. (1986). Distributions and behaviour of dissolved Cu, Zn and Mn in the Tamar Estuary. Estuar. Coastal Shelf Sci., 23., 621-640.

Allen, G. P., Salomon, J. C., Bassoullet, P., Du Penhoat, Y. and De Grandpré, C. (1980). Effects of tides on mixing and suspended sediment transport in macrotidal estuaries. Sediment. Geol., 6, 69-90.

Anderson, M. A., Tejedor-Tejedor, M. I. and Stanforth, R. R. (1985). Influence of aggregation on the uptake kinetics of phosphate by goethite. Environ. Sci. Technol., 19, 632-637.

Barrow, N. J. (1983). A mechanistic model for describing the sorption and desorption of phosphate by soil. J. Soil Sci., 34, 733-750.

Borggaard, O. K. (1982). Selective extraction of amorphous iron oxides by EDTA from selected silicates and mixtures of amorphous and crystalline iron oxides. Clay Miner., 17., 365-368.

Campbell, J. A., Gardner, M. J. and Gunn, A. M. (1985). Short-term stability of trace metals in estuarine water samples. Anal. Chim. Acta, 176, 193-200.

Cranston, R. W. and Inkley, F. A. (1957). Determination of pore structures from nitrogen adsorption isotherms. Advan. Catal., 9, 143-154.

Crosby, S. A., Glasson, D. R., Cuttler, A. H., Butler, I., Turner, D. R., Whitfield, M. and Millward, G. E. (1983). Surface areas and porosities or Fe(III)- and Fe(II)- derived oxyhydroxides. Environ. Sci., Technol., 17, 709-713.

Evans, D. W. and Cutshall, N. H. (1973). Effects of ocean water on the soluble-suspended distribution of Columbia River radionuclides. In: Radioactive Contamination of the Marine Environment. International Atomic Energy Authority, Vienna.

Glegg, G. A., Titley, J. G., Glasson, D. R., Millward, G. E. and Morris, A. W. (1987). The microstructures of estuarine particles. In: Particle Size Analysis - 1985, P. J. Lloyd (Ed)., John Wiley & Sons, London, pp 591-597.

Johnson, C. A. (1986). The regulation of trace element concentrations in river and estuarine waters contaminated with acid mine drainage: The adsorption of Cu and Zn on amorphous Fe oxyhydroxides. Geochim. Cosmochim. Acta, 50, 2433-2438.

Li, Y.-H., Burkhardt, L. and Teraoka, H. (1984). Desorption and coagulation of trace elements during estuarine mixing. Geochim. Cosmochim. Acta, 48, 1879-1884.

Madrid, L. and De Arambarri, P. (1985). Adsorption of phosphate by two iron oxides in relation to their porosity. J. Soil Sci., 36, 523-530.

Marsh, J. G., Crosby, S. A., Glasson, D. R. and Millward, G. E. (1984). B.E.T. nitrogen adsorption studies of iron oxides from natural and synthetic sources. Thermochim. Acta, 82, 221-229.

Martin, J. -M., Mouchel, J. M., and Nirel, P. (1986). Some recent developments in the characterisation of estuarine particles. Water Sci. Technol., 18, 83-92.

Morris, A. W. (1986). Removal of trace metals in the very low salinity region of the Tamar Estuary, England. Sci. Total Environ., 49, 297-304.

Morris, A. W., Bale, A. J. and Howland, R. J. M. (1982). Chemical variability in the Tamar Estuary, Southwest England. Estuar. Coastal Shelf Sci., 14, 649-661.

Nyffeler, U. P., Li, Y.-H. and Santschi, P. H. (1984). A kinetic approach to describe trace-element distribution between particles and solution in natural aquatic systems. Geochim. Cosmochim. Acta, 48, 1513-1522.

Rodiguin, N. M. and Rodiguina (1964). Consecutive Chemical Reactions. D. Van Nostrand Co. Inc., London, pp 24-31.

Ross, G. J. S. (1980). A Maximum Likelihood Program. Statistics Department, Rothampstead Experimental Station, Harpenden, U.K., 50pp.

Titley, J. G., Glegg, G. A., Glasson, D. R. and Millward, G. E. (1987). Surface areas and porosities of particulate matter in turbid estuaries. Cont. Shelf Res., In press.

Van der Weijden, C. H., Arnoldus, M. J. H. L. and Meurs, C. J. (1977). Desorption of metals from suspended material in the Rhine Estuary. Neth. J. Sea Res., 11, 130-145.

151

A20

APPENDIX 2.

**Computer Programme and Specimen Output for Pore
Size Analysis Using the Cranston and Inkley Model.**

```
L.
10 REM : PROGRAM TO CALCULATE 'CRANSTON AND INKLEY' PHYSICAL SURFACE DATA: 7TH DRAFT 86.01.87
12 REM : ++++++
13 DIM A(50). B(50) , C(50).D(50).E(50).F(50).G(50).K(50).L(50).M(50).R(50).T(50).Z(50)
14 GOTO 31
15 PRINT:PRINT:PRINT"SORRY. YOU MUST START AGAIN"
20 GOTO 32
31 CLS:PRINT:PRINT:PRINT"BEFORE ENTERING DATA.YOU MUST FIRST ENSURE THAT THE DATA IS IN AN APPROPRIATE FORM"
32 PRINT:PRINT:PRINT"THE DATA THAT THIS PROGRAMME IS DESIGNED TO ACCEPT IS THE WGT OF N2 ADSORBED PER GRAMME OF SAMPLE."
33 PRINT:PRINT "PRESS A KEY TO CONTINUE":A$=GET$
34 PRINT:PRINT"A FULL ISOTHRM MUST BE PLOTTED. AND THE WEIGHT OF N2 MUST BE READ OFF AT THE APPROPRIATE P/Po VALUES."
35 PRINT:PRINT"SEE CRANSTON AND INKLEY'S PAPER BEFORE PROCEEDING"
36 PRINT:PRINT"THE WGT OF N2 (MgN2/g OF SAMPLE) AT EACH P/Po VALUE CAN BE ENTERED DIRECTLY."
37 PRINT:PRINT:PRINT"PRESS A KEY TO CONTINUE"
38 A$=GET$
40 CLS:PRINT:PRINT:PRINT"DATA CAN ONLY BE ENTERED VIA THE KEYBOARD AT PRESENT"
50 PRINT "ENTER DATA AS FOLLOWS:"
55 PRINT "WGT OF NITROGEN AT P/Po=0.931 SHOULD BE 1ST VALUE. THEN AT .929 & SO ON."
56 PRINT:PRINT "DATA MUST BE ENTERED IN THIS ORDER (HIGHEST P/Po VALUE 1ST) OR PROGRAMME WON'T WORK."
60 PRINT"TYPE 9999 TO END INPUT."
65 LET I=1
70 INPUT A(I)
80 IF A(I)= 9999 THEN GOTO 95
90 LET I=I+1
92 GOTO 70
95 LET I=I-1
105 CLS:PRINT:PRINT:PRINT"AS DATA APPEARS ENTER Y IF CORRECT.":PRINT "N IF INCORRECT"
110 PRINT"N IF INCORRECT."
115 CLS:PRINT"THERE ARE";I;"DATA POINTS."
120 PRINT TAB(1);"NO."TAB(5);"MgN2"TAB(15);"NO."TAB(20);"MgN2"
125 FOR J=1 TO (I/2)
130 Y=((INT(I/2))+J)
135 PRINT TAB(1):J TAB(5):A(J) TAB(15):(Y) TAB(20):A(Y)
140 NEXT J
145PRINT:PRINT"IS THIS CORRECT?(Y OR N)":REPEAT:A$=GET$:UNTIL A$="Y" OR A$="N":IF A$="Y" THEN 155
150 GOTO 15
155 REM : +++++ CALCULATIONS
160 FOR Z=1 TO I
165 L(Z)=A(Z)/1.2501
170 NEXT Z
175 FOR Z=1 TO I
180 M(Z)=L(Z)-L(Z+1)
185 NEXT Z
230 LET K(1)=.50: LET K(2)=.52: LET K(3)=.54: LET K(4)=.56:LET K(5)=.58
231 LET K(6)=.6:LET K(7)=.62:LET K(8)=.65:LET K(9)=.68:LET K(10)=.71
232 LET K(11)=.75:LET K(12)=.79:LET K(13)=.84:LET K(14)=.89:LET K(15)=.95
233 LET K(16)=1.02:LET K(17)=1.1:LET K(18)=1.19:LET K(19)=1.3:LET K(20)=1.44
234 LET K(21)=1.6:LET K(22)=1.8:LET K(23)=2.08:LET K(24)=2.44:LET K(25)=1.4
235 LET K(26)=1.56:LETK(27)=1.76:LET K(28)=2.0:LET K(29)=2.34:LET K(30)=2.86
236 LET K(31)=1.34:LET K(32)=1.49:LET K(33)=1.68:LET K(34)=1.93:LET K(35)=2.26
240 LET R(1)=1.212:LET R(2)=1.219:LET R(3)=1.226:LET R(4)=1.233:LET R(5)=1.241
250 LET R(6)=1.249:LET R(7)=1.258:LET R(8)=1.268:LET R(9)=1.279:LET R(10)=1.291
251 LET R(11)=1.304:LET R(12)=1.318:LET R(13)=1.333:LET R(14)=1.35:LET R(15)=1.369
252 LET R(16)=1.391:LET R(17)=1.416:LET R(18)=1.445:LET R(19)=1.478:LET R(20)=1.518
253 LET R(21)=1.565:LET R(22)=1.624:LET R(23)=1.696:LET R(24)=1.791:LET R(25)=1.917
254 LET R(26)=2.07:LET R(27)=2.18:LET R(28)=2.315:LET R(29)=2.495:LET R(30)=2.74
255 LET R(31)=3.06:LET R(32)=3.38:LET R(33)=3.58:LET R(34)=3.71:LET R(35)=3.69:LET R(36)=3.3
260 LET T(1)=3.1E-3:LET T(2)=3.2E-3:LET T(3)=3.3E-3:LET T(4)=3.4E-3:LET T(5)=3.6E-3
261 LET T(6)=3.7E-3:LET T(7)=3.8E-3:LET T(8)=4E-3:LET T(9)=.42E-2:LET T(10)=.43E-2
262 LET T(11)=.45E-2:LET T(12)=.47E-2:LET T(13)=.5E-2:LET T(14)=.53E-2:LET T(15)=.56E-2
263 LET T(16)=.59E-2:LET T(17)=.63E-2:LET T(18)=.67E-2:LET T(19)=.72E-2:LET T(20)=.8E-2
264 LET T(21)=.87E-2:LET T(22)=.95E-2:LET T(23)=1.05E-2:LET T(24)=1.18E-2:LET T(25)=1.32E-2
265 LET T(26)=1.47E-2:LET T(27)=1.61E-2:LET T(28)=1.78E-2:LET T(29)=2.01E-2:LET T(30)=2.31E-2
266 LET T(31)=2.65E-2:LET T(32)=2.93E-2:LET T(33)=3.25E-2:LET T(34)=3.71E-2:LET T(35)=4.38E-2
```

```
267 B(1)=(M(1)*R(1))
268 C(1)=0
270 C(2)=(B(1)*T(1))
280 B(2)=(M(2)-(C(2)*K(1)))*R(2)
290 FOR J=3 TO I
300 C(J)=((B(J-1)*T(J-1))+C(J-1))
310 B(J)=((M(J)-(C(J)*K(J-1)))*R(J))
315 NEXT J
320 FOR J=1 TO I
321 D(J)=B(J)*1.584E-3
322 NEXT J
325  FOR J=1 TO 25
326 Z(J)=D(J)/10
327 NEXT J
328 FOR J=26 TO 31
329 Z(J)=D(J)/5
330 NEXT J
331 FOR J=32 TO I
332 Z(J)=D(J)/2
333 NEXT J
340 LET E(1)=295:LET E(2)=285:LET E(3)=275:LET E(4)=265:LET E(5)=255:LET E(6)=245
341 LET E(7)=235:LET E(8)=225:LET E(9)=215:LET E(10)=205: LET E(11)=195
342 LET E(12)=185:LET E(13)=175:LET E(14)=165:LET E(15)=155
343 LET E(16)=145:LET E(17)=135:LET E(18)=125:LET E(19)=115:LET E(20)=105
344 LET E(21)=95:LET E(22)=85:LET E(23)=75:LET E(24)=65:LET E(25)=55
345 LET E(26)=47.5:LET E(27)=42.5:LET E(28)=37.5:LET E(29)=32.5:LET E(30)=27.5
346 LET E(31)=22.5:LET E(32)=19:LET E(33)=17:LET E(34)=15:LET E(35)=13:LET E(36)=11
350 FOR J=1 TO I
355 IF B(J) <=0.0 THEN 363
360 F(J)=(4*1.584E-3*1E4*B(J))/E(J)
362 GOTO 365
363 F(J)=0
365 NEXT J
370 LET G(1)=F(1)
380 FOR J=2 TO I
390 G(J)=F(J)+G(J-1)
400 NEXT J
410 REM : ****** PRINT OUT OF DATA
420 CLS
430 PRINT:PRINT:PRINT"DO YOU WANT A HARD COPY OF THE DATA? (Y OR N)"
432 G$=GET$
434 IF G$="Y" OR G$="N" GOTO 438
436 GOTO 432
438 IF G$="Y" THEN VDU2
440 MODE 3
450 PRINT:PRINT:PRINT SPC(5);"SURFACE AREA AND PORE VOLUMES"
460 PRINT:PRINT:PRINT"PORE SIZE";SPC(3);"VOL(MTP)";SPC(3);"PORE VOL";SPC(2);"PORE VOL/A";SPC(4);"(D-2T)";SPC(4);"S.A";SPC(9);"CUM
S.A"
470 FOR J=1 TO I
480 IF G$="Y" AND J=18 OR J=38 THEN VDU3
490 IF J=18 OR J=38 THEN PRINT"PRESS A KEY TO CONTINUE":A$=GET$
500 IF G$="Y" AND J=18 OR J=38 THEN VDU2
510 PRINT:E(J);TAB(13);INT(1000*B(J))/1000;TAB(23);INT(1E5*D(J))/1E5;TAB(33);INT(1E6*Z(J))/1E6;TAB(45);INT(1E5*T(J))/1E5;TAB(54);
INT(1E5*F(J))/1E5;TAB(66);INT(1E5*G(J))/1E5
520 NEXT J
530 IF G$="Y" THEN VDU3
540 PRINT"PRESS A KEY TO FINISH":A$=GET$:MODE7
>
```

SURFACE AREA AND PORE VOLUMES

PORE SIZE	VOL(NTP)	PORE VOL	PORE VOL/A	(D-2T)	S.A	CUM S.A
295	9.6E-2	1.5E-4	1.5E-5	3.1E-3	2.882E-2	2.882E-2
285	8.165	2.6E-4	2.6E-5	3.2E-3	3.681E-2	5.763E-2
275	8.187	1.7E-4	1.7E-5	3.3E-3	2.473E-2	8.236E-2
265	8.166	2.6E-4	2.6E-5	3.4E-3	3.99E-2	8.12227
255	8.137	2.1E-4	2.1E-5	3.6E-3	3.423E-2	8.1565
245	8.178	2.8E-4	2.8E-5	3.7E-3	4.688E-2	8.28258
235	8.178	2.8E-4	2.8E-5	3.8E-3	4.824E-2	8.25883
225	8.2	3.1E-4	3.1E-5	4E-3	5.633E-2	8.38716
215	8.2	3.1E-4	3.1E-5	4.19E-3	5.922E-2	8.36639
285	8.232	3.6E-4	3.6E-5	4.3E-3	7.199E-2	8.43838
195	8.265	4.2E-4	4.2E-5	4.49E-3	8.624E-2	8.52463
185	8.277	4.3E-4	4.3E-5	4.7E-3	9.497E-2	8.61961
175	8.268	4.2E-4	4.2E-5	4.99E-3	9.784E-2	8.71666
165	8.334	5.2E-4	5.2E-5	5.3E-3	8.12831	8.84497
155	8.39	6.1E-4	6.1E-5	5.6E-3	8.15973	1.88471
145	8.359	5.6E-4	5.6E-5	5.9E-3	8.15721	1.16192
135	8.384	6E-4	6E-5	6.3E-3	8.18843	1.34235
125	8.398	6.3E-4	6.3E-5	6.7E-3	8.28181	1.54417
115	8.388	6.1E-4	6.1E-5	7.2E-3	8.21391	1.75889
185	8.511	8E-4	8E-5	8E-3	8.38843	2.86653
95	8.474	7.5E-4	7.5E-5	8.69E-3	8.31675	2.38328
85	8.682	1.88E-3	1.88E-4	9.5E-3	8.58885	2.89213
75	8.789	1.12E-3	1.12E-4	1.85E-2	8.59921	3.49135
65	8.83	1.31E-3	1.31E-4	1.18E-2	8.88983	4.38118
55	1.581	2.37E-3	2.37E-4	1.32E-2	1.72981	6.831
47.5	8.691	1.89E-3	2.18E-4	1.47E-2	8.92173	6.95274
42.5	8.614	9.7E-4	1.94E-4	1.61E-2	8.91599	7.86874
37.5	8.739	1.17E-3	2.34E-4	1.78E-2	1.24866	9.1174
32.5	1.852	1.66E-3	3.33E-4	2.81E-2	2.85219	11.1696
27.5	1.247	1.97E-3	3.95E-4	2.31E-2	2.8744	14.844
22.5	8.836	1.32E-3	2.64E-4	2.65E-2	2.35419	16.3982
19	8.423	6.7E-4	3.35E-4	2.93E-2	1.41146	17.88967
17	-8.288	-4.6E-4	-2.28E-4	3.25E-2	8	17.88967
15	8.386	4.8E-4	2.42E-4	3.71E-2	1.29389	19.18276
13	8.584	9.2E-4	4.63E-4	4.38E-2	2.85115	21.95392
11	1.782	2.82E-3	1.411E-3	8	18.26533	32.21925
8	8	8	8	8	8	32.21925

A23